Supporting Information

Synthesis, self-assembly and optical properties of some rigid π-bridged triphenylene dimers.

Hang Lin,[a] Ke-Xiao Zhao,[a] Min Jing,[a] Xiu-Hai Long,[a] Ke-Qing Zhao,[a,*] Ping Hu,[a] Bi-Qin Wang,[a] Peng Lei,[b] Qing-Dao Zeng,[b] Bertrand Donnio[c,*]

[a]Sichuan Normal University, Chengdu 610066, China. E-mail: kqzhao@sicnu.edu.cn

[b]Key Laboratory of Standardization and Measurement for Nanotechnology, Center for Excellence in Nanoscience, National Center for Nanoscience and Technology (NCNST), Beijing 100190, China.

[c]Institut de Physique et Chimie des Matériaux de Strasbourg (IPCMS), CNRS-Université de Strasbourg (UMR7504), Strasbourg, 67034 France. E-mail:bertrand.donnio@ipcms.unistra.fr

Table of contents

Entry	Section	Pages
1.	Experimental techniques	2
2.	Synthesis and Characterization (Schemes S1-S13)	2 - 15
3.	^{1}H, ^{13}C and ^{19}F NMR (Figures S1 – S29)	15 - 45
4.	HRMS (Figures S30 – S49)	45 - 55
5.	UV-Vis absorption and photoluminescence (Figures S50 – S52, Tables S1 – S2)	55 - 58
6.	Gels and xerogels (Figures S53 - S54)	59 - 62
7.	DFT (Figures S55 – S60, Tables S3 – S6)	63 - 88
8.	POM (Figure S61)	84 - 91
9.	TGA (Figures S62 – S63, Table S7)	92
10.	DSC (Figures S64 – S66, Table S8)	93 - 97
11.	SWAXS (Figures S67 – S70, Tables S9 – S13)	97 - 109
12.	STM (Figure S71)	110
13.	Models' variations (Figures S72 – S74)	110 - 111

1. Experimental techniques

Elemental analysis. EA were measured on a Vario Micro cube (Elementar company, German).

NMR, HRMS, UV-Vis, PL. ^{1}H NMR was measured on a Varian INOVA 400 MHz or Bruker AVANCETM 600 MHz spectrometers in $CDCl_3$ using TMS as the internal standard. ^{13}C NMR and ^{19}F NMR was recorded on a Varian UNITY INOVA-400 (100 MHz and 376 MHz). The high-resolution mass spectra (HRMS) were measured on a Fourier Transform ion cyclotron resonance mass spectrometer (7.0T FTICRMS) instrument made by Ion Spec (Varian now) with MALDI or ESI as the ion source. Ultraviolet-visible (UV-Vis) absorption spectra were measured at room temperature on a Perkin Elmer Lambda 950 spectrophotometer. Photoluminescence (PL) was measured on a HORIBA Fluoromax-4p, and the absolute quantum yields were measured by a HORIB-F-3029 Integrating Sphere, HORIBA, Kyoto, Japan.

POM, DSC and TGA. The optical textures of liquid crystals were observed using a XP-201 and an Olympus BH2 Polarised Optical Microscope (POM) equipped with a XP-201 and Mettler FP82HT hot-stages of which temperatures were controlled by a XPR-201 and Mettler FP90. The phase transition temperatures and enthalpies were investigated using a TA-DSC Q100 differential scanning calorimeter (DSC) under N_2 atmosphere with heating or cooling rate of 10 ^{o}C /min. The thermal gravimetrical analysis (TGA) was measured on a TA TGA-Q500 instrument with heating rate of 10 ^{o}C /min in N_2 atmosphere.

SWAXS. Temperature-variation SWAXS experiments were performed on a Rigaku Smartlab (3) X-Ray diffractometer equipped with a TCU 110 temperature control unit. The sample temperature was controlled within±1 K. The X-ray sources (Cu Kα, λ=0.154 nm) were provided by 40 kW ceramic tubes.

DFT. Molecular structures, orbital frontiers, HOMO and LUMO were calculated by DFT. The B3LYP-D3 method with basis set of 6-311++G(d,p)** was applied. First, the molecular structures were optimized to obtain most stable molecular geometry. Molecular structures were modelled by MM2 from Chem3D 15.0, after minimization of the energy (step interval 2fs, frame interval 10 fs, 10000 steps).

2. Synthesis and characterization

All solvents and some chemical reagents below are commercial products, and were used without further purification.

Compound	Structure	Purity	Manufacturer
2-Thiophenylboric acid	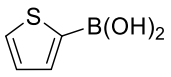	98%	Sukailu Chem. Tech. Co., Ltd.
3-Thiophenylboric acid	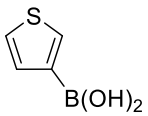	98%	Sukailu Chem. Tech. Co., Ltd.
2-Furanylboronic acid	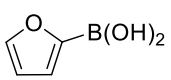	98%	Sukailu Chem. Tech. Co., Ltd.
Thieno[3,2-*b*]thiophene-2-boronic acid	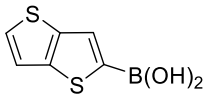	98%	Sukailu Chem. Tech. Co., Ltd.
1,4-Phenylenebisboronic acid	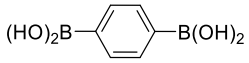	98%	Sukailu Chem. Tech. Co., Ltd.

4,4'-Biphenyldiboronic acid	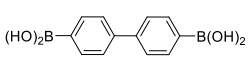	98%	Sukailu Chem. Tech. Co., Ltd.
Thieno[3,2-*b*]thiophene	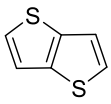	98%	Alpha Chemical Co., Ltd.
Benzo[1,2-*b*:4,5-*b*']dithiophene-4,8-dione	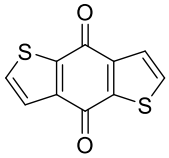	98%	Sukailu Chem. Tech. Co., Ltd.
3,4-Dimethoxybromobenzene	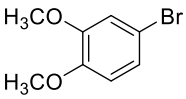	98%	Alpha Chemical Co., Ltd.
5,5’-Bis(4,4,5,5-tetramethyl-1,3,2-dioxaborolan-2-yl)-2,2’-bithiophene	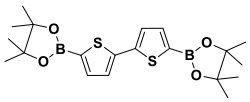	98%	Bide Pharmaceutical Tech. Co., Ltd.
Nonafluorobutanesulfonyl fluoride	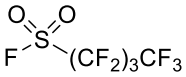	99%	Jianting Chem. Tech. Co., Ltd.

2.1. Synthesis of precursor bridges 1 and 3 (Schemes S1 and S2)

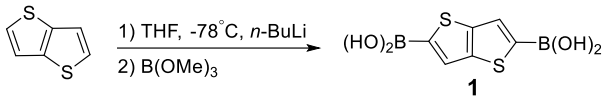

Scheme S1: Synthetic scheme bridge **1**.

1: To thieno[3,2-*b*]thiophene (2.0 g, 14.3 mmol) was slowly added a solution of *n*-butyllithium (21.4 mL, 42.8 mmol) in THF (15 mL) under argon, and the reaction was kept for 0.5h. After stirring at room temperature for 1h, the reaction was cooled down to -78°C, and trimethyl borate (7.19 mL, 64.2 mmol) was added quickly. The mixture was stirred at room temperature for 12h. Then, it was slowly poured into ice water. Diluted hydrochloric acid was added dropwise until the mixture was acidic. After being filtered through a funnel, it was dried in vacuum under argon to yield **2** (1.98g, 61%).

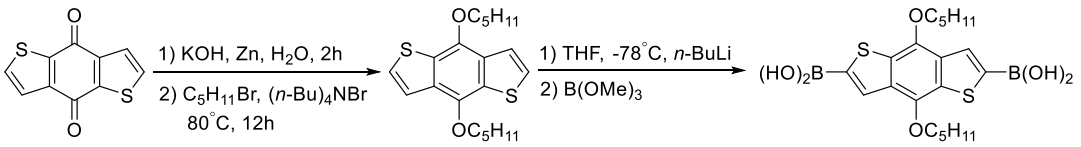

Scheme S2: Synthetic scheme of bridge **3**.

2 and **3:** A mixture of benzo[1,2-b:4,5-b']dithiophene-4,8-dione (2.0 g, 9.08 mmol), KOH (1.33 g, 23.61 mmol) and zinc powder (1.49 g, 22.70 mmol) in water (50 mL) was heated to reflux with stirring for 2h. Then 1-bromopentane (3.15 g, 20.88 mmol) and tetrabutylammonium bromide (0.55 g, 1.36 mmol) were added into the reacting solution and continued to react for 12h at 80°C. After cooling to room temperature, the mixture was washed by water and the product extracted by CH_2Cl_2. The organic layer was dried over anhydrous $MgSO_4$ and filtered through a funnel, and condensed on a rotary evaporator. The crude product was purified by silica-gel column chromatography with elution of CH_2Cl_2/petroleum ether (1/4, v/v) to yield **2** (2.79 g, 85%). **3** was synthesized according to the same procedure used for **1**: **2** (1.0 g, 2.76

mmol), *n*-butyllithium (5.5 mL, 11.03 mmol), THF (30 mL), trimethyl borate (1.85 mL, 16.55 mmol). It was dried in vacuum under argon to yield **3** (0.66 g, 53%).

2.2. Synthesis of triphenylene precursors M0-1 - M0-4 (Schemes S3-S4)

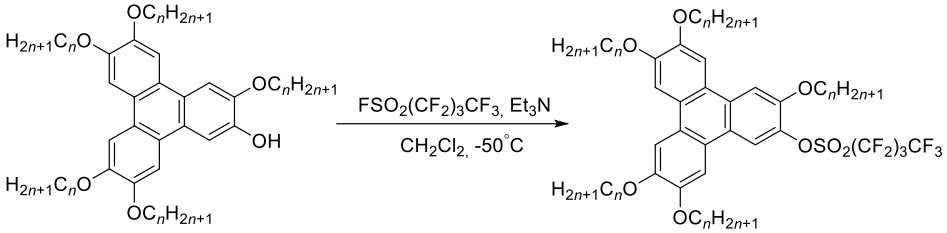

$\mathbf{4}_6$ (*n* = 6) **M0-1** (*n* = 6)
$\mathbf{4}_8$ (*n* = 8) **M0-2** (*n* = 8)

Scheme S3: Synthetic procedure of TP precursor **M0-1** and **M0-2**.

M0-1: Under argon, a solution of $\mathbf{4}_6$[1] (3.0g，0.0040 mol) in CH_2Cl_2 (150 mL), was cooled to -50°C, and were successively added, Et_3N (5.60 mL, 0.0403 mol) and nonafluorobutanesulfonyl fluoride (2.84 mL, 0.0161 mol). The mixture was stirred at -50°C for 1h, and then maintained at room temperature for 12h. Water was then added, the mixture extracted with CH_2Cl_2, dried over $MgSO_4$, and the organic solvent removed under vacuum. The residue was purified by silica column chromatography with elution of CH_2Cl_2/petroleum ether (1:2, v/v), and crystallized in EtOAc-EtOH to yield a white solid[2] (3.75g. 90.65%). ^{1}H NMR ($CDCl_3$, TMS, 400MHz) δ (ppm): 8.16 (s, 1H), 7.83 (s, 1H), 7.78 (s, 3H), 7.68 (s, 1H), 4.28-4.20 (m, 10H), 2.00-1.94 (m, 10H), 1.60-1.57 (m, 10H), 1.42-1.37 (m, 20H), 0.95 (t, *J* = 7.0 Hz, 15H). ^{13}C NMR ($CDCl_3$, 100MHz) δ (ppm): 150.29, 149.40, 149.37, 148.97, 148.87, 138.44, 129.44, 125.10, 123.40, 122.77, 122.16, 116.39, 107.91, 107.15, 106.55, 106.37, 106.29, 69.87, 69.74, 69.35, 69.29, 31.69, 31.68, 31.63, 31.57, 29.42, 29.39, 29.35, 29.29, 29.03, 25.85, 25.84, 25.76, 25.58, 22.66, 22.61, 22.56, 14.04, 14.00, 13.97. ^{19}F NMR ($CDCl_3$, 376 MHz) δ (ppm): -80.64 (t, *J* = 9.7 Hz, 3F, CF_3), -109.74 (t, *J* = 13.8 Hz, 2F, SCF_2), -120.71 – -120.79 (m, 2F, CF_2), -120.80 – -120.89 (m, 2F, CF_2).

M0-2 were synthesized accordingly to the above method. $\mathbf{4}_8$ (3.0 g, 0.0034 mol), Et_3N (4.71 mL, 0.0339 mol), nonafluorobutanesulfonyl fluoride (2.39 mL, 0.0136 mmol): **M0-2** (3.33 g, 84.1%). ^{1}H NMR ($CDCl_3$, TMS, 400MHz) δ (ppm): 8.14 (s, 1H), 7.79 (s, 1H), 7.75 (s, 3H), 7.65 (s, 1H), 4.24-4.19 (m, 10H), 1.95 (s, 10H), 1.59 (s, 10H), 1.43-1.27 (m, 40H), 0.91 (t, *J* = 4.0 Hz, 15H). ^{13}C NMR ($CDCl_3$, 100 MHz) δ (ppm): 150.21, 149.31, 149.29, 148.89, 148.78, 138.36, 129.38, 125.03, 123.32, 122.71, 122.68, 122.09, 116.33, 107.78, 107.02, 106.40, 106.24, 106.12, 69.81, 69.69, 69.29, 69.21, 31.87, 31.83, 31.82, 29.51, 29.48, 29.46, 29.40, 29.36, 29.32, 29.23, 29.08, 26.21, 26.11, 25.91, 22.70, 22.69, 22.67, 14.11, 14.08. ^{19}F NMR ($CDCl_3$, 376 MHz) δ (ppm): -80.65 (t, *J* = 9.3 Hz, 3F, CF_3), -109.82 (t, *J* = 12.2 Hz, 2F, SCF_2), -120.80 (s, 2F, CF_2), -125.86 – -125.92 (m, 2F, CF_2).

M0-3: To a stirred solution of 3,3',4,4'-tetra(methoxy)-1,1-biphenyl[3] (500.0 mg, 1.823 mmol) and 2-bromoanisole (511.4 mg, 2.73 mmol) in dry CH_2Cl_2 (30.0 mL), a solution of $FeCl_3$ (886.9 mg, 5.468 mmol) in CH_3NO_2 (1.0 mL) was added dropwise at room temperature. After around 0.5h, methanol (5 mL) and water (5 mL) were added to quench the reaction. The extraction with CH_2Cl_2 and purification by silica gel column chromatography (light petroleum/CH_2Cl_2, 1.5:1, v/v) and recrystallization in ethyl acetate and ethanol yielded a yellow solid, **6** (533.2 mg, 64%). Subsequently, under argon, **6** (500.0 mg, 1.093 mmol) was added to a reaction tube, stirring with dry CH_2Cl_2 (10.0 mL). The above mixture was placed and stirred at -78 °C, then

[1] S. Kumar, B. Lakshmi. A convenient and economic method for the synthesis of monohydroxy-pentaalkoxy- and hexaalkoxytriphenylene discotics. *Tetrahedron Lett*., 2005, 46, 2603-2605.

[2] S. J. Mahoney, M. M. Ahmida, H. Kayal, N. Fox, Y. Shimizu, S. H. Eichhorn. Synthesis, mesomorphism and electronic properties of nonaflate and cyano-substituted pentyloxy and 3-methylbutyloxy triphenylenes. *J. Mater. Chem*., 2009,19, 9221-9232.

[3] J. F. Hang, H. Lin, K. Q. Zhao, P. Hu, B. Q. Wang, H. Monobe, C. H. Zhu, B. Donnio. Butterfly Mesogens Based on Carbazole, Fluorene or Fluorenone: Mesomorphous, Gelling, Photophysical, and Photoconductive Properties. *Eur. J. Org. Chem.,* 2021, 1989-2002.

BBr_3 (0.62 mL, 6.56 mmol) was injected into the reaction system, and kept stirring overnight. It was extracted by ethyl acetate, dried with $MgSO_4$, organic solvent evaporated under vacuum to yield the black solid, 11-bromotriphenylene-2,3,6,7,10-pentaol. Soon afterwards, in a 100 mL round bottom flask, all 11-bromotriphenylene-2,3,6,7,10-pentaol, *n*-bromohexane (1.28 g, 7.748 mmol), K_2CO_3 (5.35 g, 38.741 mmol), zinc powder (211.1 mg, 3.23 mmol), KI (21.5 mg, 0.129 mmol) were introduced and DMF (20.0 mL) added. The reaction was heated to 90°C and let stirred for 24h. The mixture was cooled and poured in a 500 mL beaker in ice-water and dilute hydrochloric acid added to the solution till acidity, stirred, and filtered in a Buchner funnel. The solution was dried and solvent evaporated. The product was purified by silica gel column chromatography (dichloromethane/petroleum ether 1:1.5 v/v) and recrystallized from ethanol and ethyl acetate to obtain white powder **M0-3** (618.4 g, 70%). ^{1}H NMR ($CDCl_3$, TMS, 400MHz) δ (ppm): 8.57 (s, 1H), 7.84 (s, 1H), 7.78 (s, 3H), 7.77 (s, 1H), 4.26-4.21 (m, 10H), 2.00-1.90 (m, 10H), 1.65-1.57 (m, 10H), 1.41-1.34 (m, 20H), 0.96-0.92 (m, 15H). ^{13}C NMR ($CDCl_3$, 100 MHz) δ (ppm): 153.50, 149.90, 149.28, 148.94, 148.72, 129.25, 127.66, 124.75, 124.01, 123.05, 122.74, 122.63, 112.16, 107.54, 107.12, 106.68, 106.03, 105.57, 69.78, 69.73, 69.41, 69.38, 69.20, 31.69, 31.67, 31.61, 29.42, 29.40, 29.34, 29.33, 29.18, 25.85, 25.83, 25.82, 25.80, 22.66, 22.63, 14.06.

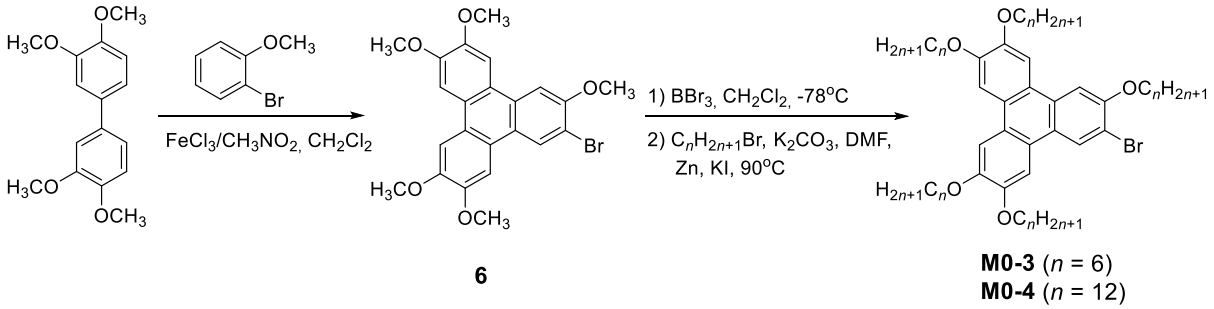

Scheme S4: Synthetic procedure of TP precursor **M0-3** and **M0-4**.

M0-4: As for compound **M0-3**: **6** (500.0 mg, 1.093 mmol), BBr_3 (0.62 mL, 6.56 mmol), 1-bromododecane (1.93 g, 7.748 mmol), K_2CO_3 (5.36 g, 38.741 mmol), zinc powder (211.1 mg, 3.23 mmol), KI (21.5 mg, 0.129 mmol). Silica gel column chromatography (eluting with light petroleum/CH_2Cl_2, 1.5:1, v/v) and recrystallization in ethyl acetate and ethanol yielded a white solid **M0-4** (994.1 mg, 74%). ^{1}H NMR ($CDCl_3$, TMS, 400MHz) δ (ppm): 8.56 (s, 1H), 7.83 (s, 1H), 7.78 (d, *J* = 1.9 Hz, 3H), 7.75 (s, 1H), 4.25-4.21 (m, 10H), 2.00-1.90 (m, 10H), 1.63-1.54 (m, 10H), 1.43-1.27 (m, 80H), 0.88 (t, *J* = 6.9 Hz, 15H). ^{13}C NMR ($CDCl_3$, 100 MHz) δ (ppm): 153.53, 149.91, 149.30, 148.96, 148.73, 129.28, 127.69, 124.78, 124.03, 123.08, 122.77, 122.65, 112.19, 107.59, 107.16, 106.72, 106.08, 105.60, 69.81, 69.75, 69.43, 69.41, 69.22, 31.93, 29.74, 29.71, 29.69, 29.64, 29.56, 29.52, 29.47, 29.46, 29.39, 29.38, 29.23, 26.21, 26.19, 26.16, 26.14, 22.70, 14.13.

2.3. Synthesis of triphenylene derivatives M1-M5 (Scheme S5)

M1: Under argon, **M0-1** (400.0 mg, 0.39 mmol), 2-thiophenylboric acid (64.77 mg, 0.51 mmol), K_2CO_3(1076.35 mg, 7.79 mmol), and $Pd(PPh_3)_4$ (45.0 mg, 0.039 mmol) were added to a reaction tube. Degassed water (2 mL) and THF (8 mL) were injected into the reaction mixture. The mixture was stirred at 70°C for 24h. Then, it was cooled, extracted with CH_2Cl_2 and dried with $MgSO_4$. The organic solvent was removed by distillation, and the residue was purified by silica gel column chromatography (light petroleum/CH_2Cl_2 2:1, v/v) to yield **M1** as a yellow solid (284.33 mg, 90%). ^{1}H NMR ($CDCl_3$, TMS, 400MHz) δ (ppm): 8.65 (s, 1H), 7.93 (s, 1H), 7.87 (s, 1H), 7.81 (s, 3H), 7.70 (d, *J* = 2.8 Hz, 1H), 7.42 (d, *J* = 4.9 Hz, 1H), 7.19 (dd, *J* = 5.1, 3.7 Hz, 1H), 4.31-4.23 (m, 10H), 2.05-1.95 (m, 10H), 1.65-1.57 (m, 10H), 1.47-1.36 (m, 20H), 0.95 (t, *J* = 6.7 Hz, 15H). ^{13}C NMR ($CDCl_3$, 100 MHz) δ (ppm): 153.92, 149.82, 149.21, 148.84, 148.75, 139.96, 129.26, 126.81, 125.63, 125.59, 124.85, 123.78, 123.17, 123.14, 122.99, 122.90, 122.76, 107.86, 107.43, 106.89, 106.64, 104.48, 69.85, 69.78, 69.45, 69.37, 68.93, 31.69, 31.66, 29.44, 29.38, 29.31, 26.04, 25.86, 25.85, 22.67, 22.61, 14.06. Elemental analysis: calculated for $C_{52}H_{74}O_5S$ (811.219), C 76.99%, H 9.20%, S 3.95%; found, C 76.84%, H 9.01%, S 3.94%.

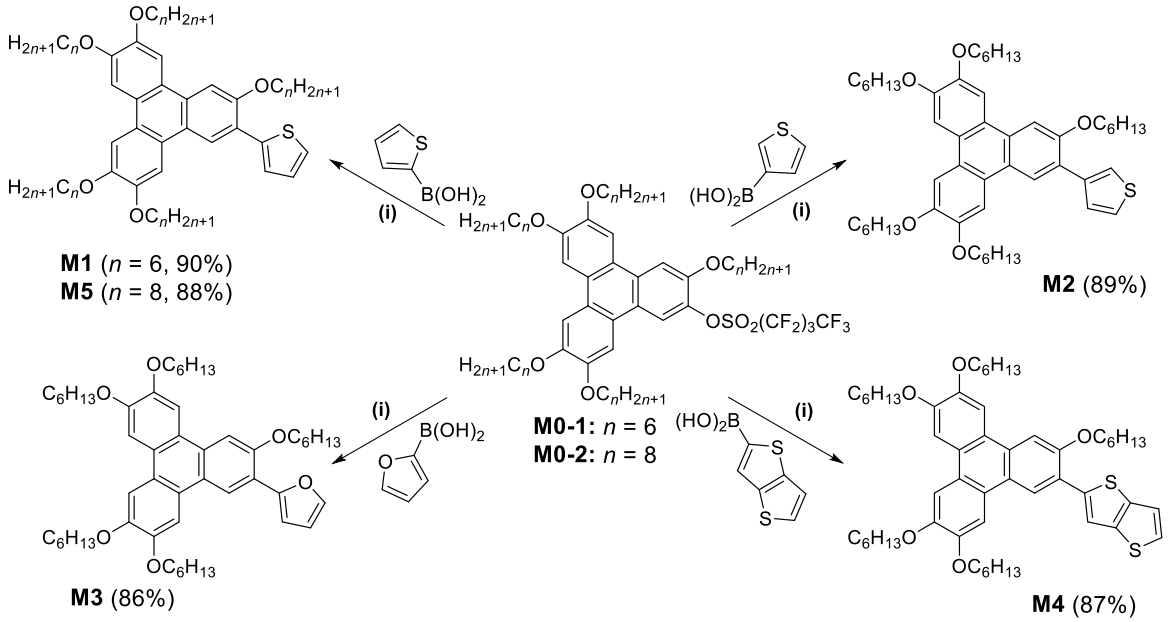

Scheme S5: Synthetic procedure for the monomeric species **M1**-**M5**: (i) $Pd(PPh_3)_4$, K_2CO_3, THF/H_2O.

M2-M5 were synthesized according to the same procedure used for **M1**.

M2: The coupling of **M0-1** (400.0 mg, 0.39 mmol) with 3-thiophenylboric acid (64.77 mg, 0.51 mmol) resulted in **M2** (723.61 mg, 89.2%). ^{1}H NMR ($CDCl_3$, TMS, 400MHz) δ (ppm): 8.51 (s, 1H), 7.94 (s, 1H), 7.90 (s, 1H), 7.83 (s, 3H), 7.79 (s, 1H), 7.64 (s, 1H), 7.44 (s, 1H), 4.25-4.24 (m, 10H), 1.96 (s, 10H), 1.60 (s, 10H), 1.42 (s, 20H), 0.96 (s, 15H). ^{13}C NMR ($CDCl_3$, 100 MHz) δ (ppm): 154.81, 149.71, 149.19, 148.75, 148.72, 138.69, 129.18, 128.90, 124.82, 124.76, 124.35, 124.24, 123.87, 123.33, 123.08, 122.75, 107.80, 107.40, 106.88, 106.57, 104.63, 69.80, 69.76, 69.44, 69.37, 68.62, 31.68, 31.59, 29.43, 29.38, 29.30, 25.95, 25.85, 22.66, 22.60, 14.06. Elemental analysis: calculated for $C_{52}H_{74}O_5S$ (811.219), C 76.99%, H 9.20%, S 3.95%; found, C 77.29%, H 9.36%, S 3.95%.

M3: The coupling of **M0-1** (400.0 mg, 0.39 mmol) with 2-furanylboronic acid (56.65 mg, 0.51 mmol) resulted in **M3** (264.75 mg, 85.5%). ^{1}H NMR ($CDCl_3$, TMS, 400MHz) δ (ppm): 8.90 (s, 1H), 8.03 (s, 1H), 7.86 (s, 1H), 7.81 (s, 2H), 7.78 (s, 1H), 7.60 (s, 1H), 7.13 (s, 1H), 6.59 (s, 1H), 4.30-4.24 (m, 10H), 2.04-1.96 (m, 10H), 1.62-1.60 (m, 10H), 1.42 (s, 20H), 0.96 (s, 15H). ^{13}C NMR ($CDCl_3$, 100 MHz) δ (ppm): 153.59, 150.59, 149.74, 149.23, 148.75, 148.67, 141.15, 128.82, 124.88, 124.08, 123.05, 123.02, 122.67, 120.32, 119.18, 111.93, 110.30, 107.86, 107.34, 106.86, 106.81, 103.94, 69.84, 69.77, 69.42, 69.35, 68.44, 31.70, 31.69, 29.45, 29.42, 29.40, 29.38, 26.07, 25.85, 22.67, 22.61, 14.06. Elemental analysis: calculated for $C_{52}H_{74}O_6$ (795.158), C 78.55%, H 9.38%; found, C 78.21%, H 9.54%.

M4: The coupling of **M0-1** (400.0 mg, 0.39 mmol) with thieno[3,2-*b*]thiophene-2-boronic acid (93.17 mg, 0.51 mmol) resulted in **M4** (294.84 mg, 87.3%). ^{1}H NMR ($CDCl_3$, TMS, 400MHz) δ (ppm): 8.58 (s, 1H), 7.87 (s, 2H), 7.80 (s, 1H), 7.76 (s, 2H), 7.72 (s, 1H) 7.40 (d, *J* = 5.1 Hz, 1H), 7.32 (d, *J* = 5.1 Hz, 1H), 4.26-4.21 (m, 10H), 2.04-1.92 (m, 10H), 1.62-1.60 (m, 10H), 1.43 (s, 20H), 0.96 (t, *J* = 6.4 Hz, 10H). ^{13}C NMR ($CDCl_3$, 100 MHz) δ (ppm): 153.90, 149.80, 149.16, 148.78, 148.64, 142.43, 139.43, 139.38, 129.37, 126.60, 124.86, 123.60, 123.08, 123.04, 122.95, 122.81, 122.72, 119.47, 118.06, 107.70, 107.27, 106.68, 106.36, 104.43, 69.77, 69.72, 69.35, 69.26, 68.91, 31.73, 31.72, 31.71, 31.70, 31.66, 29.45, 29.39, 29.29, 26.01, 25.89, 25.88, 25.86, 22.69, 22.67, 22.60, 14.09, 14.07. Elemental analysis: calculated for $C_{54}H_{74}O_5S_2$ (867.301), C 74.78%, H 8.60%, S 7.39%; found, C 74.30%, H 8.26%, S 7.52%.

M5: The coupling of **M0-2** (400.0 mg, 0.34 mmol) with 2-thiophenylboric acid (57.0 mg, 0.45 mmol) resulted in **M5** (287.5 mg, 88.2%). ^{1}H NMR ($CDCl_3$, TMS, 400MHz) δ (ppm): 8.65 (s, 1H), 7.94 (s, 1H), 7.87 (s, 1H), 7.81 (s, 3H), 7.70 (d, *J* = 3.8 Hz, 1H), 7.42 (d, *J* = 4.8 Hz, 1H), 7.19 (dd, *J* = 4.8, 3.8 Hz, 1H), 4.30-4.23 (m, 10H), 2.03-1.96 (m, 10H), 1.61-1.58 (m, 10H), 1.44-1.34 (m, 40H), 0.92 (t, *J* = 8.0 Hz, 15H). ^{13}C NMR ($CDCl_3$, 100 MHz) δ (ppm): 153.95, 149.87, 149.26,

148.90, 148.80, 140.01, 129.28, 126.82, 125.64, 125.56, 124.90, 123.83, 123.19, 123.05, 122.94, 122.80, 107.98, 107.55, 107.02, 106.78, 104.55, 69.92, 69.85, 69.52, 69.44, 68.98, 31.87, 31.84, 29.50, 29.46, 29.45, 29.35, 29.26, 26.38, 26.22, 22.70, 14.10. Elemental analysis: calculated for $C_{62}H_{94}O_5S$ (951.489), C 78.26%, H 9.96%, S 3.37%; found, C 78.31%, H 9.71%, S 3.21%.

2.4. Synthesis of the unsymmetrical fused heterocycles Tp^6T^6 and Tp^6Dt^6 (Schemes S6-S7)

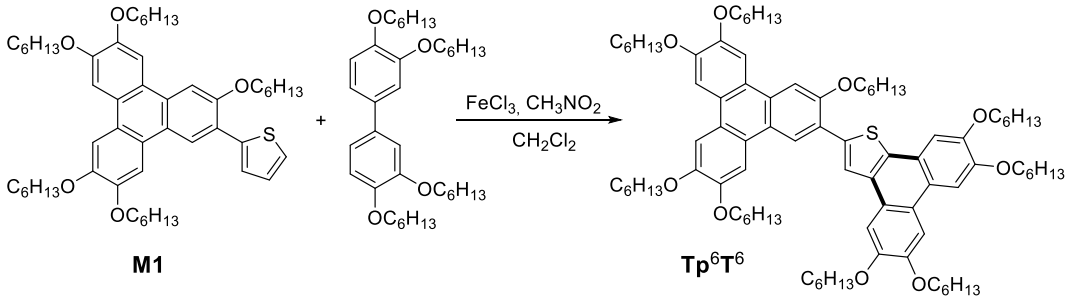

Scheme S6: Synthetic procedure for Tp^6T^6.

Tp^6T^6: Tp^6T^6 was synthesized by intermolecular cyclodehydrogenation (cross oxidation). To a solution of 3,3',4,4'-tetra(hexyloxy)-1,1-biphenyl[4] (120.0 mg, 0.220 mmol) and stirring $FeCl_3$ (43.0 mg, 0.250 mmol) in CH_3NO_2 (1 mL) in CH_2Cl_2 (8 mL), were added with **M1** (50 mg, 0.062 mmol) in CH_2Cl_2. After around 1h, cold CH_3OH (2 mL) and H_2O (2 mL) were added. It was extracted by CH_2Cl_2, dried with $MgSO_4$, organic solvent evaporated under vacuum, the residue purified by silica column with elution of light petroleum/CH_2Cl_2 1:1, v/v), and recrystallized from EtOAc-EtOH to get a yellow solid Tp^6T^6 (10.0 mg, 24%) and some amount of dimer $Tp^6Th_2Tp^6$ (20.5 mg, 41%). ^{1}H NMR ($CDCl_3$, TMS, 600MHz) δ (ppm): δ 8.80 (s, 1H), 8.43 (s, 1H), 8.08 (s, 1H), 7.94 (s, 1H), 7.91 (s, 2H), 7.89 (s, 1H), 7.85 (s, 2H), 7.74 (s, 1H), 7.50 (s, 1H), 4.38 (t, *J* = 6.4 Hz, 2H), 4.31-4.23 (m, 16H), 2.11-2.06 (m, 2H), 1.99-1.94 (m, 16H), 1.74-1.69 (m, 2H), 1.63-1.56 (m, 16H), 1.46-1.36 (m, 36H), 0.96-0.88 (m, 27H). ^{13}C NMR ($C_2D_2Cl_4$, 151 MHz) δ (ppm): 154.43, 150.18, 149.57, 149.36, 149.31, 148.98, 148.58, 138.01, 134.25, 133.62, 129.44, 124.88, 123.78, 123.63, 123.39, 123.11, 122.99, 122.88, 122.71, 122.68, 122.31, 122.18, 108.60, 108.15, 108.10, 108.07, 107.39, 106.92, 104.70, 70.16, 70.13, 69.97, 69.63, 69.23, 68.92, 31.66, 31.59, 31.57, 29.43, 29.41, 29.40, 29.38, 29.35, 29.32, 29.22, 26.08, 25.77, 25.76, 25.75, 25.71, 22.63, 22.60, 22.57, 14.12, 14.09, 14.08. HRMS (MALDI): $[M+H]^+$ calcd for $C_{88}H_{128}O_9S$, m/z: 1360.9279 (100.0%), 1361.9313 (95.2%), 1362.9346 (44.8%), 1364.9413 (3.1%); found, 1361.9311, 1360.9278, 1362,9357, 1363.9420. Elemental analysis: calculated for $C_{88}H_{128}O_9S$ (1362.04), C 77.60%, H 9.47%, S 2.35%; found, C 77.69%, H 9.31%, S 2.45%.

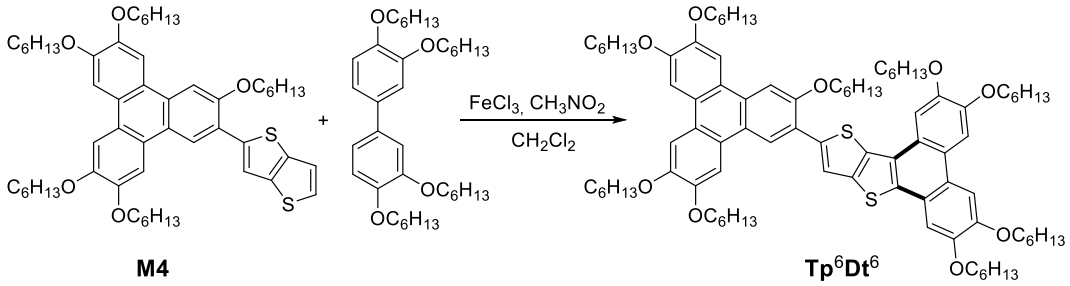

Scheme S7: Synthetic procedure for Tp^6Dt^6.

Tp^6Dt^6 was synthesized according to the same procedure used for Tp^6T^6. **M4** (50.0 mg, 0.058 mmol), $FeCl_3$ (38.0 mg, 0.230 mmol), CH_3NO_2 (1.0 mL), 3,3',4,4'-tetra(hexyloxy)-1,1-biphenyl (120.0 mg, 0.220 mmol). Silica gel column chromatography (eluting with light petroleum/CH_2Cl_2, 1:1, v/v) and recrystallization in ethyl acetate and ethanol yielded a yellow solid Tp^6Dt^6 (26.3 mg, 64%) and small amount of dimer $Tp^6Tt_2Tp^6$ (9.5 mg, 19%). ^{1}H NMR ($CDCl_3$, TMS, 600MHz) δ (ppm): 8.78 (s, 1H), 8.02 (s, 1H), 8.02 (s, 1H), 7.96 (s, 1H), 7.92 (s, 1H), 7.90 (s,

[4] K. Q. Zhao, Y. Gao, W. H. Yu, P. Hu, B. Q. Wang, B. Heinrich, B. Donnio. Discogens Possessing Aryl Side Groups Synthesized by Suzuki Coupling of Triphenylene Triflates and Their Self-Organization Behavior. *Eur.J.Org. Chem*., 2016, 2802-2814.

3H), 7.84 (s, 2H), 7.42 (s, 1H), 4.38 (t, *J* = 6.3 Hz, 4H), 4.33-4.20 (m, 14H), 2.12-2.08 (m, 2H), 2.03-1.93 (m, 16H), 1.67-1.57 (m, 18H), 1.46-1.35 (m, 36H), 0.97-0.88 (m, 27H). ^{13}C NMR ($CDCl_3$, 151 MHz) δ (ppm): 150.79, 146.84, 146.34, 146.17, 146.12, 145.84, 145.65, 145.15, 138.70, 133.60, 132.85, 126.43, 123.34, 121.85, 120.55, 120.11, 120.09, 120.06, 120.01, 119.94, 119.84, 119.78, 119.64, 118.71, 115.17, 104.85, 104.32, 104.20, 104.12, 104.04, 103.75, 103.61, 102.83, 101.60, 66.77, 66.74, 66.69, 66.63, 66.31, 66.29, 65.92, 65.73, 28.56, 28.52, 28.50, 28.49, 28.46, 28.42, 26.29, 26.27, 26.25, 26.21, 26.19, 26.14, 26.01, 22.87, 22.79, 22.74, 22.68, 22.67, 22.64, 19.47, 10.86, 10.83. HRMS (MALDI): $[M+H]^+$ calcd for $C_{90}H_{128}O_9S_2$, m/z: 1416.9000 (100.0%), 1417.9033 (97.3%), 1418.9067 (46.9%), 1419.9076 (1.8%); found, 1417.9032, 1416.8990, 1418.9057, 1419.9079. Elemental analysis: calculated for $C_{90}H_{128}O_9S_2$ (1418.125), C 76.23%, H 9.10%, S 4.52%; found, C 76.14%, H 9.06%, S 4.45%.

2.5. Synthesis of the symmetrical bridged dimers by Scholl cyclohydrogenation (Schemes S8-S9)

Tp^{6}Th$_2$Tp^6: To a stirred solution of **M1** (100.0 mg, 0.120 mmol) in dry CH_2Cl_2 (15 mL), a solution of $FeCl_3$ (42.0 mg, 0.260 mmol) in CH_3NO_2 (1.0 mL) was added dropwise at room temperature. After around 1h, methanol (3 mL) and water (3 mL) were added to quench the reaction. The extraction with CH_2Cl_2 and purification by silica gel column chromatography (light petroleum/CH_2Cl_2, 1:1, v/v) and recrystallization in ethyl acetate and ethanol yielded a yellow solid, **Tp^{6}Th$_2$Tp^6** (75.4 mg, 76%). ^{1}H NMR ($CDCl_3$, TMS, 600MHz) δ (ppm): 8.69 (s, 2H), 7.98 (s, 2H), 7.89 (s, 2H), 7.84 (s, 2H), 7.83 (s, 4H), 7.67 (d, *J* = 3.8 Hz, 2H), 7.32 (d, *J* = 3.8 Hz, 2H), 4.34 (t, *J* = 6.3 Hz, 4H), 4.29-4.22 (m, 16H), 2.09-2.04 (m, 4H), 1.99-1.93 (m, 16H), 1.72-1.67 (m, 4H), 1.63-1.59 (m, 16H), 1.48-1.40 (m, 40H), 0.97-0.93 (m, 30H). ^{13}C NMR ($C_2D_2Cl_4$, 151 MHz) δ (ppm): 153.76, 150.08, 149.37, 149.10, 148.91, 138.55, 137.53, 129.15, 126.41, 124.80, 123.57, 123.46, 123.14, 122.82, 122.59, 122.46, 122.35, 108.48, 107.94, 107.35, 104.46, 70.12, 69.96, 69.73, 69.61, 69.05, 31.65, 31.61, 29.42, 29.39, 29.35, 29.24, 26.08, 25.77, 22.65, 22.63, 14.13, 14.10. HRMS (MALDI): $[M]^+$ calcd for $C_{104}H_{146}O_{10}S_2$, m/z: 1620.0391 (100.0%), 1619.0357 (88.9%), 1621.0425 (55.7%), 1622.0458 (18.9%); found, 1620.0381, 1619.0358, 1621.0467, 1622.0467. Elemental analysis: calculated for $C_{104}H_{146}O_{10}S_2$ (1620.42), C 77.09%, H 9.08%, S 3.96%; found, C 76.95%, H 9.19%, S 4.03%.

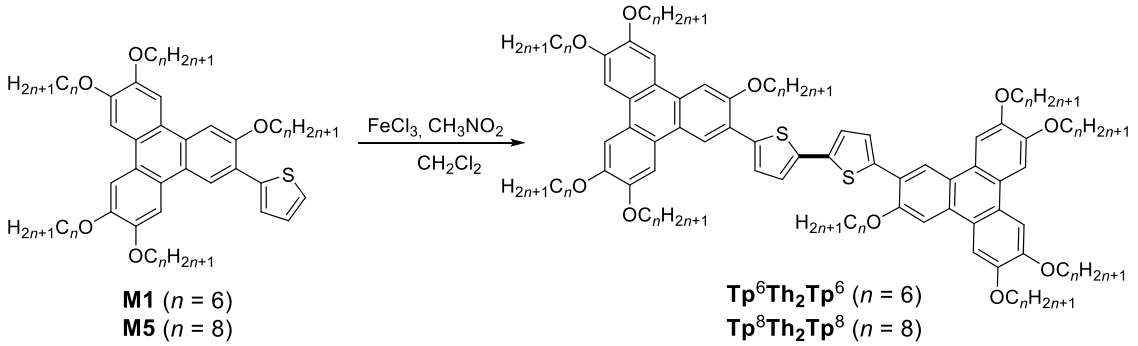

M1 (*n* = 6)
M5 (*n* = 8)

Tp^{6}Th$_2$Tp^6 (*n* = 6)
Tp^{8}Th$_2$Tp^8 (*n* = 8)

Scheme S8: Synthetic procedure for **Tp^{6}Th$_2$Tp^6** and **Tp^{8}Th$_2$Tp^8**.

Tp^{8}Th$_2$Tp^8: As for **Tp^{6}Th$_2$Tp^6. M5** (100.0 mg, 0.105 mmol), CH_2Cl_2 (15 mL), $FeCl_3$ (37.51 mg, 0.231 mmol), CH_3NO_2 (1.0 mL). Silica gel column chromatography (eluting with light petroleum/CH_2Cl_2, 1:1, v/v) and recrystallization in ethyl acetate and ethanol yielded a yellow solid **Tp^{8}Th$_2$Tp^8** (72.7 mg, 73%). ^{1}H NMR ($CDCl_3$, TMS, 600MHz) δ (ppm): 8.69 (s, 2H), 7.98 (s, 2H), 7.90 (s, 2H), 7.85 (s, 2H), 7.83 (s, 4H), 7.67 (d, *J* = 3.4 Hz, 2H), 7.33 (d, *J* = 3.4 Hz, 2H), 4.35 (t, *J* = 6.2 Hz, 4H), 4.28-4.23 (m, 16H), 2.09-2.04 (m, 4H), 1.99-1.93 (m, 16H), 1.71-1.66 (m, 4H), 1.63-1.58 (m, 16H), 1.50-1.32 (m, 80H), 0.92-0.87 (m, 30H). ^{13}C NMR ($CDCl_3$, 100 MHz) δ (ppm): 153.85, 149.86, 149.25, 148.91, 148.76, 138.79, 137.72, 129.29, 126.34, 124.90, 123.76, 123.36, 123.21, 122.99, 122.83, 122.62, 122.50, 107.90, 107.49, 106.95, 106.80, 104.48, 69.89, 69.81, 69.48, 69.03, 31.90, 31.88, 29.55, 29.53, 29.53, 29.49, 29.37, 26.53, 26.25, 26.24, 22.70, 14.11. HRMS (MALDI): $[M]^+$ calcd for $C_{124}H_{186}O_{10}S_2$, m/z: 1900.3521 (100.0%), 1899.3487 (74.6%), 1901.3555 (66.5%), 1902.3588 (29.2%), 1903.3622 (8.7%); found, 1900.3520, 1901.3554, 1899.3481, 1902.3584, 1903.3624. Elemental analysis: calculated for $C_{124}H_{186}O_{10}S_2$

(1900.96), C 78.35%, H 9.86%, S 3.37%; found, C 78.00%, H 9.97%, S 3.37%.

Tp^{6}β-Th$_2$Tp^6, **Tp^{6}Fu$_2$Tp^6**, and **Tp^{6}Tt$_2$Tp^6** were synthesized according to the same procedure used for **Tp^{6}Th$_2$Tp^6** (**Scheme S9**).

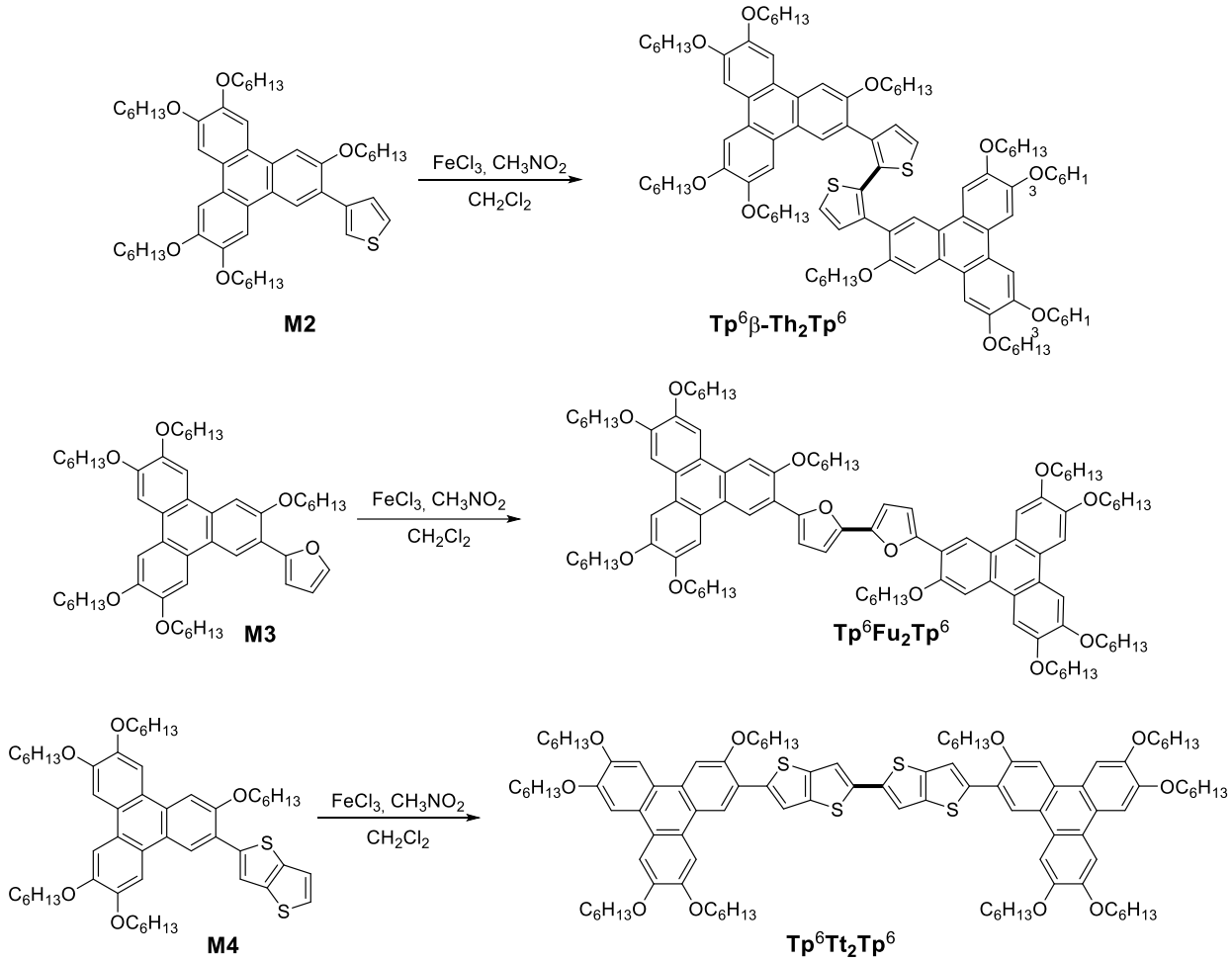

Scheme S9: Synthetic procedure for **Tp^{6}β-Th$_2$Tp^6**, **Tp^{6}Fu$_2$Tp^6**, and **Tp^{6}Tt$_2$Tp^6**.

Tp^{6}β-Th$_2$Tp^6: M2 (100.0 mg, 0.120 mmol), CH_2Cl_2 (15 mL), $FeCl_3$ (42.0 mg, 0.260 mmol), CH_3NO_2 (1.0 mL). Silica gel column chromatography (eluting with light petroleum/CH_2Cl_2, 1:1, v/v) and recrystallization in ethyl acetate and ethanol yielded a yellow solid **Tp^{6}β-Th$_2$Tp^6** (64.1 mg, 64%). ^{1}H NMR ($CDCl_3$, TMS, 600MHz) δ (ppm): 7.85 (s, 2H), 7.77 (s, 2H), 7.71 (s, 2H), 7.55 (s, 2H), 7.32 (d, *J* = 5.2 Hz, 2H), 7.21 (s, 2H), 7.19 (d, *J* = 5.2 Hz, 2H), 7.07 (s, 2H), 4.23 (t, *J* = 6.4 Hz, 4H), 4.17 (s, 4H), 4.12 (t, *J* = 5.2 Hz, 4H), 3.87 (s, 4H), 3.08 (s, 4H), 1.99-1.82 (m, 16H), 1.63-1.34 (m, 50H), 1.22-1.16 (m, 4H), 1.06-1.01 (m, 10H), 0.97-0.92 (m, 24H), 0.86 (t, *J* = 7.3 Hz, 6H). ^{13}C NMR ($CDCl_3$, 100 MHz) δ (ppm): 154.51, 149.42, 149.05, 148.43, 148.10, 136.89, 132.23, 131.72, 128.58, 126.00, 124.59, 124.26, 123.90, 123.46, 123.12, 122.15, 107.37, 107.02, 106.65, 105.25, 102.95, 69.80, 69.68, 69.40, 68.49, 67.41, 31.78, 31.75, 31.73, 31.58, 29.53, 29.49, 29.28, 28.45, 25.95, 25.91, 25.90, 25.87, 25.59, 22.71, 22.68, 22.60, 14.10, 14.06. HRMS (MALDI): $[M]^+$ calculated for $C_{104}H_{146}O_{10}S_2$, m/z: 1620.0391 (100.0%), 1619.0357 (88.9%), 1621.0425 (55.7%), 1622.0458 (18.9%); found, 1620.0381, 1619.0355, 1621.0416, 1622.0471. Elemental analysis: calculated for $C_{104}H_{146}O_{10}S_2$ (1620.42), C 77.09%, H 9.08%, S 3.96%; found, C 76.75%, H 9.08%, S 3.96%.

Tp^{6}Fu$_2$Tp^6: M3 (100.0 mg, 0.120 mmol), CH_2Cl_2 (15 mL), $FeCl_3$ (42.0 mg, 0.260 mmol), CH_3NO_2 (1.0 mL). Silica gel column chromatography (eluting with light petroleum/CH_2Cl_2, 1:1, v/v) and recrystallization in ethyl acetate and ethanol yielded a yellow solid **Tp^{6}Fu$_2$Tp^6** (66.9 mg, 67%). ^{1}H NMR ($CDCl_3$, TMS, 600MHz) δ (ppm): 9.03 (s, 2H), 8.08 (s, 2H), 7.90 (s, 2H), 7.84 (s, 2H), 7.83 (s, 2H), 7.83 (s, 2H), 7.25 (d, J = 3.5 Hz, 2H), 6.87 (d, J = 3.5 Hz, 2H), 4.36 (t, J = 6.5 Hz, 4H), 4.26 (t, J = 6.5 Hz, 4H), 4.25 (t, J = 6.5 Hz, 4H), 4.21 (t, J = 6.6 Hz, 4H), 4.18 (t, J = 6.7 Hz, 4H), 2.10-

2.05 (m, 4H), 1.99-1.89 (m, 12H), 1.74-1.65 (m, 8H), 1.62-1.57 (m, 10H), 1.50-1.33 (m, 36H), 1.28-1.20 (m, 10H), 0.98-0.92 (m, 24H), 0.86 (t, J = 7.0 Hz, 6H). ^{13}C NMR ($CDCl_3$, 100 MHz) δ (ppm): 153.75, 150.12, 149.84, 149.35, 148.77, 148.70, 145.29, 128.90, 125.01, 124.09, 123.07, 123.02, 122.78, 120.14, 118.87, 112.36, 107.99, 107.71, 107.63, 106.90, 106.54, 103.94, 69.94, 69.91, 69.44, 69.20, 68.51, 31.74, 31.72, 31.66, 29.50, 29.45, 29.41, 29.25, 26.08, 25.90, 25.88, 25.67, 22.68, 22.65, 22.61, 14.07. HRMS (MALDI): $[M]^+$ calcd for $C_{104}H_{146}O_{12}$, m/z: 1588.0848 (100.0%), 1587.0814 (88.9%), 1589.0881 (55.7%), 1590.0915 (18.9%); found, 1588.0850, 1587.0849, 1589.0851,1590.0866. Elemental analysis: calculated for $C_{104}H_{146}O_{12}$ (1588.30), C 78.65%, H 9.27%; found, C 78.98%, H 9.20%.

$Tp^6Tt_2Tp^6$: M4 (100.0 mg, 0.120 mmol), CH_2Cl_2 (15 mL), $FeCl_3$ (43.0 mg, 0.250 mmol), CH_3NO_2 (1.0 mL). Silica gel column chromatography (eluting with light petroleum/CH_2Cl_2, 1:1, v/v) and recrystallization in toluene and light petroleum yielded a yellow solid **$Tp^6Tt_2Tp^6$** (71.0 mg, 71%). ^{1}H NMR ($CDCl_3$, TMS, 600MHz) δ (ppm): 8.60 (s, 2H), 7.90 (s, 2H), 7.83 (s, 2H), 7.79 (s, 2H), 7.76 (s, 2H), 7.74 (s, 2H), 7.73 (s, 2H), 7.44 (s, 2H), 4.28 (t, *J* = 6.0 Hz, 4H), 4.27 (t, *J* = 6.0 Hz, 4H), 4.24-4.21 (m, 12H), 2.07-1.92 (m, 20H), 1.68-1.58 (m, 20H), 1.48-1.38 (m, 40H), 0.99-0.94 (m, 30H). ^{13}C NMR ($CDCl_3$, 151 MHz) δ (ppm): 153.90, 149.89, 149.24, 148.89, 148.71, 142.43, 140.16, 138.97, 138.34, 129.44, 124.92, 123.64, 123.15, 122.87, 122.84, 122.81, 117.93, 115.78, 107.78, 107.37, 106.76, 106.55, 104.52, 69.83, 69.78, 69.40, 69.04, 31.76, 31.74, 31.73, 31.71, 29.48, 29.45, 29.41, 29.36, 26.08, 25.93, 25.90, 25.88, 22.72, 22.68, 22.64, 14.11, 14.07. HRMS (MALDI): $[M]^+$ calcd for $C_{108}H_{146}O_{10}S_4$, m/z: 1731.9832 (100.0%), 1730.9799 (85.6%), 1732.9866 (57.9%), 1733.9899 (19.8%), 1734.9824 (10.5%); found, 1731.9836, 1732.9862, 1730.9792, 1733.9893, 1734.9891. Elemental analysis: calculated for $C_{108}H_{146}O_{10}S_4$ (1732.59), C 74.87%, H 8.49%, S 7.40%; found, C 74.93%, H 8.48%, S 7.54%.

2.6. Synthesis of the symmetrical bridged dimers by Suzuki cross-coupling (Schema 10)

Tp^6PhTp^6: Under argon, **M0-1** (250.0 mg, 0.244 mmol), 1,4-phenylenebisboronic acid (16.14 mg, 0.097 mmol), K_2CO_3 (403.63 mg, 2.921 mmol), $Pd(PPh_3)_4$ (28.13 mg, 0.024 mmol), were mixed and stirred in a H_2O/THF (2 mL:8 mL) solvent mixture. The mixture was heated to 70°C for 24h with stirring. When cooled, the mixture was extracted with CH_2Cl_2, dried over $MgSO_4$, and the solvent removed under vacuum. The residue was purified by silica column chromatography with elution of CH_2Cl_2/petroleum ether 1:1 (v/v). Recrystallization in ethyl acetate-ethanol yielded a white solid (119.4 mg, 80%). ^{1}H NMR ($CDCl_3$, TMS, 600MHz) δ (ppm): 8.49 (s, 2H), 7.98 (d, *J* = 5.3 Hz, 4H), 7.93 (s, 2H), 7.87 (s, 4H), 7.86 (s, 4H), 4.29-4.26 (m, 12H), 4.24 (d, *J* = 6.6 Hz, 4H), 4.25 (t, *J* = 6.6 Hz, 4H), 4.22 (t, *J* = 6.6 Hz, 4H), 1.99-1.88 (m, 16H), 1.63-1.53 (m, 20H), 1.46-1.34 (m, 40H), 0.95 (t, *J* = 6.6 Hz, 18H), 0.91 (t, *J* = 6.6 Hz, 6H), 0.91 (t, *J* = 6.6 Hz, 6H). ^{13}C NMR ($CDCl_3$, 100 MHz) δ (ppm): 155.02, 149.77, 149.29, 148.73, 137.51, 130.41, 129.49, 125.62, 124.86, 124.02, 123.14, 123.05, 122.97, 107.90, 107.49, 106.91, 106.46, 104.80, 69.84, 69.47, 69.31, 68.66, 31.71, 31.69, 31.65, 31.50, 29.44, 29.39, 29.37, 29.17, 25.87, 25.85, 25.81, 22.67, 22.63, 14.07, 14.04. HRMS (MALDI): $[M]^+$ calcd for $C_{102}H_{146}O_{10}$, m/z: 1532.0950 (100.0%), 1531.0916 (90.6%), 1533.0983 (54.7%), 1534.1017 (19.6%); found, 1532.0946, 1531.0918, 1533.0996, 1534.1063. Elemental analysis: calculated for $C_{102}H_{146}O_{10}$ (1532.28), C 79.95%, H 9.60%; found, C 79.77%, H 9.89%.

All the other D-π-D molecules were synthesized according to the above method.

Tp^8PhTp^8: M0-2 (250.0 mg, 0.214 mmol), 1,4-phenylenebisboronic acid (14.20 mg, 0.086 mmol), K_2CO_3 (355.13 mg, 2.570 mmol), $Pd(PPh_3)_4$ (24.75 mg, 0.022 mmol): **Tp^8PhTp^8** (112.3 mg, 72%). ^{1}H NMR ($CDCl_3$, TMS, 600MHz) δ (ppm): 8.49 (s, 2H), 7.98 (d, *J* = 4.6 Hz, 4H), 7.93 (s, 2H), 7.86 (s, 8H), 4.28-4.26 (m, 12H), 4.24 (t, *J* = 6.6 Hz, 4H), 4.21 (t, *J* = 6.6 Hz, 4H), 1.99-1.88 (m, 20H), 1.62-1.52 (m, 20H), 1.46-1.26 (m, 80H), 0.92-0.83 (m, 30H). ^{13}C NMR ($CDCl_3$, 100 MHz) δ (ppm): 155.01, 149.78, 149.31, 148.75, 148.73, 137.50, 130.38, 129.49, 125.62, 124.85, 124.06, 123.17, 123.04, 122.98, 107.94, 107.54, 106.94, 106.48, 104.77, 69.87, 69.49, 69.32, 68.64, 31.86, 31.83, 31.81, 29.50, 29.45, 29.35, 29.31, 29.24, 26.22, 26.19, 26.15, 22.70, 22.66, 14.12, 14.09. HRMS (MALDI): $[M]^+$ calcd for $C_{122}H_{186}O_{10}$, m/z: 1812.4080 (100.0%), 1811.4046 (75.8%), 1813.4113 (65.4%), 1814.4147 (28.4%); found, 1812.4072, 1811.4045, 1813.4115, 1814.40. Elemental analysis: calculated for $C_{122}H_{186}O_{10}$ (1812.82), C 80.83%, H 10.34%; found, C 80.42%, H 10.54%.

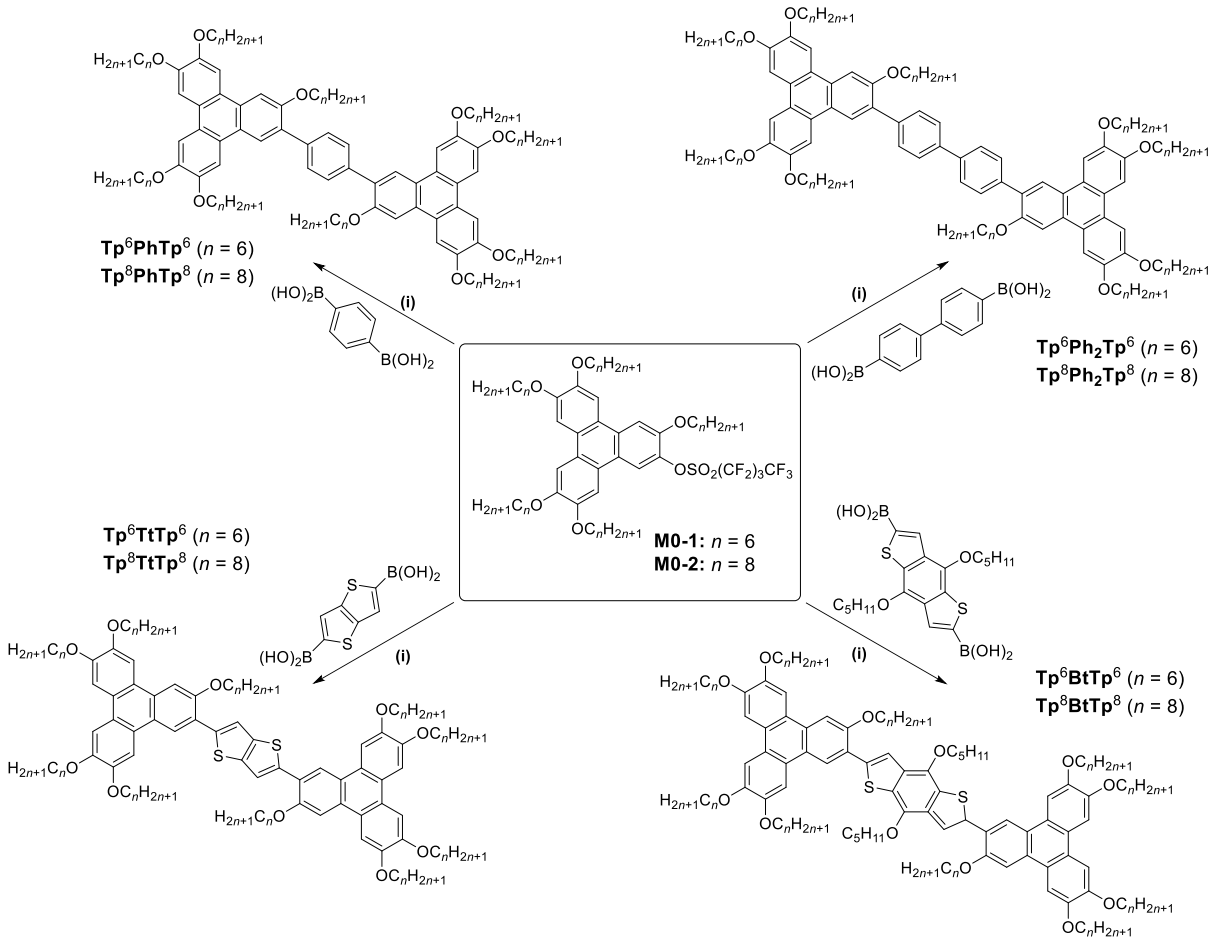

Scheme S10: Synthetic procedure for symmetrical dimers by Suzuki cross-coupling. (i) Pd $(PPh_3)_4$, K_2CO_3, THF/H_2O.

$Tp^6Ph_2Tp^6$: M0-1 (250.0 mg, 0.244 mmol), 4,4'-biphenyldiboronic acid (23.54 mg, 0.097 mmol), K_2CO_3 (403.63 mg, 2.921 mmol), $Pd(PPh_3)_4$ (28.13 mg, 0.024 mmol): **$Tp^6Ph_2Tp^6$** (123.5 mg, 78%). ^{1}H NMR ($CDCl_3$, TMS, 600MHz) δ (ppm): 8.45 (s, 2H), 7.97 (d, *J* = 6.4 Hz, 4H), 7.92 (s, 2H), 7.86-7.82 (m, 12H), 4.28-4.21 (m, 20H), 1.99-1.86 (m, 20H), 1.63-1.51 (m, 20H), 1.46-1.35 (m, 40H), 0.96-0.91 (m, 30H). ^{13}C NMR ($C_2D_2Cl_4$, 151 MHz) δ (ppm): 154.97, 150.02, 149.46, 148.95, 139.11, 137.60, 130.40, 129.97, 129.35, 126.51, 125.33, 124.76, 123.91, 122.98, 122.77, 108.57, 108.06, 107.46, 107.18, 104.92, 70.12, 70.05, 69.67, 68.75, 31.59, 31.56, 31.44, 29.42, 29.36, 29.12, 25.83, 25.77, 25.71, 22.62, 22.59, 14.10, 14.07. HRMS (MALDI): $[M]^+$ calcd for $C_{108}H_{150}O_{10}$, m/z: 1608.1263 (100.0%), 1607.1229 (85.6%), 1609.1296 (57.9%), 1610.1330 (12.1%); found, 1608.1258, 1607.1228, 1609.1306, 1610.1354. Elemental analysis: calculated for $C_{108}H_{150}O_{10}$ (1608.38), C 80.65%, H 9.40%; found, C 80.39%, H 9.03%.

$Tp^8Ph_2Tp^8$: M0-2 (250.0 mg, 0.214 mmol), 4,4'-biphenyldiboronic acid (20.72 mg, 0.086 mmol), K_2CO_3 (355.13 mg, 2.570 mmol), $Pd(PPh_3)_4$ (24.75 mg, 0.022 mmol): **$Tp^8Ph_2Tp^8$** (116.2 mg, 72%). ^{1}H NMR ($CDCl_3$, TMS, 600MHz) δ (ppm): 8.45 (s, 2H), 7.97 (d, *J* = 6.1 Hz, 4H), 7.92 (s, 2H), 7.86-7.83 (m, 12H), 4.28-4.21 (m, 20H), 1.99-1.86 (m, 20H), 1.62-1.51 (m, 20H), 1.46-1.28 (m, 80H), 0.92-0.87 (m, 30H). ^{13}C NMR ($C_2D_2Cl_4$,151 MHz) δ (ppm): 154.96, 150.01, 149.46, 148.93, 139.09, 137.59, 130.38, 129.99, 129.35, 126.49, 125.34, 124.77, 123.89, 122.99, 122.76, 108.58, 108.10, 107.48, 107.19, 104.96, 70.15, 70.08, 69.70, 69.64, 68.78, 31.77, 31.74, 29.48, 29.41, 29.38, 29.27, 29.24, 29.19, 26.20, 26.13, 26.11, 26.05, 22.65, 14.16. HRMS (MALDI): $[M]^+$ calcd for $C_{128}H_{190}O_{10}$, m/z: 1888.4393 (100.0%), 1887.4359 (72.2%), 1889.4426 (68.7%), 1890.4460 (31.1%), 1891.4493 (10.5%); found, 1888.4391, 1889.4429, 1887.4358, 1890.4465, 1891.4502. Elemental analysis: calculated for $C_{128}H_{190}O_{10}$ (1888.92), C 81.39%, H 10.14%; found, C 80.93%, H 10.39%.

Tp^6TtTp^6: M0-1 (250.0 mg, 0.244 mmol), thieno[3,2-*b*]thiophene-2,5-diboronic acid (22.18 mg,

0.097 mmol), K_2CO_3 (403.63 mg, 2.921 mmol), $Pd(PPh_3)_4$ (28.13 mg, 0.024 mmol): **Tp^{6}TtTp^6** (106.0 mg, 68%). ^{1}H NMR ($CDCl_3$, TMS, 600MHz) δ (ppm): 8.72 (s, 2H), 7.99 (s, 2H), 7.95 (s, 2H), 7.90 (s, 2H), 7.87 (s, 2H), 7.83 (s, 4H), 4.36 (t, *J* = 6.4 Hz, 4H), 4.30 (t, *J* = 6.5 Hz, 4H), 4.27-4.23(m, 12H), 2.10-2.05 (m, 4H), 2.01-1.93 (m, 16H), 1.71-1.57 (m, 20H), 1.50-1.37 (m, 40H), 0.98-0.93 (m, 30H). ^{13}C NMR ($CDCl_3$, 100 MHz) δ (ppm): 157.49, 149.54, 149.09, 148.72, 148.59, 130.31, 124.59, 124.34, 123.94, 123.24, 122.93, 122.84, 114.43, 107.36, 107.28, 106.85, 106.66, 106.37, 69.76, 69.49, 69.46, 69.17, 68.21, 31.67, 29.43, 29.40, 29.35, 29.31, 25.82, 22.65, 14.06. HRMS (MALDI): $[M]^+$ calcd for $C_{102}H_{144}O_{10}S_2$, m/z: 1594.0234 (100.0%), 1593.0201 (90.6%), 1595.0268 (54.6%), 1596.0302 (19.6%); found, 1594.0234, 1593.0198, 1595.0276, 1596.0304. Elemental analysis: calculated for $C_{102}H_{144}O_{10}S_2$ (1594.38), C 76.84%, H 9.10%, S 4.02%; found, C 77.09%, H 9.10%, S 4.06%.

Tp^{8}TtTp^8: M0-2 (250.0 mg, 0.214 mmol), thieno[3,2-*b*]thiophene-2,5-diboronic acid (19.52 mg, 0.086 mmol), K_2CO_3 (355.13 mg, 2.570 mmol), $Pd(PPh_3)_4$ (24.75 mg, 0.022 mmol): **Tp^{8}TtTp^8** (107.8 mg, 67%). ^{1}H NMR ($CDCl_3$, TMS, 600MHz) δ (ppm): 8.72 (s, 2H), 8.00 (s, 2H), 7.94 (s, 2H), 7.91 (s, 2H), 7.87 (s, 2H), 7.84 (s, 4H), 4.36 (t, *J* = 6.5 Hz, 4H), 4.29 (t, *J* = 6.5 Hz, 4H), 4.27-4.23 (m, 12H), 2.10-2.05 (m, 4H), 2.00-1.93(m, 16H), 1.69-1.57 (m, 20H), 1.50-1.32 (m, 80H), 0.92-0.88 (m, 30H). ^{13}C NMR ($CDCl_3$, 100 MHz) δ (ppm): 154.06, 149.88, 149.30, 148.93, 148.76, 141.79, 139.89, 129.37, 124.94, 123.75, 123.36, 123.22, 123.12, 122.95, 118.30, 107.91, 107.46, 106.91, 106.74, 104.73, 69.89, 69.81, 69.47, 69.10, 31.87, 31.85, 29.54, 29.46, 29.37, 29.30, 26.40, 26.24, 26.23, 22.70, 14.14, 14.12. HRMS (MALDI): $[M]^+$ calcd for $C_{122}H_{184}O_{10}S_2$, m/z: 1874.3364 (100.0%), 1873.3331 (75.8%), 1875.3398 (65.4%), 1876.3432 (28.4%); found, 1874.3340, 1875.3399, 1873.3290, 1876.3516. Elemental analysis: calculated for $C_{122}H_{184}O_{10}S_2$ (1874.92), C 78.15%, H 9.89%, S 3.42%; found, C 78.34%, H 9.68%, S 3.34%.

Tp^{6}BtTp^6: M0-1 (250.0 mg, 0.244 mmol), 4,8-bis(pentyloxy)benzo[1,2-*b*:4,5-*b*']thiophene diboronic acid (43.83 mg, 0.097 mmol), K_2CO_3 (403.63 mg, 2.921 mmol), $Pd(PPh_3)_4$ (28.13 mg, 0.024 mmol): **Tp^{6}BtTp^6** (112.7 mg, 64%). ^{1}H NMR ($CDCl_3$, TMS, 600MHz) δ (ppm): 8.78 (s, 2H), 8.15 (s, 2H), 8.04 (s, 2H), 7.94 (s, 2H), 7.91 (s, 2H), 7.85 (s, 4H), 4.43 (t, *J* = 6.5 Hz, 4H), 4.38 (t, *J* = 6.4 Hz, 4H), 4.31-4.24 (m, 16H), 2.12-2.07 (m, 4H), 2.03-1.93 (m, 20H), 1.72-1.57 (m, 24H), 1.52-1.37 (m, 44H), 0.99 (t, *J* = 7.4 Hz, 6H), 0.96-0.92 (m, 30H). ^{13}C NMR ($C_2D_2Cl_4$, 151 MHz) δ (ppm): 154.57, 150.31, 149.52, 149.20, 148.95, 143.77, 139.54, 132.36, 129.81, 129.64, 125.06, 124.22, 123.60, 123.19, 122.75, 122.64, 119.53, 108.74, 108.16, 107.35, 104.68, 70.23, 70.07, 69.72, 69.62, 69.05, 31.66, 31.60, 31.57, 30.26, 29.41, 29.39, 29.33, 28.16, 26.03, 25.76, 22.62, 22.58, 22.53, 14.13, 14.10. HRMS (MALDI): $[M]^+$ calcd for $C_{116}H_{166}O_{12}S_2$, m/z: 1816.1854 (100.0%), 1815.1821 (79.7%), 1817.1888 (62.2%), 1818.1921 (25.6%), 1819.1846 (5.6%); found, 1816.1855, 1815.1818, 1817.1893, 1818.1925, 1819.1943. Elemental analysis: calculated for $C_{116}H_{166}O_{12}S_2$ (1816.71), C 76.69%, H 9.21%, S 3.53%; found, C 76.90%, H 9.13%, S 3.60%.

Tp^{8}BtTp^8: M0-2 (250.0 mg, 0.214 mmol), 4,8-bis(pentyloxy)benzo[1,2-*b*:4,5-*b*']thiophene diboronic acid (38.56 mg, 0.086 mmol), K_2CO_3 (355.13 mg, 2.570 mmol), $Pd(PPh_3)_4$ (24.75 mg, 0.022 mmol): **Tp^{8}BtTp^8** (108.5 mg, 60%). ^{1}H NMR ($CDCl_3$, TMS, 600MHz) δ (ppm): 8.78 (s, 2H), 8.15 (s, 2H), 8.04 (s, 2H), 7.94 (s, 2H), 7.91 (s, 2H), 7.85 (s, 4H), 4.43 (t, *J* = 6.6 Hz, 4H), 4.38 (t, *J* = 6.4 Hz, 4H), 4.31-4.24 (m, 16H), 2.12-2.07 (m, 4H), 2.03-1.93 (m, 20H), 1.71-1.57 (m, 24H), 1.52-1.32 (m, 84H), 0.99 (t, *J* = 7.4 Hz, 6H), 0.92-0.88 (m, 30H). ^{13}C NMR ($C_2D_2Cl_4$, 151 MHz) δ (ppm): 154.57, 150.31, 149.53, 149.19, 148.95, 143.78, 139.54, 132.37, 129.79, 129.66, 129.63, 125.06, 124.22, 123.61, 123.19, 122.76, 122.65, 119.55, 108.74, 108.18, 107.35, 104.69, 70.24, 70.10, 69.72, 69.63, 69.06, 31.82, 31.77, 30.27, 29.48, 29.45, 29.43, 29.40, 29.28, 29.27, 29.24, 28.18, 26.35, 26.13, 26.12, 22.65, 22.63, 22.53, 14.16, 14.14. HRMS (MALDI): $[M]^+$ calcd for $C_{136}H_{206}O_{12}S_2$, m/z: 2096.4984 (100.0%), 2097.5018 (73.0%), 2095.4951 (68.0%); found, 2096.4983, 2097.5023, 2095.4943. Elemental analysis: calculated for $C_{136}H_{206}O_{12}S_2$ (2097.25), C 77.89%, H 9.90%, S 3.06%; found, C 77.63%, H 9.68%, S 3.02%.

2.7. Synthesis of the unsymmetrical bridged dimers Tp^{6}Ph$_2$Tp^{12} and Tp^{6}Th$_2$Tp^{12} by double Suzuki cross-coupling (Schemes S11-S12)

Tp^{6}Ph$_2$Tp^{12}/Tp^{12}Ph$_2$Tp^{12}: Under argon, 4,4'-biphenyldiboronic acid (36.4 mg, 0.151 mmol), **M0-4** (203.5 mg, 0.166 mmol), K_2CO_3 (416.1 mg, 3.011 mmol), $Pd(PPh_3)_4$ (17.4 mg, 0.015 mmol), were mixed and stirred in a H_2O/THF (2 mL:8 mL) solvent mixture. The mixture was heated to

70°C for 6h with stirring. Subsequently, the reaction was cooled to room temperature, and **M0-3** (133.8 mg, 0.166 mmol) and additional $Pd(PPh_3)_4$ (34.8 mg, 0.030 mmol) were added. The temperature was reheated to 70°C under argon, and the reaction was stirred for 12h. When cooled, the mixture was extracted with CH_2Cl_2, dried over $MgSO_4$, and the solvent removed under vacuum. The residue was purified by silica column chromatography with elution of CH_2Cl_2/petroleum ether 1:1 (v/v). Recrystallizing from EtOAc-EtOH yield a white solid **Tp^{6}Ph$_2$Tp^{12}** (73.3 mg, 24%) and some amount of the symmetrical compounds **Tp^{12}Ph$_2$Tp^{12}** (114.4 mg, 31%) and **Tp^{6}Ph$_2$Tp^6** (65.4 mg, 27%). **Tp^{6}Ph$_2$Tp^{12}**: ^{1}H NMR ($CDCl_3$, TMS, 600MHz) δ (ppm): 8.45 (s, 2H), 7.97 (s, 2H), 7.96 (s, 2H), 7.91 (s, 2H), 7.86-7.83 (m, 12H), 4.26 (s, 20H), 1.98-1.86 (m, 20H), 1.63-1.53 (m, 20H), 1.44-1.28 (m, 100H), 0.96-0.83 (m, 30H). ^{13}C NMR ($CDCl_3$, 151 MHz) δ (ppm): 155.00, 149.78, 149.30, 148.78, 139.58, 137.86, 130.34, 130.13, 129.55, 126.66, 125.45, 124.85, 124.01, 123.13, 122.99, 107.89, 107.49, 106.92, 106.58, 104.90, 69.83, 69.47, 69.36, 68.72, 31.93, 31.91, 31.71, 31.69, 31.66, 31.53, 29.74, 29.71, 29.69, 29.66, 29.64, 29.56, 29.51, 29.44, 29.39, 29.36, 29.27, 29.22, 26.26, 26.23, 26.21, 26.15, 25.90, 25.87, 25.85, 25.81, 22.69, 22.67, 22.63, 14.11, 14.10, 14.06, 14.04. HRMS (MALDI): $[M]^+$ calcd for $C_{138}H_{210}O_{10}$, m/z: 2028.5958 (100.0%), 2027.5924 (67.0%), 2029.5991 (45.4%), 2030.6025 (17.0%); found, 2028.5902, 2029.5945, 2027.5854, 2030.5997. Elemental analysis: calculated for $C_{138}H_{210}O_{10}$ (2029.19), C 81.68%, H 10.43%; found, C 81.47%, H 10.26%. **Tp^{12}Ph$_2$Tp^{12}**: ^{1}H NMR ($CDCl_3$, TMS, 600MHz) δ (ppm): 8.45 (s, 2H), 7.97 (s, 2H), 7.96 (s, 2H), 7.92 (s, 2H), 7.87-7.83 (m, 12H), 4.27-4.25 (m, 20H), 1.98-1.87 (m, 20H), 1.62-1.51 (m, 20H), 1.46-1.28 (m, 160H), 0.90-0.84 (m, 30H). ^{13}C NMR ($CDCl_3$, 151 MHz) δ (ppm): 154.99, 149.81, 149.31, 148.79, 139.57, 137.86, 130.34, 130.16, 129.56, 126.66, 125.45, 124.86, 124.03, 123.12, 123.00, 107.92, 107.52, 106.95, 106.60, 104.91, 69.86, 69.49, 69.38, 68.73, 31.93, 31.91, 29.74, 29.72, 29.69, 29.56, 29.51, 29.45, 29.39, 29.37, 29.27, 26.26, 26.23, 26.21, 26.17, 22.70, 22.68, 14.12. HRMS (MALDI): $[M]^+$ calcd for $C_{168}H_{270}O_{10}$, m/z: 2449.0653 (100.0%), 2450.0686 (66.8%), 2448.0619 (55.0%), 2451.0720 (54.0%), 2452.0753 (17.1%); found, 2449.0656, 2450.0616, 2451.0612, 2448.0689, 2452.0641. Elemental analysis: calculated for $C_{168}H_{270}O_{10}$ (2449.99), C 82.36%, H 11.11%; found, C 82.42%, H 10.87%.

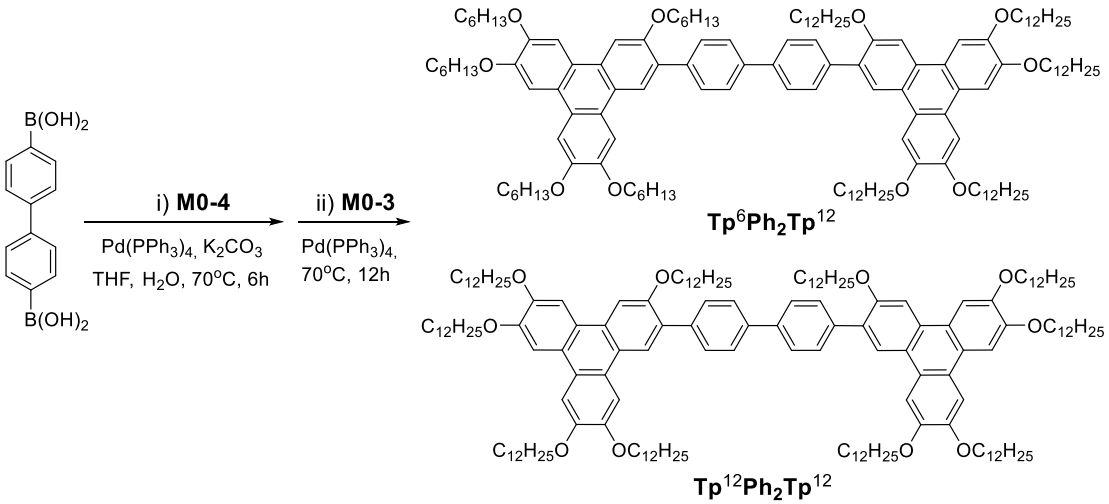

Scheme S11: Synthetic procedure for unsymmetrical dimer **Tp^{6}Ph$_2$Tp^{12}**.

Tp^{6}Th$_2$Tp^{12}/Tp^{12}Th$_2$Tp^{12}: Under argon, 2,2'-Bithiophene-5,5'-diboronic acid bis(pinacol) ester (108.2 mg, 0.259 mmol), **M0-3** (230.0 mg, 0.285 mmol), **M0-4** (349.8 mg, 0.285 mmol), K_2CO_3 (715.2 mg, 5.175 mmol), $Pd(PPh_3)_4$ (89.7 mg, 0.078 mmol), were mixed and stirred in a H_2O/THF (2 mL:8 mL) solvent mixture. The mixture was heated to 70°C for 24h with stirring. When cooled, the mixture was extracted with CH_2Cl_2, dried over $MgSO_4$, and the solvent removed under vacuum. The residue was purified by silica column chromatography with elution of CH_2Cl_2/petroleum ether 1:1 (v/v). Recrystallized from EtOAc-EtOH to get a yellow solid **Tp^{6}Th$_2$Tp^{12}** (132.1 mg, 25%) and some amount of symmetrical compounds **Tp^{12}Th$_2$Tp^{12}** (101.9 mg, 16%) and **Tp^{6}Th$_2$Tp^6** (96.4 mg, 23%). **Tp^{6}Th$_2$Tp^{12}**: ^{1}H NMR ($CDCl_3$, TMS, 600MHz) δ (ppm): 8.69 (s, 2H), 7.98 (s, 2H), 7.89 (s, 2H), 7.84 (s, 2H), 7.82 (s, 4H), 7.67 (s, 2H), 7.33 (s, 2H), 4.34 (s, 4H), 4.27-4.23 (m, 16H), 2.08-2.05 (m, 4H), 1.95-1.93 (m, 16H), 1.71-1.67 (m, 4H), 1.62-

1.57 (m, 16H), 1.48-1.21 (m, 100H), 0.97-0.93 (m, 15H), 0.89-0.81 (m, 15H). ^{13}C NMR ($CDCl_3$, 151 MHz) δ (ppm): 153.91, 149.89, 149.26, 148.94, 148.79, 138.76, 137.72, 129.32, 126.42, 124.92, 123.77, 123.38, 123.23, 123.02, 122.87, 122.72, 122.64, 107.89, 107.46, 106.93, 106.83, 106.78, 104.55, 69.88, 69.80, 69.47, 69.04, 31.93, 31.90, 31.72, 31.71, 31.70, 31.68, 29.74, 29.72, 29.69, 29.57, 29.51, 29.47, 29.44, 29.39, 29.37, 26.50, 26.23, 26.15, 25.89, 25.86, 22.69, 22.67, 14.12, 14.06. HRMS (MALDI): $[M]^+$ calcd for $C_{134}H_{206}O_{10}S_2$, m/z: 2040.5086 (100.0%), 2041.5120 (71.9%), 2039.5052 (69.0%), 2042.5153 (35.2%), 2043.5187 (14.4%); found, 2040.5073, 2041.5100, 2039.5033, 2042.5120, 2043.5151. Elemental analysis: calculated for $C_{134}H_{206}O_{10}S_2$ (2041.23), C 78.85%, H 10.17%, S 3.14%; found, C 79.15%, H 9.97%, S 3.26%. **Tp^{12}Th$_2$Tp^{12}**: ^{1}H NMR ($CDCl_3$, TMS, 600MHz) δ (ppm): 8.69 (s, 2H), 7.98 (s, 2H), 7.90 (s, 2H), 7.85 (s, 2H), 7.83 (s, 4H), 7.67 (d, *J* = 3.5 Hz, 2H), 7.33 (d, *J* = 3.5 Hz, 2H), 4.35 (t, *J* = 6.1 Hz, 4H), 4.28-4.23 (m, 16H), 2.09-2.04 (m, 4H), 1.99-1.95 (m, 16H), 1.71-1.66 (m, 4H), 1.62-1.58 (m, 16H), 1.49-1.21 (m, 160H), 0.89-0.81 (m, 30H). ^{13}C NMR ($CDCl_3$, 151 MHz) δ (ppm): 153.91, 149.89, 149.27, 148.95, 148.80, 138.75, 137.74, 129.33, 126.41, 124.93, 123.78, 123.35, 123.24, 123.03, 122.88, 122.74, 122.63, 107.93, 107.49, 106.96, 106.82, 104.56, 69.90, 69.82, 69.49, 69.04, 31.93, 31.91, 29.74, 29.72, 29.69, 29.57, 29.51, 29.47, 29.44, 29.39, 26.50, 26.22, 22.69, 22.67, 14.12. HRMS (MALDI): $[M]^+$ calcd for $C_{164}H_{266}O_{10}S_2$, m/z: 2460.9781 (100.0%), 2461.9815 (88.1%), 2459.9747 (56.4%), 2462.9848 (60.5%), 2463.9882 (22.4%); found, 2460.9770, 2461.9787, 2459.9751, 2462.9803, 2463.9831. Elemental analysis: calculated for $C_{164}H_{266}O_{10}S_2$ (2462.04), C 80.01%, H 10.89%, S 2.60%; found, C 79.82%, H 10.61%, S 2.59%.

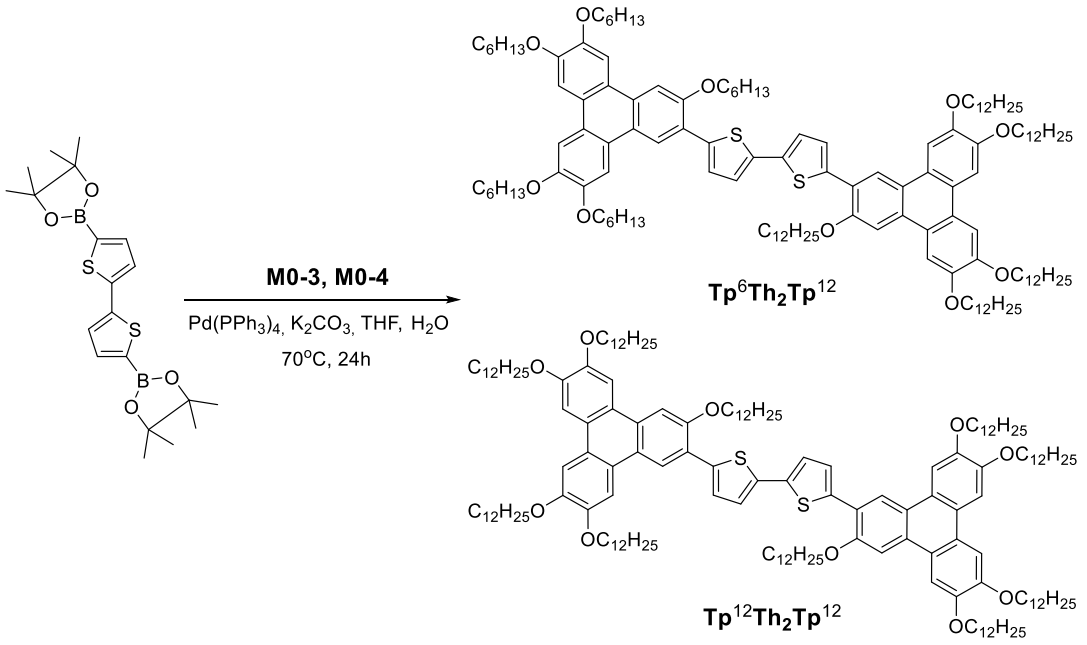

Scheme S12: Synthetic procedure of unsymmetrical **Tp^{6}Th$_2$Tp^{12}**.

2.8. Synthesis of the non-bridged dimers Tp^{6}Tp^6 by Suzuki cross-coupling (Schemes S13)

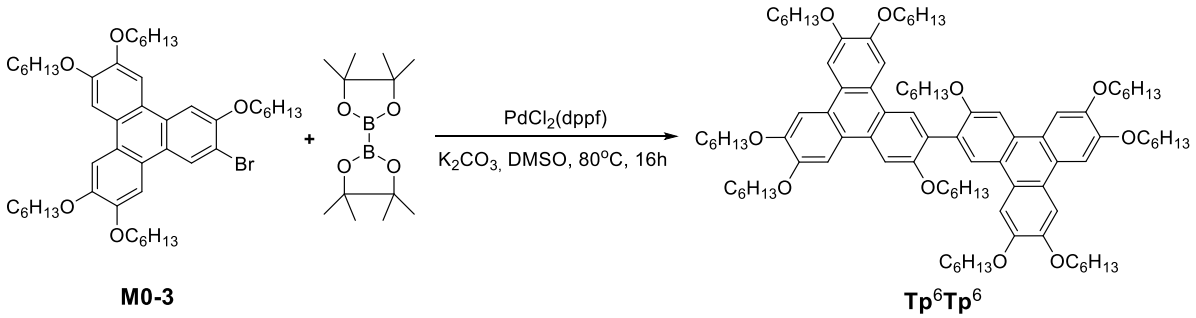

Scheme S13: Synthetic procedure of **Tp^{6}Tp^6**.

Tp^{6}Tp^6: A dry flask with an argon atmosphere was charged with **M0-3** (400.0 mg, 0.495 mmol), bis(pinacolato)diboron (68.9 mg, 0.248 mmol), $PdCl_2$(dppf) (14.5 mg, 4.0 mol %), K_2CO_3 (205.3 mg, 1.49 mmol), 4.0 mol % of dppf (11.0 mg) were added. After addition of 10 mL of DMSO, the reaction was stirred at 80°C for 16h. The reaction mixture was cooled to room temperature and extracted with CH_2Cl_2, dried over $MgSO_4$, evaporated and the residue purified by column chromatography (eluent light petroleum/dichloromethane, 1/1.5, v/v). Recrystallized from EtOAc-EtOH to get a white solid **Tp^{6}Tp^6** (256.2 mg, 71%).[5] ^{1}H NMR ($CDCl_3$, TMS, 600MHz) δ (ppm): 8.47 (s, 2H), 8.00 (s, 2H), 7.93 (s, 2H), 7.92 (s, 2H), 7.88 (s, 4H), 4.28 (t, *J* = 6.3 Hz, 8H), 4.24 (m, 4H), 4.18 (m, 4H), 4.14 (m, 4H), 2.00-1.91 (m, 12H), 1.89-1.84 (m, 4H), 1.72-1.68 (m, 4H), 1.63-1.58 (m, 12H), 1.52-1.47 (m, 4H), 1.45-1.38 (m, 24H), 1.34-1.28 (m, 12H), 1.20-1.11 (m, 8H), 0.96-0.92 (m, 18H), 0.85 (t, *J* = 7.0 Hz, 6H), 0.72 (t, *J* = 7.1 Hz, 6H). ^{13}C NMR ($CDCl_3$, 151 MHz) δ (ppm): 156.02, 149.70, 149.37, 148.71, 148.54, 129.64, 128.54, 126.23, 124.82, 124.24, 123.37, 122.90, 122.60, 107.96, 107.69, 106.92, 106.30, 104.41, 69.96, 69.87, 69.48, 69.16, 68.77, 31.70, 31.68, 31.59, 31.53, 29.44, 29.40, 29.35, 29.30, 25.87, 25.82, 25.76, 22.66, 22.65, 22.55, 22.48, 14.06, 13.96, 13.88. HRMS (MALDI): $[M]^+$ calcd for $C_{96}H_{142}O_{10}$, m/z: 1456.0637 (100.0%), 1455.0603 (96.3%), 1457.0670 (51.4%), 1458.0704 (17.0%); found, 1456.0621, 1455.0572, 1457.0663, 1458.0703. Elemental analysis: calculated for $C_{96}H_{142}O_{10}$ (1455.0603), C 79.18%, H 9.83%; found, C 78.86%, H 9.85%.

3. ^{1}H, ^{13}C and ^{19}F NMR

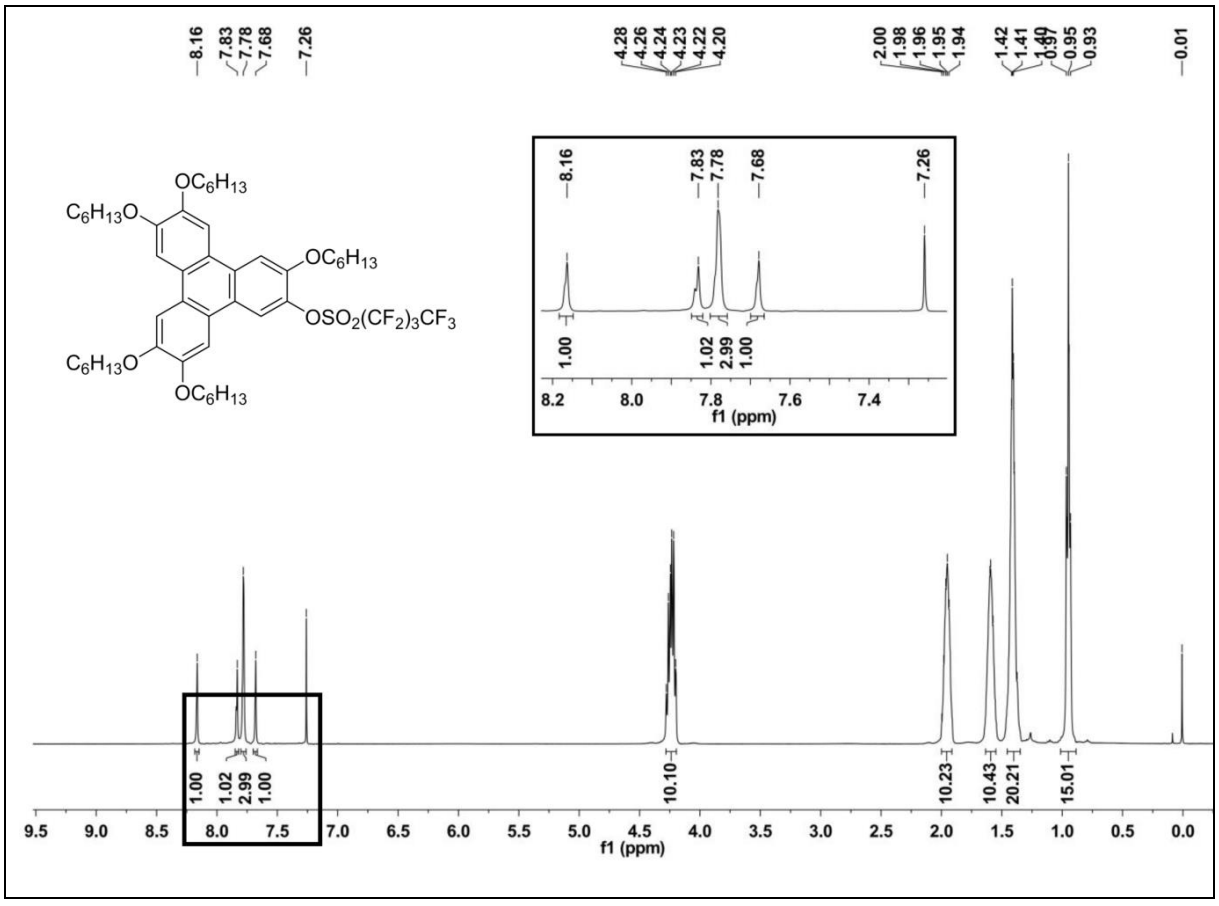

[5] C. F. Nising, U. K. Schmid, M. Nieger, S. Bräse. A New Protocol for the One-Pot Synthesis of Symmetrical Biaryls. *J. Org. Chem.,* 2004, 69, 6830-6833.

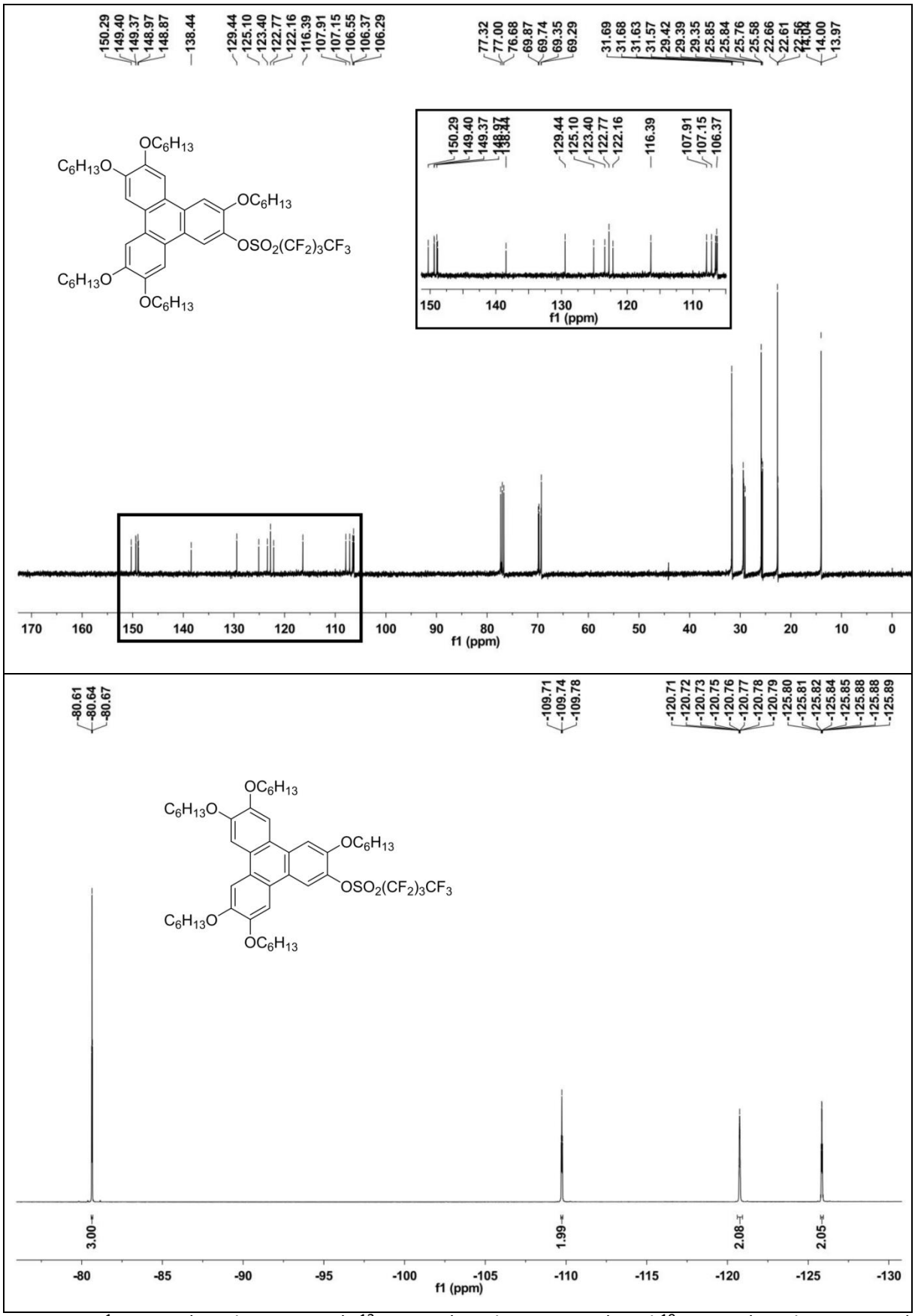

Figure S1. ^{1}H NMR ($CDCl_3$, 400MHz), ^{13}C NMR ($CDCl_3$, 100 MHz) and ^{19}F NMR ($CDCl_3$, 376 MHz) spectra of **M0-1**.

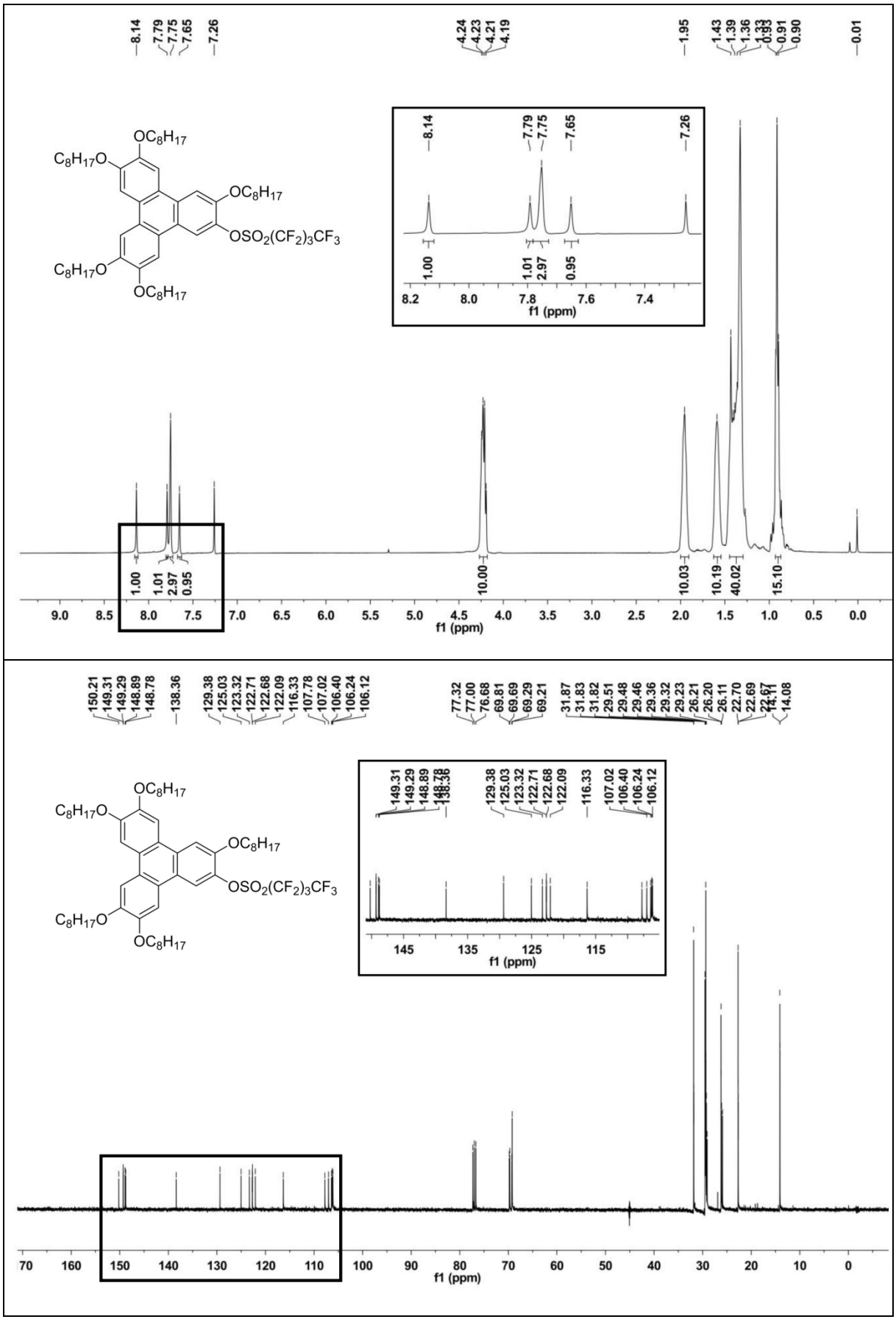
8.14
7.79
7.75
7.65
7.26
4.24
4.23
4.21
4.19
1.95
1.43
1.39
1.36
1.33
0.91
0.90
0.01
OC8H17
C8H17O
OC8H17
OSO2(CF2)3CF3
C8H17O
OC8H17
1.00
1.01
2.97
0.95
10.00
10.03
10.19
40.02
15.10
f1 (ppm)
150.21
149.31
149.29
148.89
148.78
138.36
129.38
125.03
123.32
122.71
122.68
122.09
116.33
107.78
107.02
106.40
106.24
106.12
77.32
77.00
76.68
69.81
69.69
69.29
69.21
31.87
31.83
31.82
29.51
29.48
29.46
29.36
29.32
29.23
26.21
26.20
26.11
22.70
22.69
14.08
f1 (ppm)

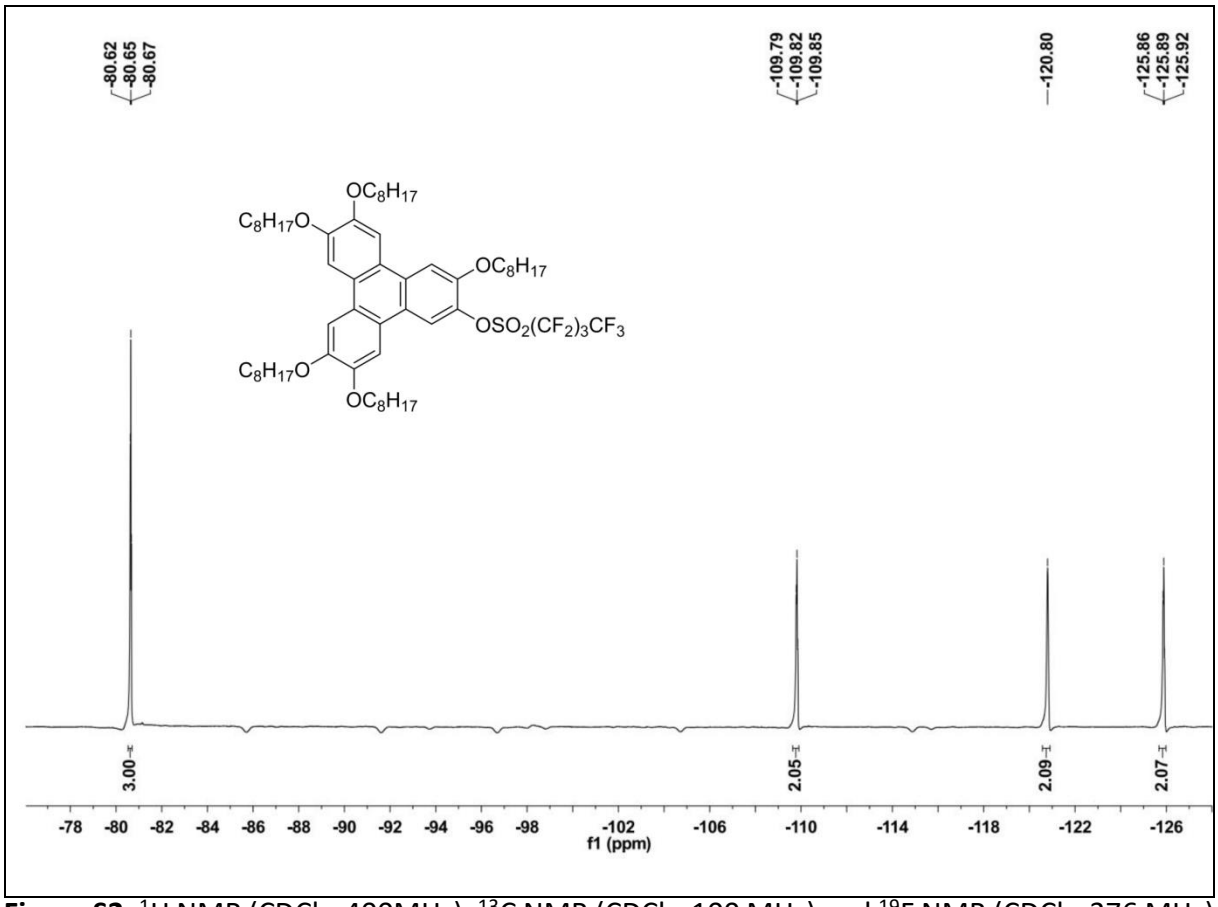

Figure S2. ^{1}H NMR ($CDCl_3$, 400MHz), ^{13}C NMR ($CDCl_3$, 100 MHz) and ^{19}F NMR ($CDCl_3$, 376 MHz) spectra of **M0-2**.

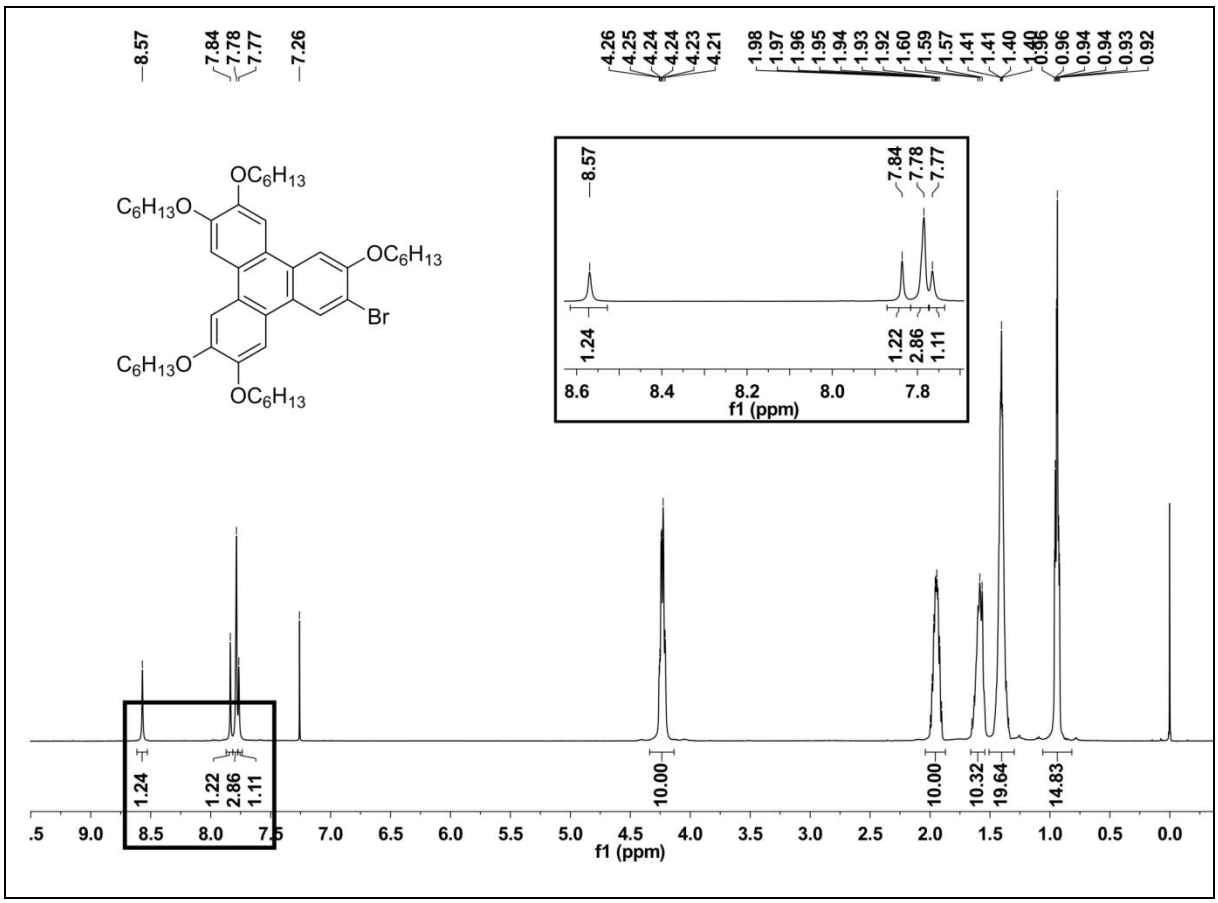

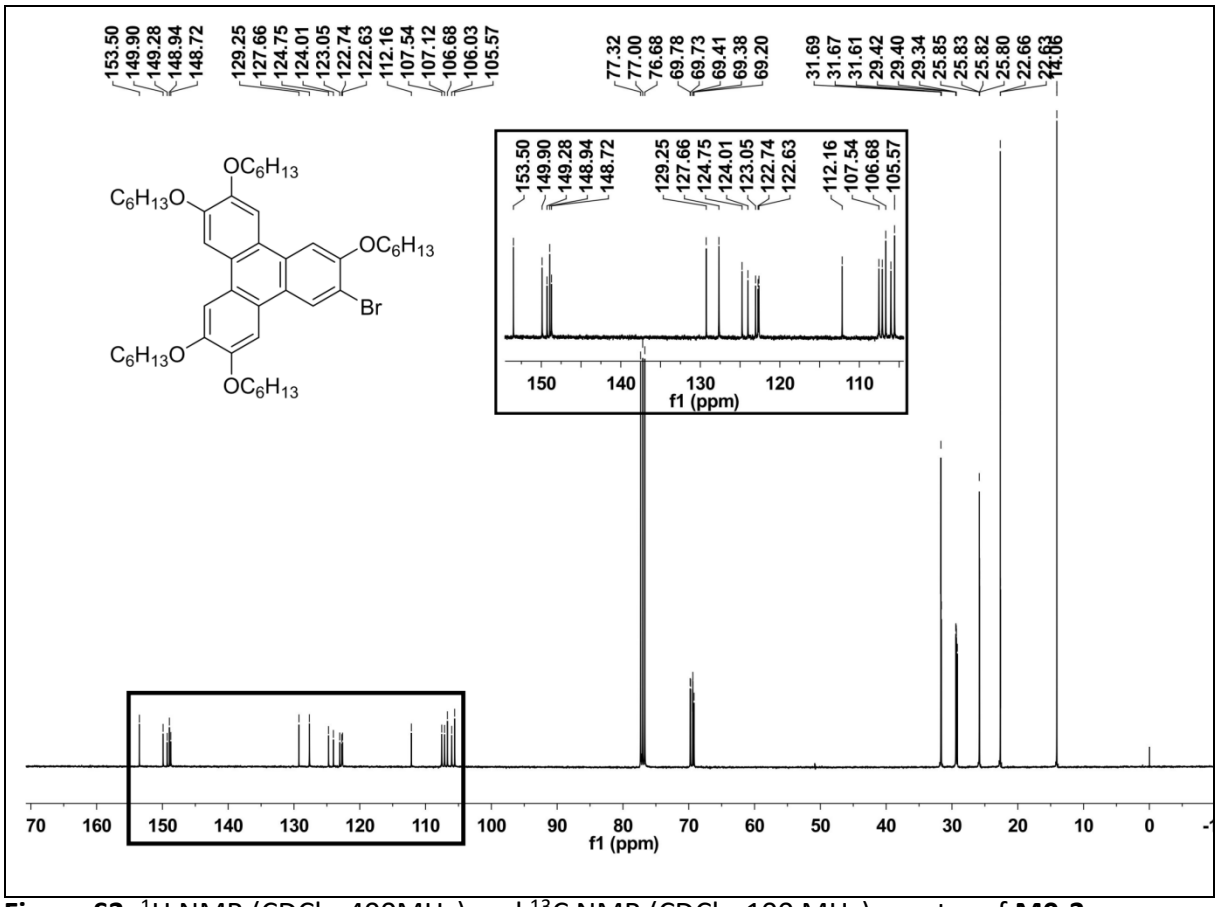

Figure S3. ^{1}H NMR ($CDCl_3$, 400MHz) and ^{13}C NMR ($CDCl_3$, 100 MHz) spectra of **M0-3**.

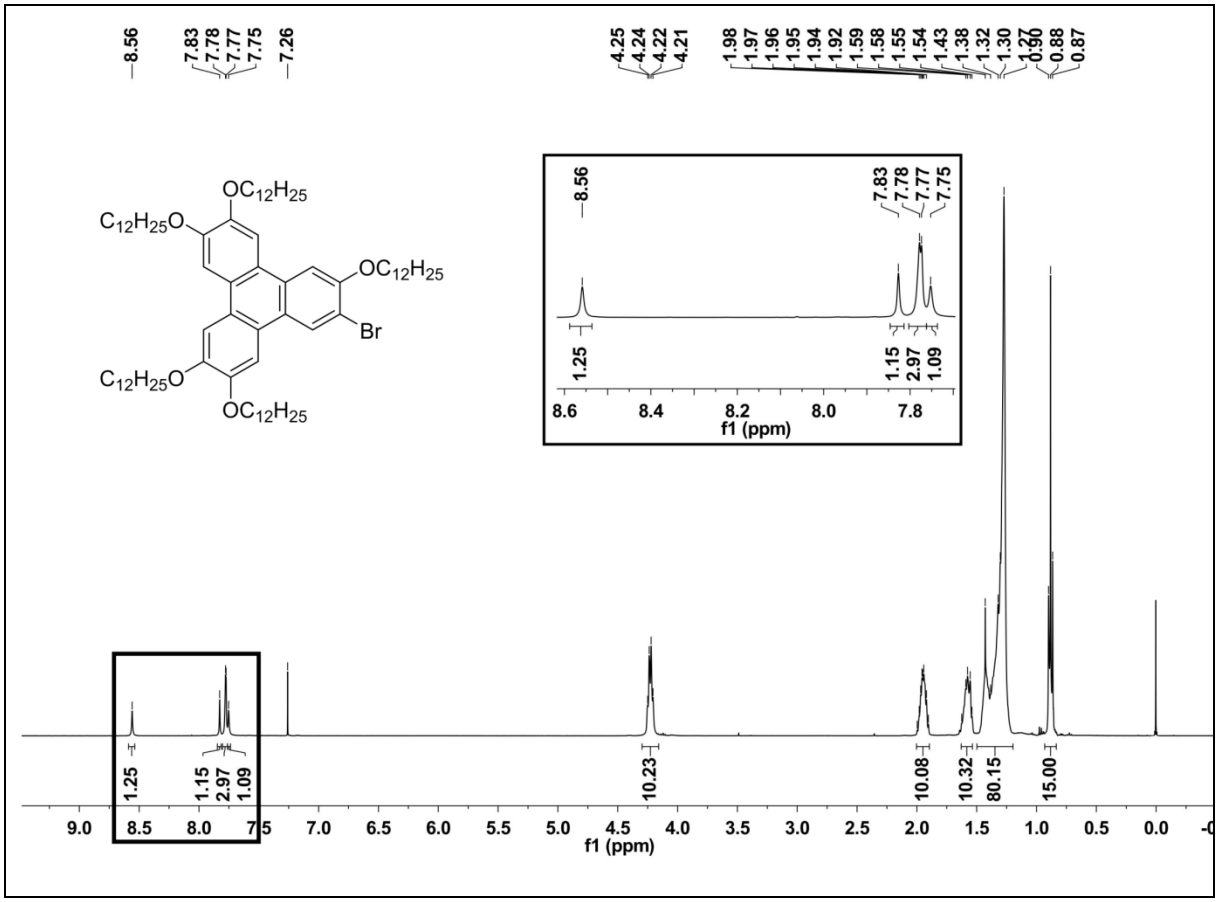

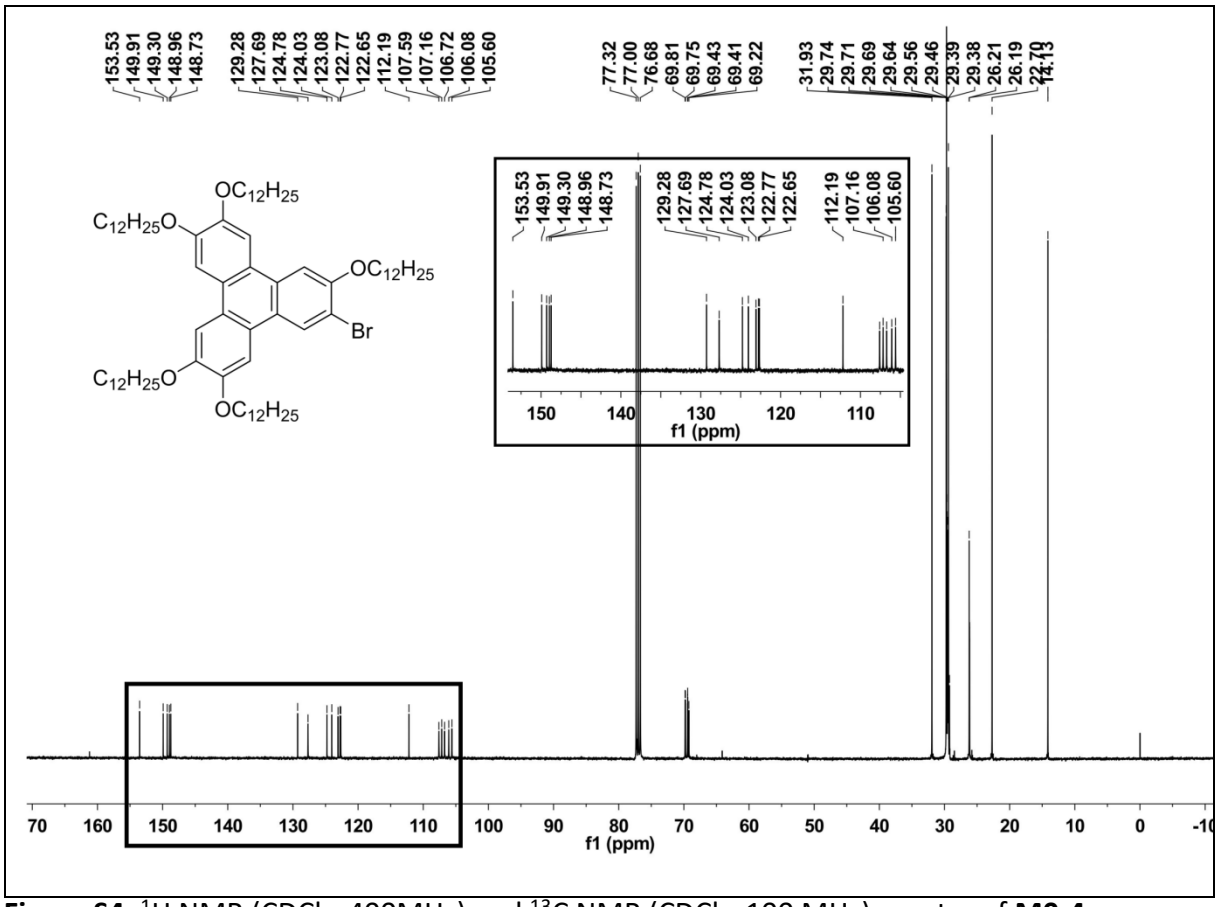

Figure S4. ^{1}H NMR ($CDCl_3$, 400MHz) and ^{13}C NMR ($CDCl_3$, 100 MHz) spectra of **M0-4**.

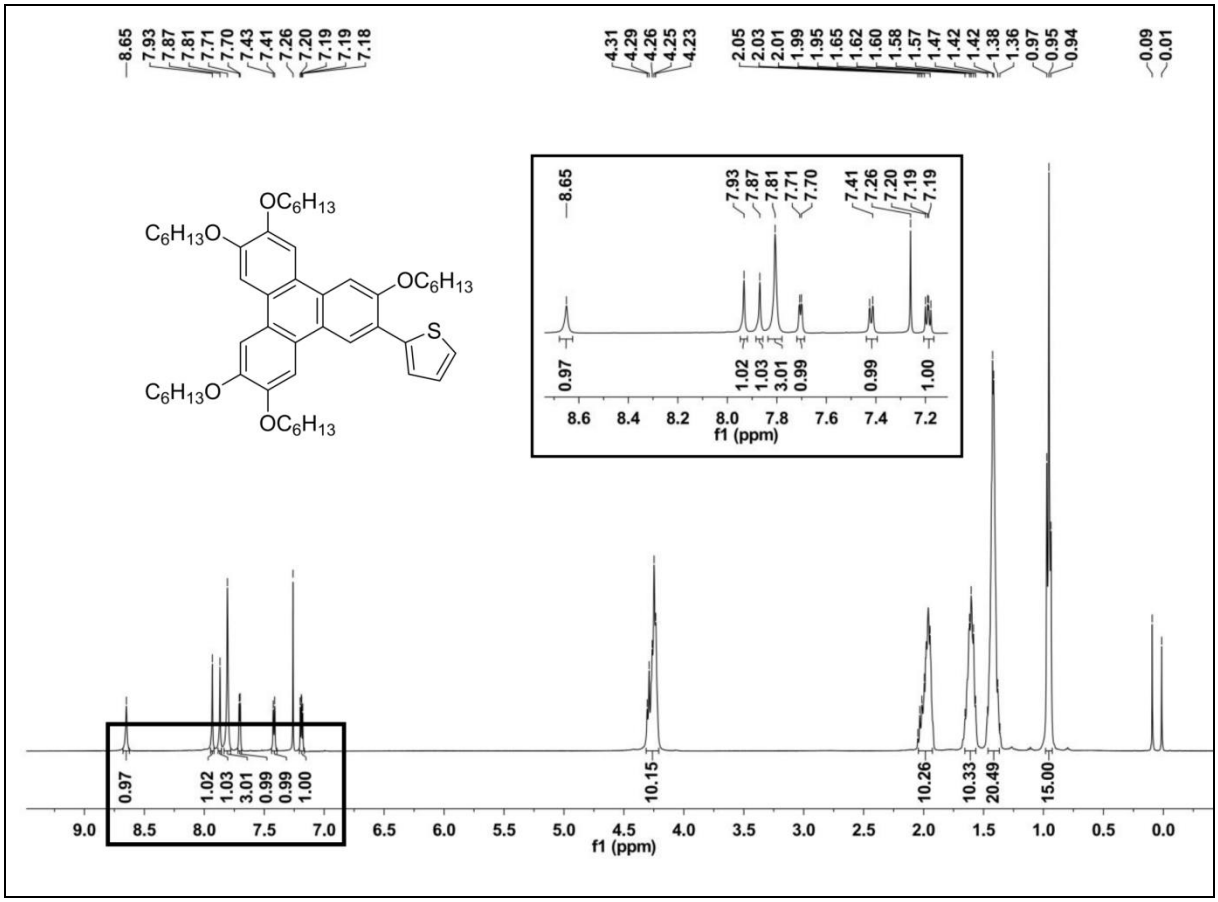

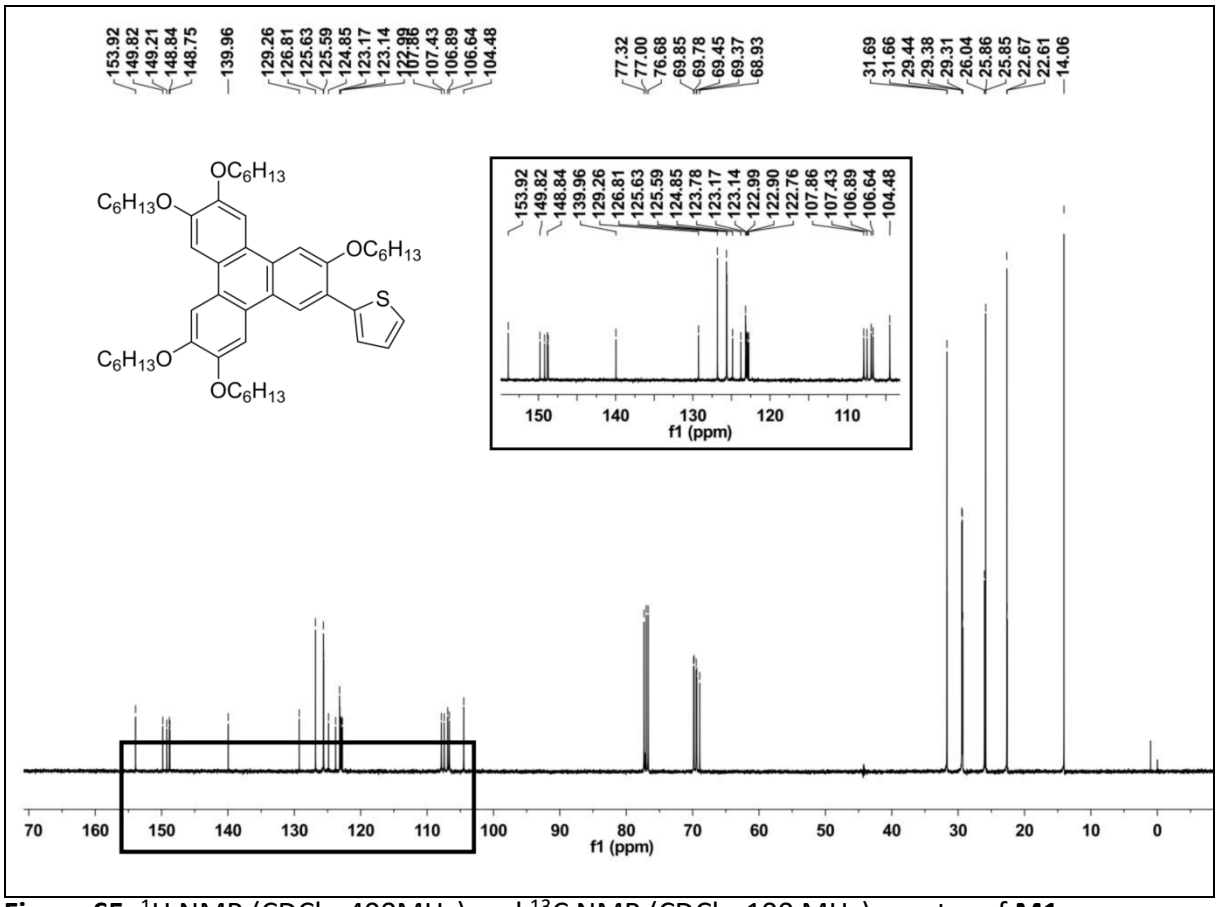

Figure S5. ^{1}H NMR ($CDCl_3$, 400MHz) and ^{13}C NMR ($CDCl_3$, 100 MHz) spectra of **M1**.

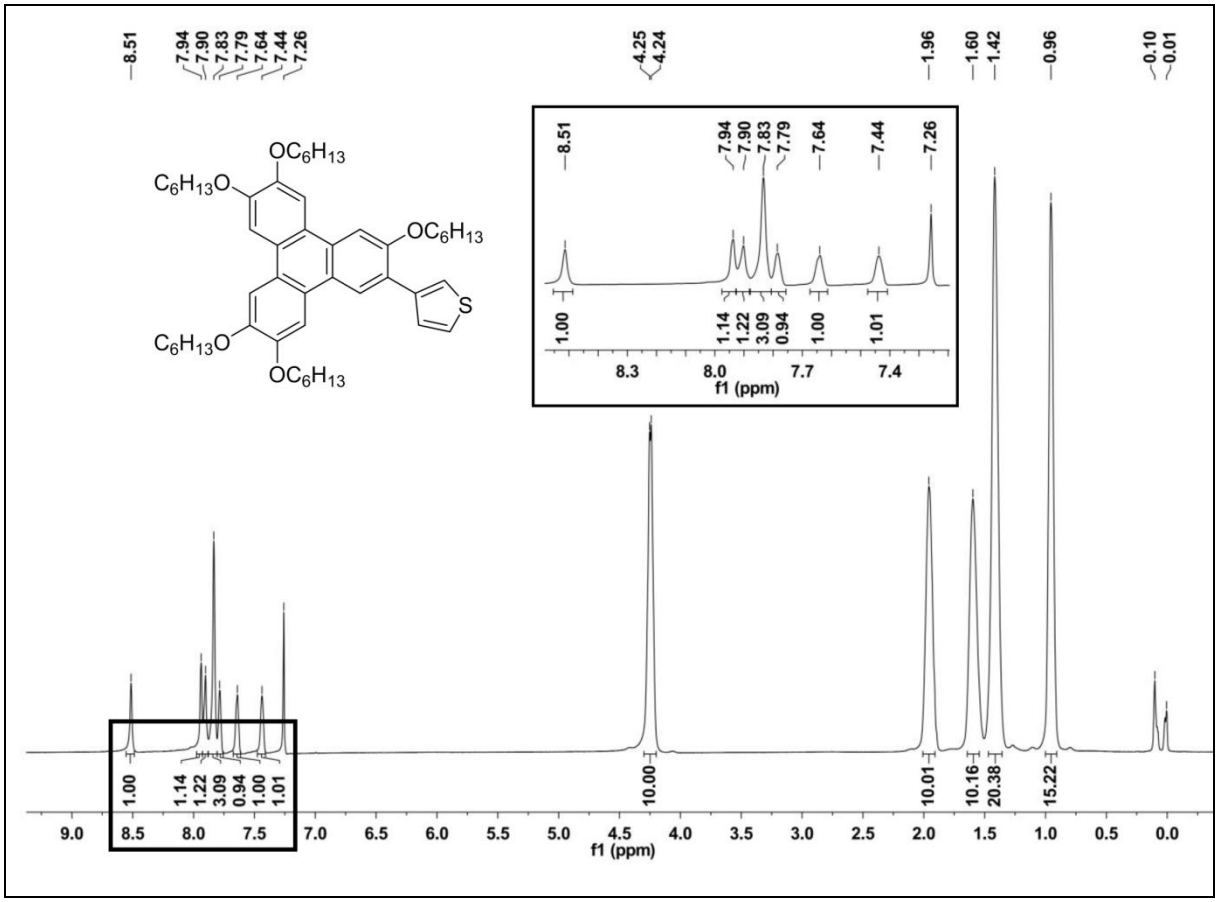

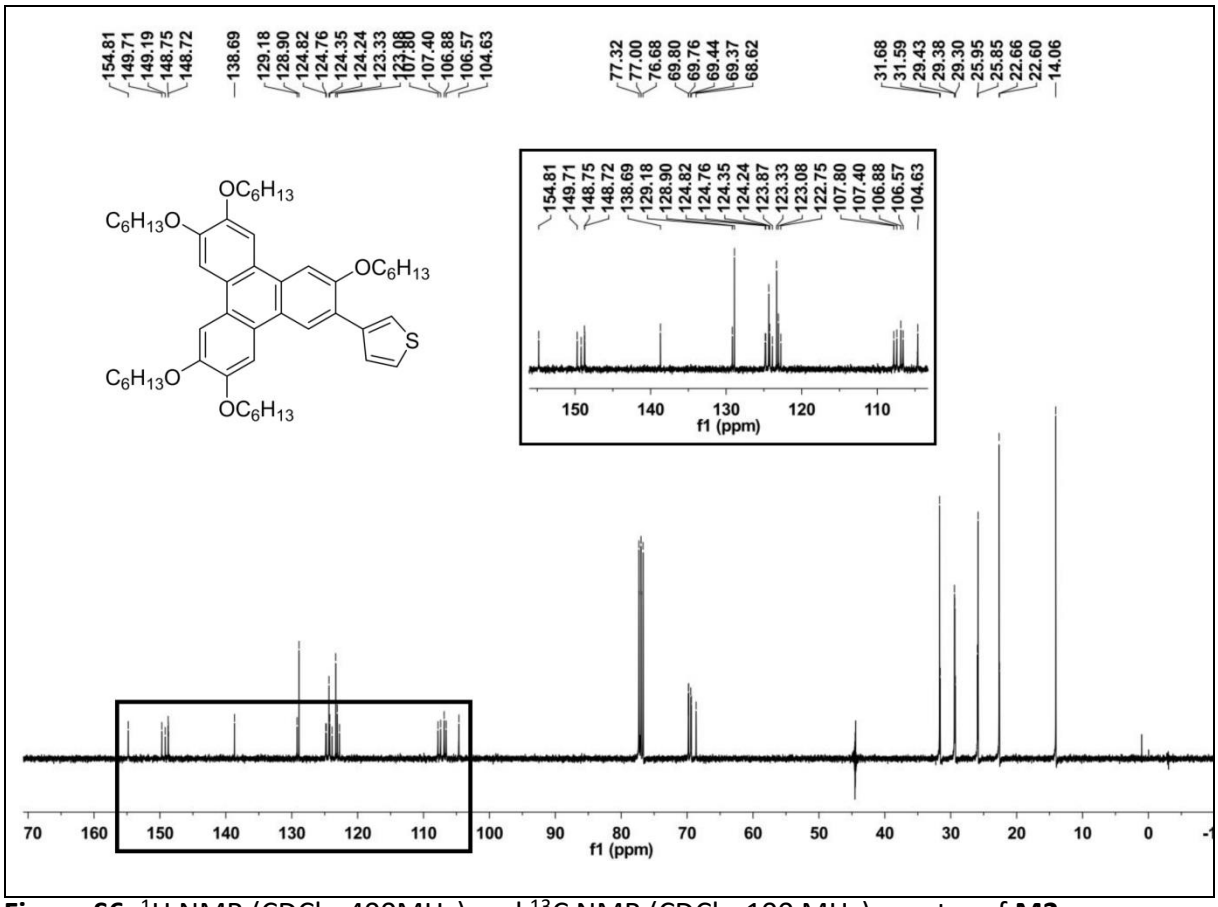

Figure S6. ^{1}H NMR ($CDCl_3$, 400MHz) and ^{13}C NMR ($CDCl_3$, 100 MHz) spectra of **M2**.

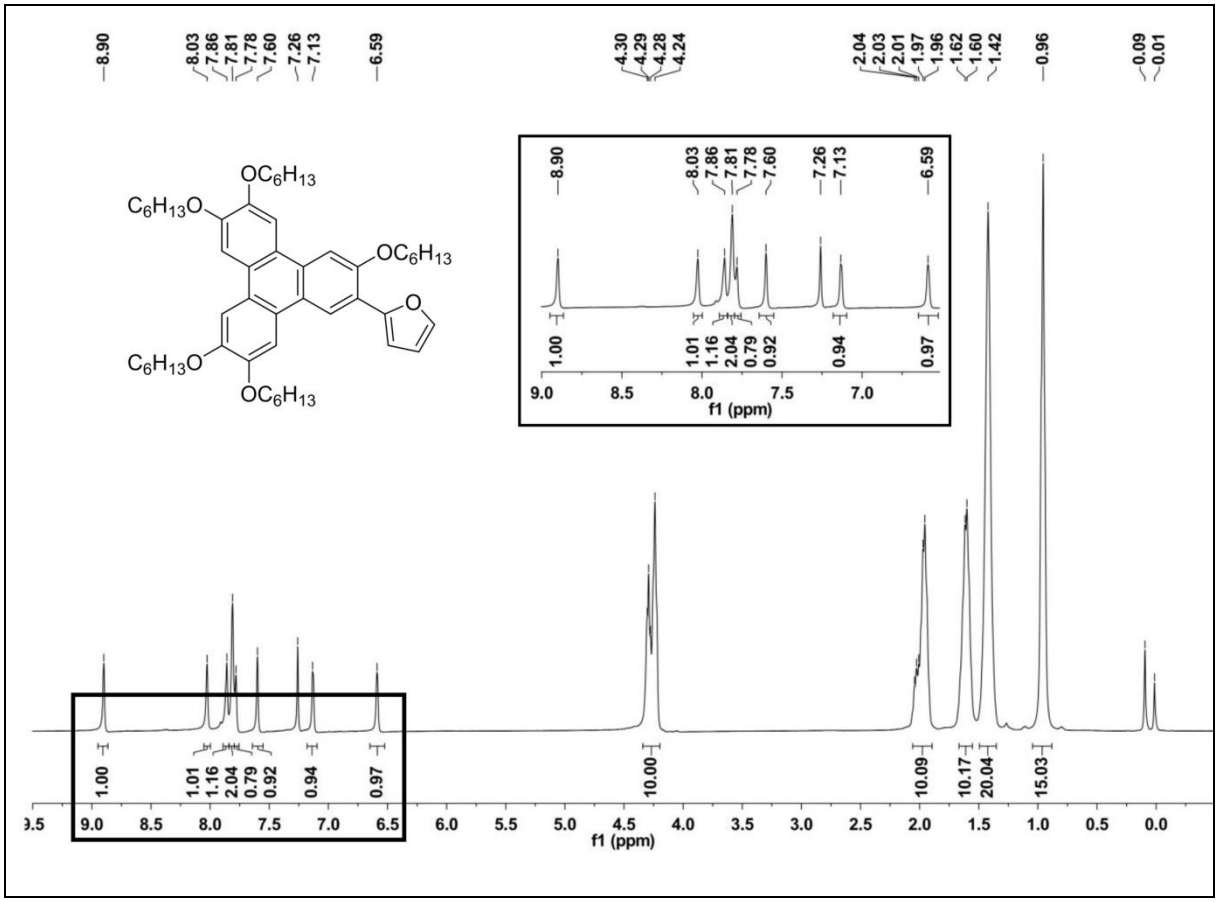

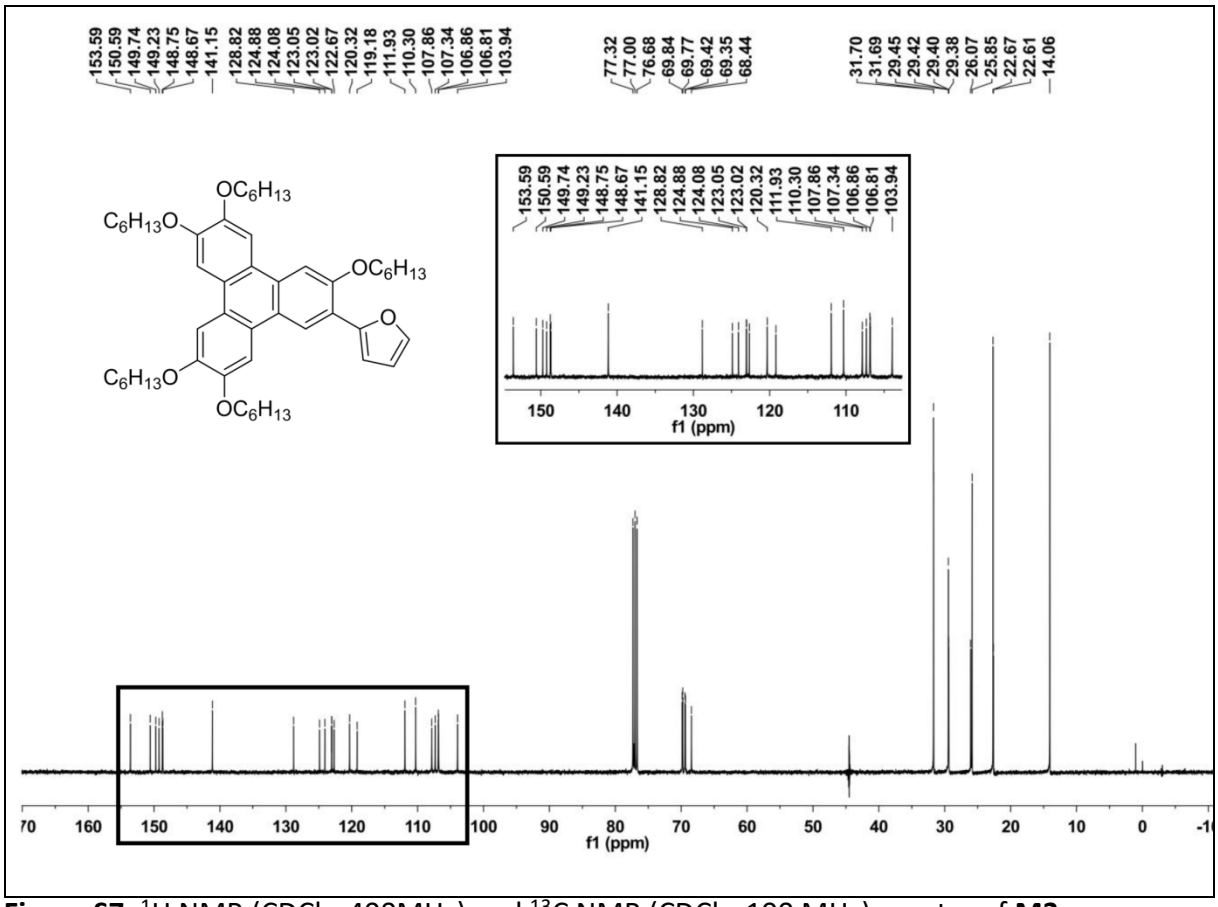

Figure S7. ^{1}H NMR ($CDCl_3$, 400MHz) and ^{13}C NMR ($CDCl_3$, 100 MHz) spectra of **M3**.

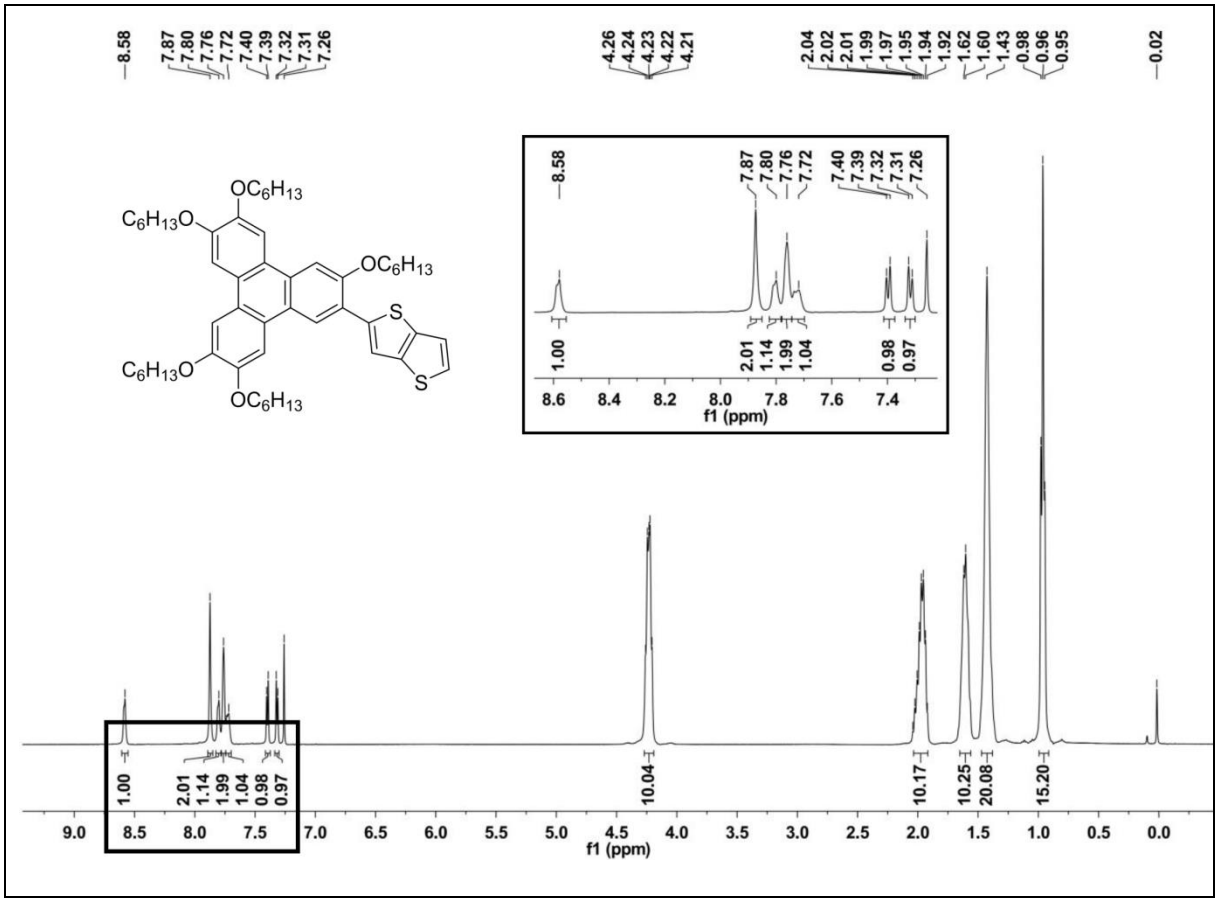

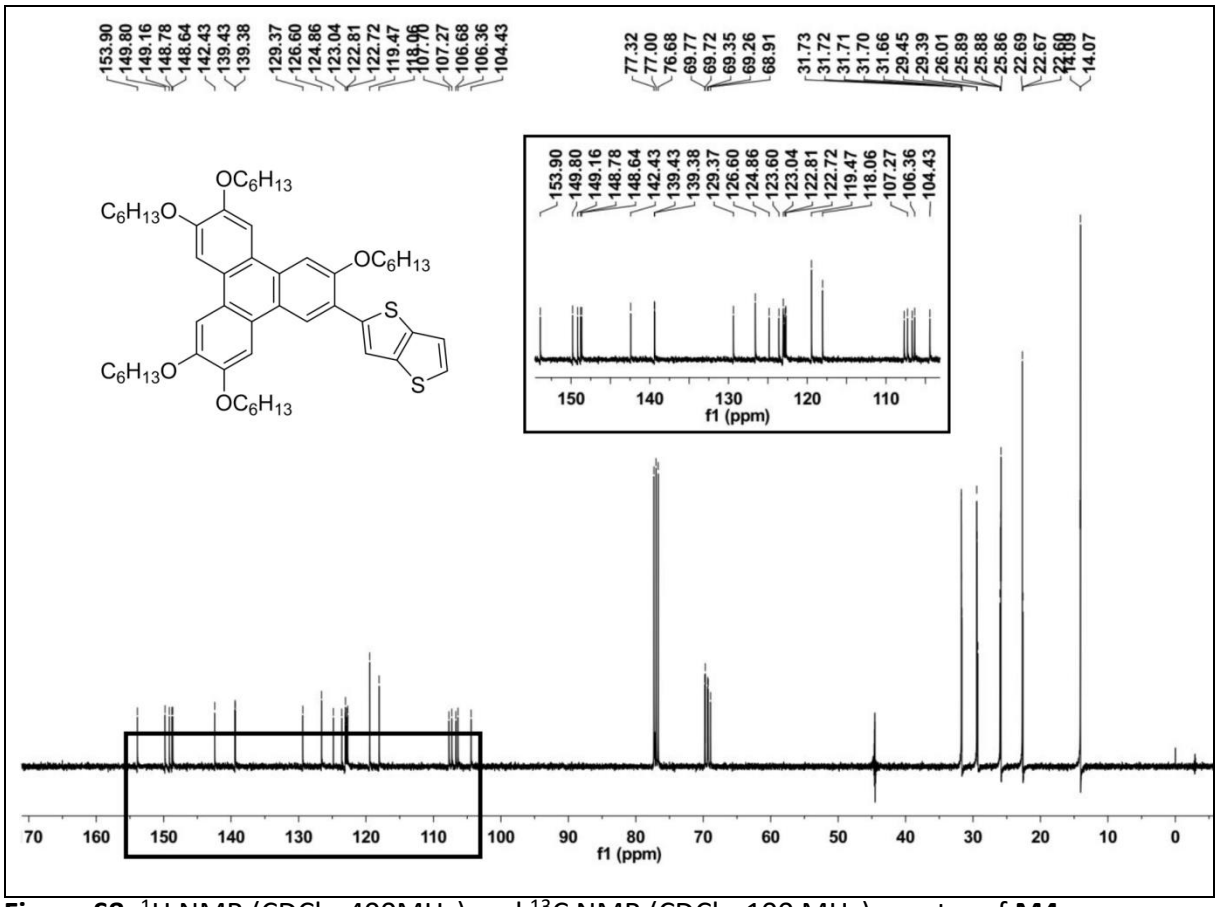

Figure S8. ^{1}H NMR ($CDCl_3$, 400MHz) and ^{13}C NMR ($CDCl_3$, 100 MHz) spectra of **M4**.

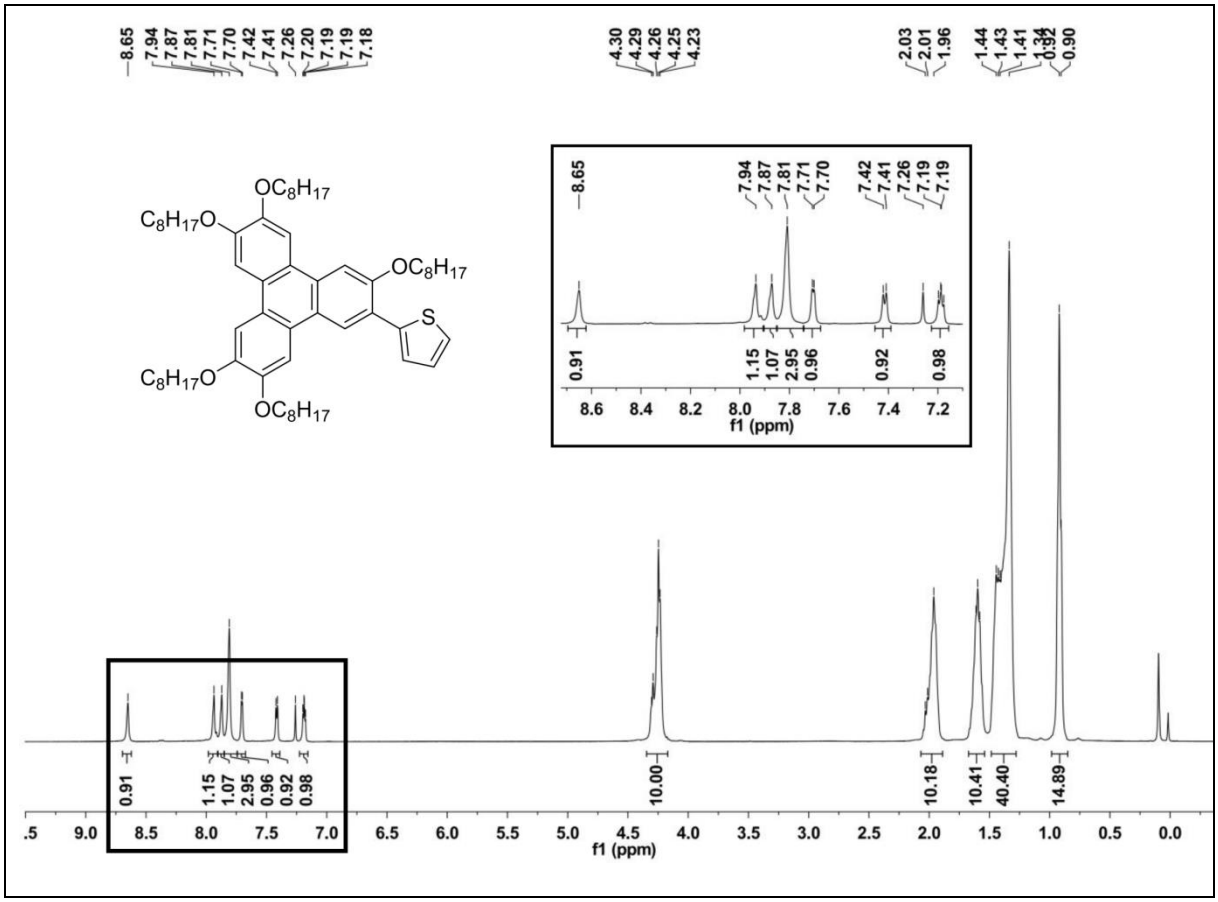

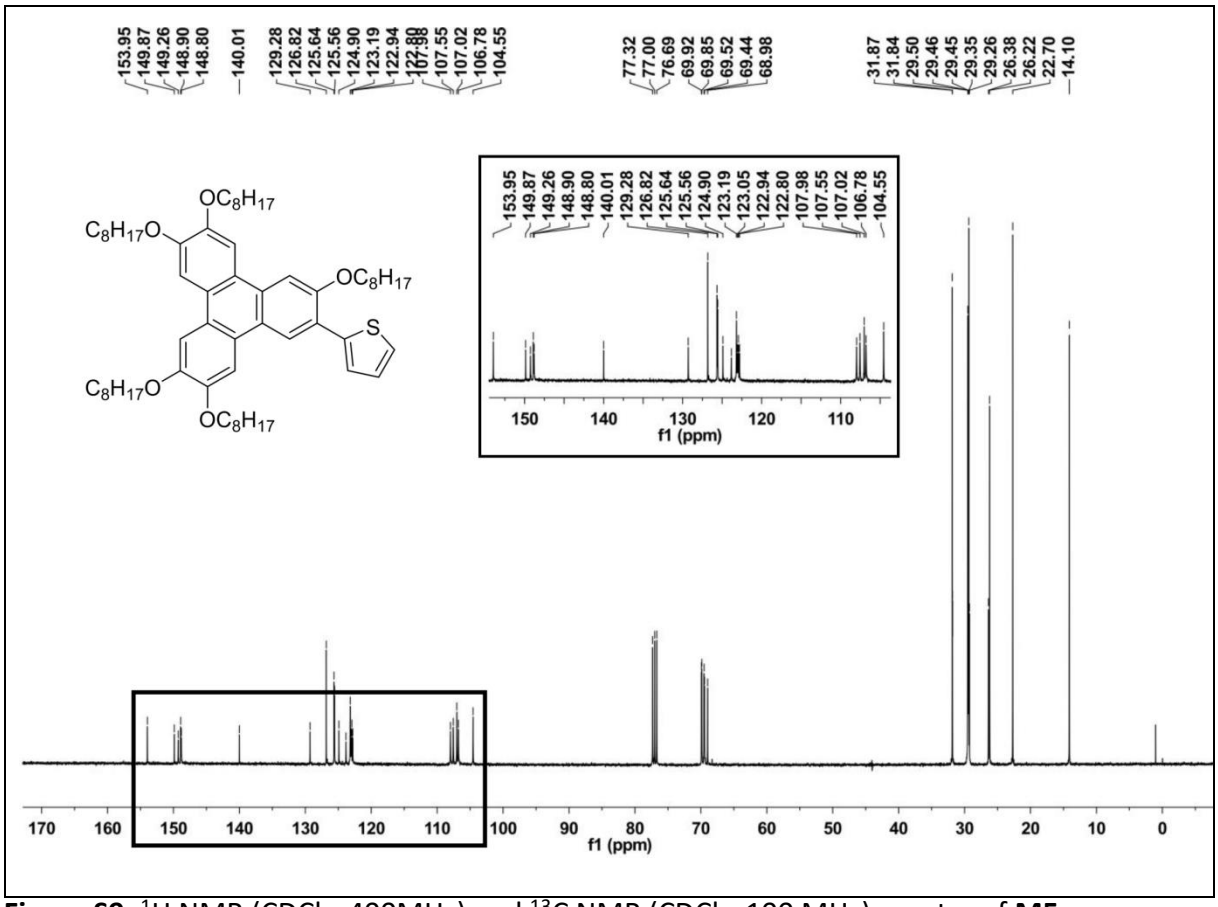

Figure S9. ^{1}H NMR ($CDCl_3$, 400MHz) and ^{13}C NMR ($CDCl_3$, 100 MHz) spectra of **M5**.

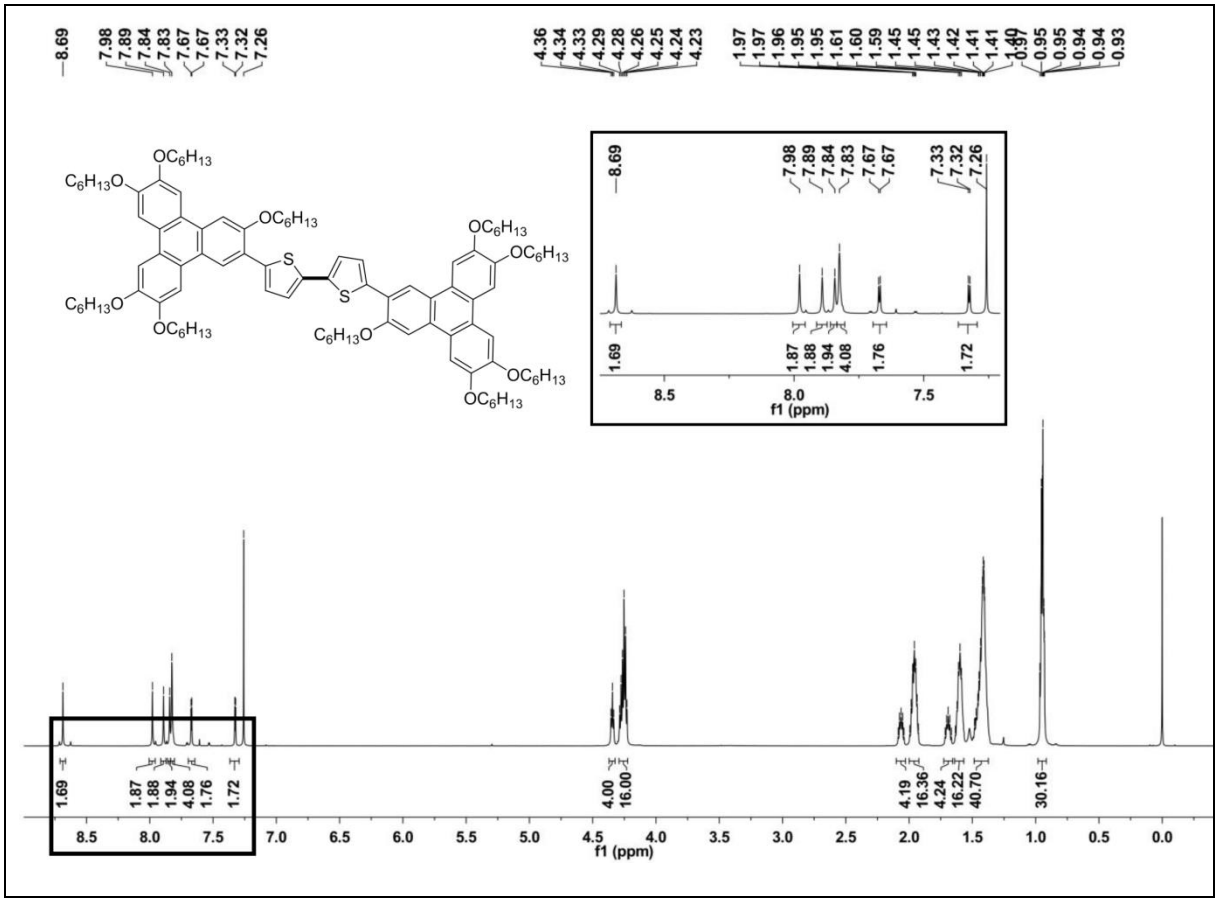

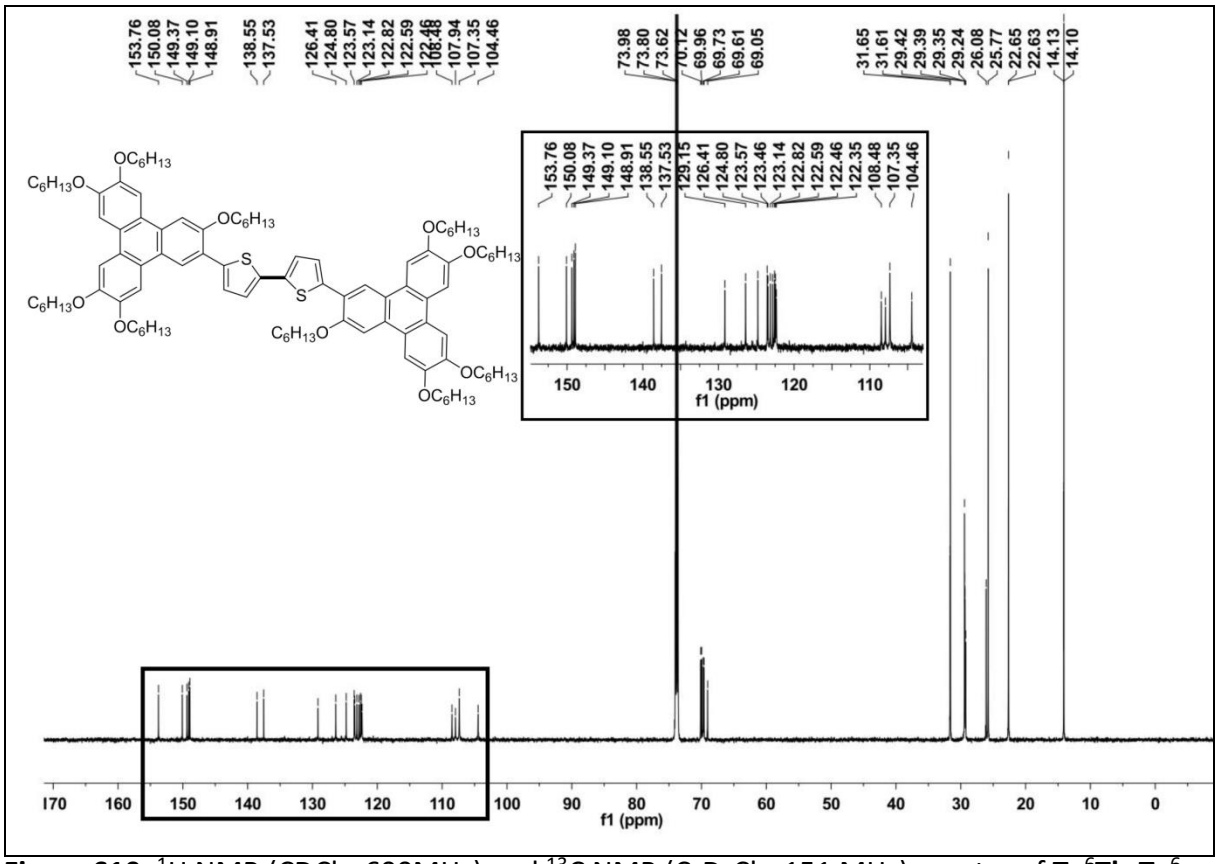

Figure S10. ^{1}H NMR ($CDCl_3$, 600MHz) and ^{13}C NMR ($C_2D_2Cl_4$, 151 MHz) spectra of **Tp^{6}Th$_2$Tp^{6}**.

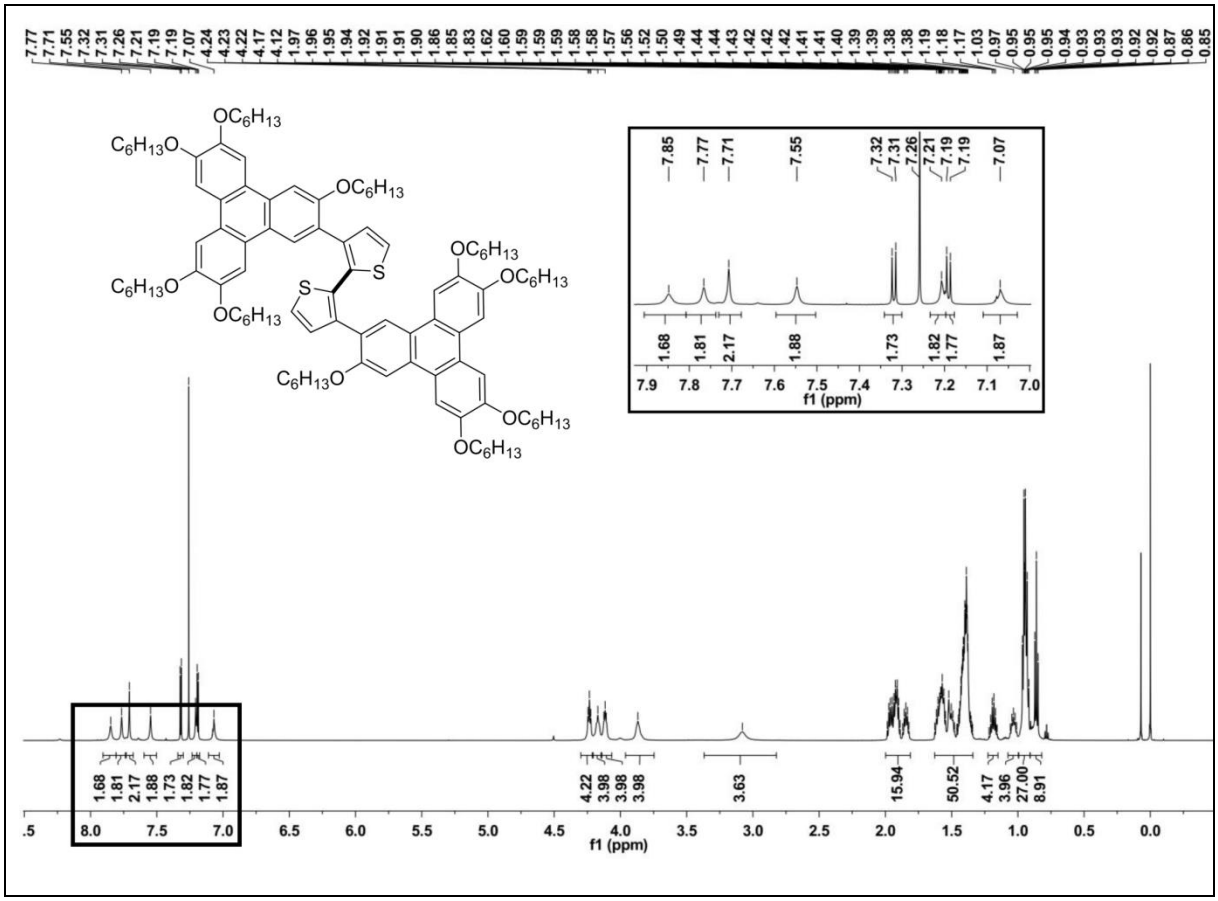

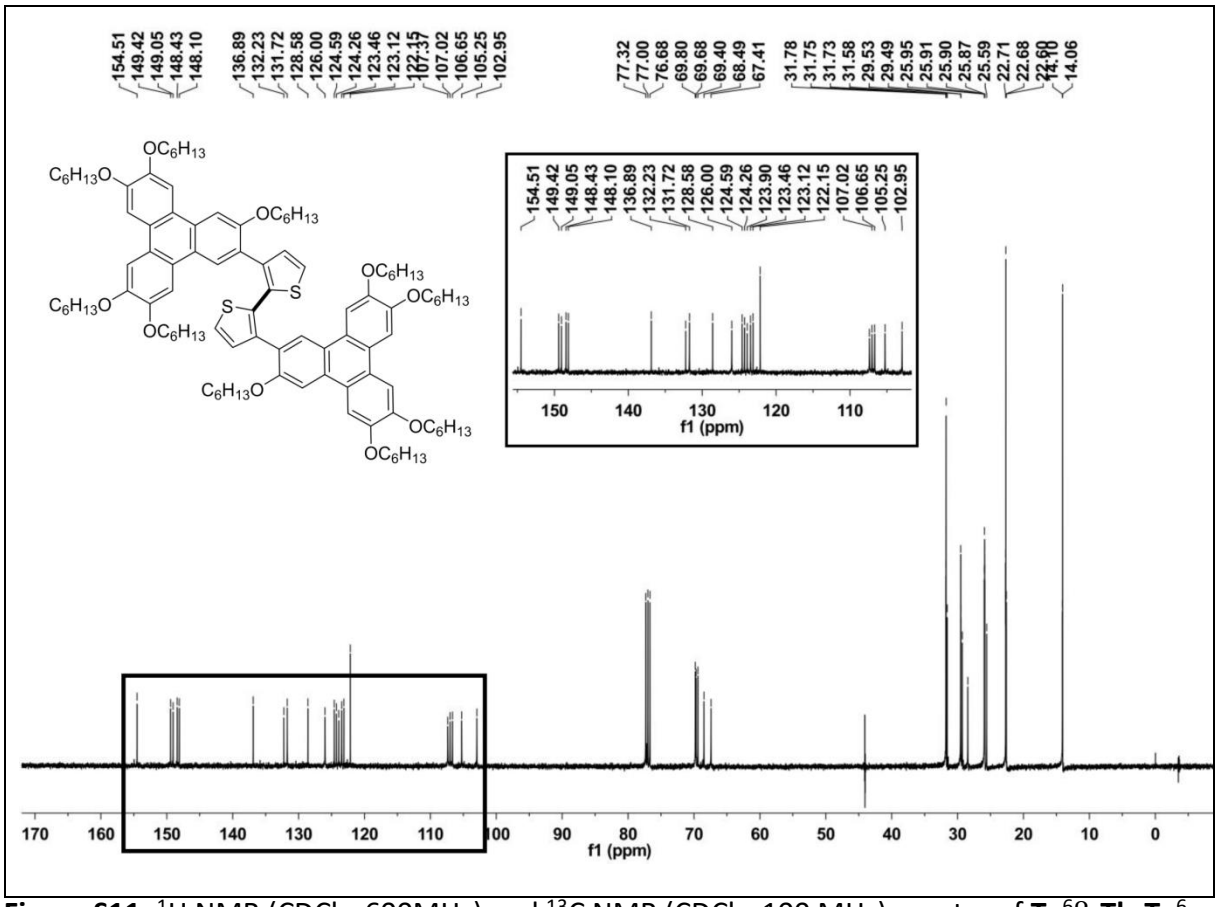

Figure S11. ^{1}H NMR ($CDCl_3$, 600MHz) and ^{13}C NMR ($CDCl_3$, 100 MHz) spectra of **Tp**$^{6}\beta$-**Th$_2$Tp**^{6}.

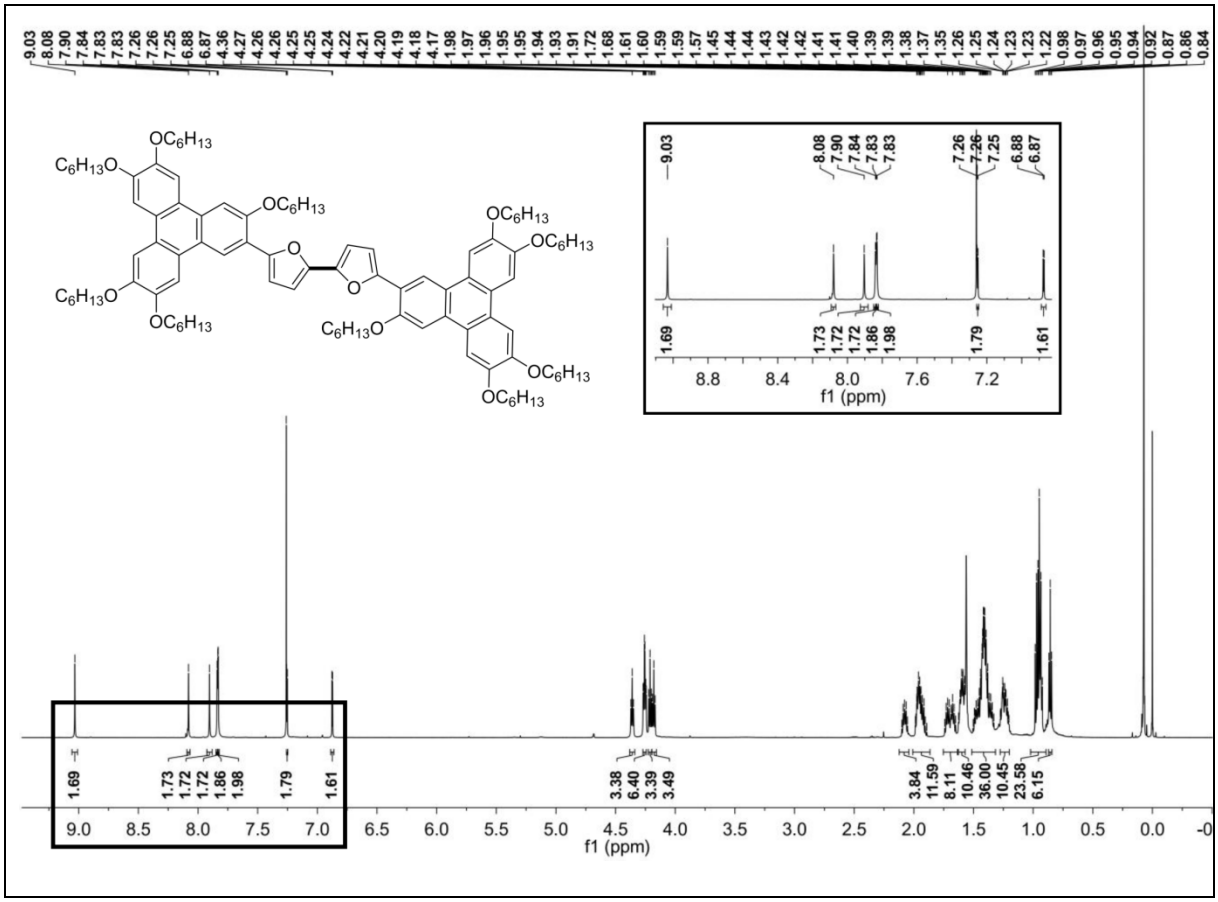

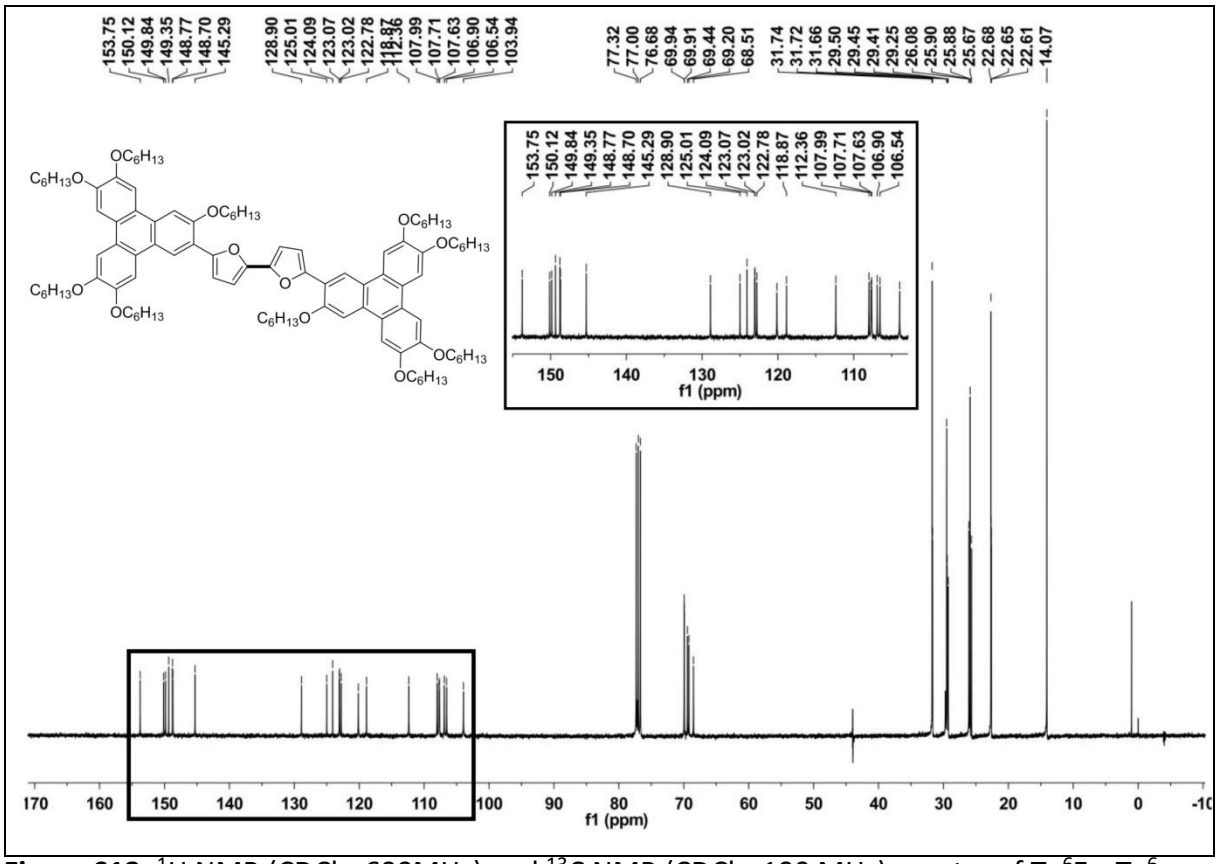

Figure S12. ^{1}H NMR ($CDCl_3$, 600MHz) and ^{13}C NMR ($CDCl_3$, 100 MHz) spectra of **Tp^{6}Fu$_2$Tp^{6}**.

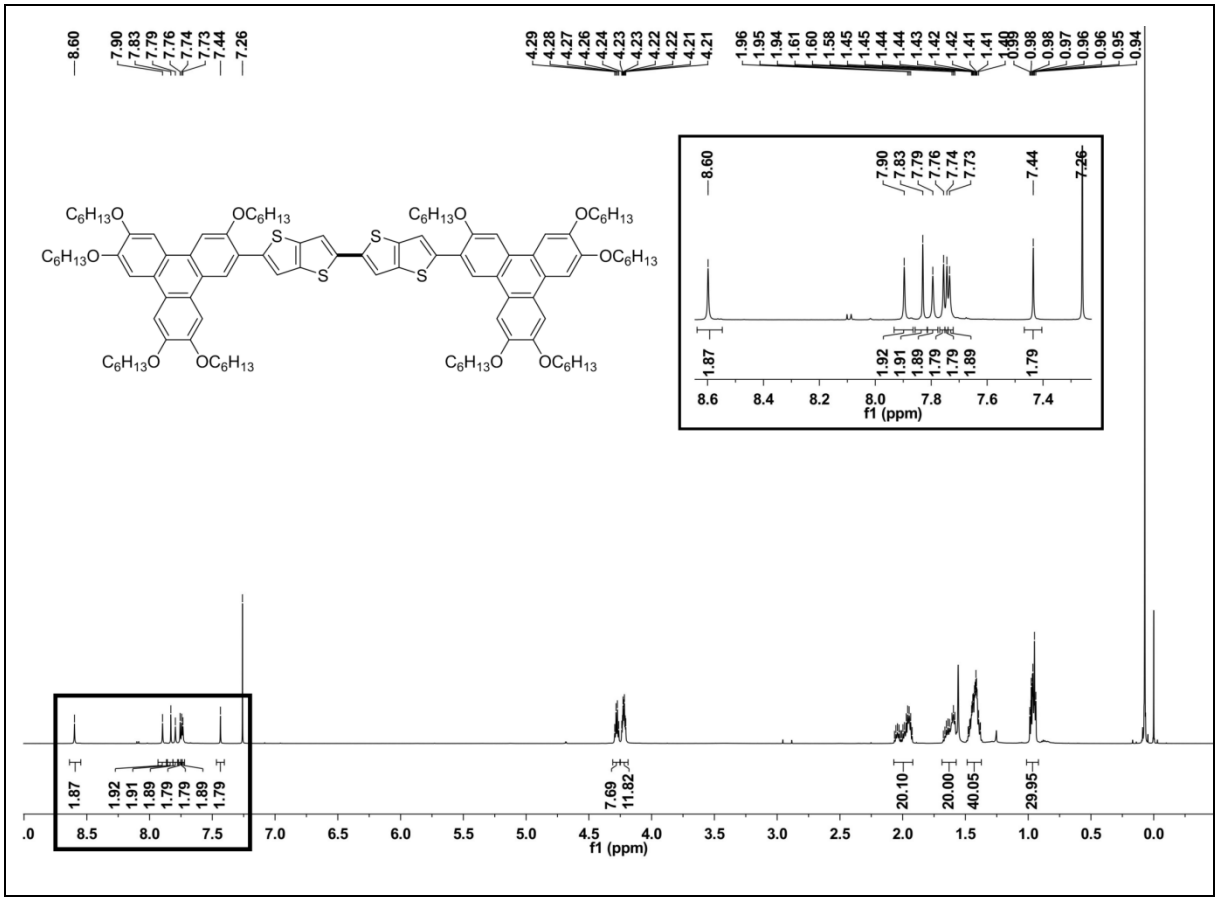

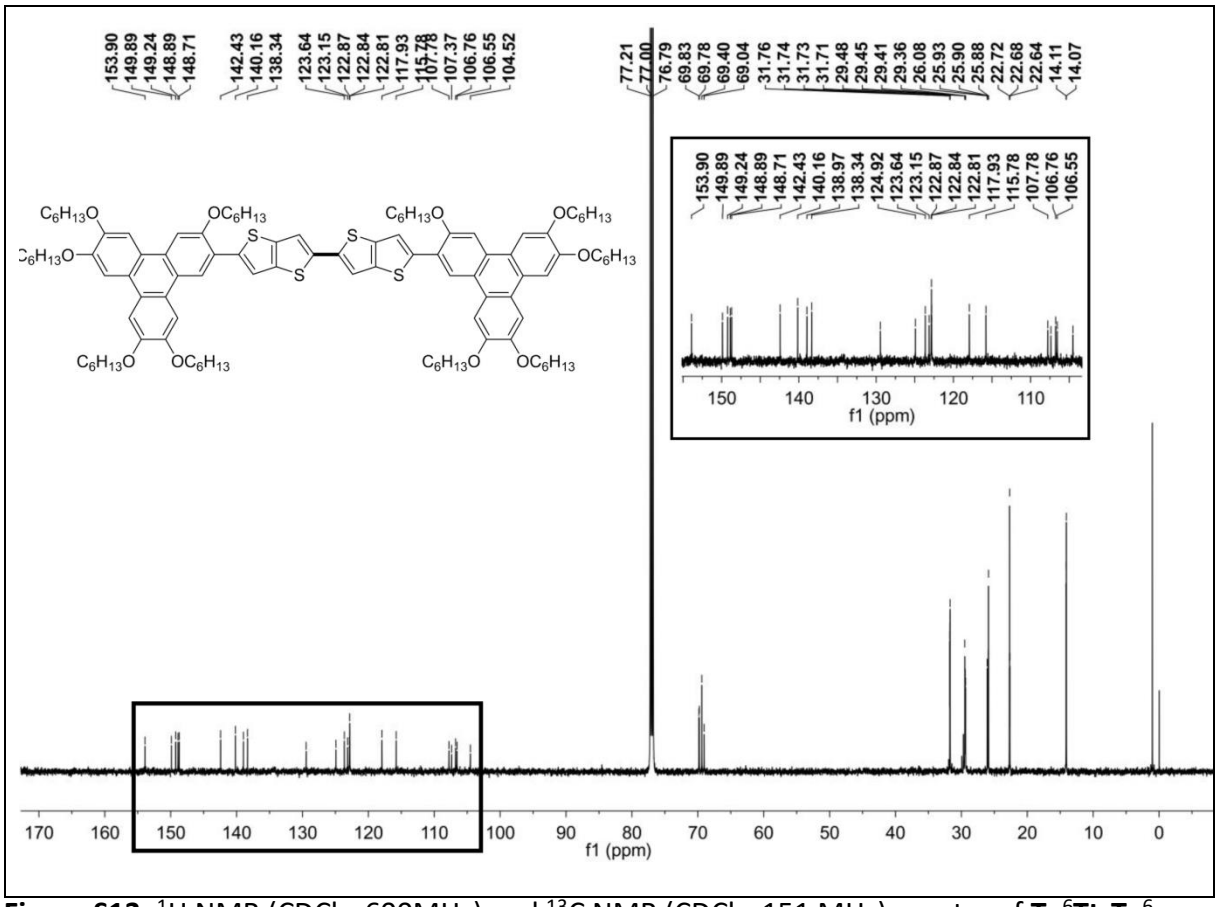

Figure S13. ^{1}H NMR ($CDCl_3$, 600MHz) and ^{13}C NMR ($CDCl_3$, 151 MHz) spectra of **Tp^{6}Tt$_2$Tp^{6}**.

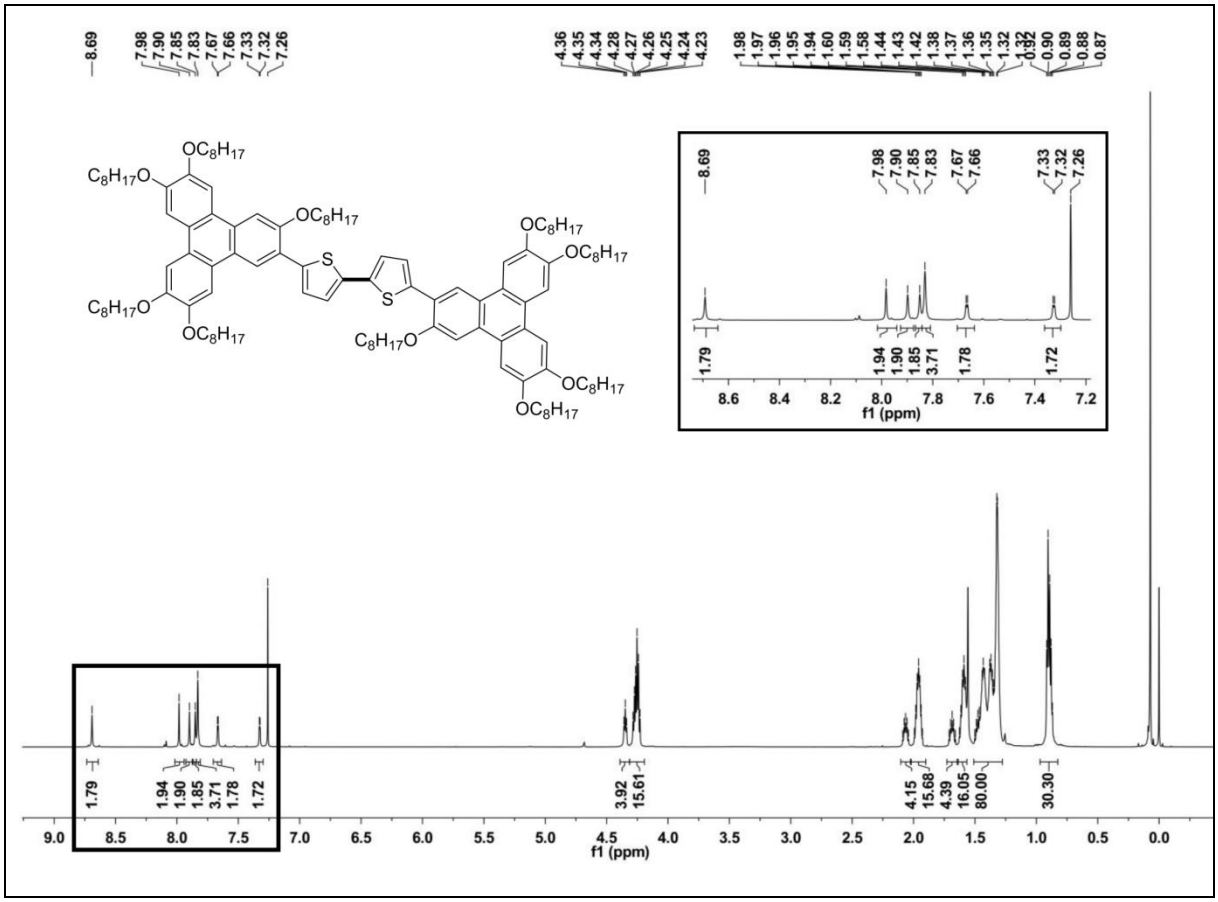

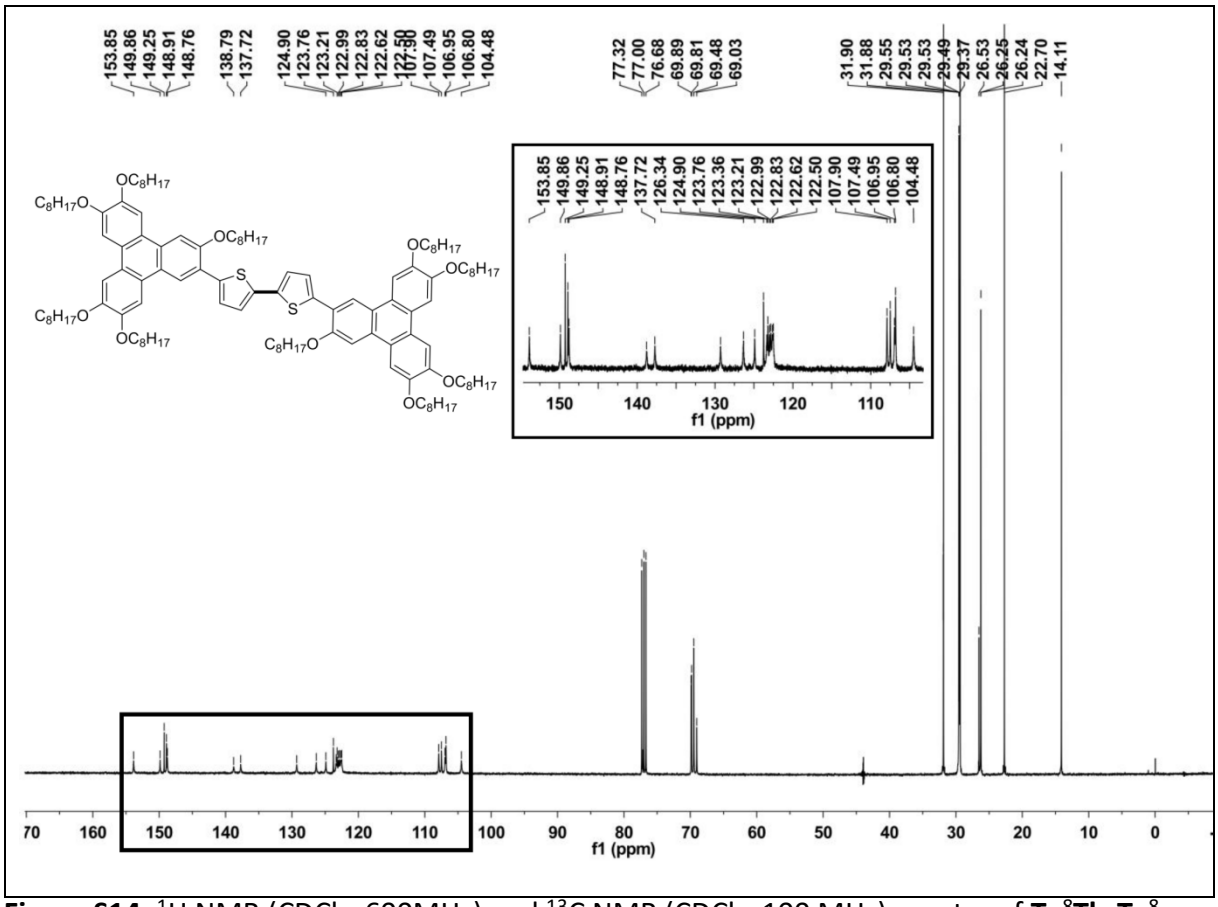

Figure S14. ^{1}H NMR ($CDCl_3$, 600MHz) and ^{13}C NMR ($CDCl_3$, 100 MHz) spectra of **Tp^{8}Th$_2$Tp^{8}**.

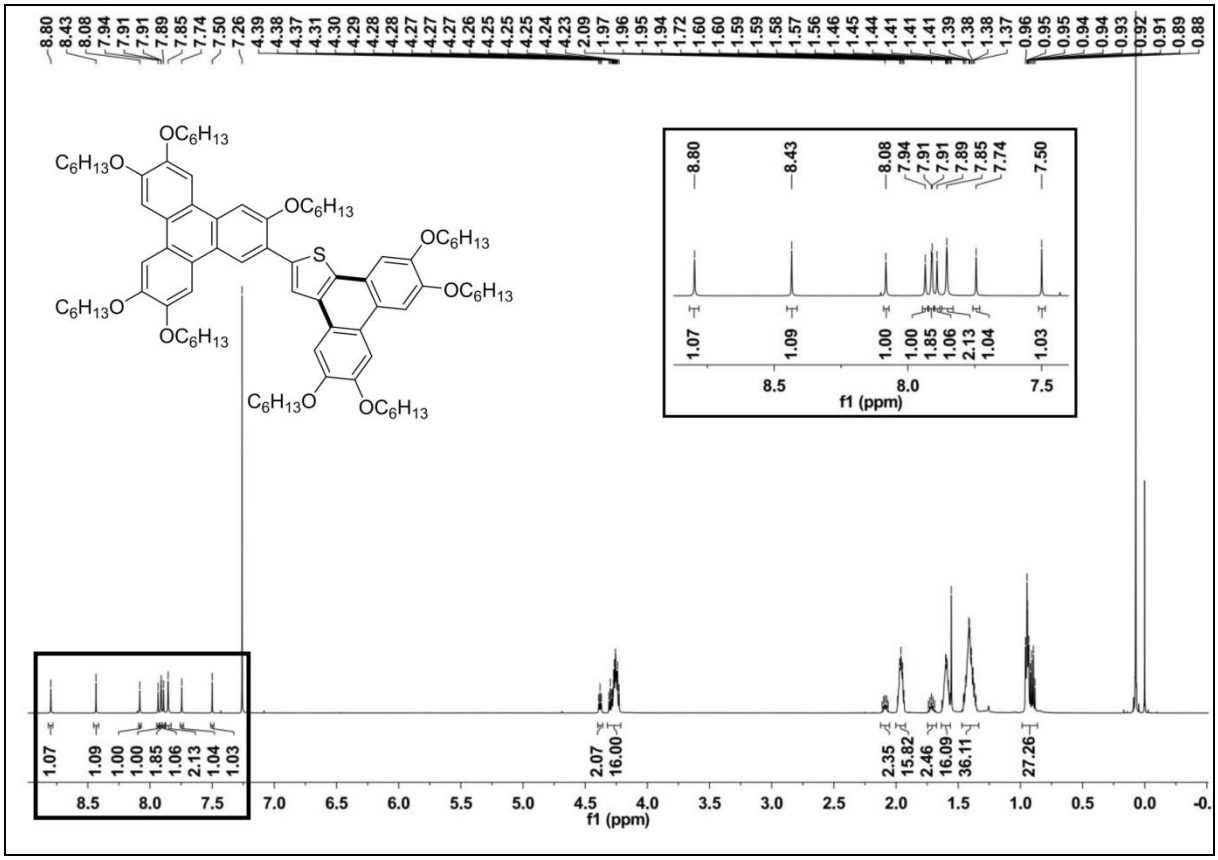

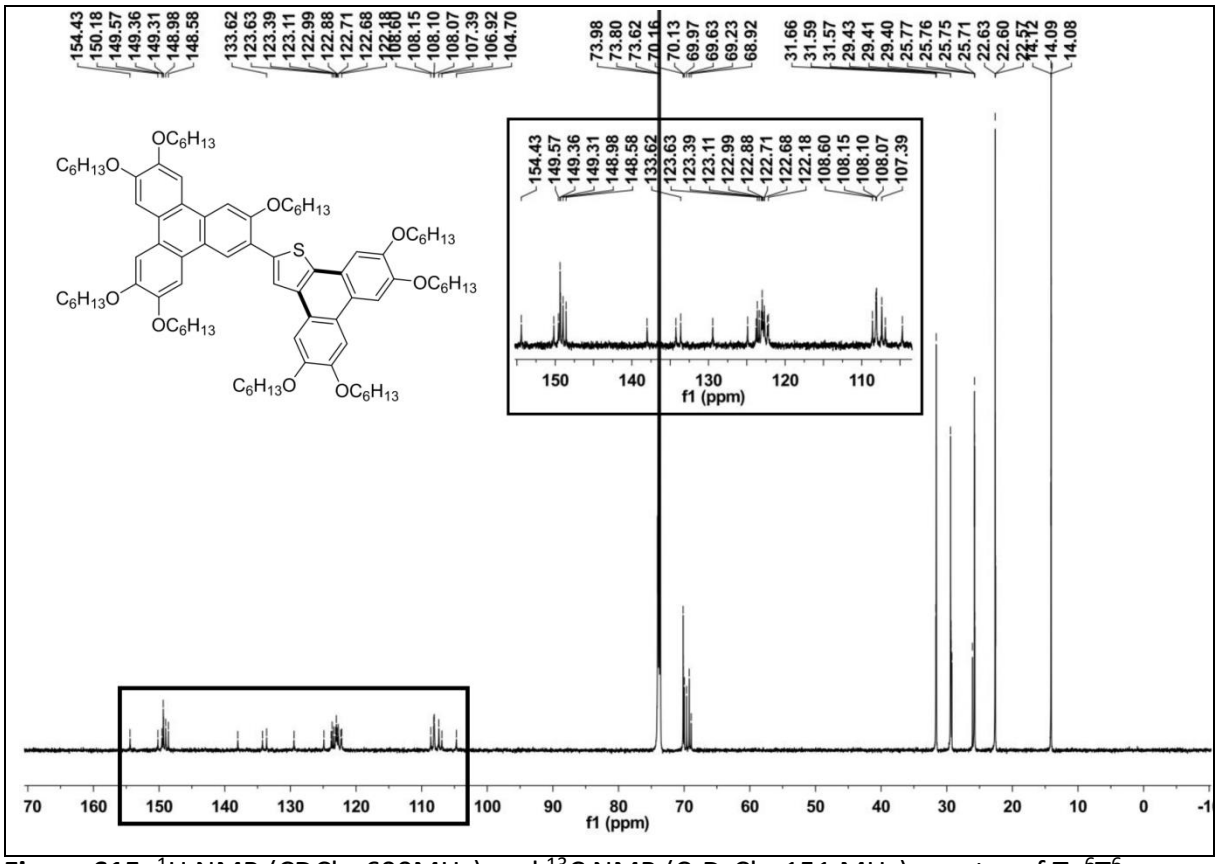

Figure S15. ^{1}H NMR ($CDCl_3$, 600MHz) and ^{13}C NMR ($C_2D_2Cl_4$, 151 MHz) spectra of **Tp^{6}T^{6}**.

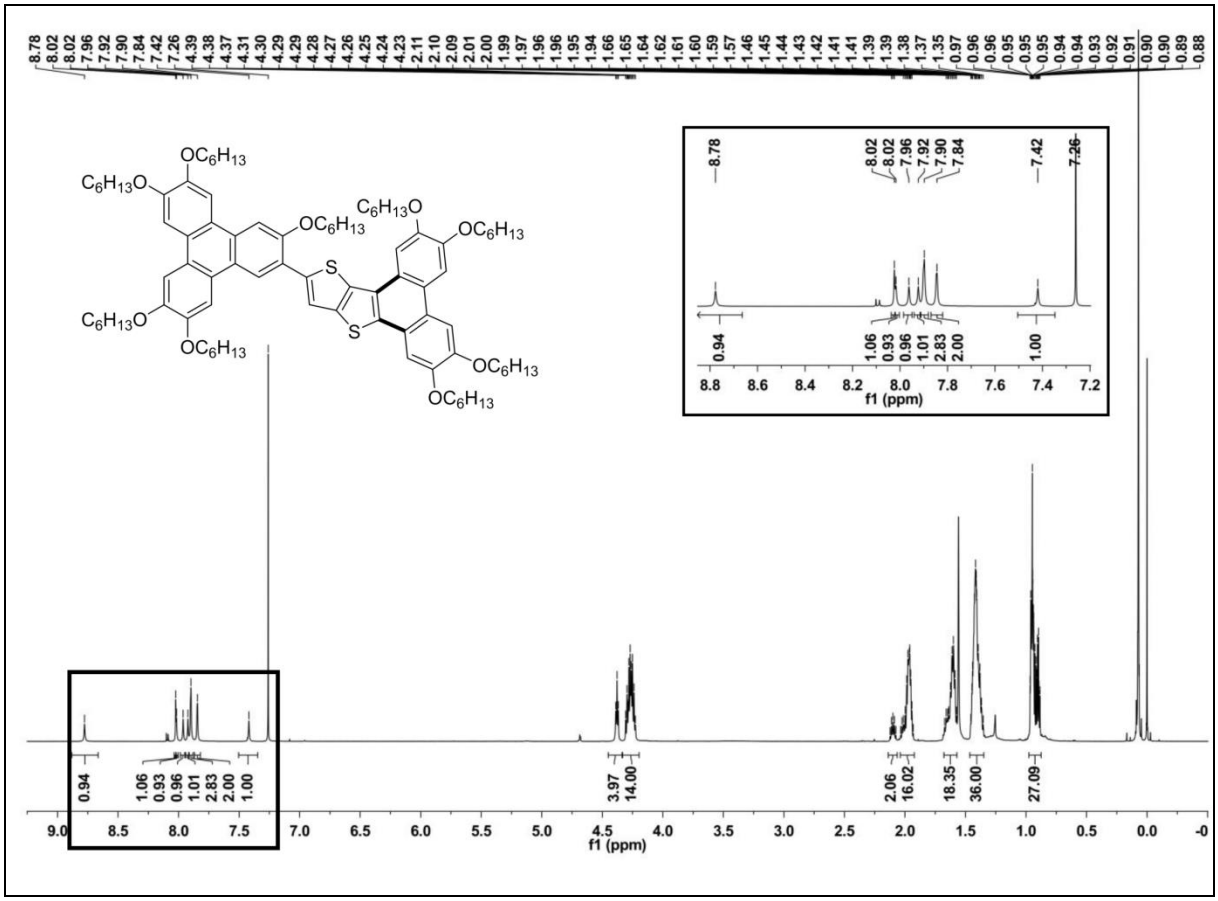

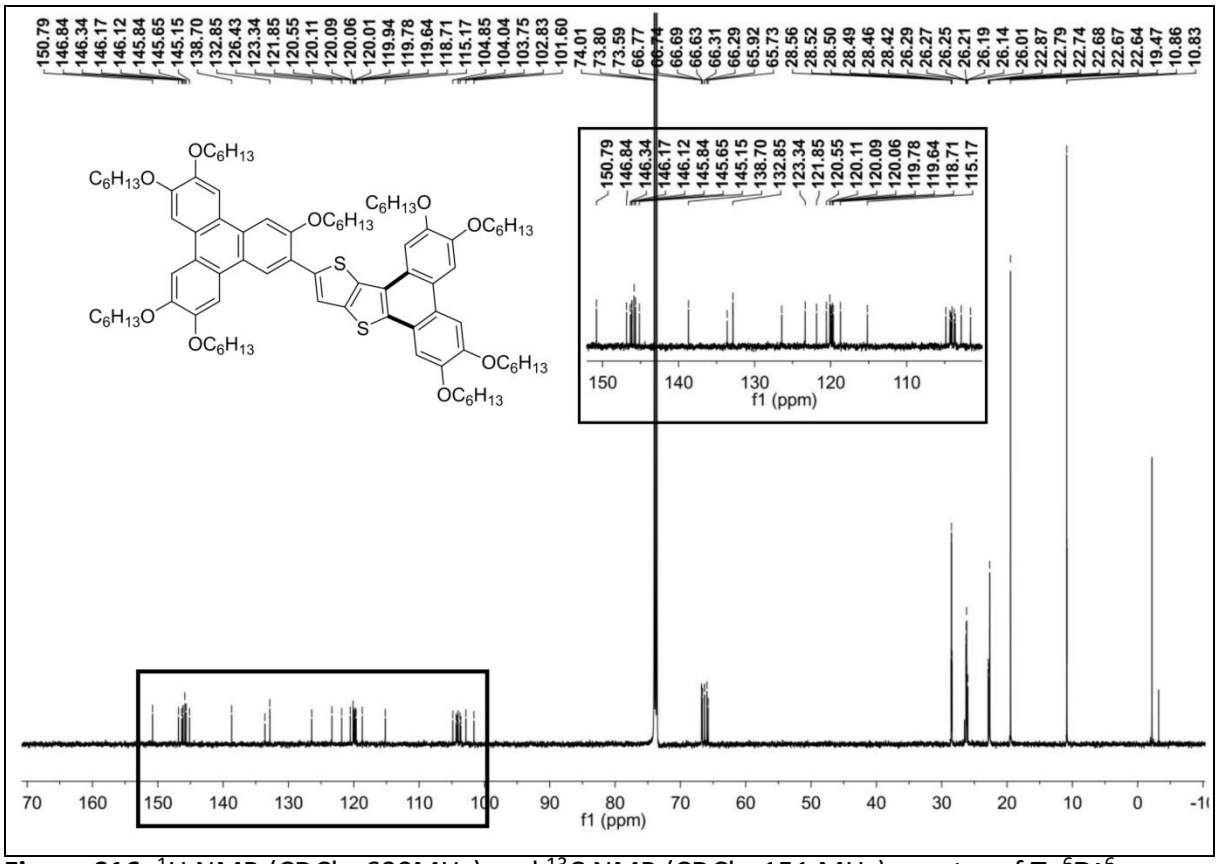

Figure S16. ^{1}H NMR ($CDCl_3$, 600MHz) and ^{13}C NMR ($CDCl_3$, 151 MHz) spectra of **Tp^{6}Dt^{6}**.

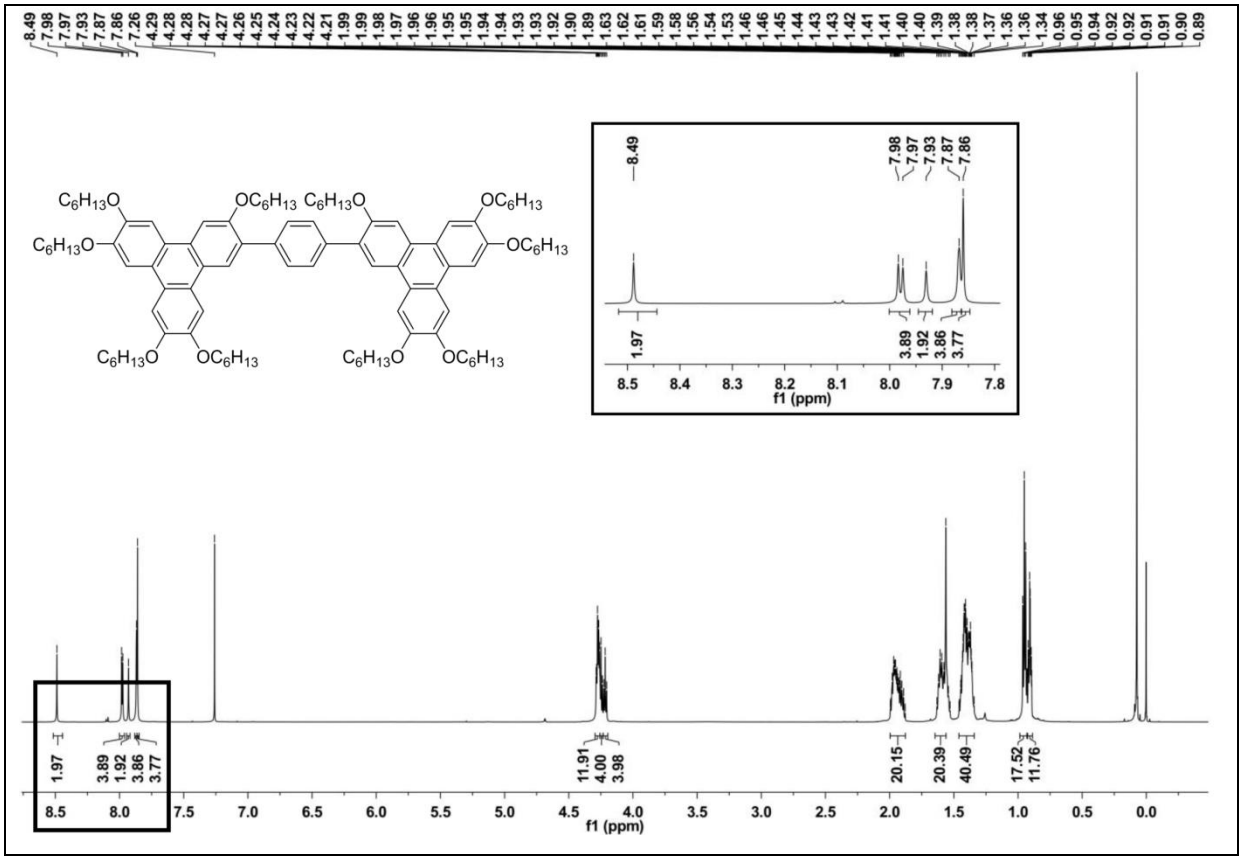

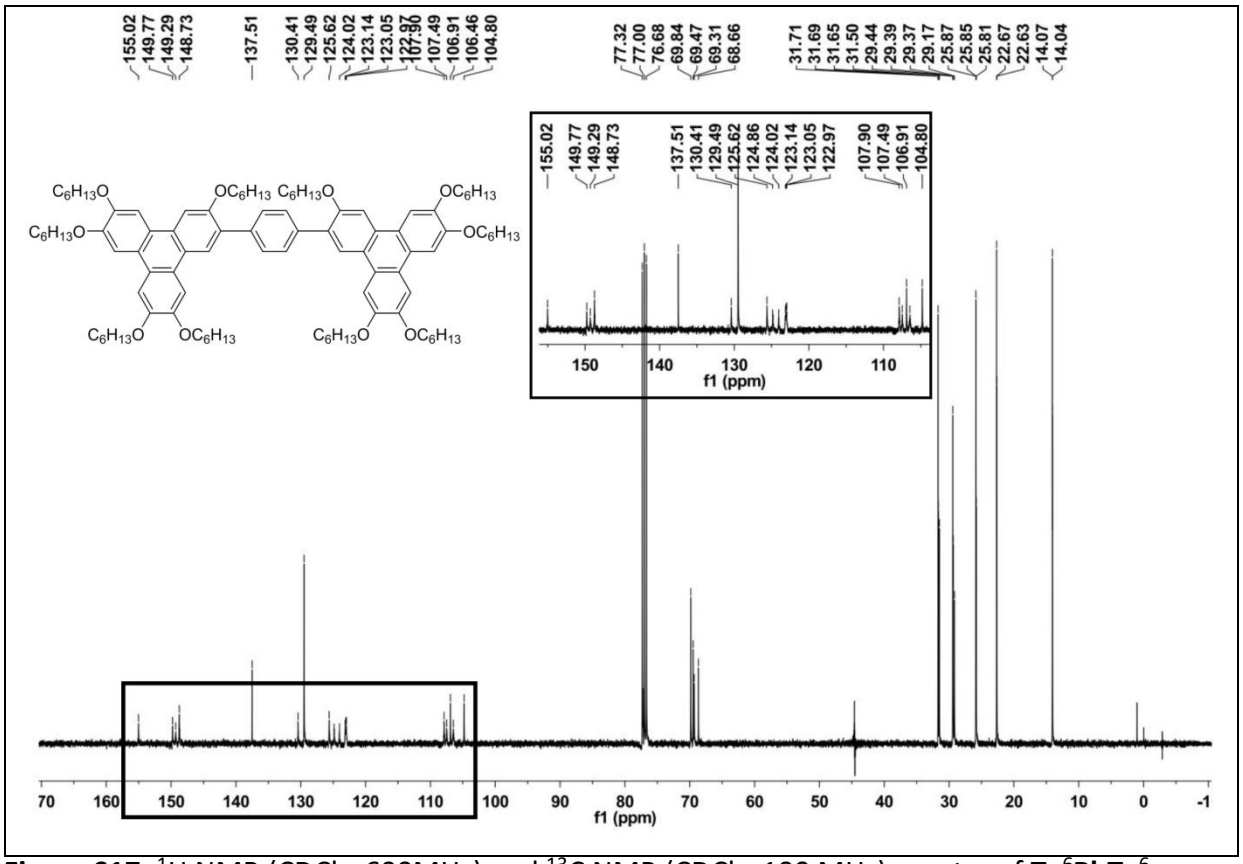

Figure S17. ^{1}H NMR ($CDCl_3$, 600MHz) and ^{13}C NMR ($CDCl_3$, 100 MHz) spectra of **Tp^{6}PhTp^{6}**.

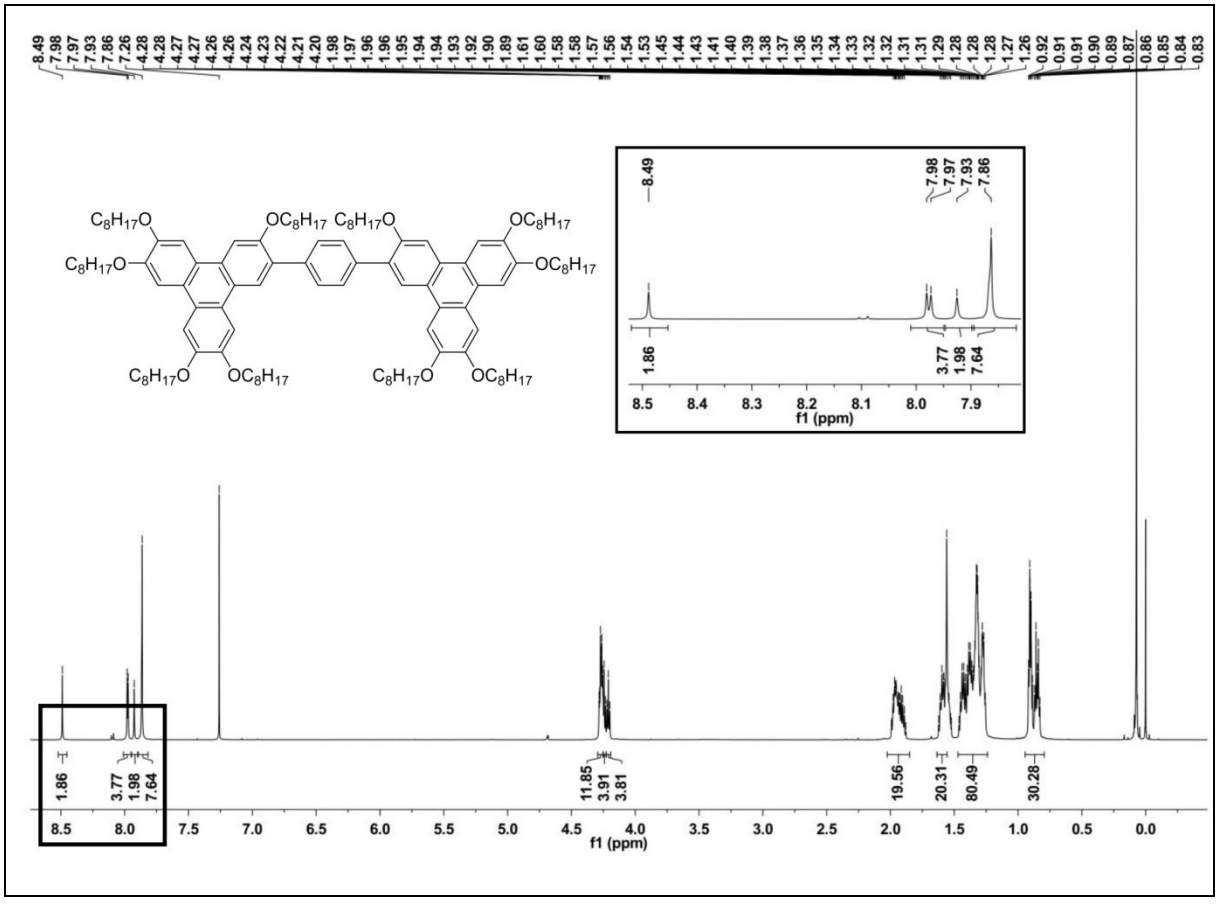

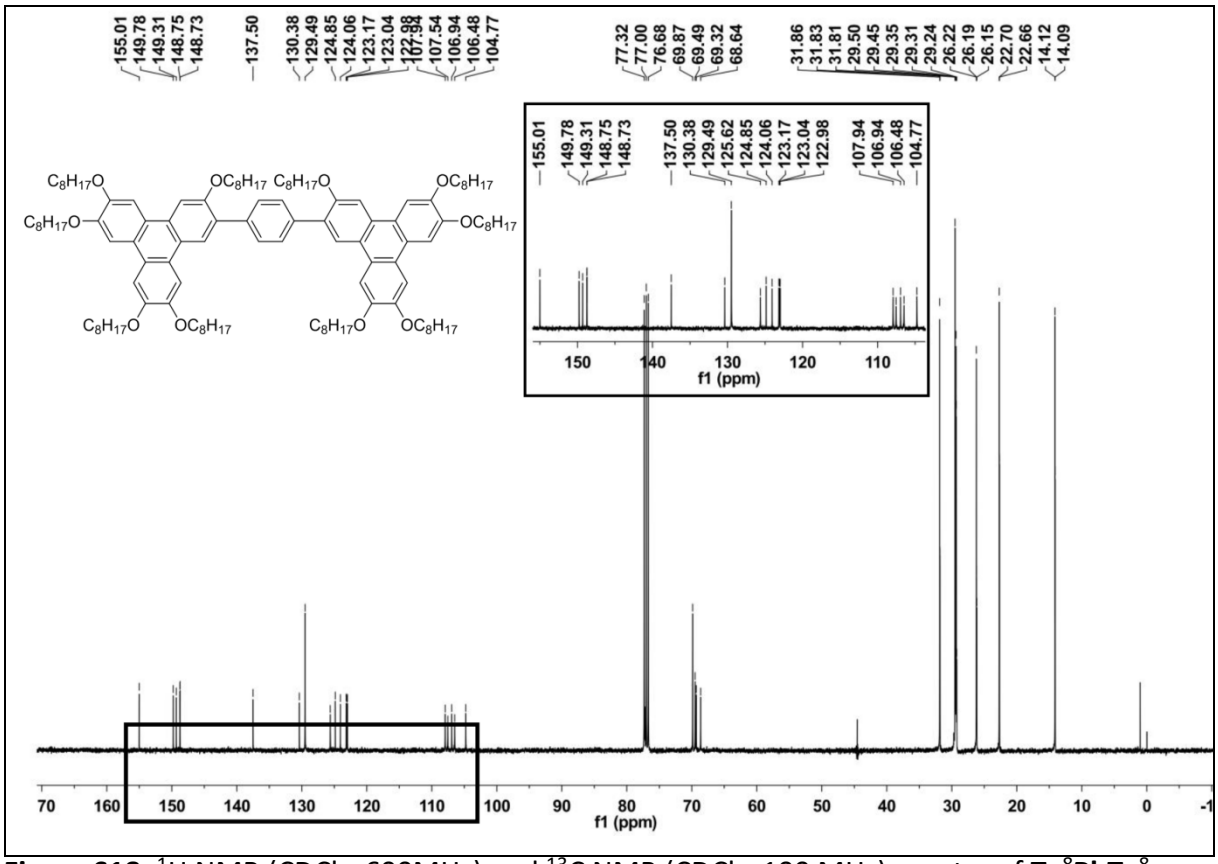

Figure S18. ^{1}H NMR ($CDCl_3$, 600MHz) and ^{13}C NMR ($CDCl_3$, 100 MHz) spectra of **Tp^{8}PhTp^{8}**.

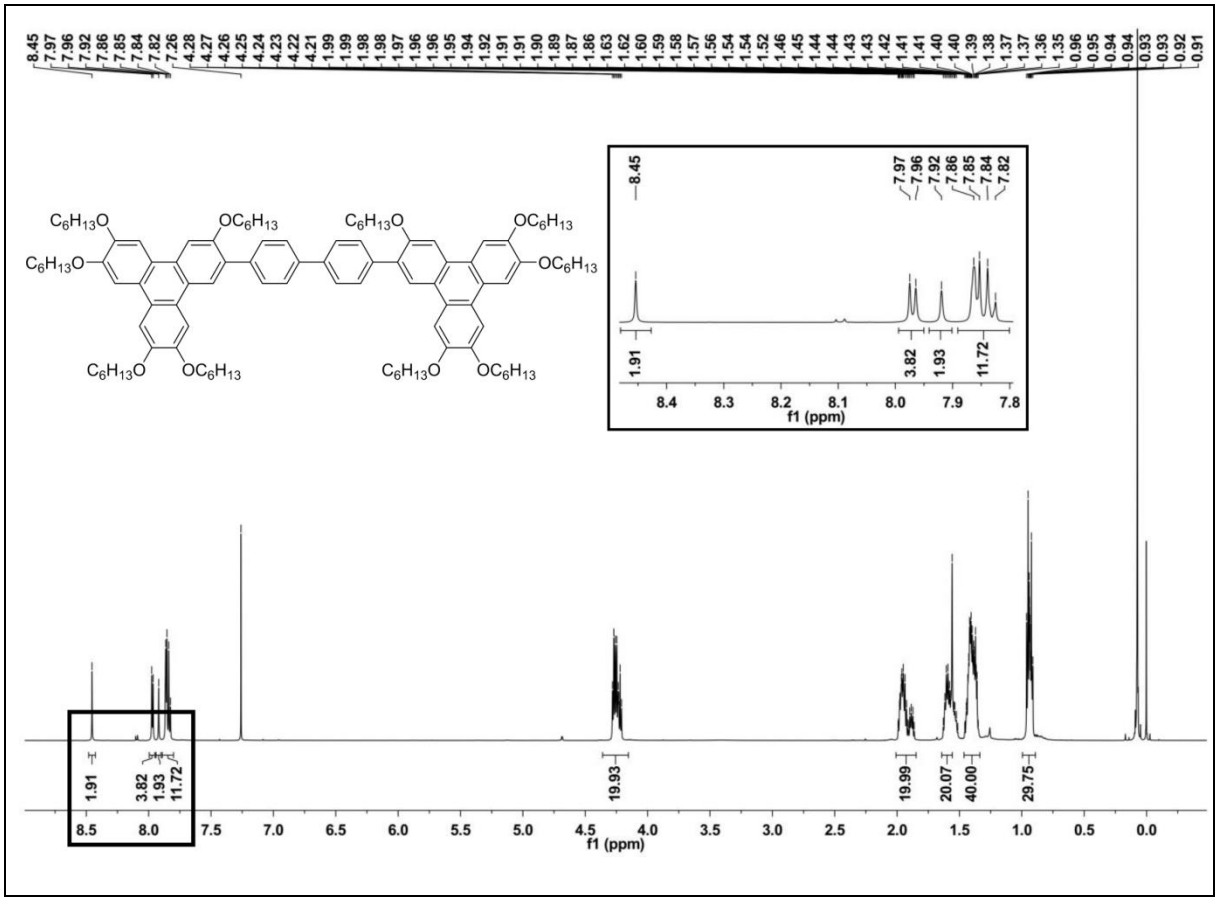

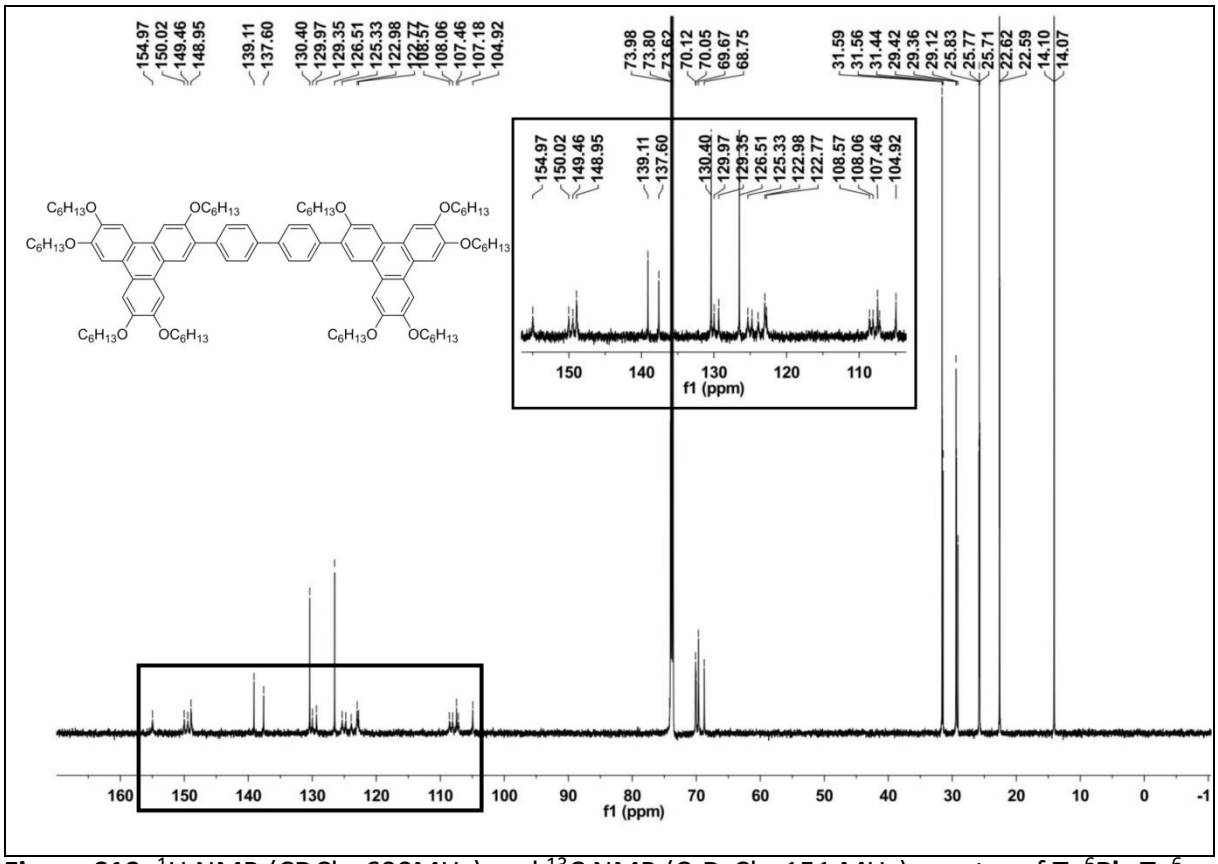

Figure S19. ^{1}H NMR ($CDCl_3$, 600MHz) and ^{13}C NMR ($C_2D_2Cl_4$, 151 MHz) spectra of **Tp^{6}Ph$_2$Tp^{6}**.

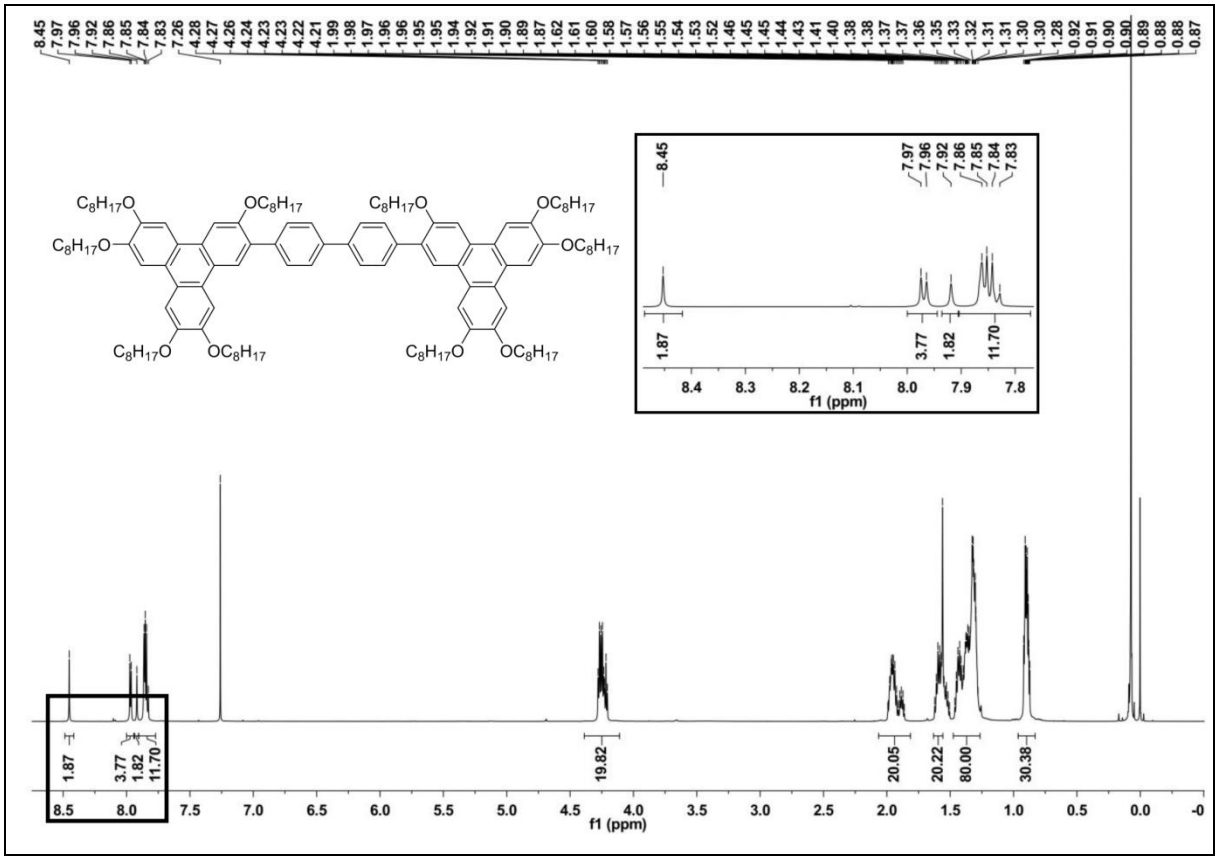

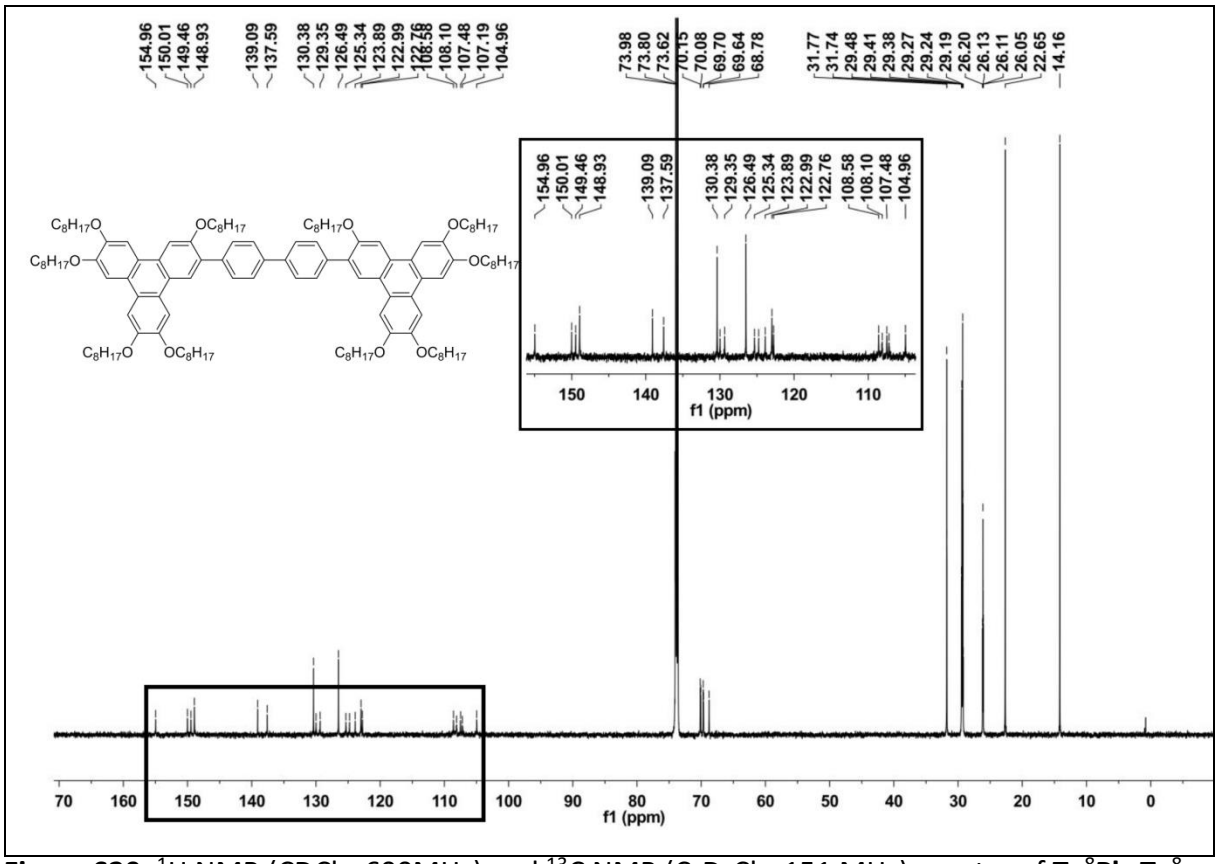

Figure S20. ^{1}H NMR ($CDCl_3$, 600MHz) and ^{13}C NMR ($C_2D_2Cl_4$, 151 MHz) spectra of **Tp^{8}Ph$_2$Tp^{8}**.

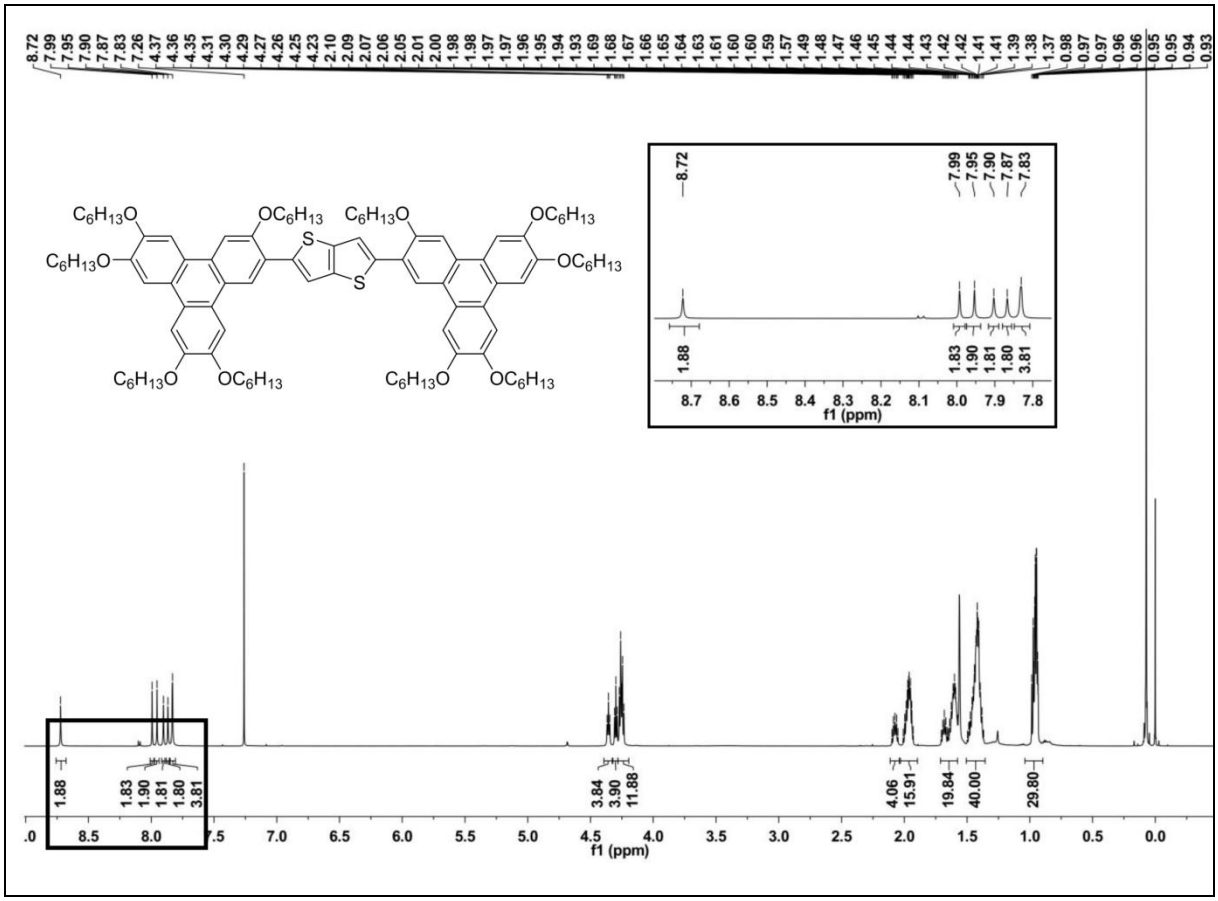

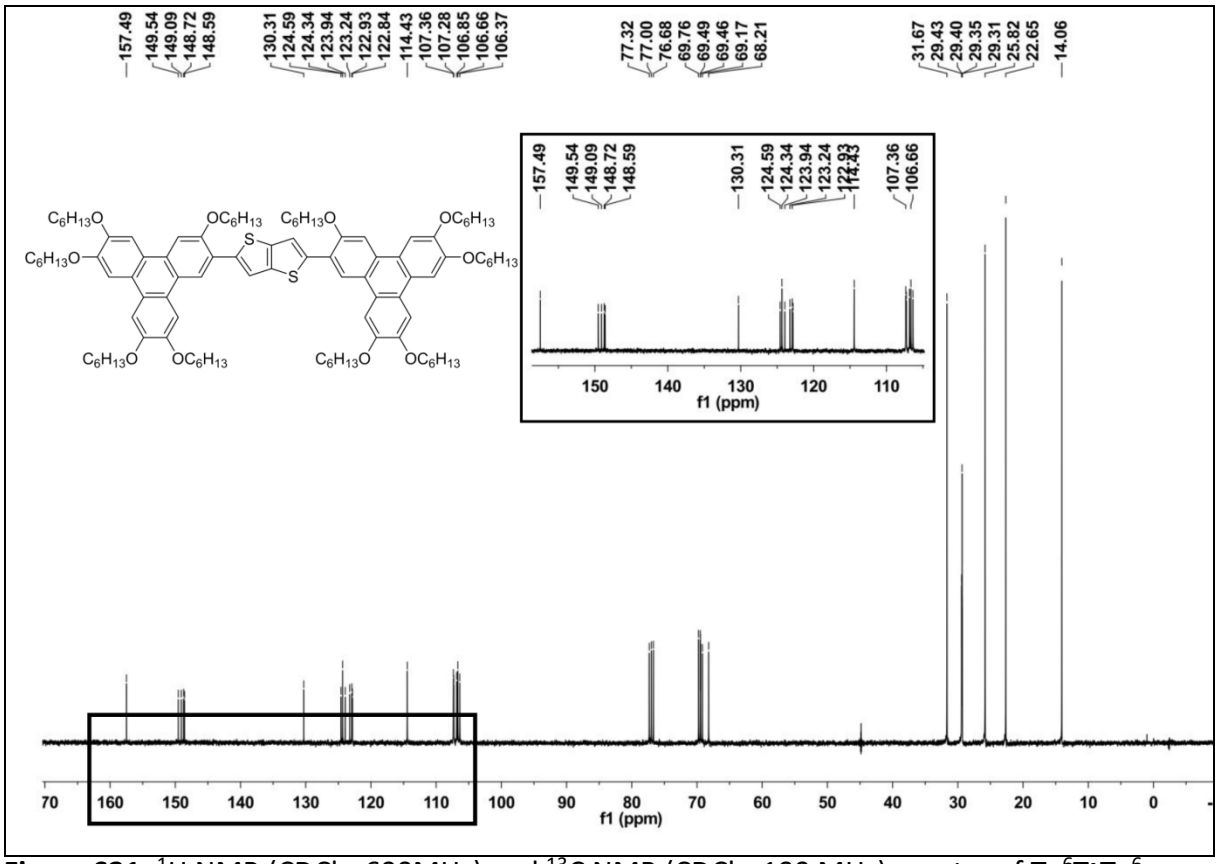

Figure S21. ^{1}H NMR ($CDCl_3$, 600MHz) and ^{13}C NMR ($CDCl_3$, 100 MHz) spectra of **Tp^{6}TtTp^{6}**.

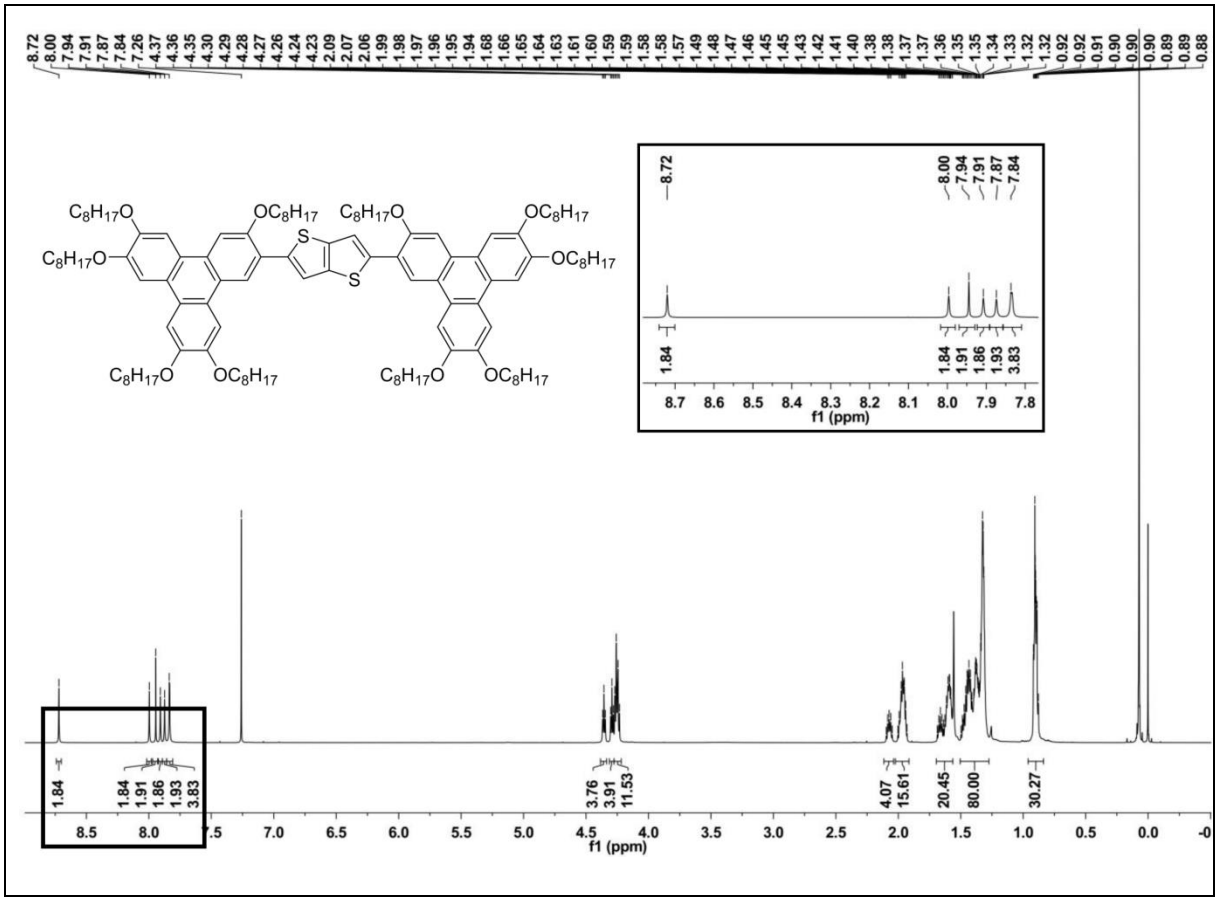

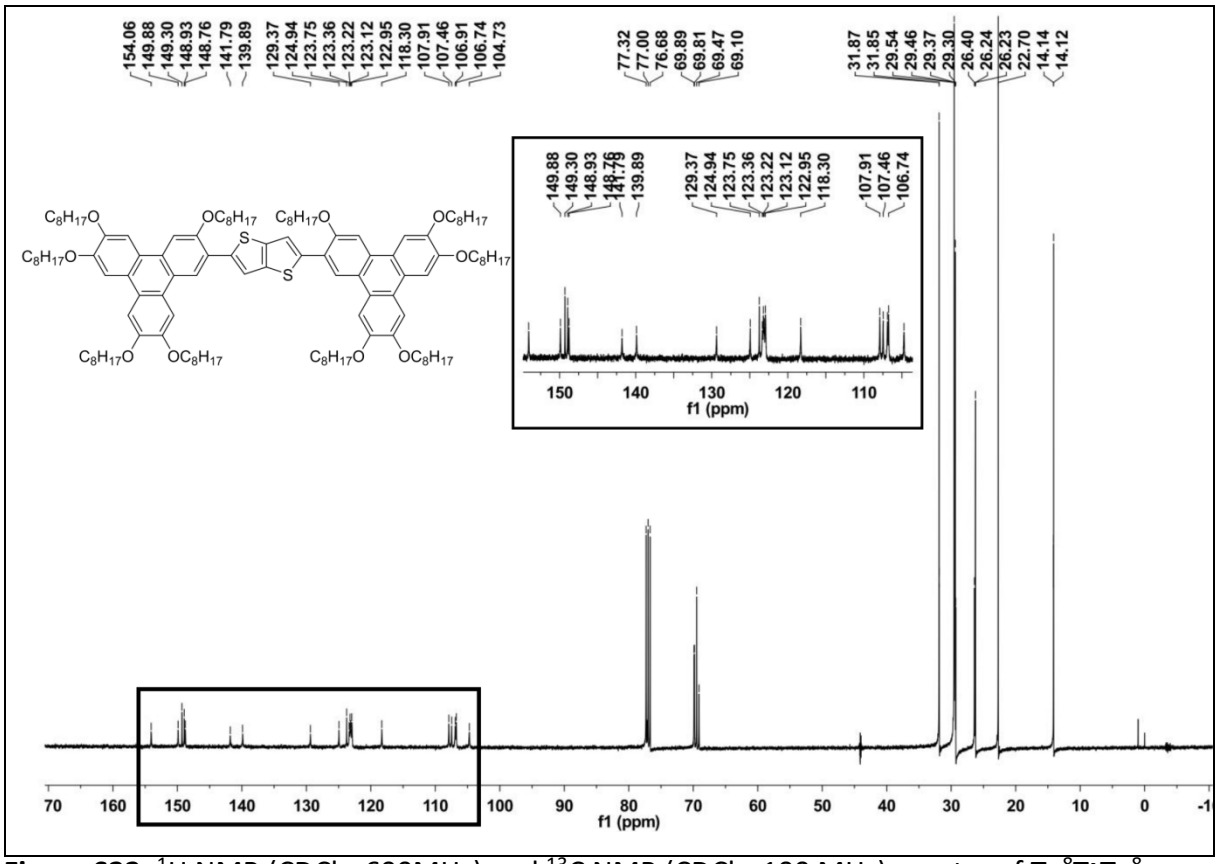

Figure S22. ^{1}H NMR ($CDCl_3$, 600MHz) and ^{13}C NMR ($CDCl_3$, 100 MHz) spectra of **Tp^{8}TtTp^{8}**.

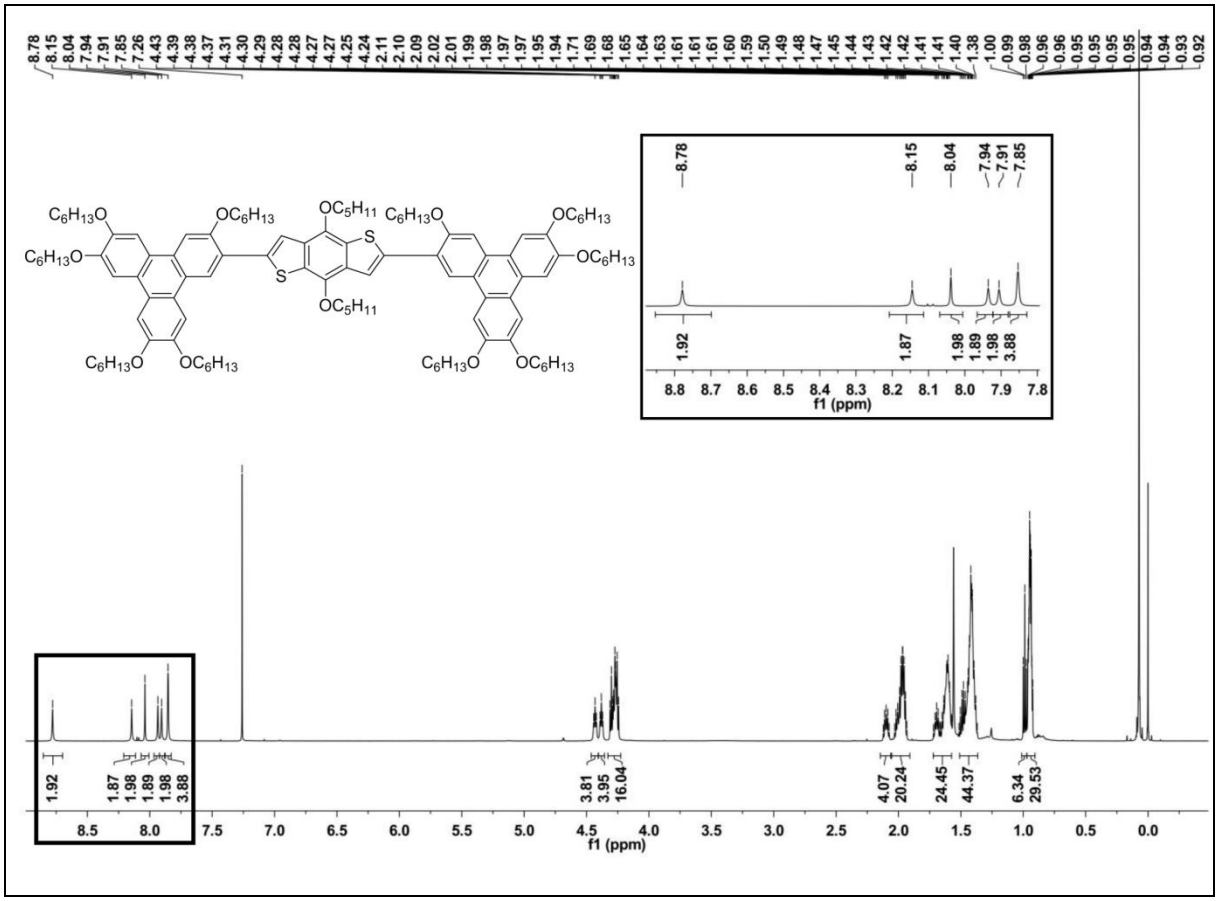

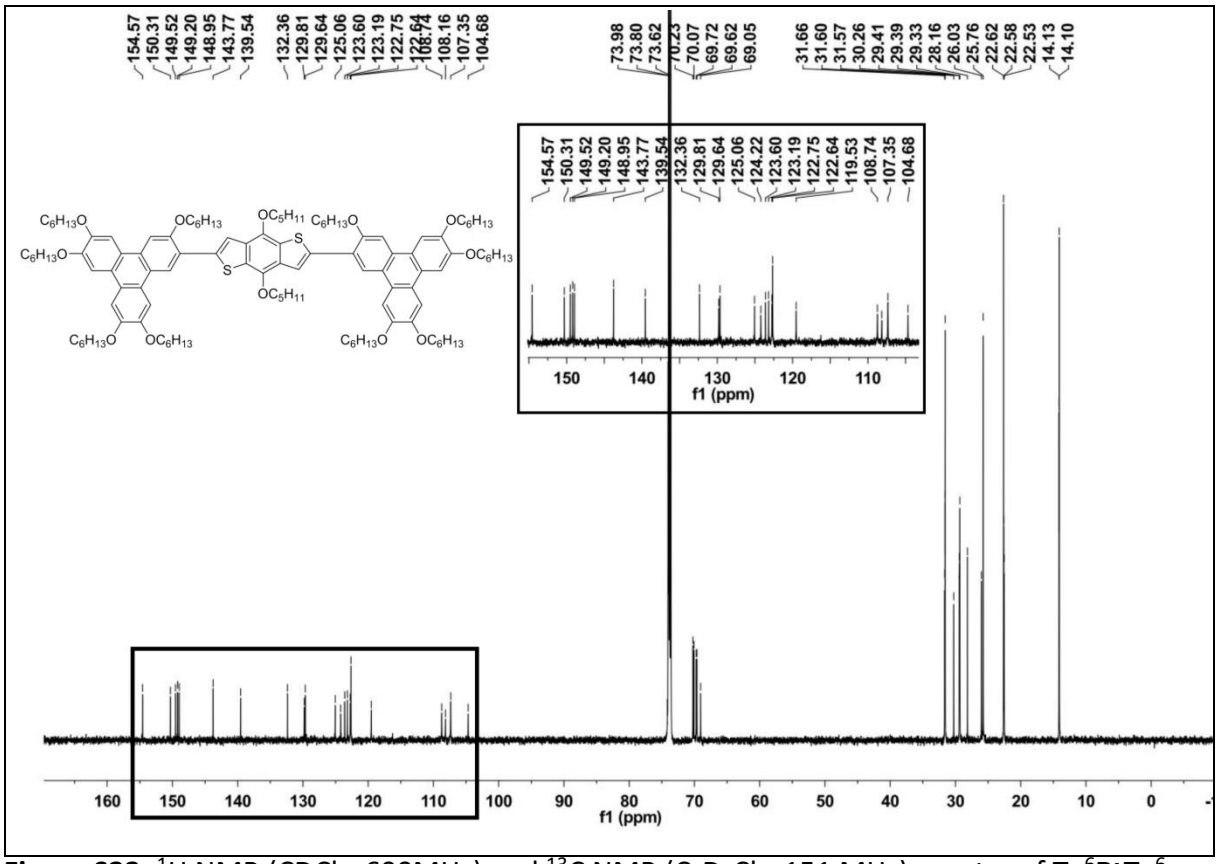

Figure S23. ^{1}H NMR ($CDCl_3$, 600MHz) and ^{13}C NMR ($C_2D_2Cl_4$, 151 MHz) spectra of **Tp^{6}BtTp^{6}**.

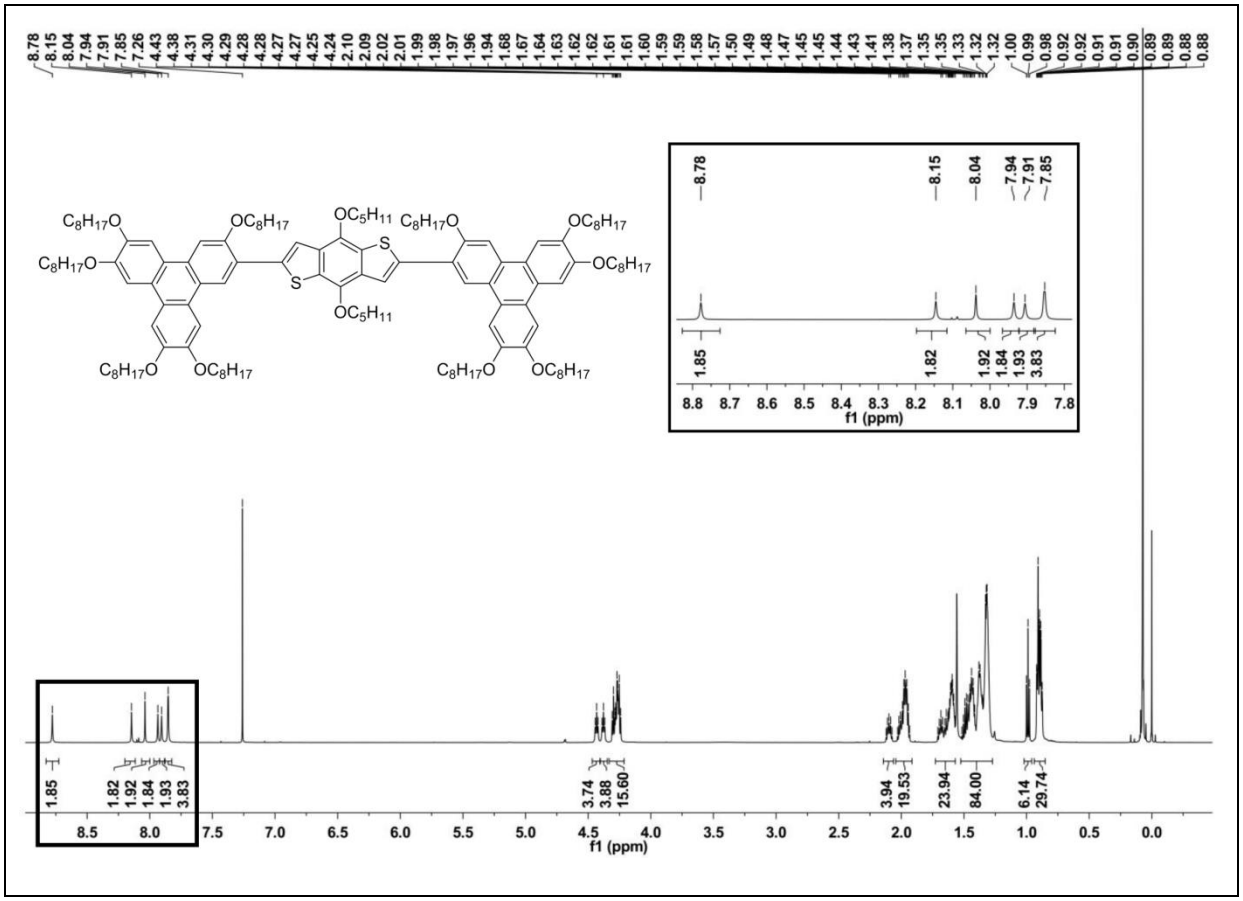

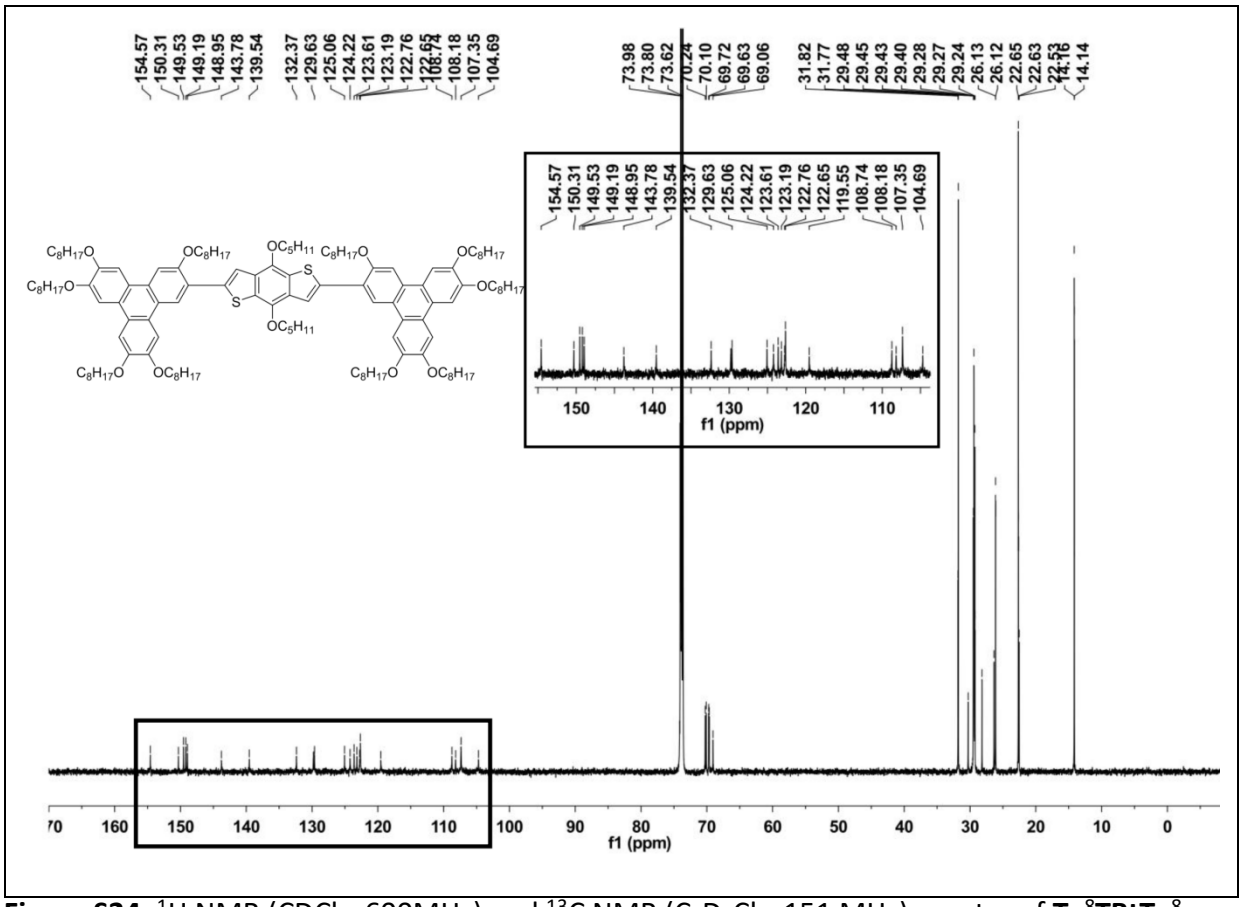

Figure S24. ^{1}H NMR ($CDCl_3$, 600MHz) and ^{13}C NMR ($C_2D_2Cl_4$, 151 MHz) spectra of **Tp**[8]**TBtTp**[8].

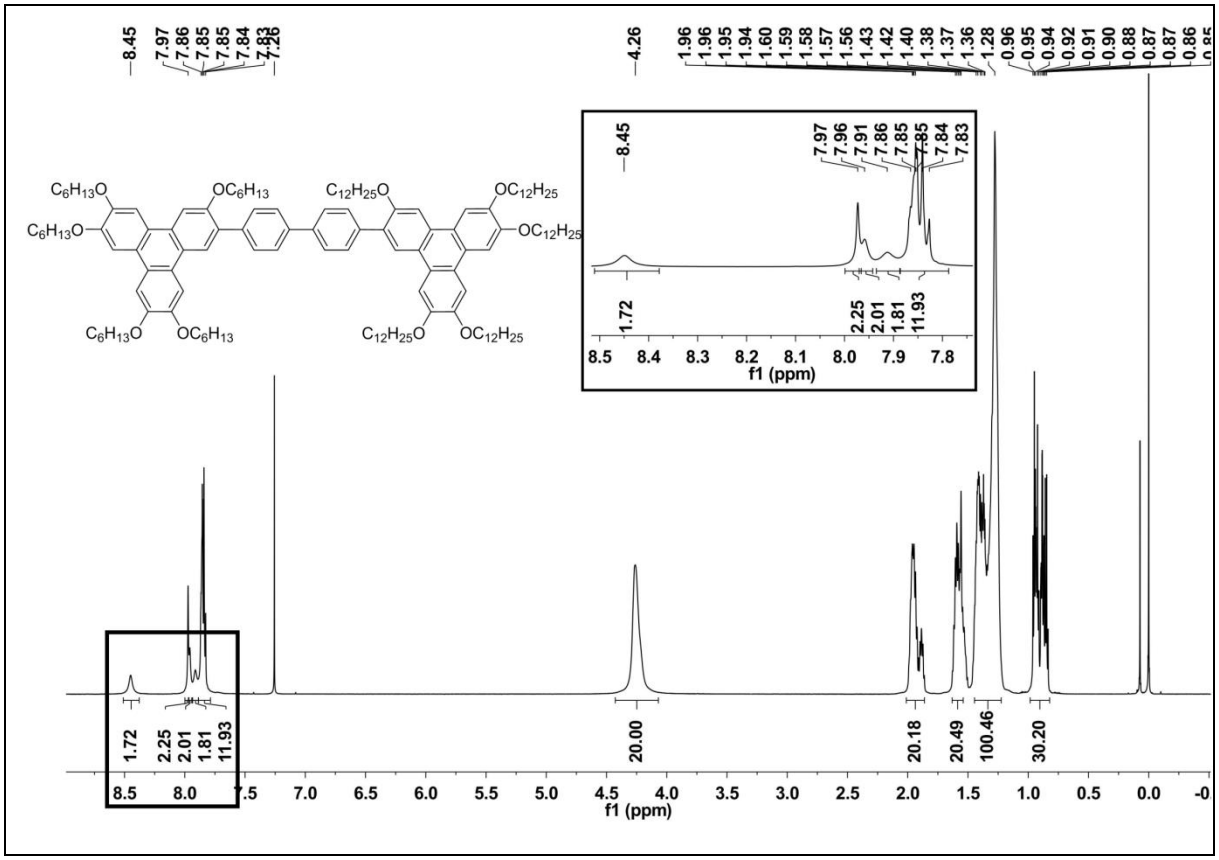

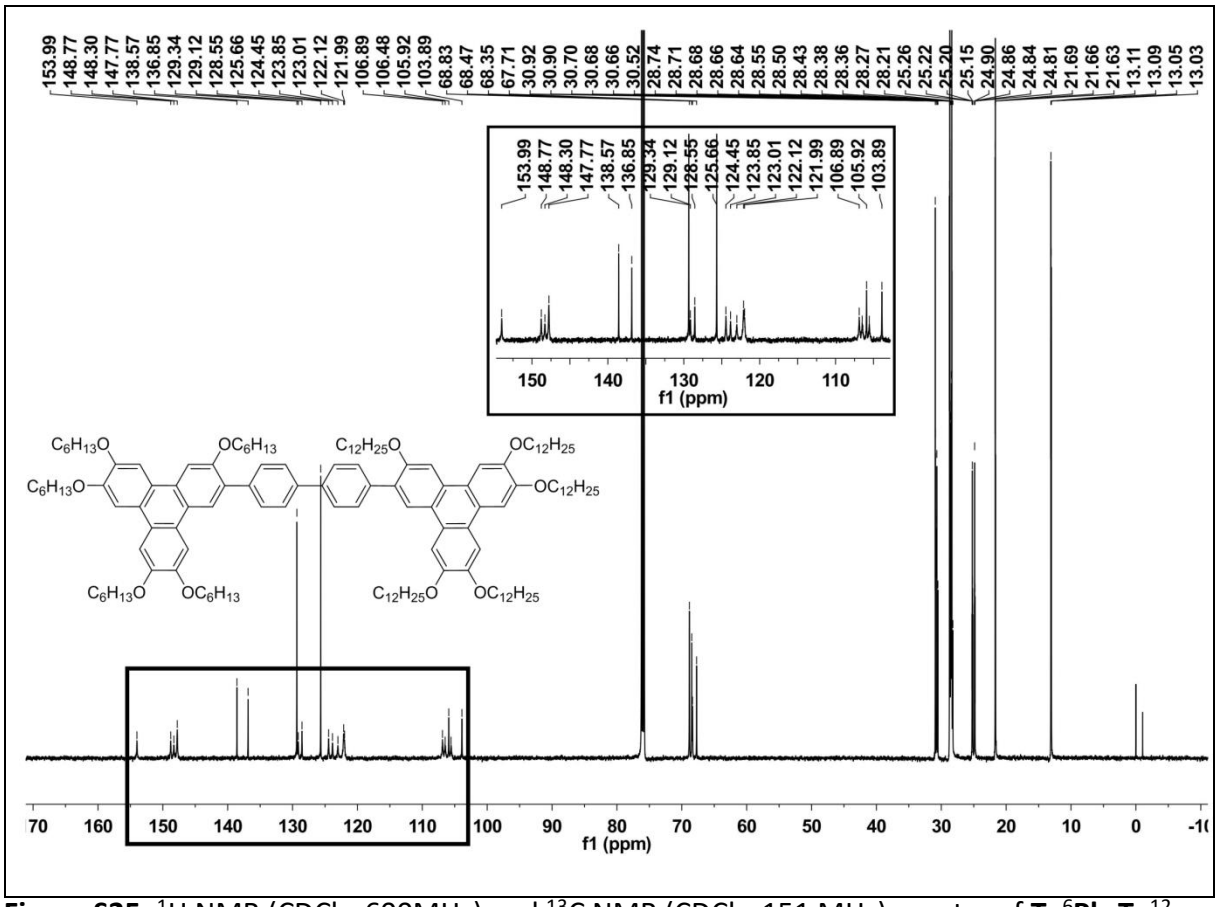

Figure S25. ^{1}H NMR ($CDCl_3$, 600MHz) and ^{13}C NMR ($CDCl_3$, 151 MHz) spectra of **Tp^{6}Ph$_2$Tp^{12}**.

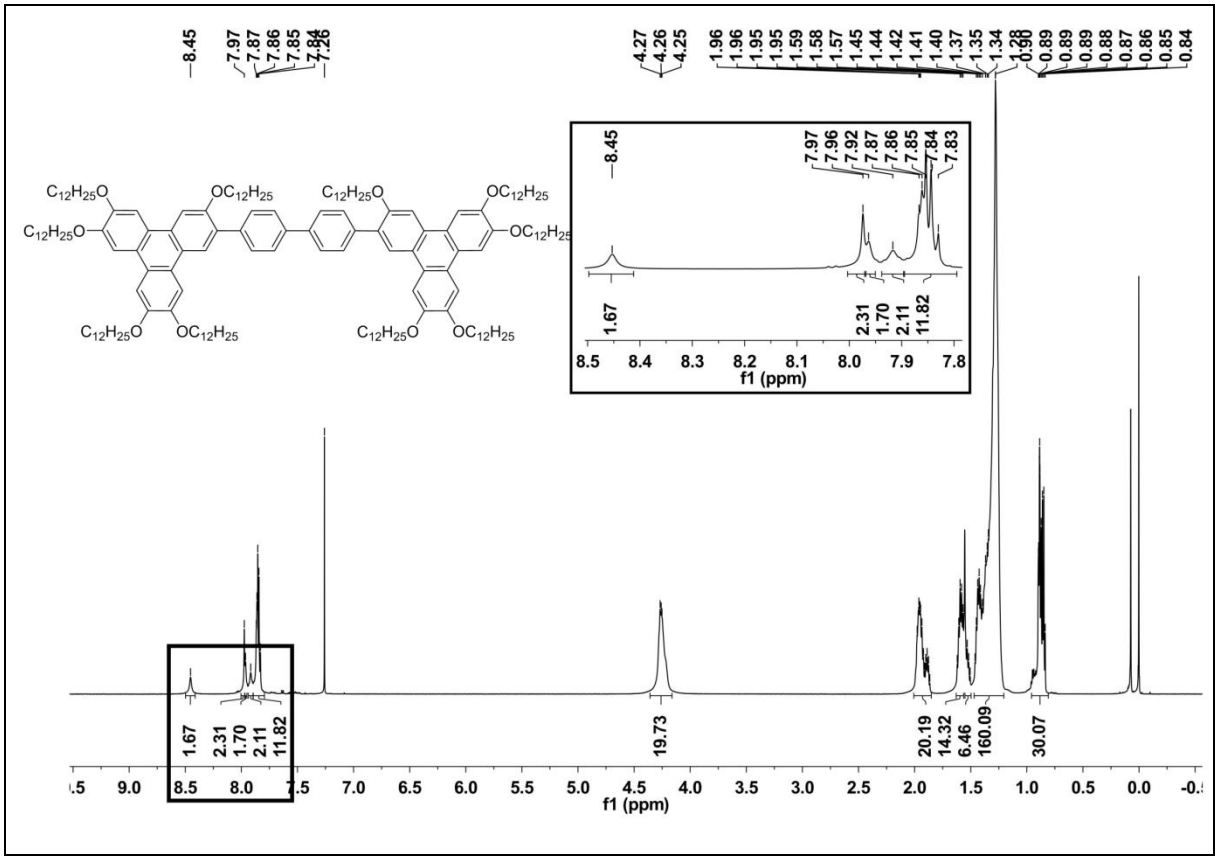

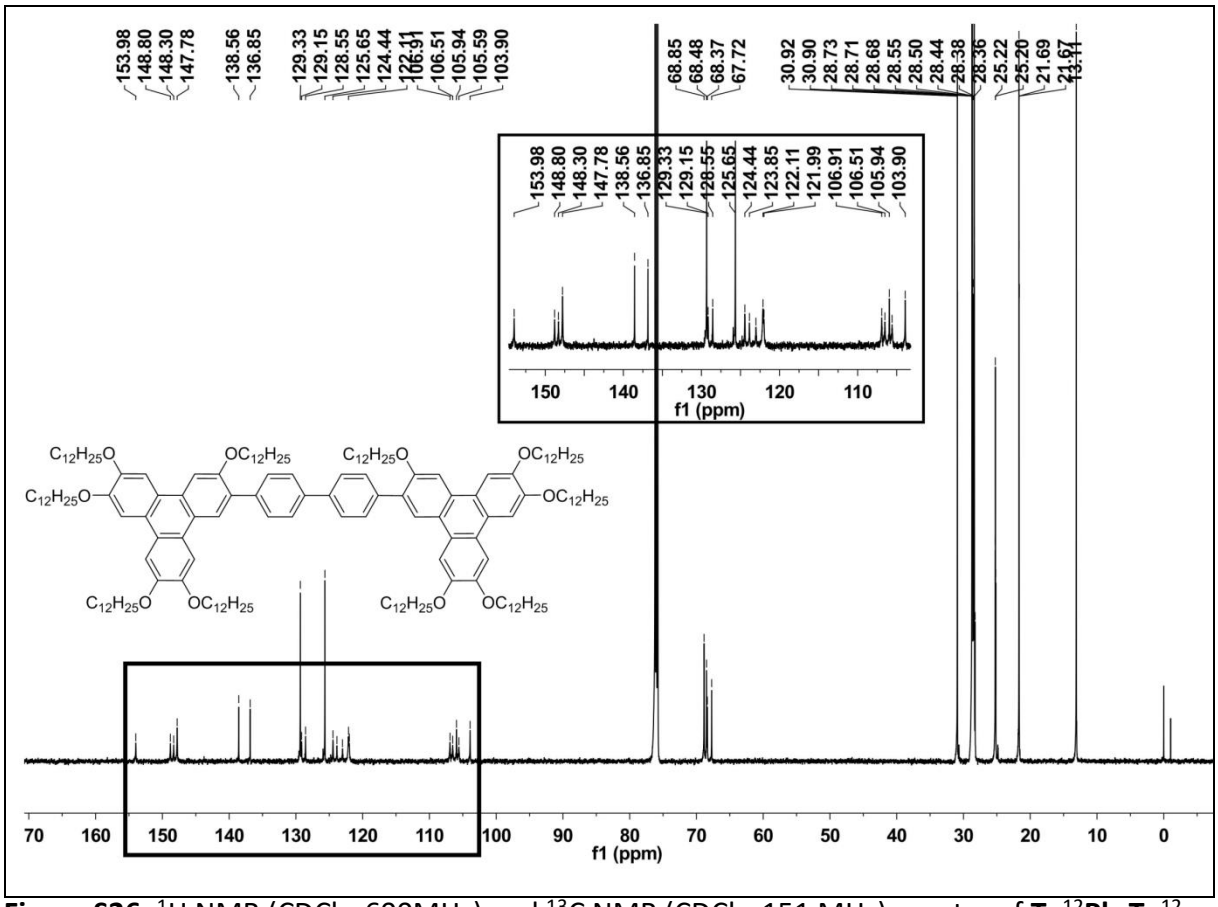

Figure S26. ^{1}H NMR ($CDCl_3$, 600MHz) and ^{13}C NMR ($CDCl_3$, 151 MHz) spectra of **Tp^{12}Ph$_2$Tp^{12}**.

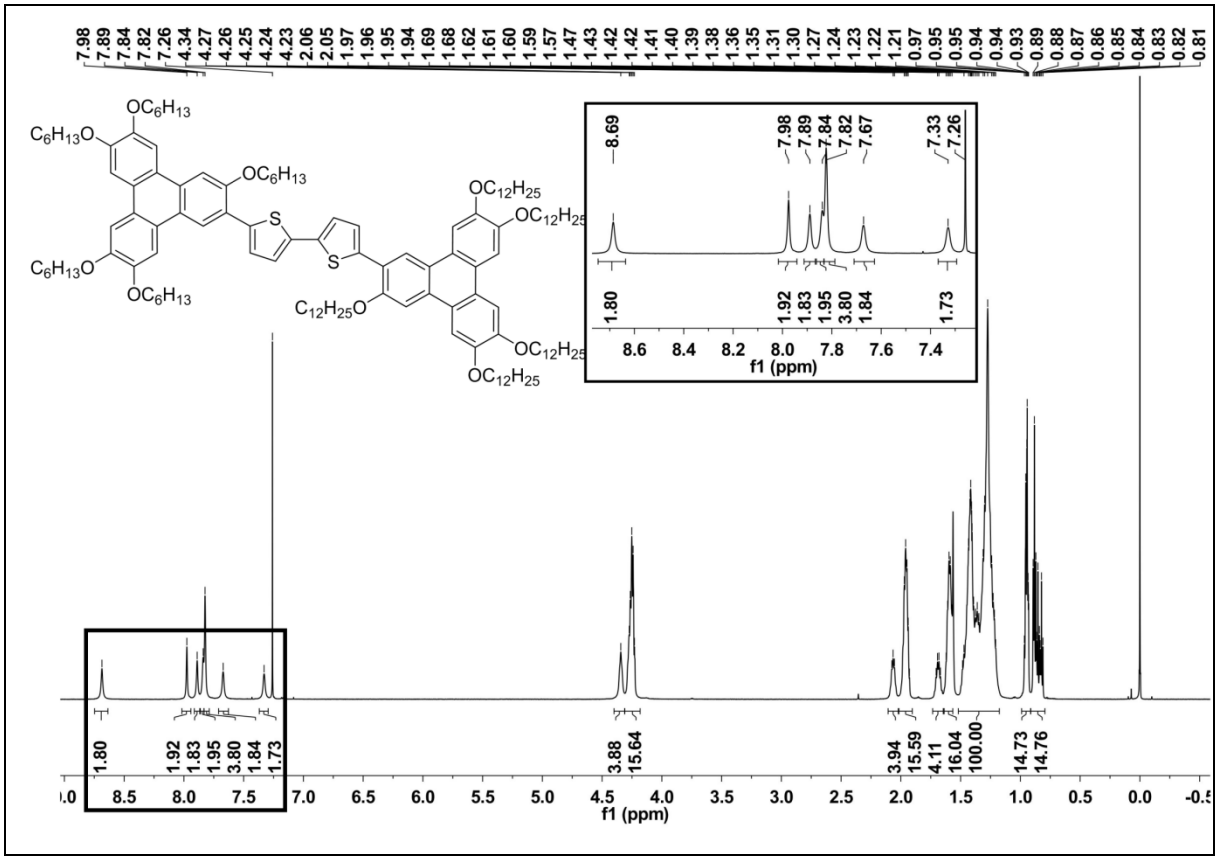

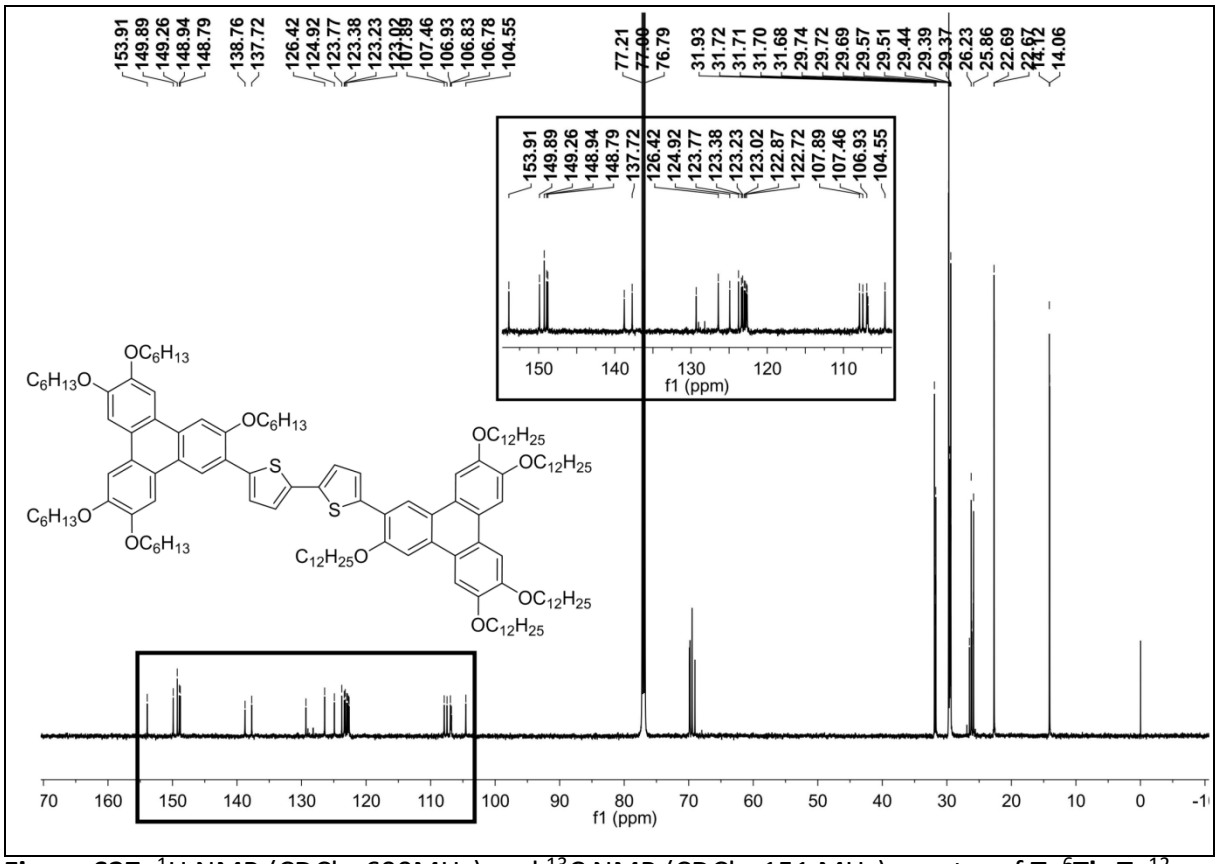

Figure S27. ^{1}H NMR ($CDCl_3$, 600MHz) and ^{13}C NMR ($CDCl_3$, 151 MHz) spectra of **Tp^{6}Th$_2$Tp^{12}**.

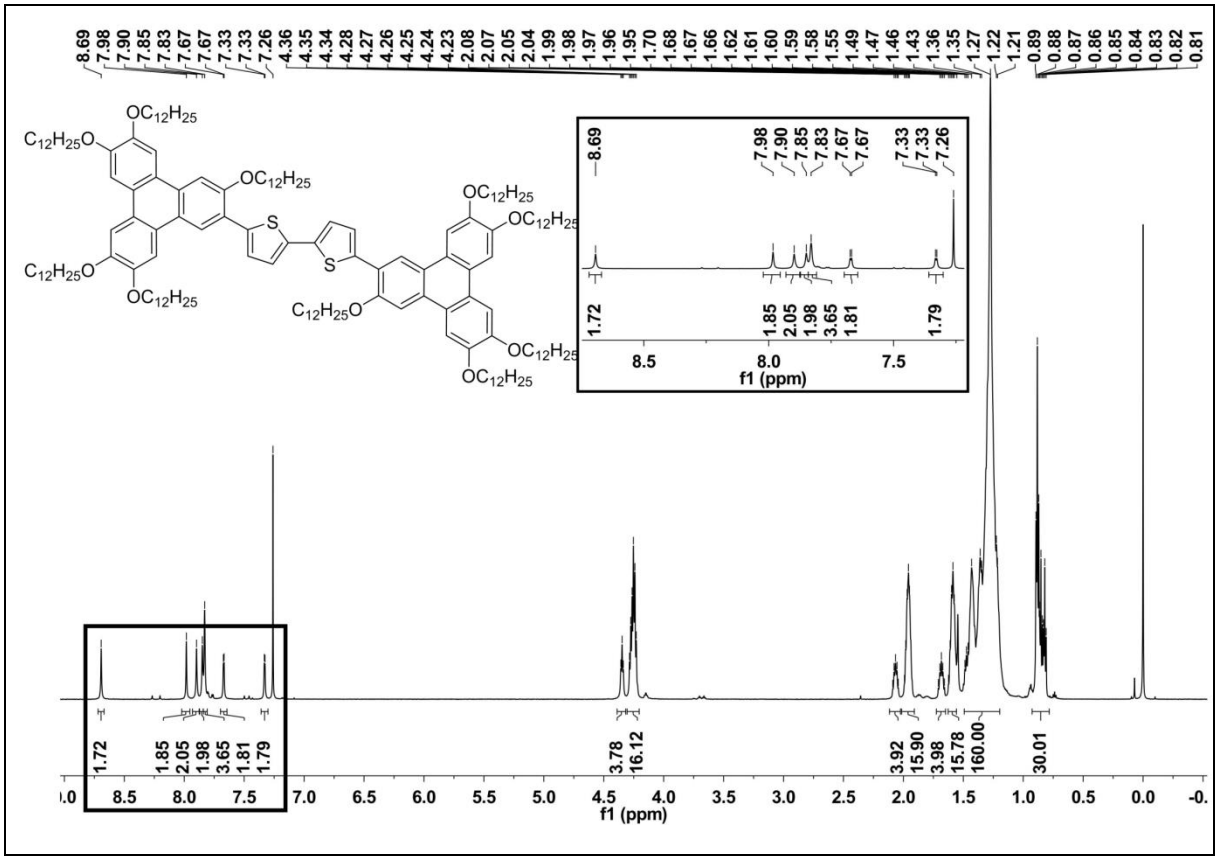

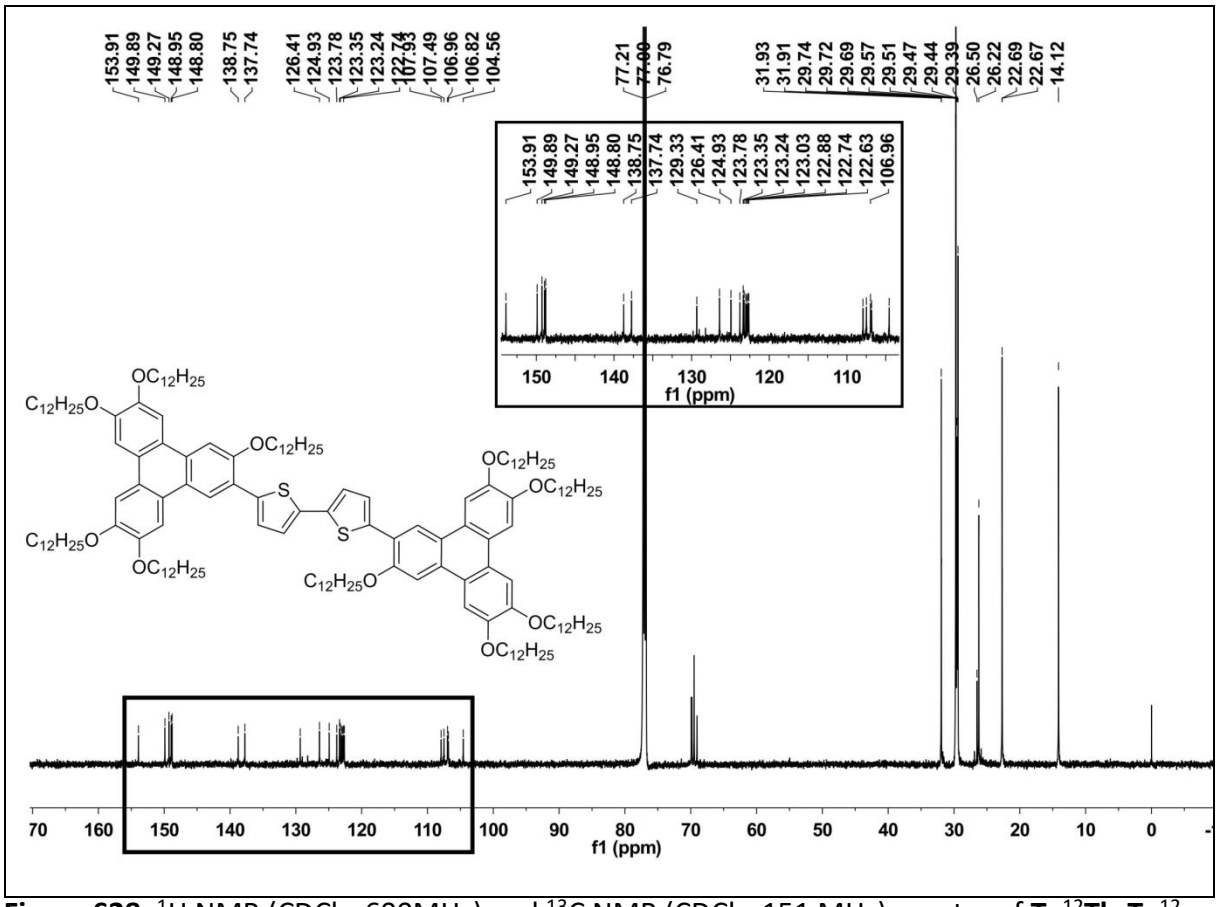

Figure S28. ^{1}H NMR ($CDCl_3$, 600MHz) and ^{13}C NMR ($CDCl_3$, 151 MHz) spectra of **Tp^{12}Th$_2$Tp^{12}**.

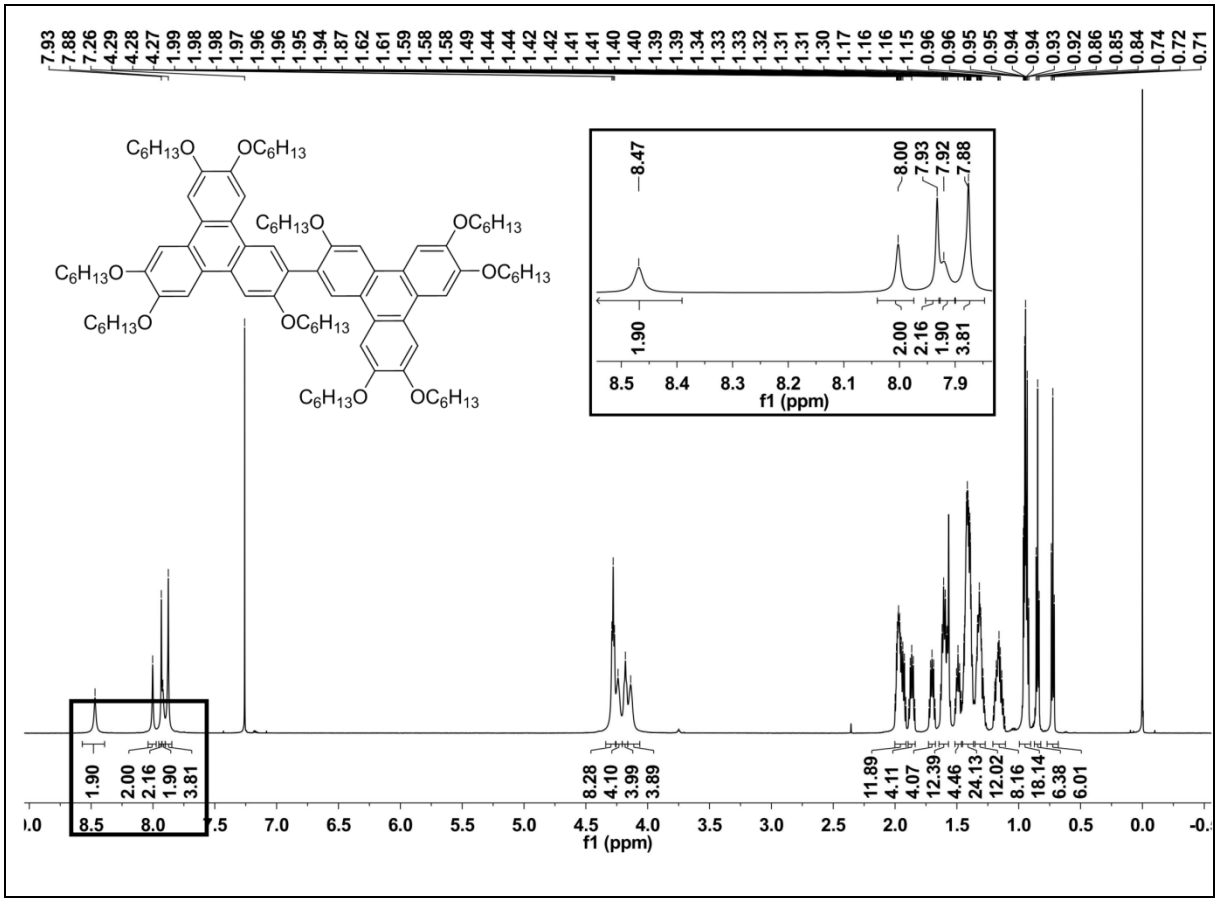

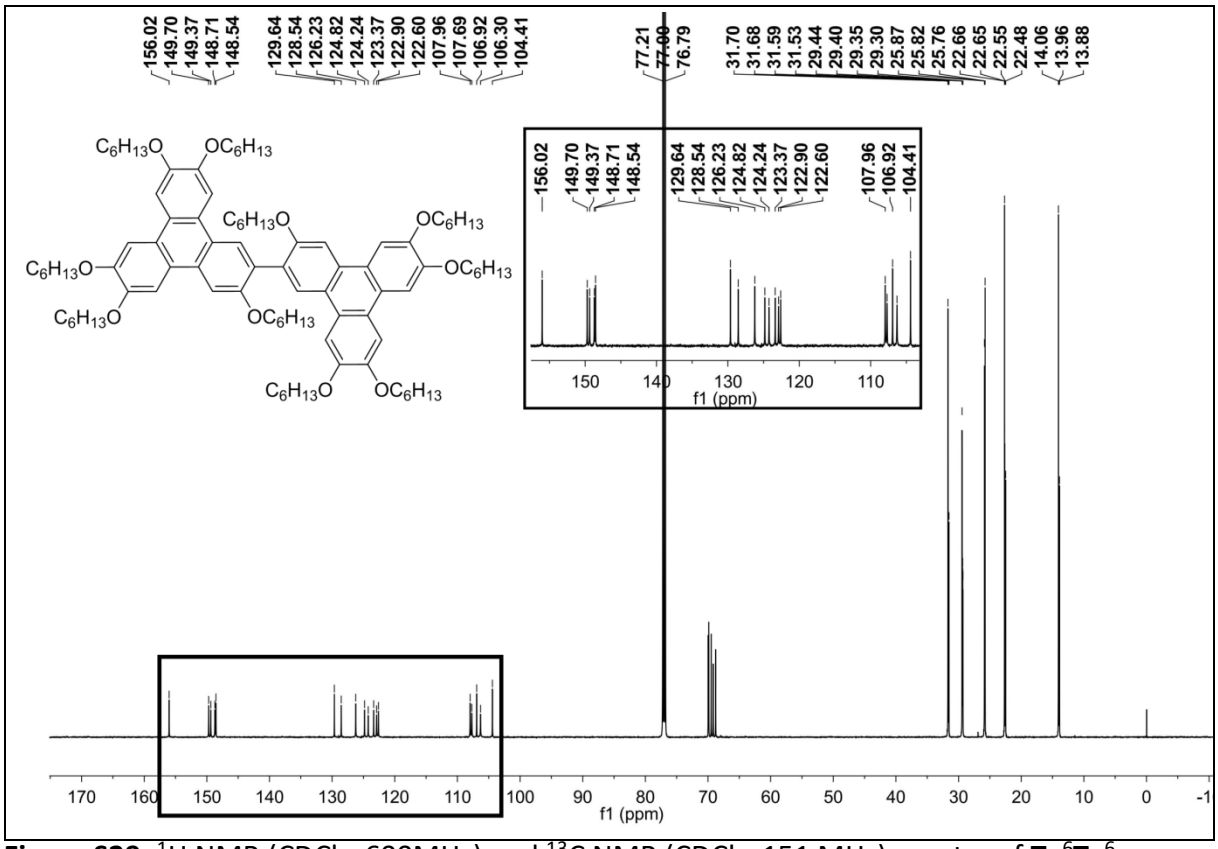

Figure S29. ^{1}H NMR ($CDCl_3$, 600MHz) and ^{13}C NMR ($CDCl_3$, 151 MHz) spectra of **Tp^{6}Tp^{6}**.

4. HRMS

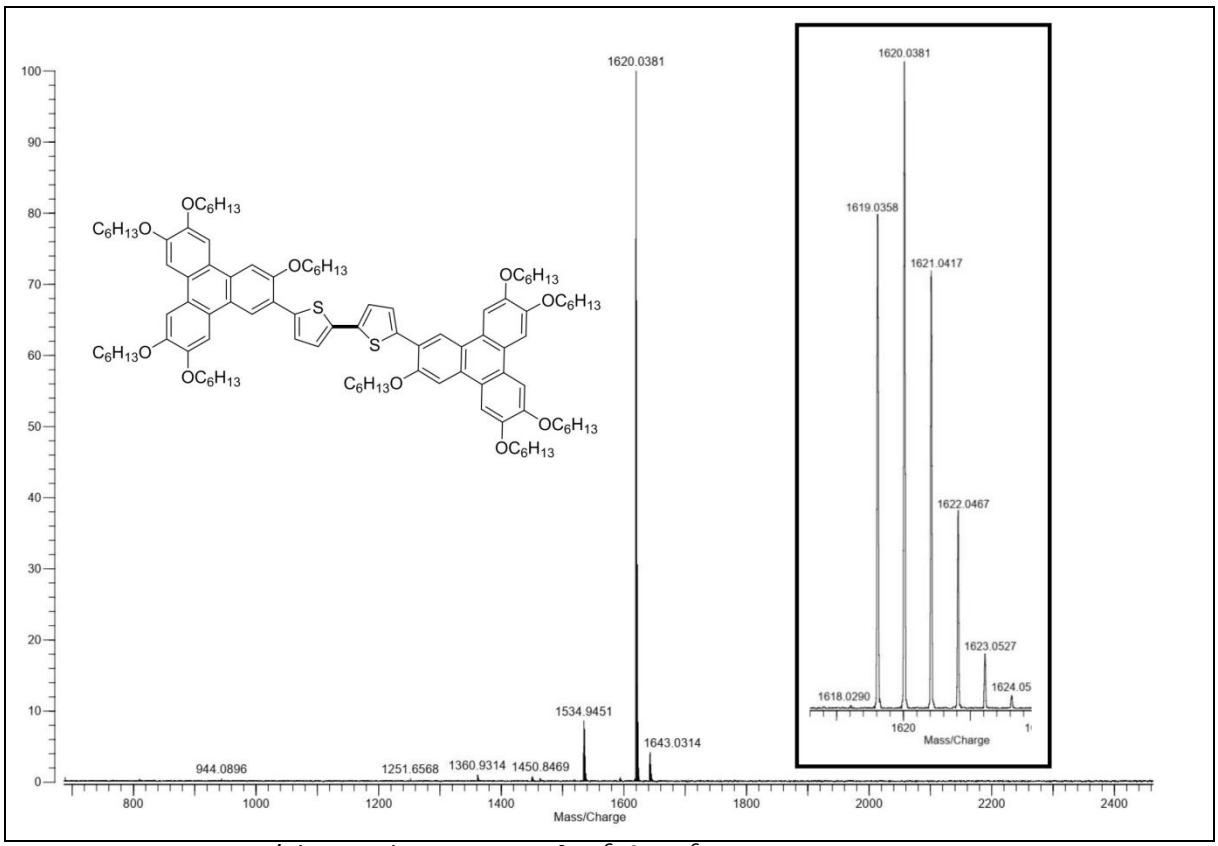

Figure S30. HRMS m/z(MALDI) spectrum of **Tp^{6}Th$_2$Tp^{6}.**

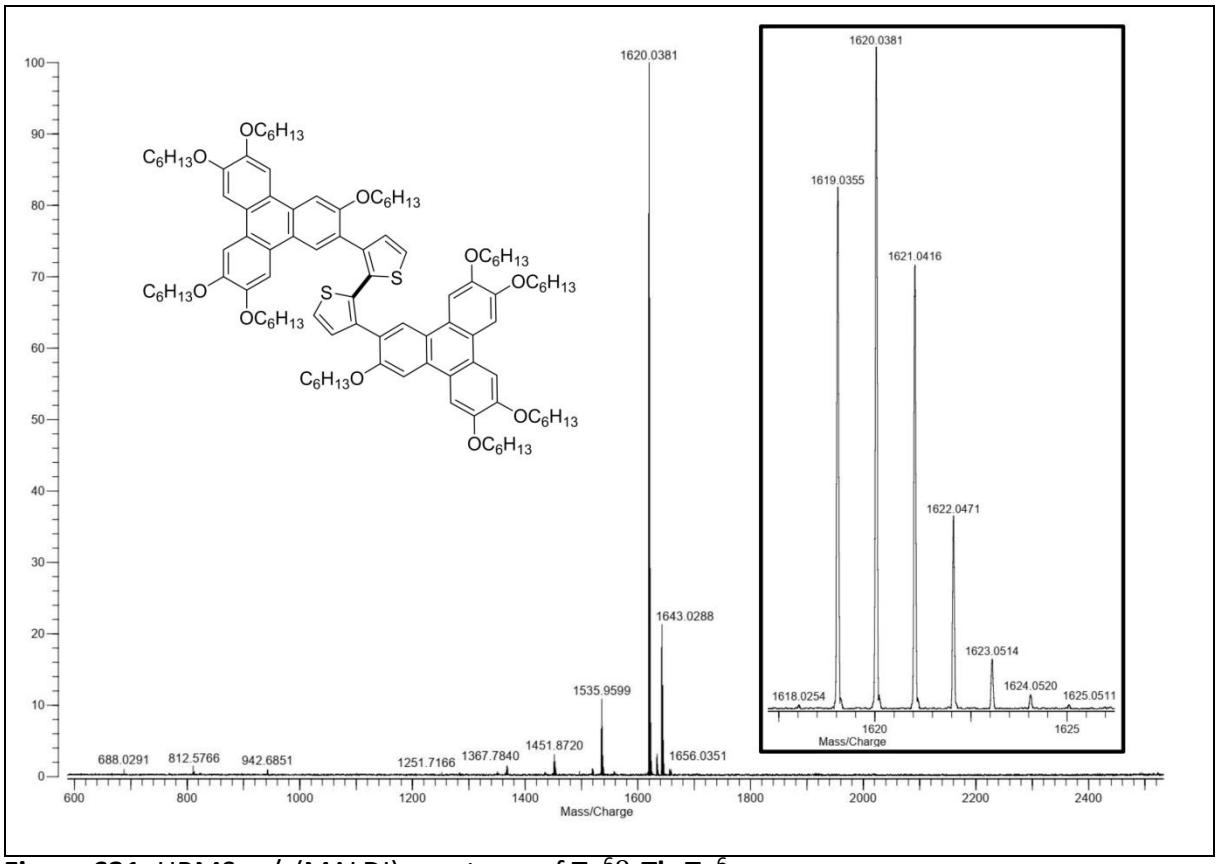

Figure S31. HRMS m/z(MALDI) spectrum of **Tp^{6}β-Th$_2$Tp^6.**

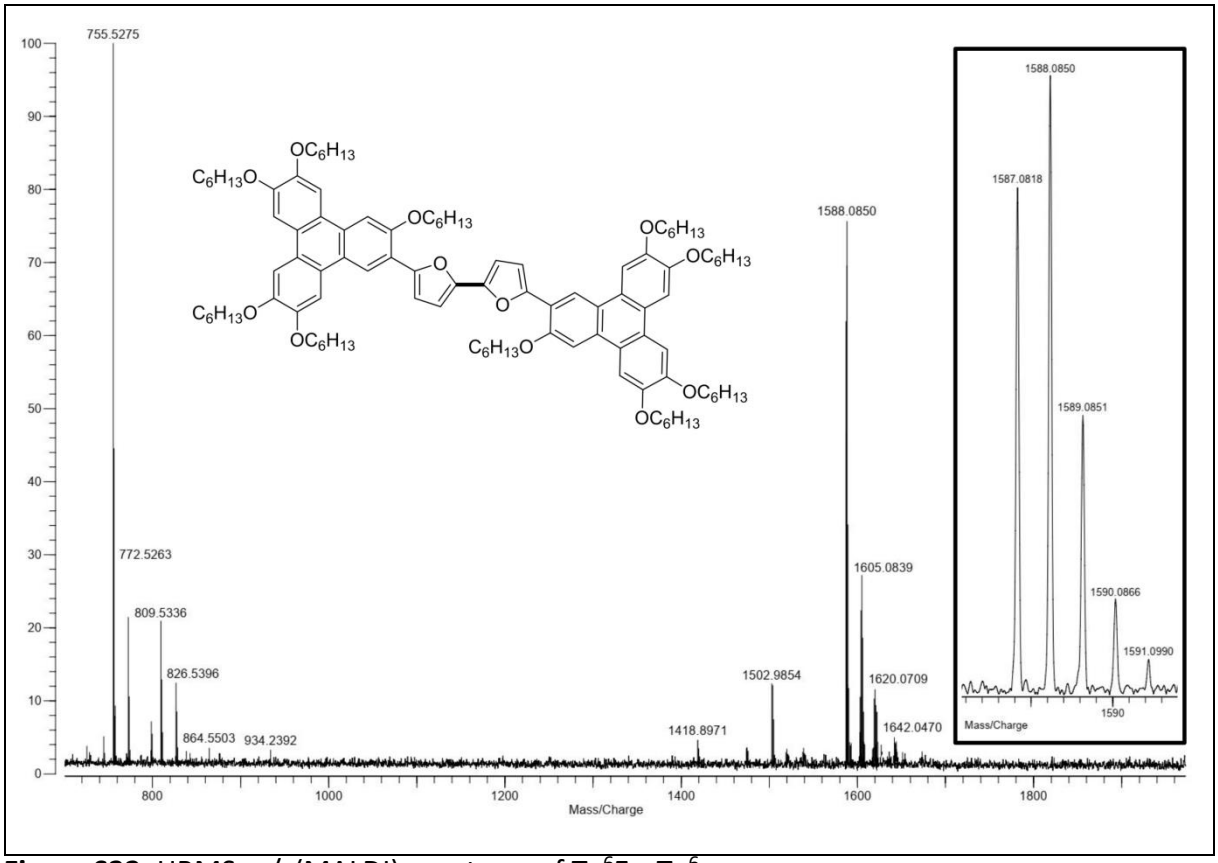

Figure S32. HRMS m/z(MALDI) spectrum of **Tp^{6}Fu$_2$Tp^6.**

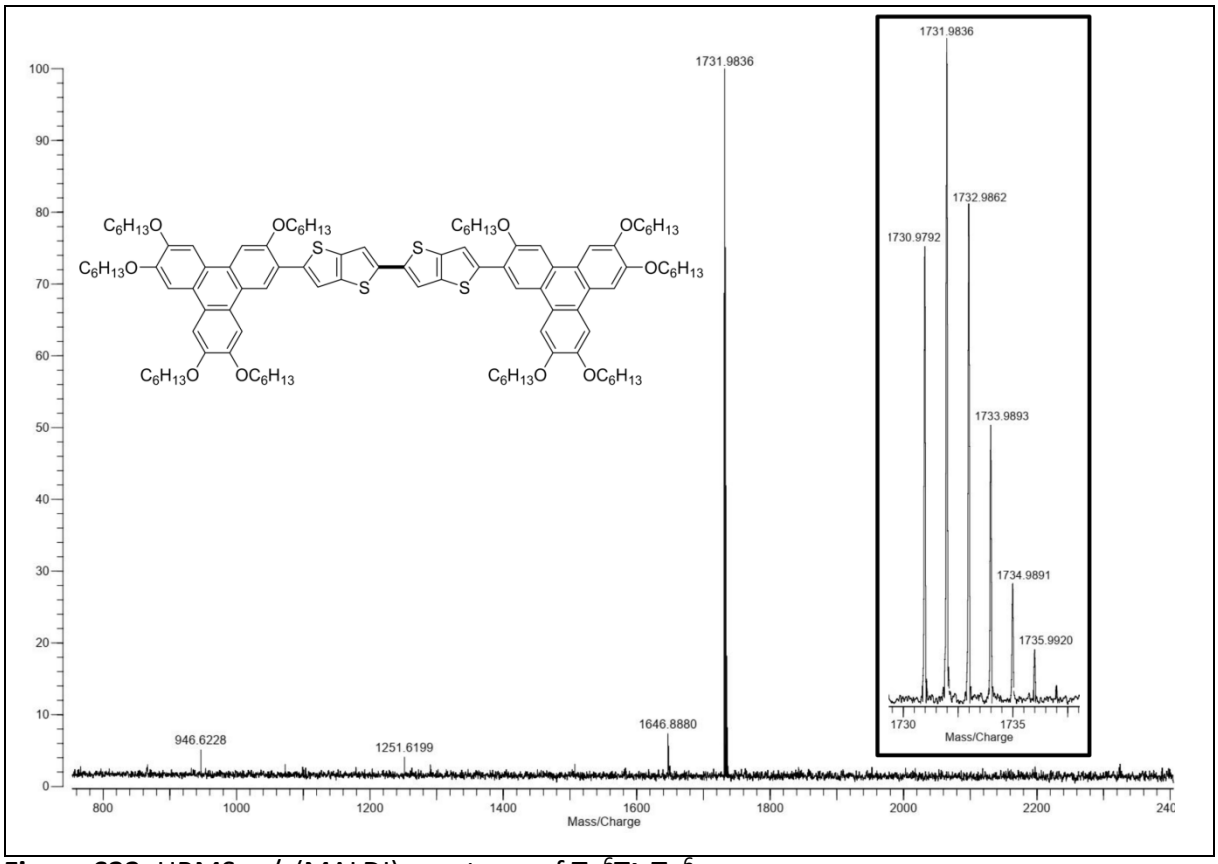

Figure S33. HRMS m/z(MALDI) spectrum of **Tp^{6}Tt$_{2}$Tp^{6}.**

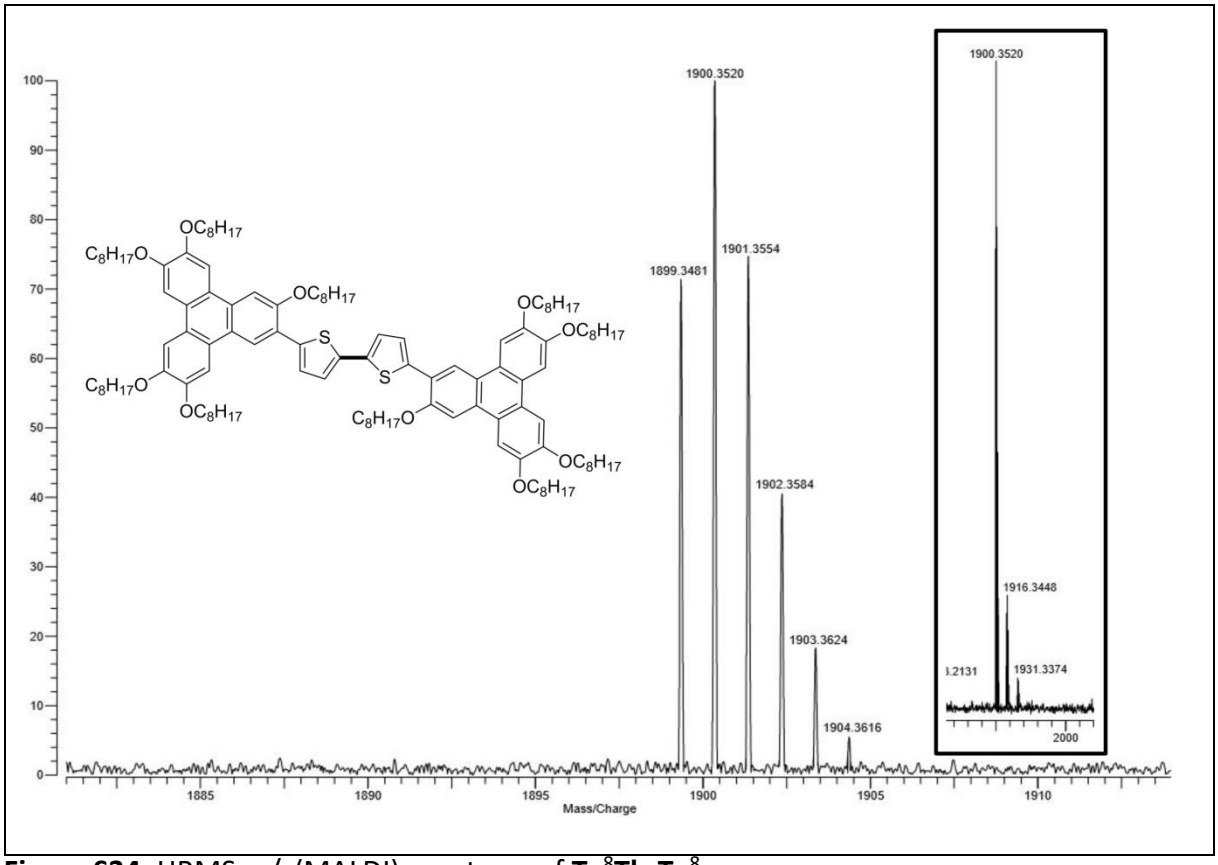

Figure S34. HRMS m/z(MALDI) spectrum of **Tp^{8}Th$_{2}$Tp^{8}.**

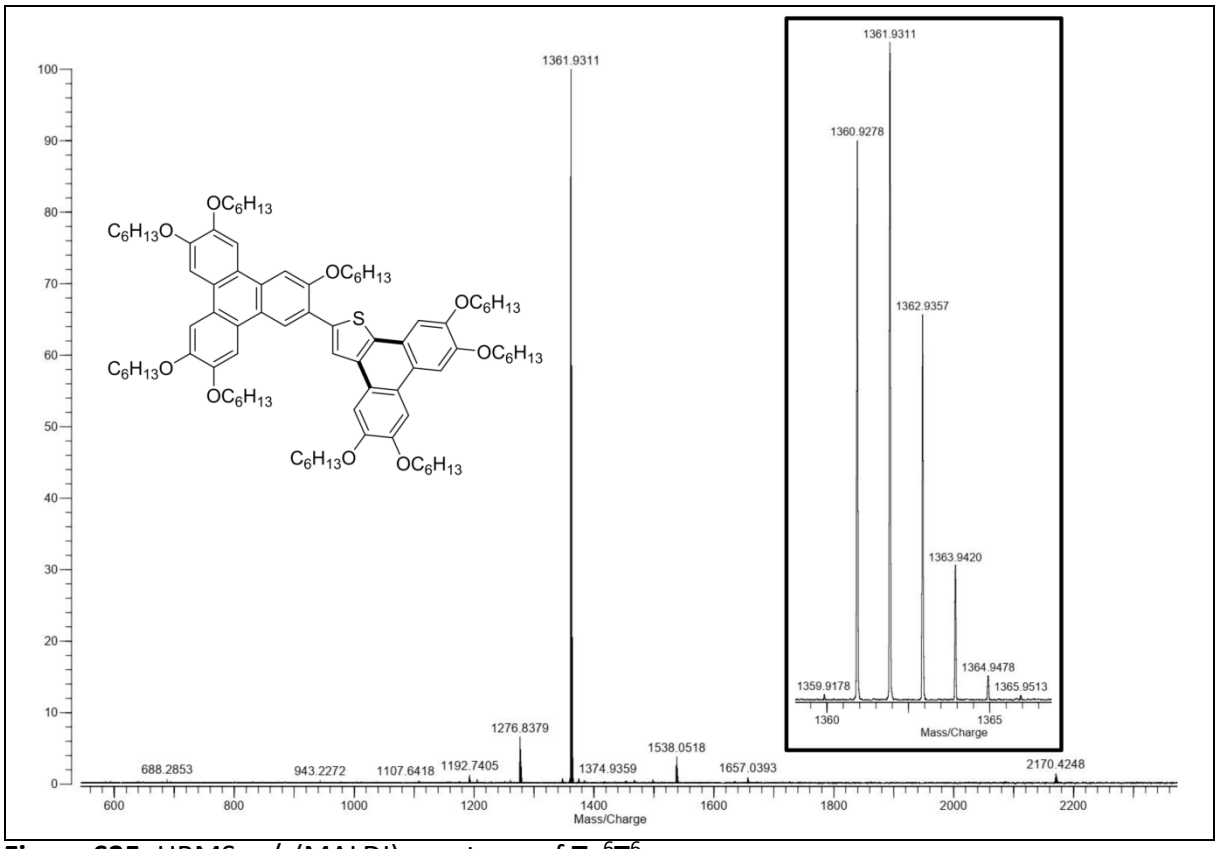

Figure S35. HRMS m/z(MALDI) spectrum of **Tp^{6}T^6.**

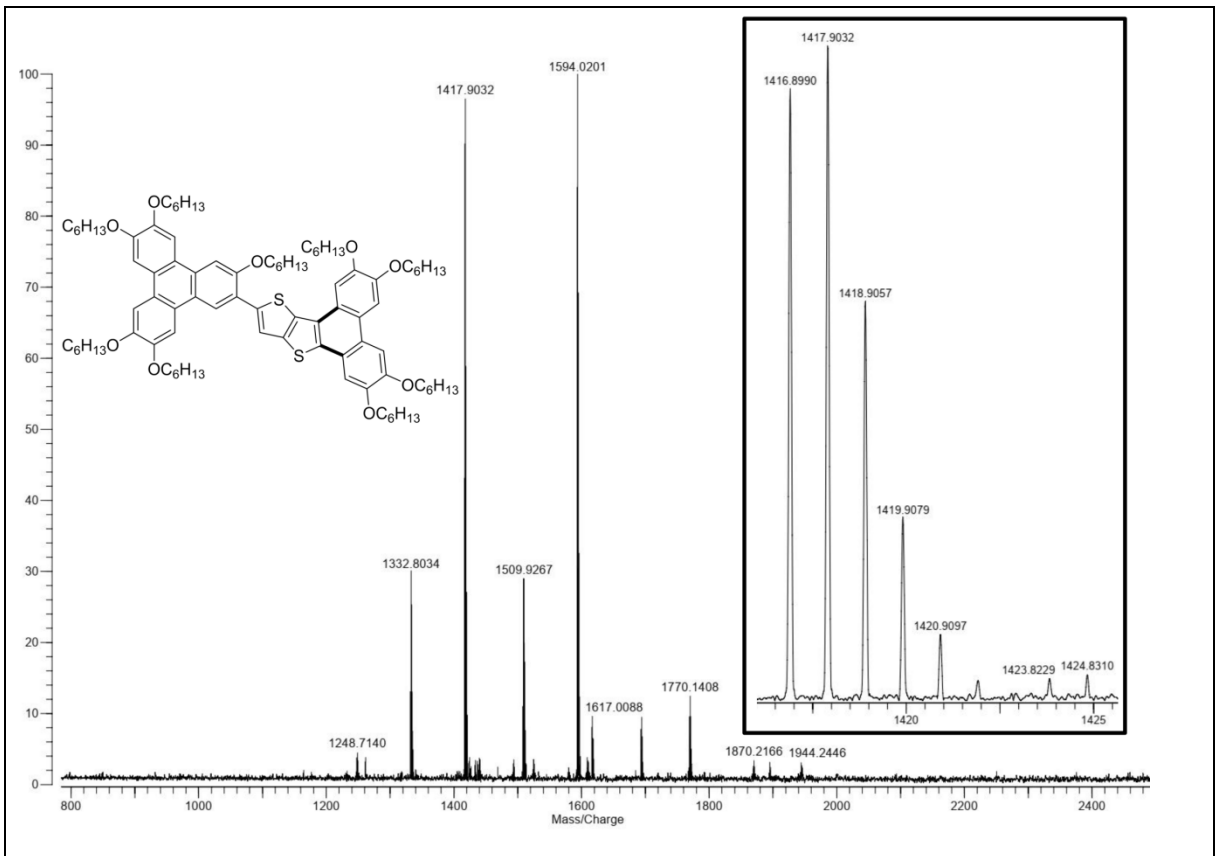

Figure S36. HRMS m/z(MALDI) spectrum of **Tp^{6}Dt^6.**

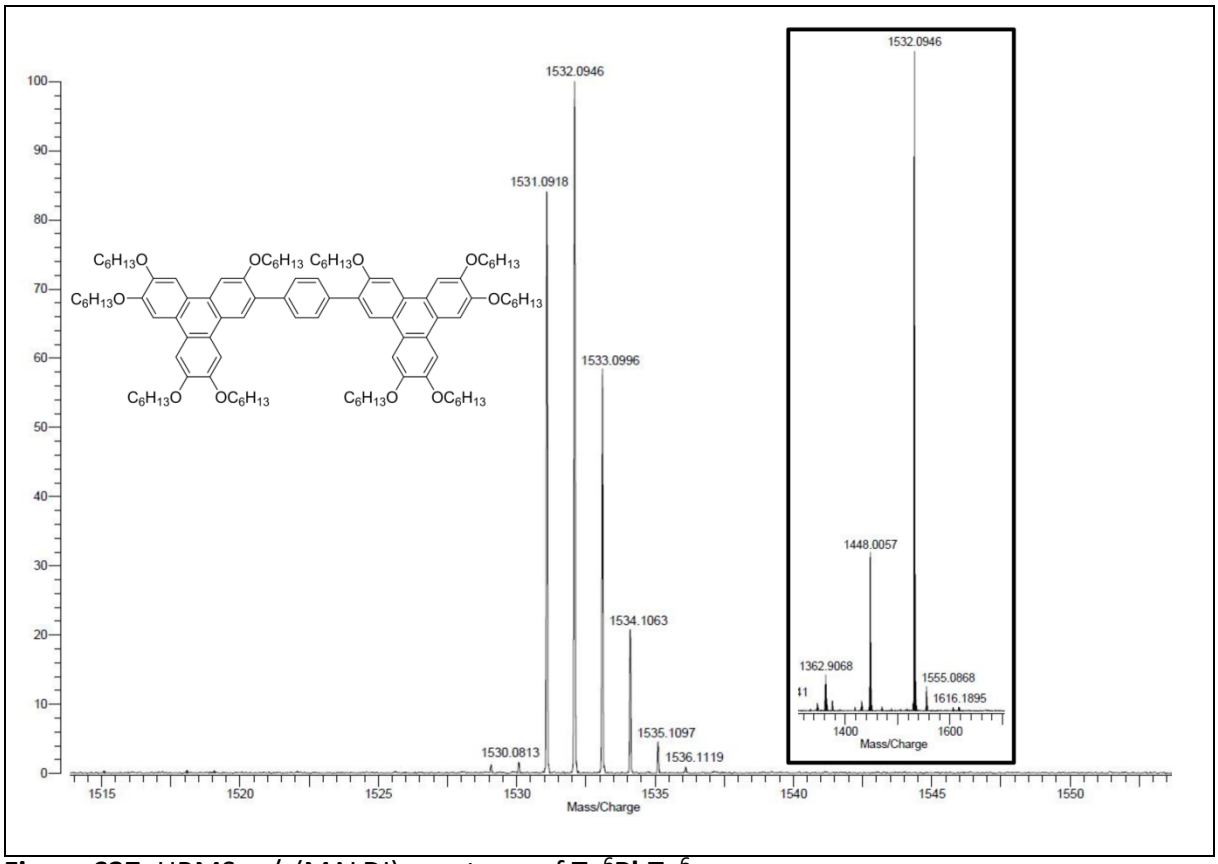

Figure S37. HRMS m/z(MALDI) spectrum of **Tp^{6}PhTp^{6}.**

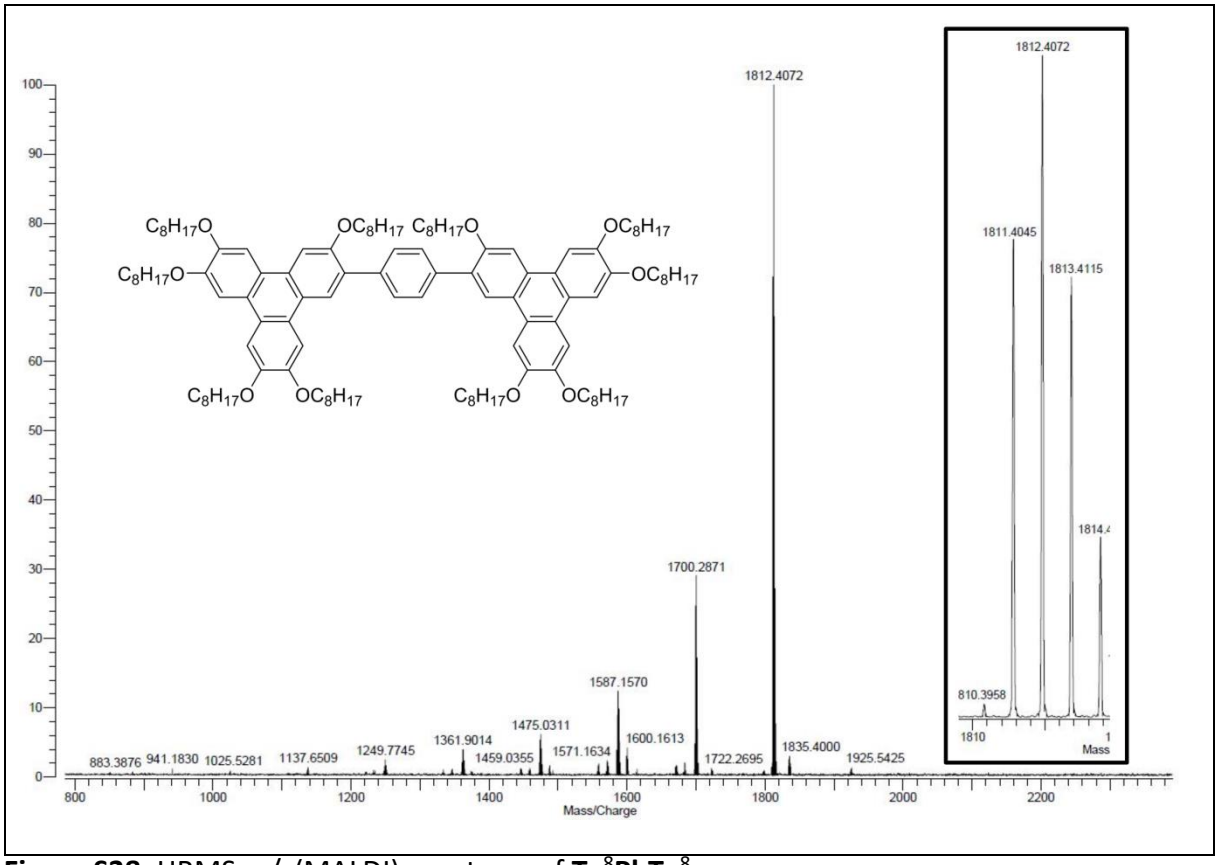

Figure S38. HRMS m/z(MALDI) spectrum of **Tp^{8}PhTp^{8}.**

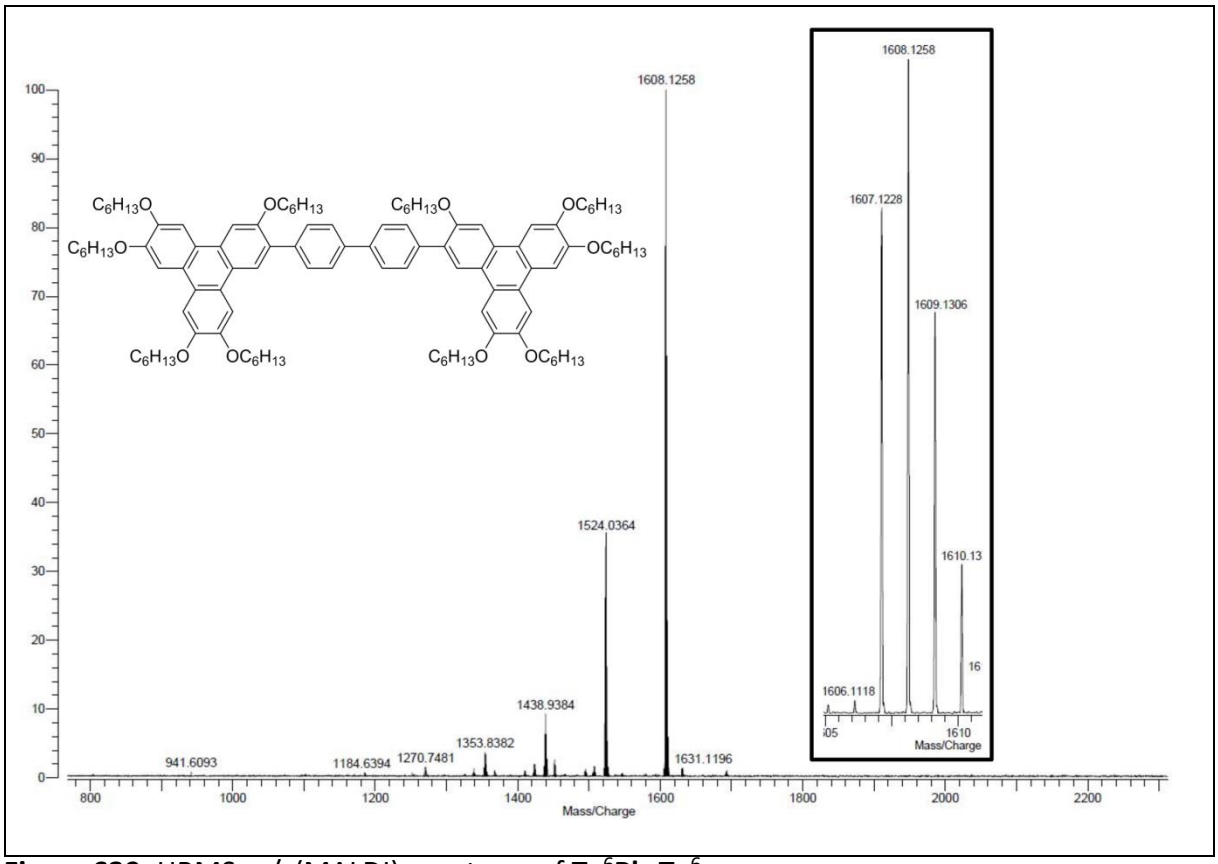

Figure S39. HRMS m/z(MALDI) spectrum of **Tp^{6}Ph$_2$Tp^{6}.**

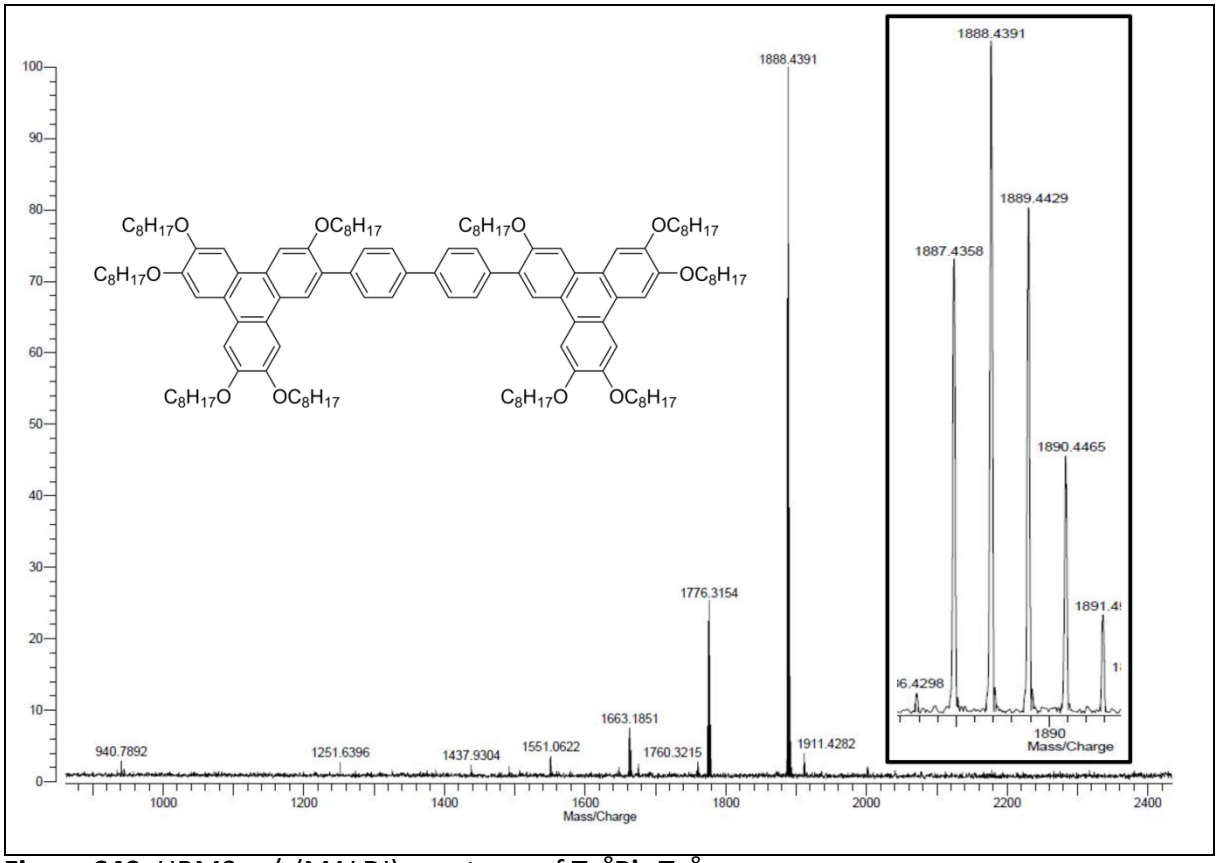

Figure S40. HRMS m/z(MALDI) spectrum of **Tp^{8}Ph$_2$Tp^{8}.**

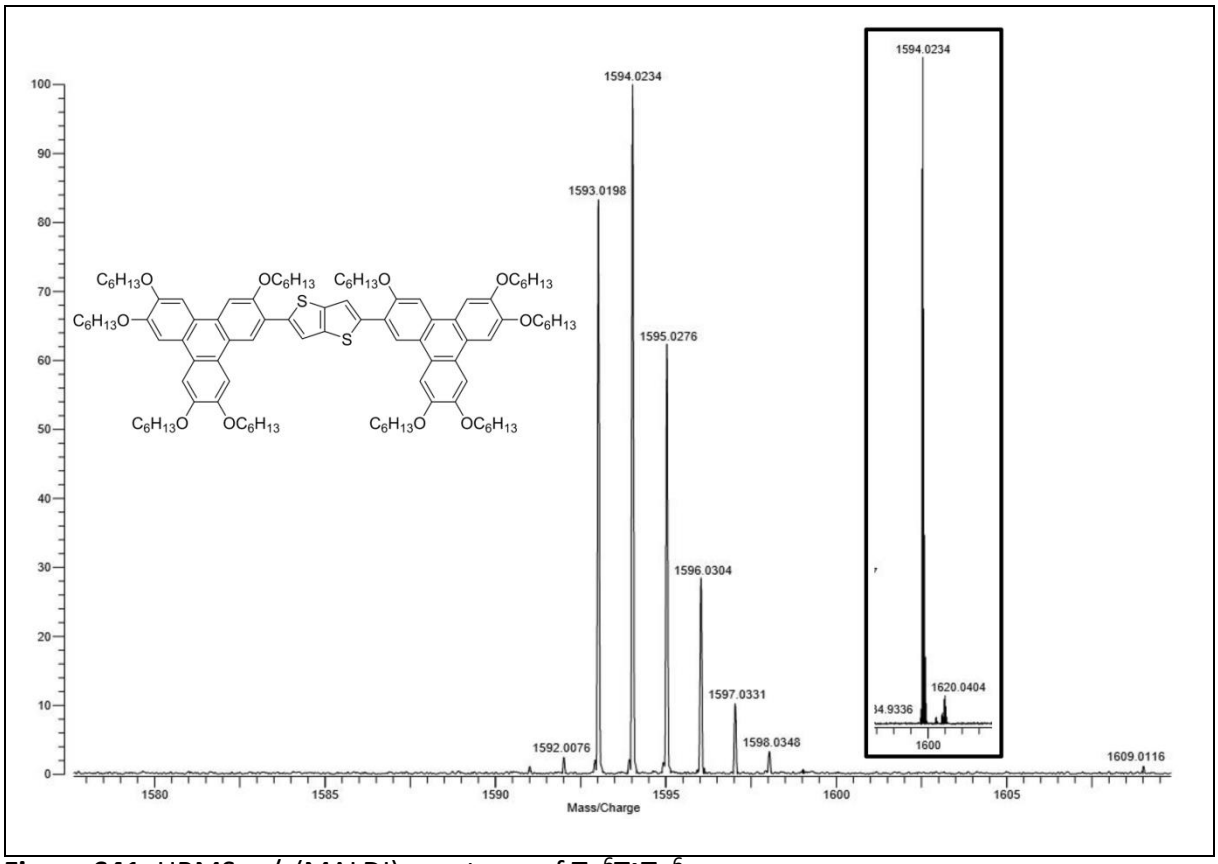

Figure S41. HRMS m/z(MALDI) spectrum of **Tp^{6}TtTp^{6}.**

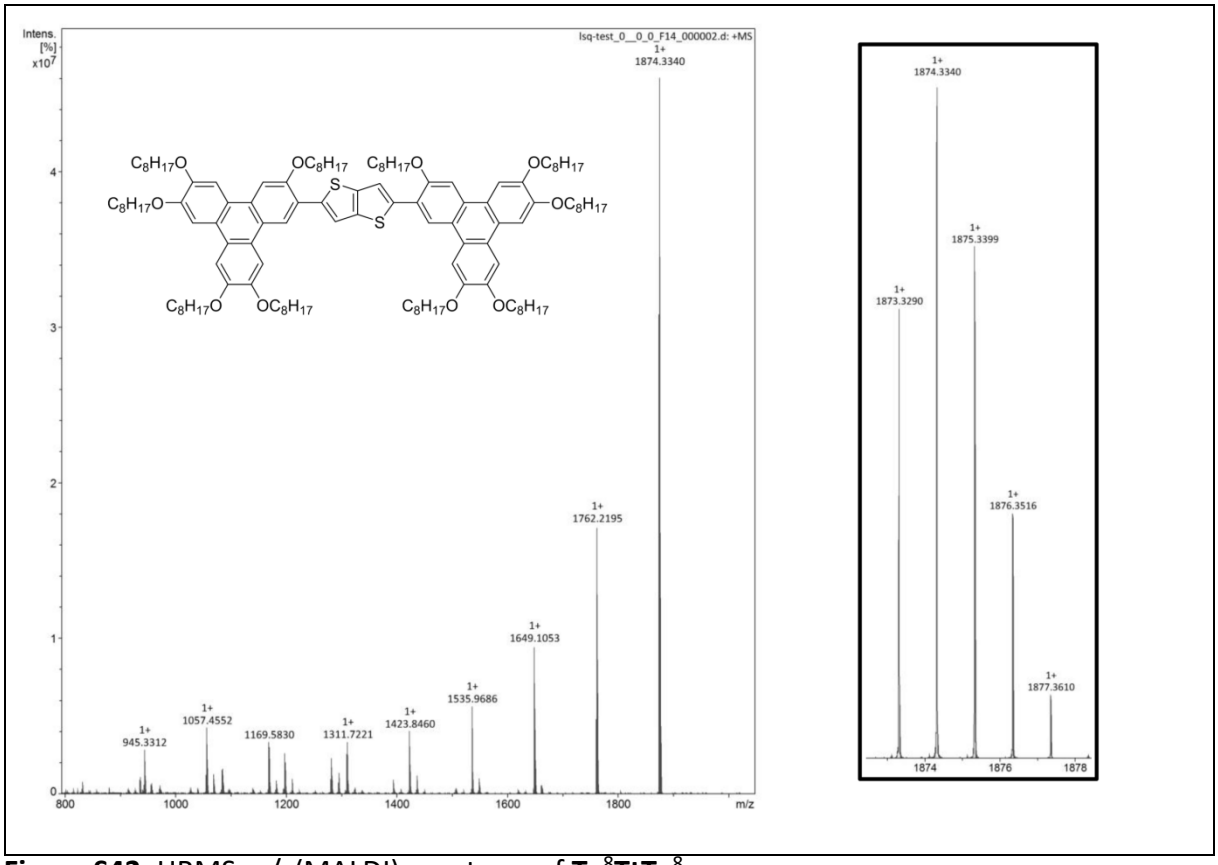

Figure S42. HRMS m/z(MALDI) spectrum of **Tp^{8}TtTp^{8}.**

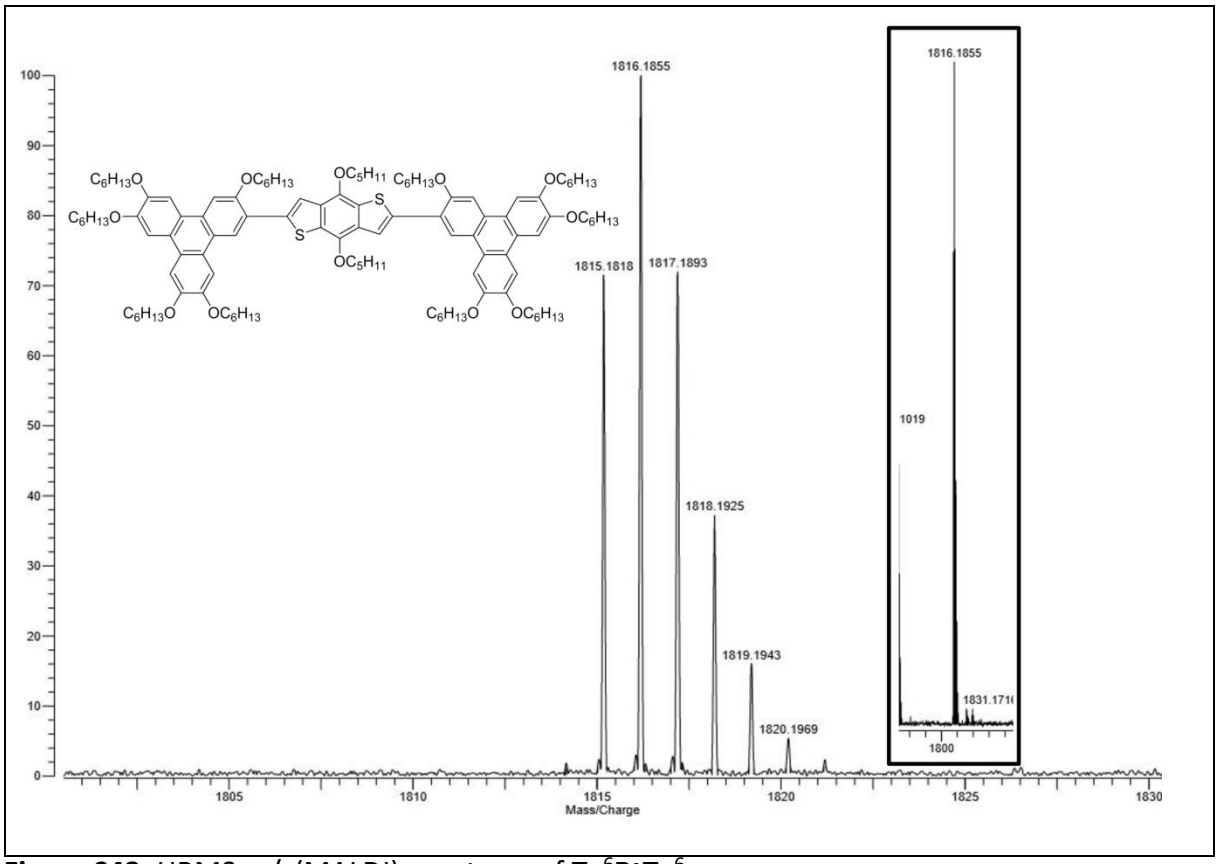

Figure S43. HRMS m/z(MALDI) spectrum of **Tp^{6}BtTp^{6}.**

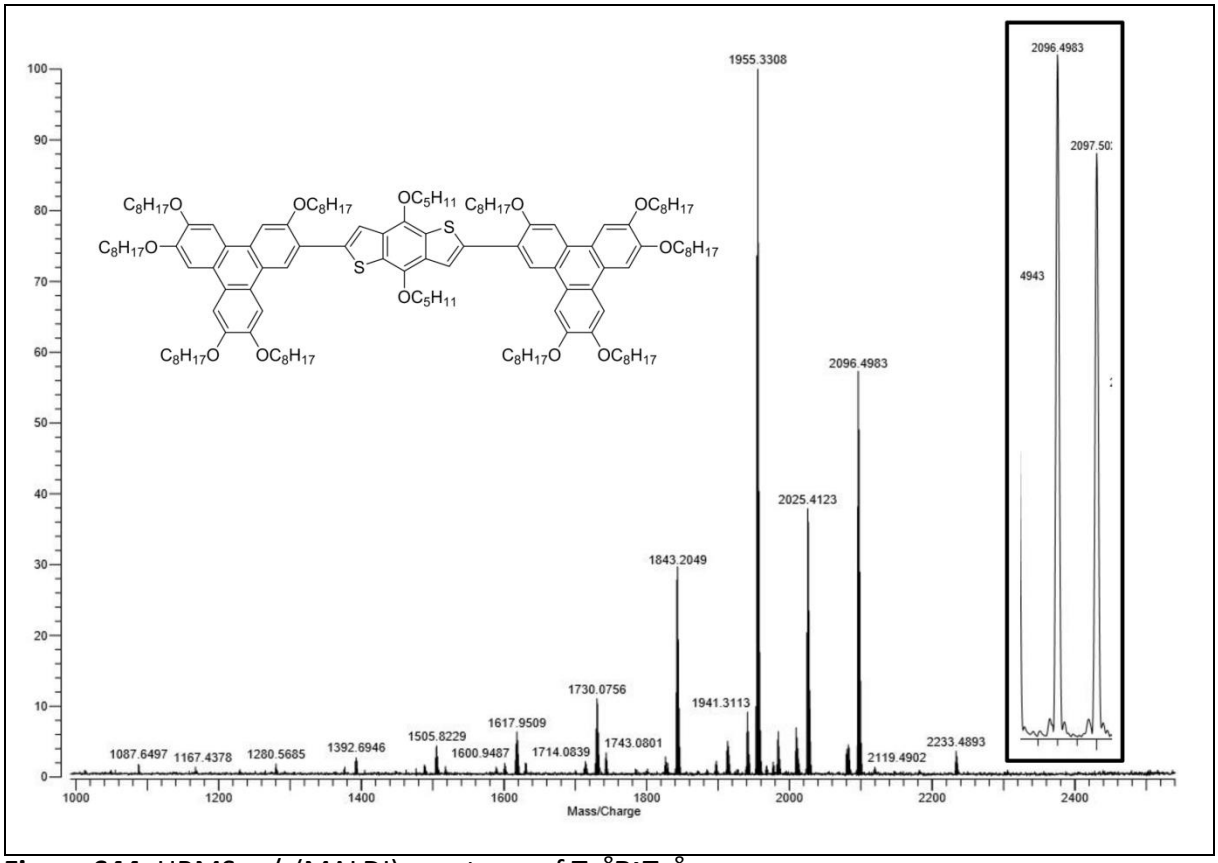

Figure S44. HRMS m/z(MALDI) spectrum of **Tp^{8}BtTp^{8}.**

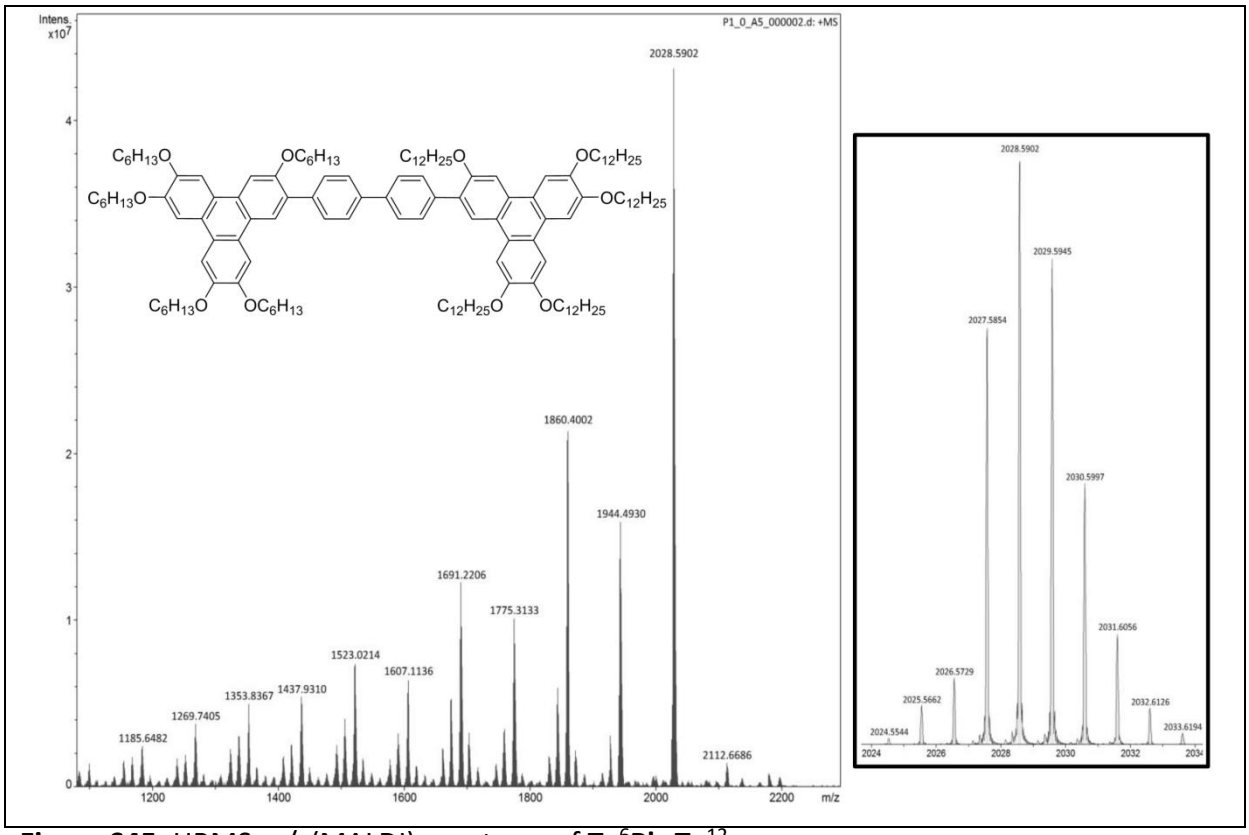

Figure S45. HRMS m/z(MALDI) spectrum of **Tp^{6}Ph$_2$Tp^{12}.**

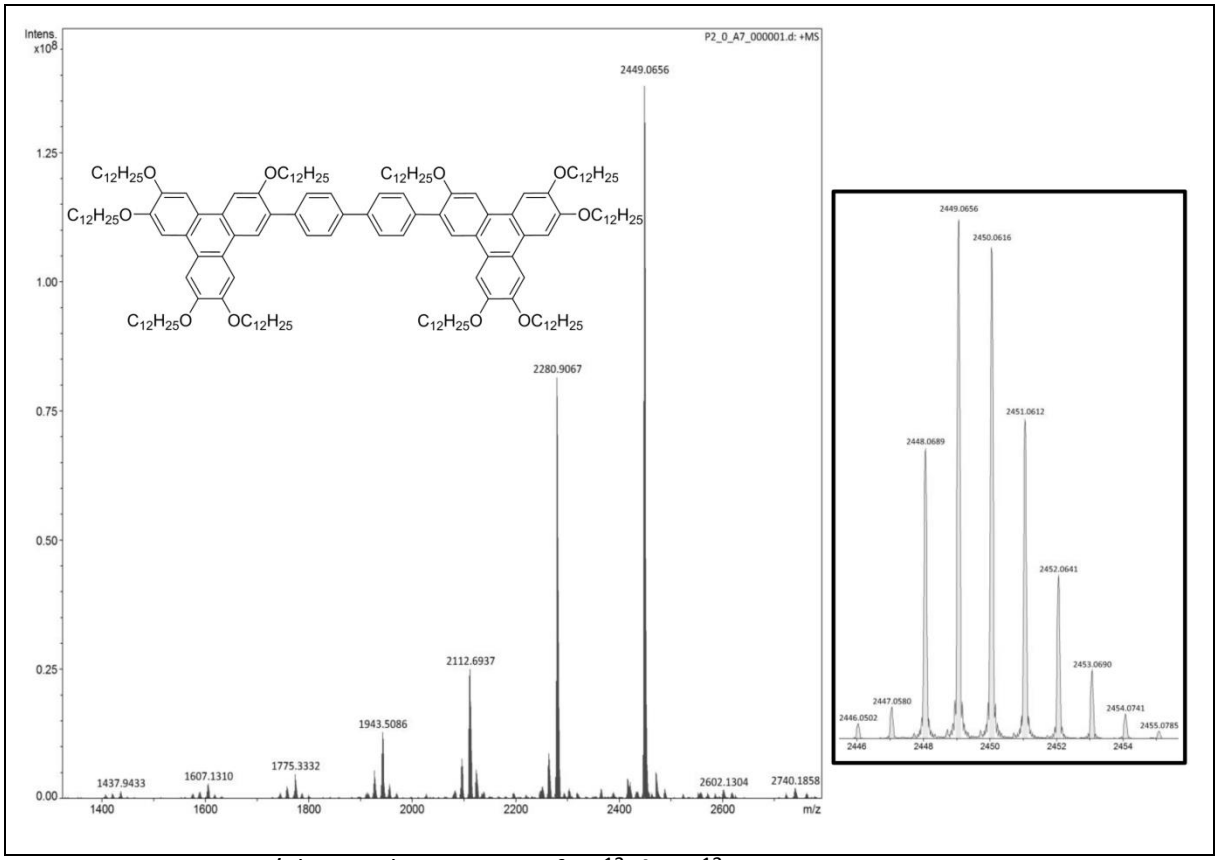

Figure S46. HRMS m/z(MALDI) spectrum of **Tp^{12}Ph$_2$Tp^{12}.**

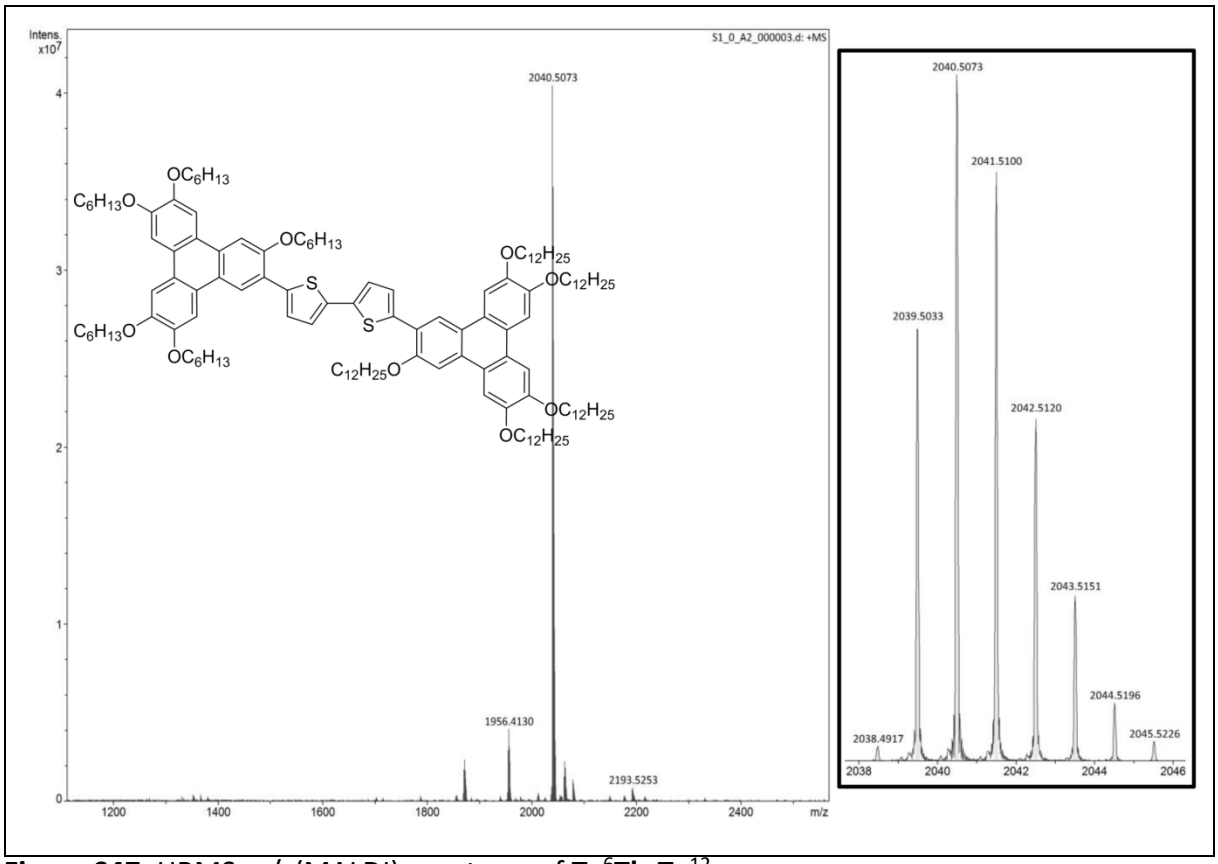

Figure S47. HRMS m/z(MALDI) spectrum of **Tp^{6}Th$_2$Tp^{12}.**

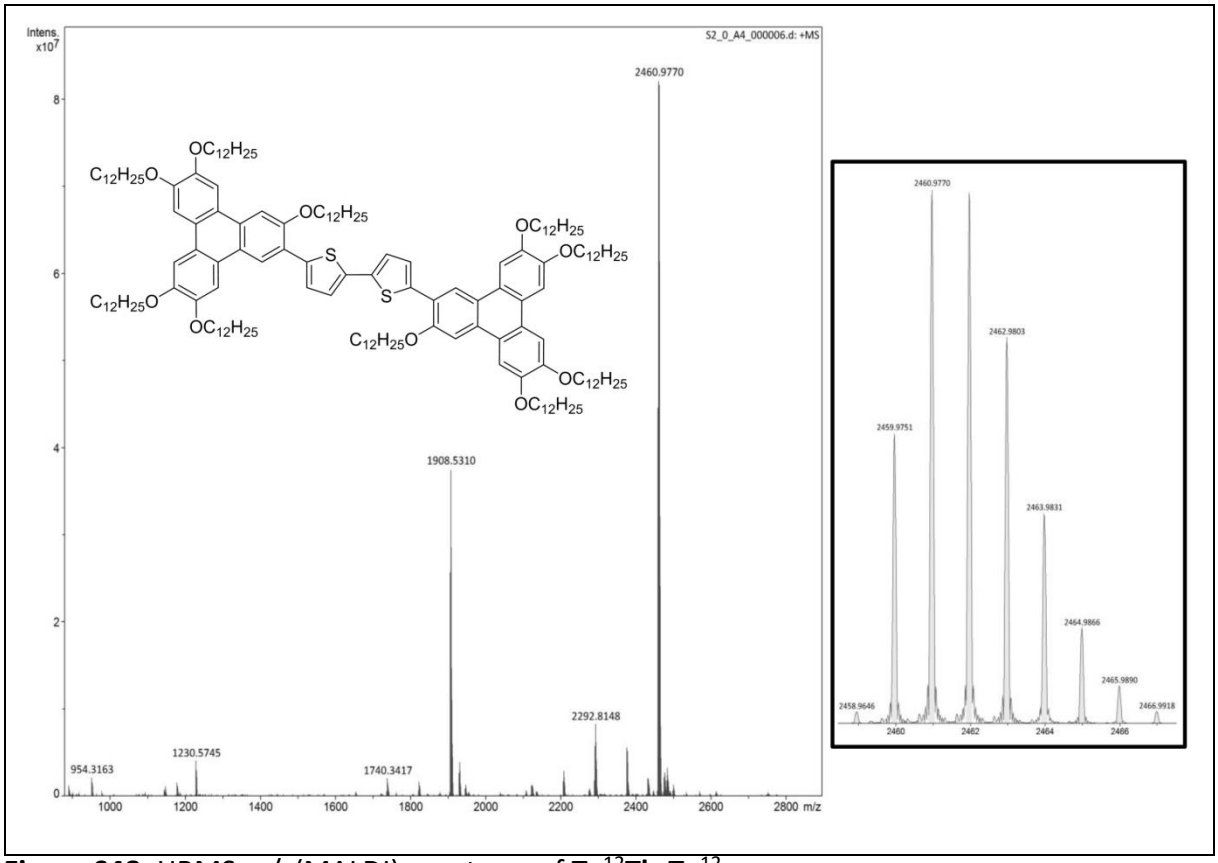

Figure S48. HRMS m/z(MALDI) spectrum of **Tp^{12}Th$_2$Tp^{12}.**

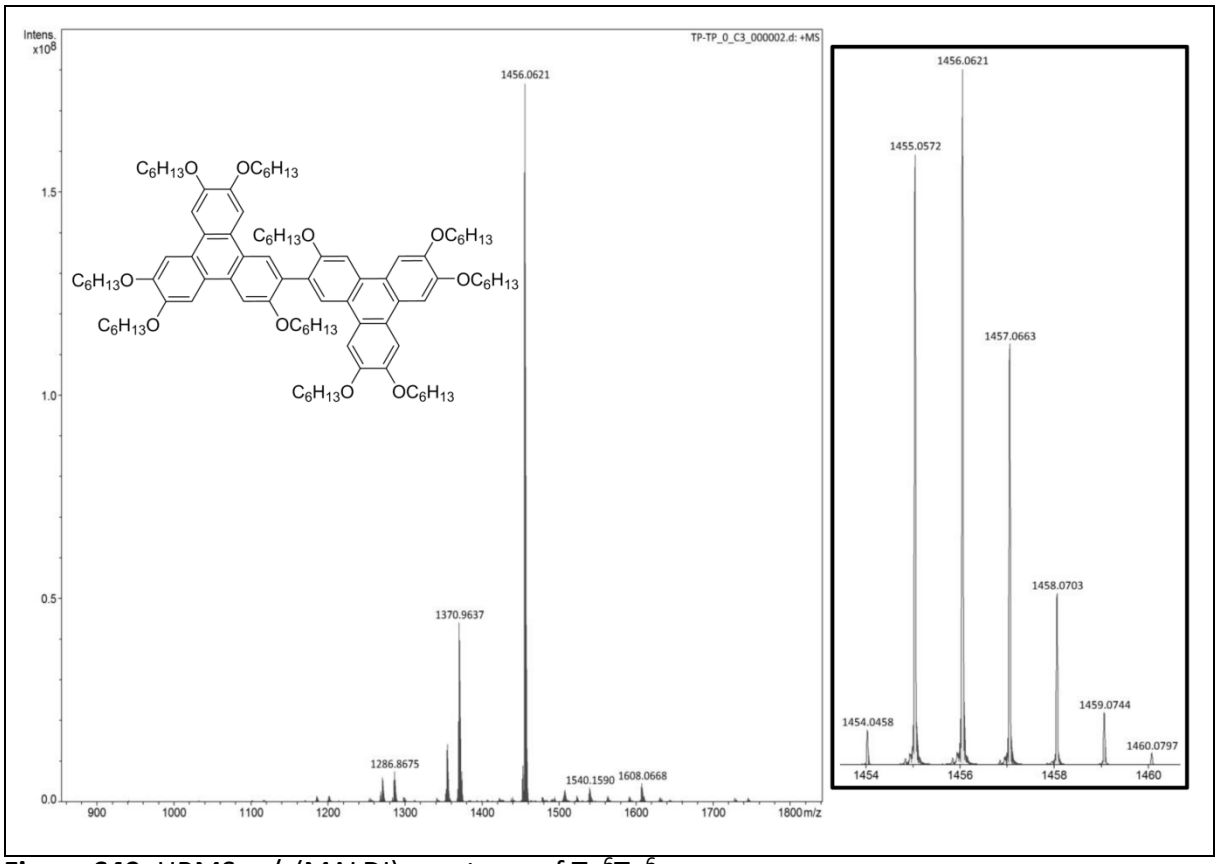

Figure S49. HRMS m/z(MALDI) spectrum of **Tp^{6}Tp^6.**

5. UV-Vis absorption and photoluminescence

Table S1. Summary of the UV/vis absorption[a] and fluorescence spectroscopic properties of the monomers in solution[b] and films[c].

Compound	λ_{abs} (nm)	ε (×10^4, L mol^{-1}cm^{-1})	λ_{em} (nm) solution	λ_{em} (nm) film	QY[d] [%] solution
M1	261 290 345	4.60 8.74 2.52	400 412	420 431	19.70
M2	252 262 284 320 337	2.34 3.07 7.73 1.79 1.35	391 403	406	15.87
M3	261 290 334 349 378	4.09 10.61 3.00 3.13 0.40	391 409	411 492	25.18
M4	263 294 359	5.10 6.78 3.45	401 422	437 459 483	30.05
M5	261 290 346	4.68 8.63 2.47	401 411	436	19.10

M0-1	260	5.87	370	---	---
	269	8.81	391		
	278	12.24	412		
	309	3.11			
M0-2	260	5.49	371	---	---
	269	8.06	391		
	278	10.98	412		
	309	2.82			

[a] UV-vis absorption measured in THF solution with a concentration of 1×10^{-5} mol L^{-1} (λ in nm, absorption coefficient, ε, in $\times10^4$ L $mol^{-1}cm^{-1}$). [b] In micromolar THF solutions with solution concentration of 1×10^{-5} mol L^{-1}. Excitation wavelength: 310 nm for all monomers. [c] The thin films were obtained by drop-casting dilute THF solution and evaporation of solvent. Excitation wavelength: 320 nm for **M3** and 340 nm for others. [d] Quantum yields (QY) in % were measured with solution concentration of 1×10^{-5} mol L^{-1} in THF excited at 310 nm as well.

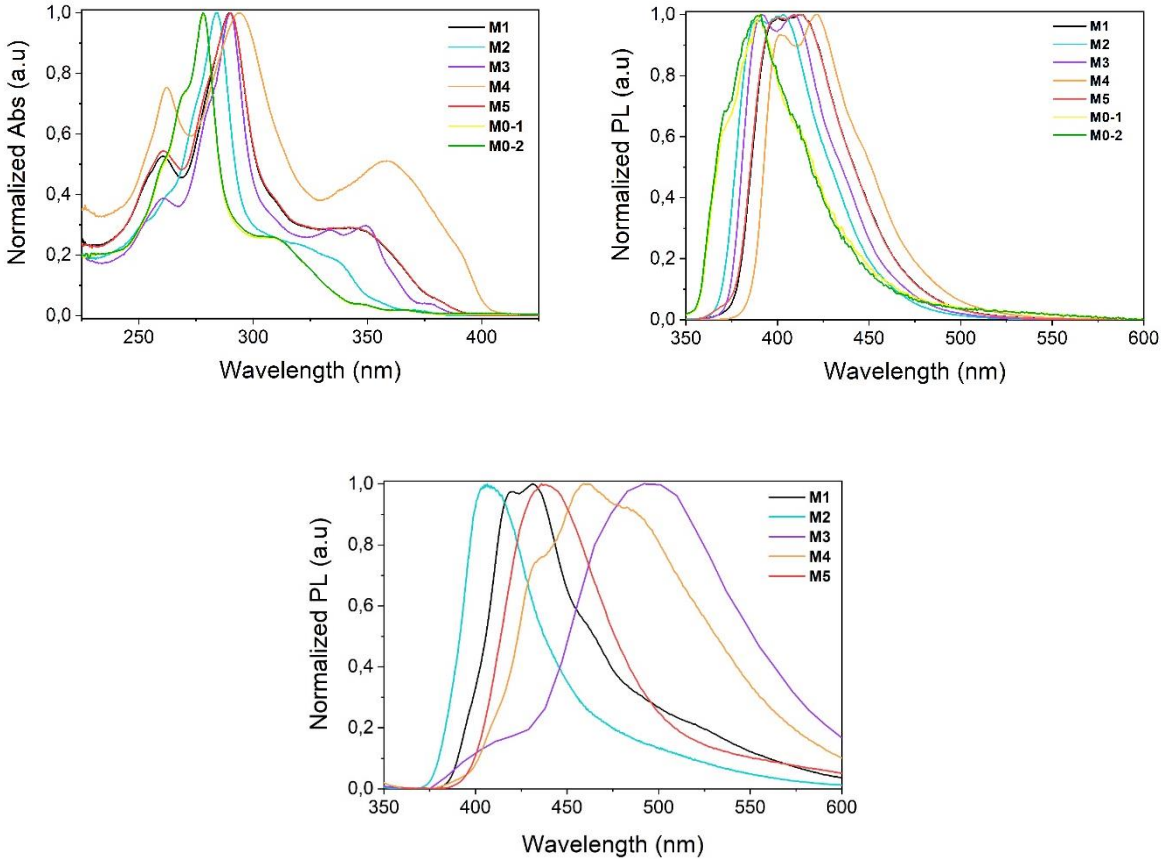

Figure S50. Absorption and photoluminescence of the monomeric precursors. From top to bottom: UV/Vis absorption spectra; photoluminescence spectra in micromolar THF solution; and photoluminescence spectra in thin-films.

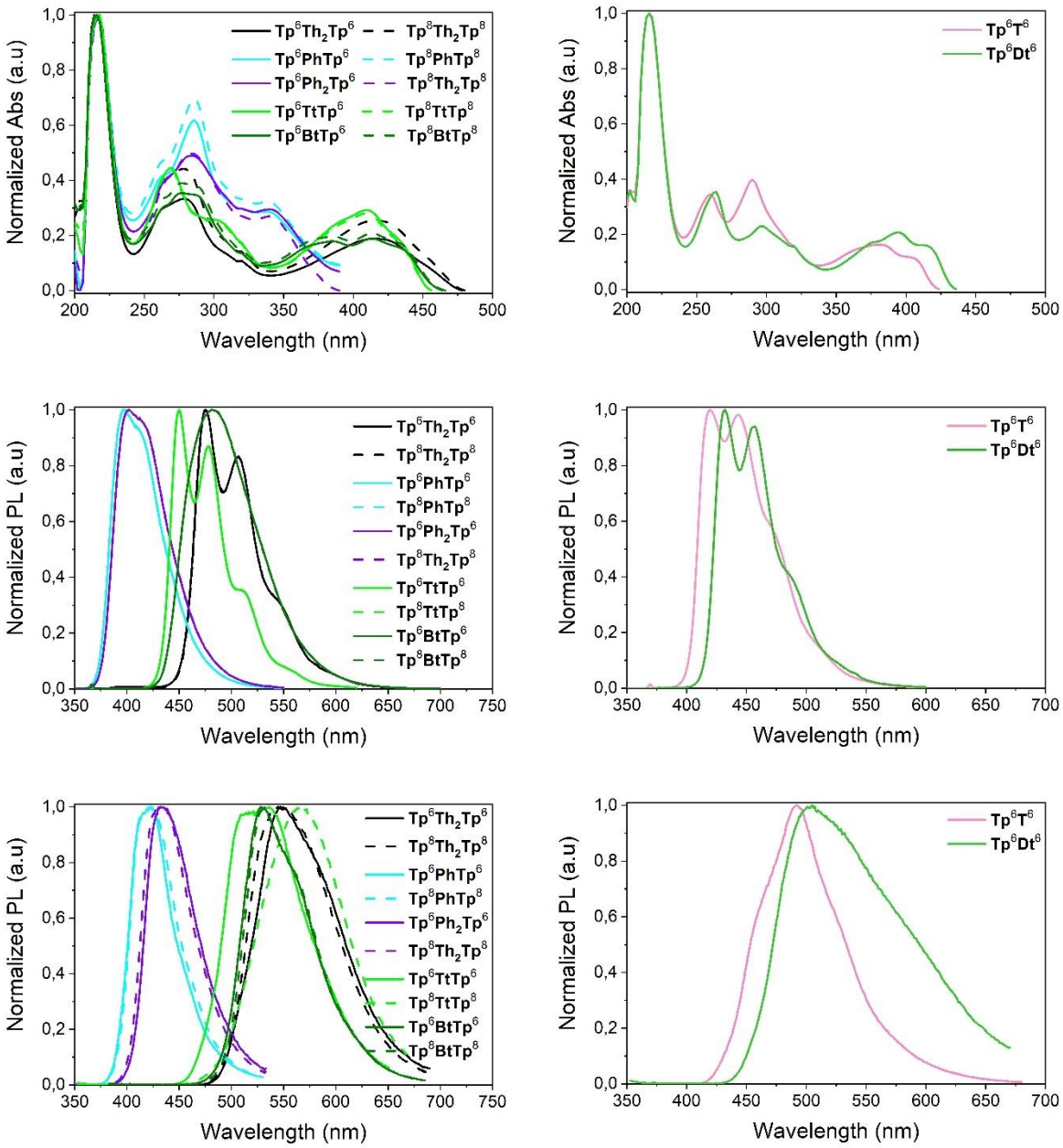

Figure S51. From top to bottom, and left to right: UV/Vis absorption spectra; photoluminescence spectra in micromolar THF solution; and photoluminescence spectra in thin-films of symmetrical dimeric compounds (effect of the chain-length, n = 6 and 8) and for unsymmetrical dimers **Tp^{6}T^6** and **Tp^{6}Dt^6** (effect of the chain-length).

Table S2. Summary of the UV/vis absorption[a] and fluorescence spectroscopic properties of the unsymmetrical dimeric compounds in solution[b] and films[c].

Compound	λ_{abs}[a]	ε[a]	λ_{em}[b]	λ_{em}[c]	QY[d] [%] solution
Tp^{6}T^6	216	28.01	419 443 472	492	26.82
	260	9.68			
	290	11.16			
	320	4.43			
	382	4.57			
	404	3.28			

	216	27.20			
	264	9.68			
	296	6.31	432		
Tp^{6}Dt^6	320	4.33	457	505	45.12
	376	4.72	487		
	394	5.70			
	414	4.43			

[a] UV-vis absorption measured in THF solution with a concentration of 1×10^{-5} mol L^{-1} (λ_{abs} in nm, absorption coefficient, ε, in $\times10^4$ L mol^{-1}cm^{-1}). [b] Emission (λ_{em} in nm) in THF solutions with solution concentration of 1×10^{-5} mol L^{-1}. Excitation wavelength: 370 nm for **Tp^{6}T^6**; 270 nm for **Tp^{6}Dt^6**. [c] Emission (λ_{em} in nm) in thin films. The thin films were obtained by drop-casting dilute THF solution and evaporation of solvent. Excitation wavelength: 370 nm for **Tp^{6}T^6**; 340 nm for **Tp^{6}Dt^6**. [d] Quantum yields (QY) in % were measured with solution concentration of 1×10^{-5} mol L^{-1} in THF excited at different wavelengths (with the same excitation wavelengths used for [b]).

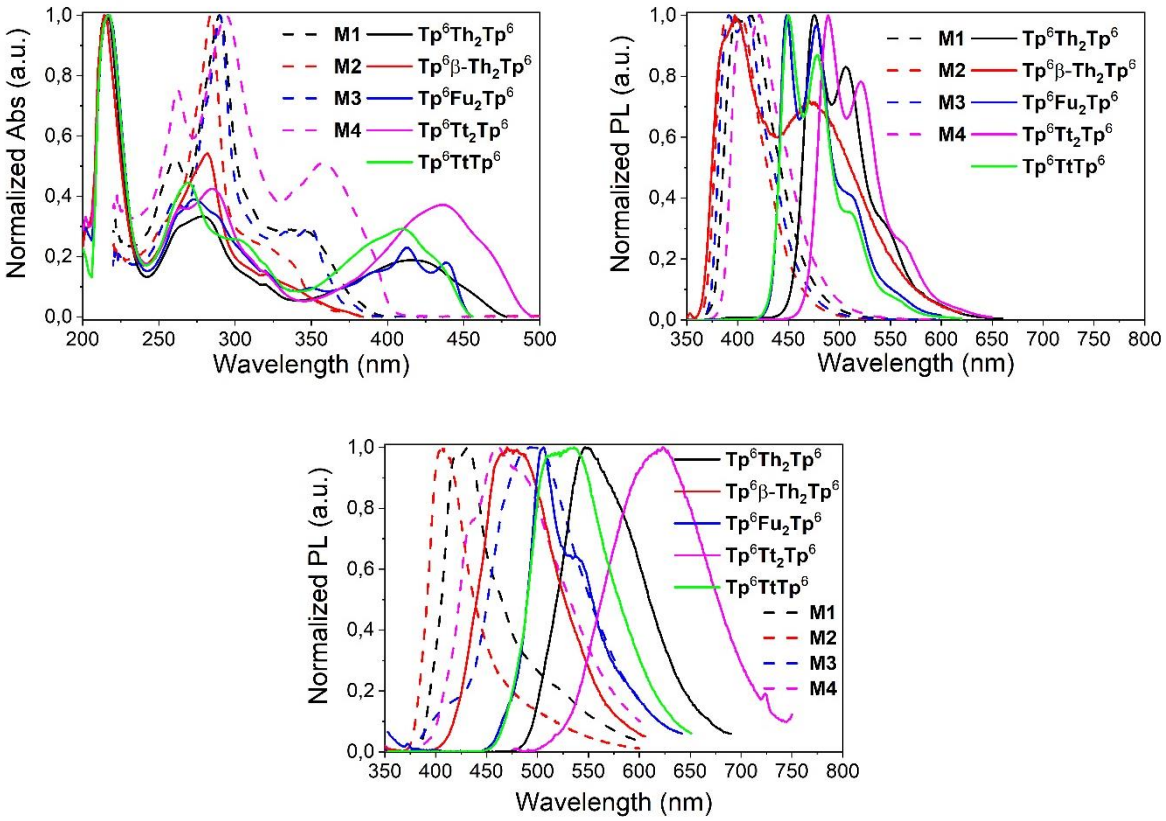

Figure S52. Comparison of the absorption and photoluminescence (solution and film) of the monomeric precursors and corresponding p-bridged dimers.

6. Gels and xerogels

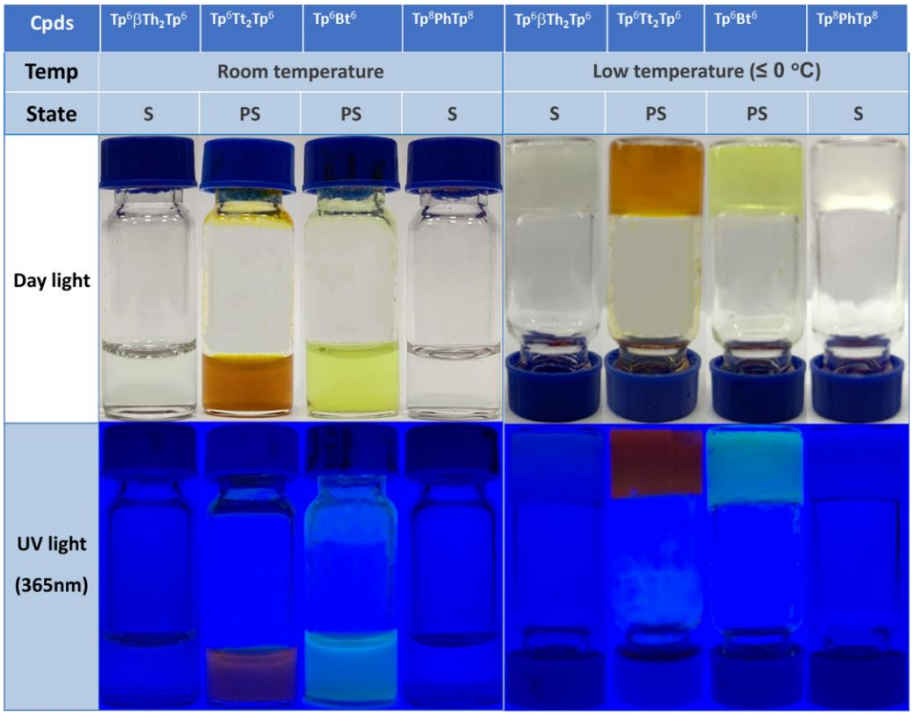

Figure S53. Effect of temperature on gel formation in day light (top) and under UV irradiation (365 nm, bottom). S and PS indicate the state of the mixture corresponding to solution and poor solution, respectively. The numbers in brackets correspond to the critical (minimum) gelation concentration (CGC/MGC) in mg mL^{-1}.

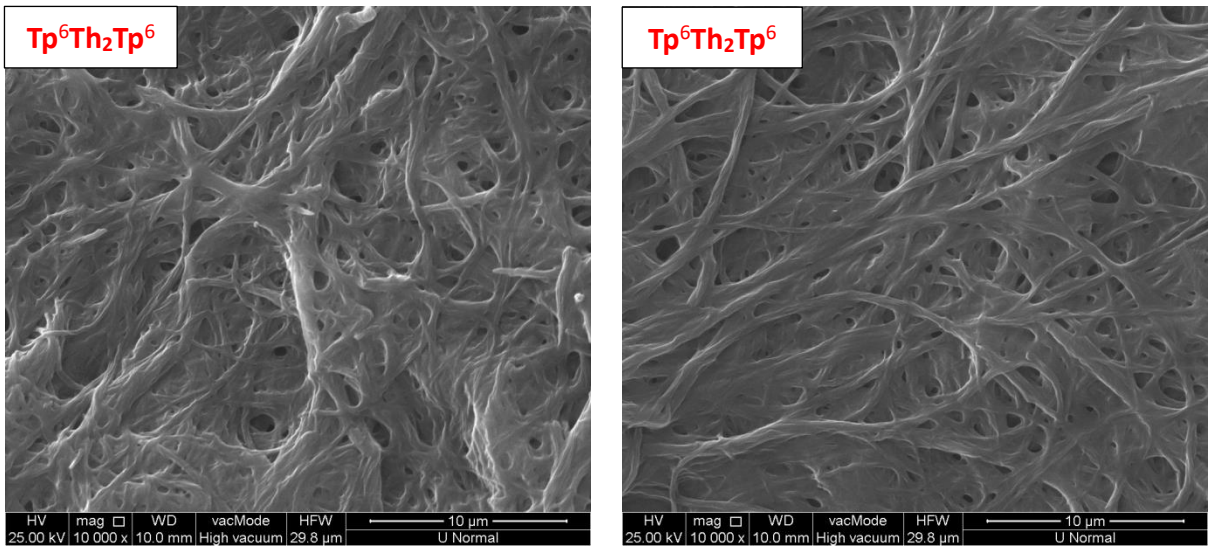

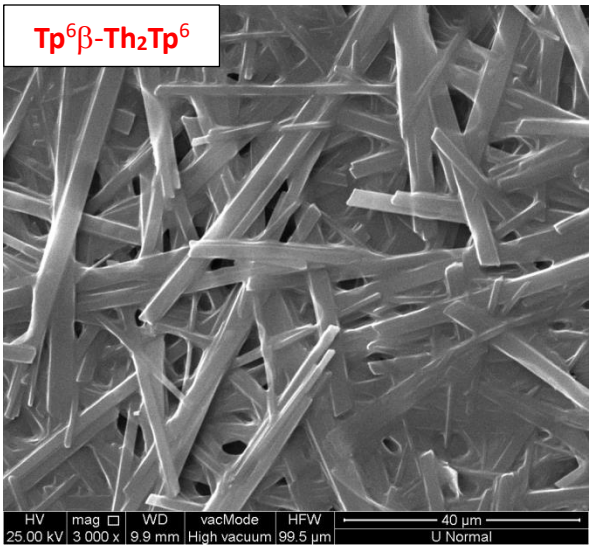
Tp⁶β-Th₂Tp⁶
HV 25.00 kV
mag 3 000 x
WD 9.9 mm
vacMode High vacuum
HFW 99.5 µm
40 µm
U Normal

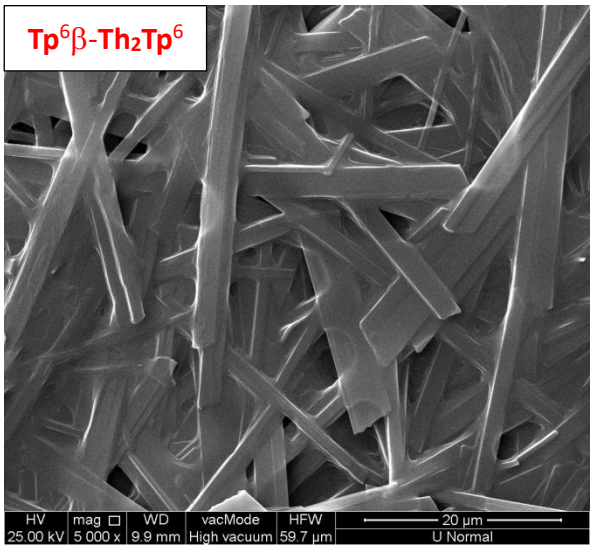
Tp⁶β-Th₂Tp⁶
HV 25.00 kV
mag 5 000 x
WD 9.9 mm
vacMode High vacuum
HFW 59.7 µm
20 µm
U Normal

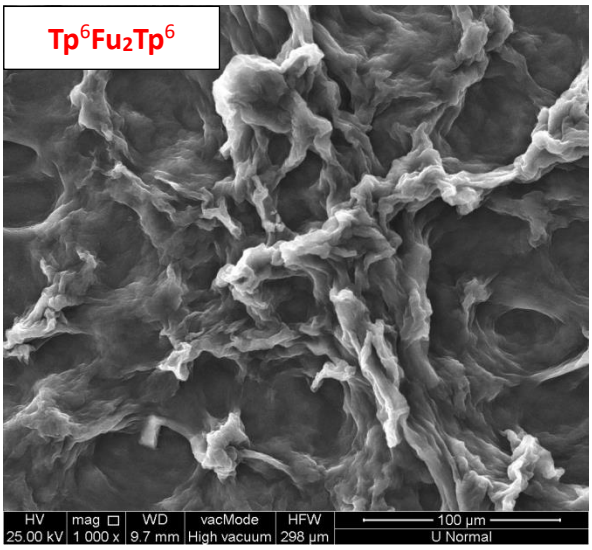
Tp⁶Fu₂Tp⁶
HV 25.00 kV
mag 1 000 x
WD 9.7 mm
vacMode High vacuum
HFW 298 µm
100 µm
U Normal

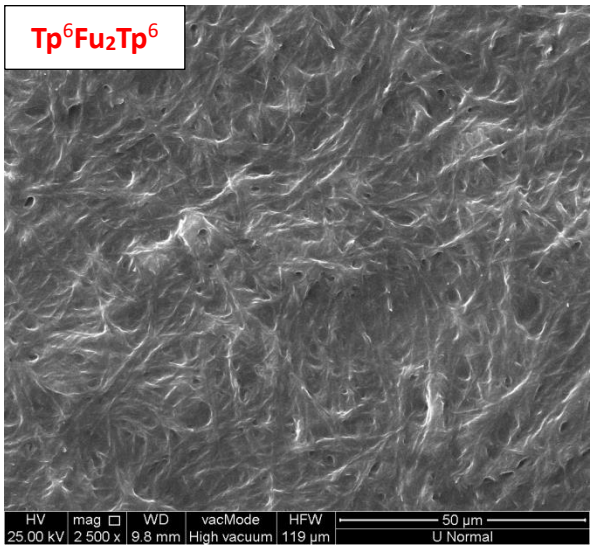
Tp⁶Fu₂Tp⁶
HV 25.00 kV
mag 2 500 x
WD 9.8 mm
vacMode High vacuum
HFW 119 µm
50 µm
U Normal

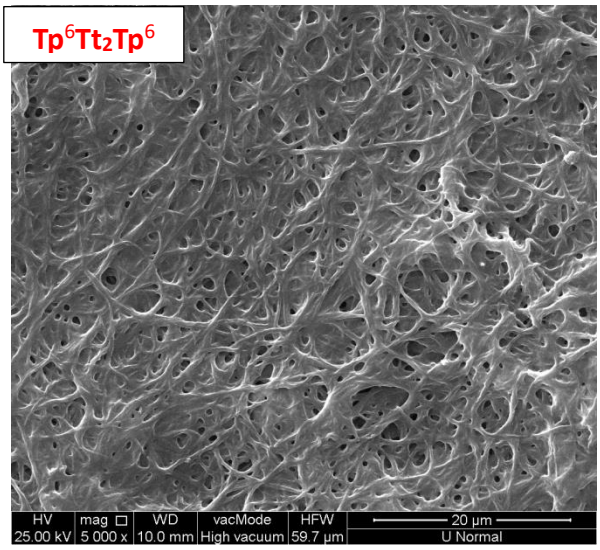
Tp⁶Tt₂Tp⁶
HV 25.00 kV
mag 5 000 x
WD 10.0 mm
vacMode High vacuum
HFW 59.7 µm
20 µm
U Normal

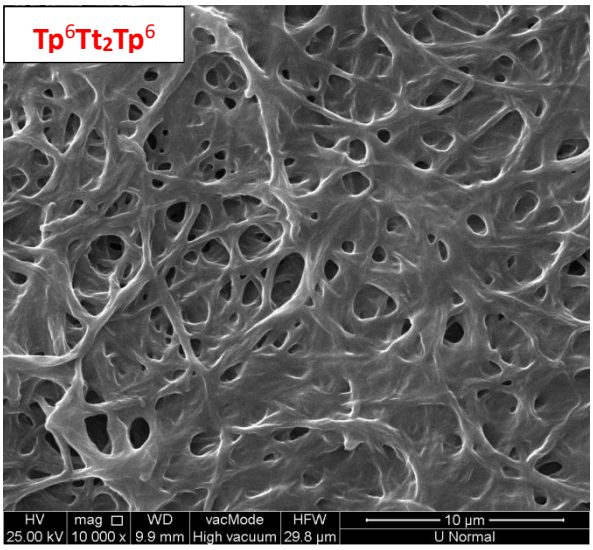
Tp⁶Tt₂Tp⁶
HV 25.00 kV
mag 10 000 x
WD 9.9 mm
vacMode High vacuum
HFW 29.8 µm
10 µm
U Normal

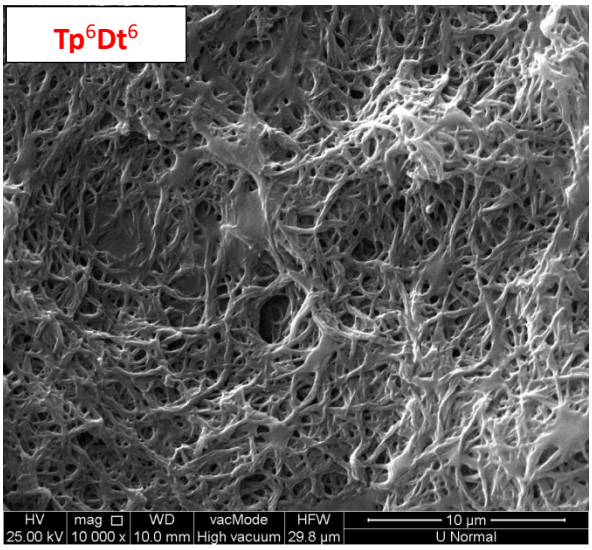
Tp6Dt6
HV 25.00 kV
mag 10 000 x
WD 10.0 mm
vacMode High vacuum
HFW 29.8 µm
10 µm
U Normal

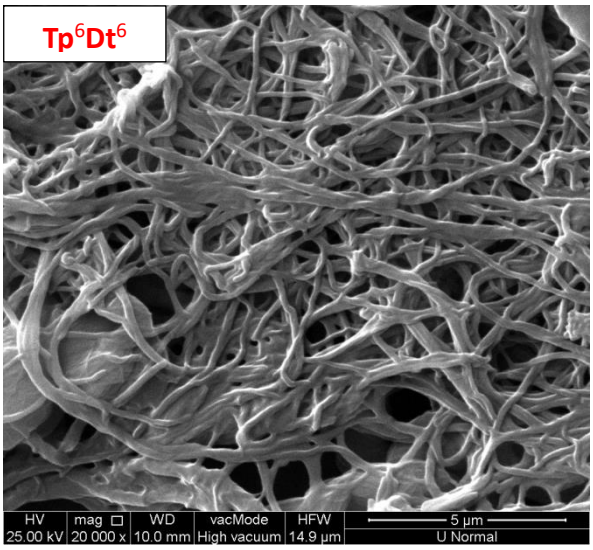
Tp6Dt6
HV 25.00 kV
mag 20 000 x
WD 10.0 mm
vacMode High vacuum
HFW 14.9 µm
5 µm
U Normal

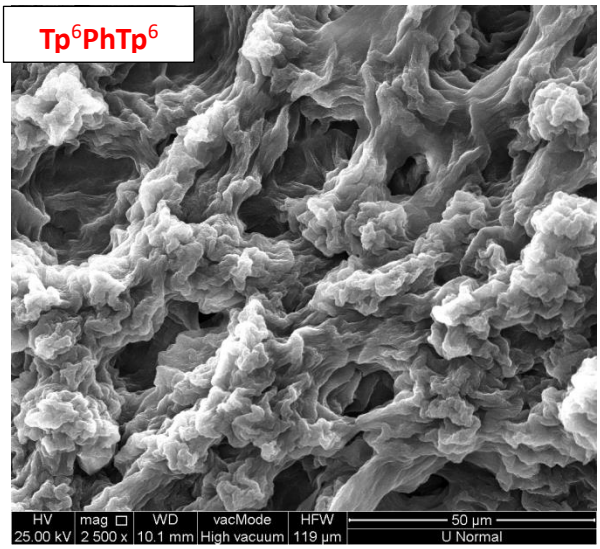
Tp6PhTp6
HV 25.00 kV
mag 2 500 x
WD 10.1 mm
vacMode High vacuum
HFW 119 µm
50 µm
U Normal

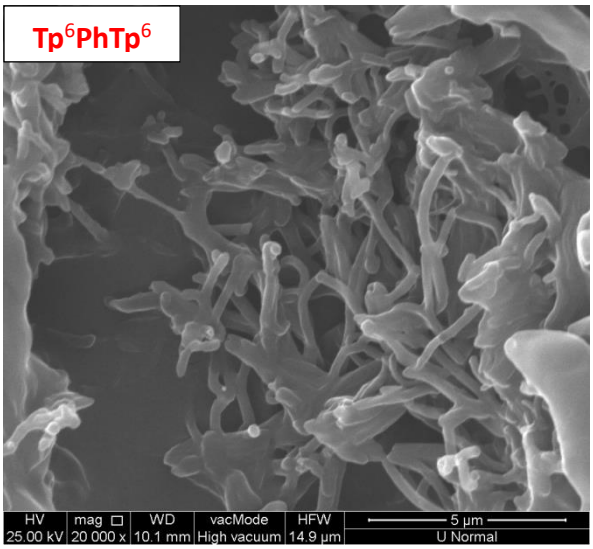
Tp6PhTp6
HV 25.00 kV
mag 20 000 x
WD 10.1 mm
vacMode High vacuum
HFW 14.9 µm
5 µm
U Normal

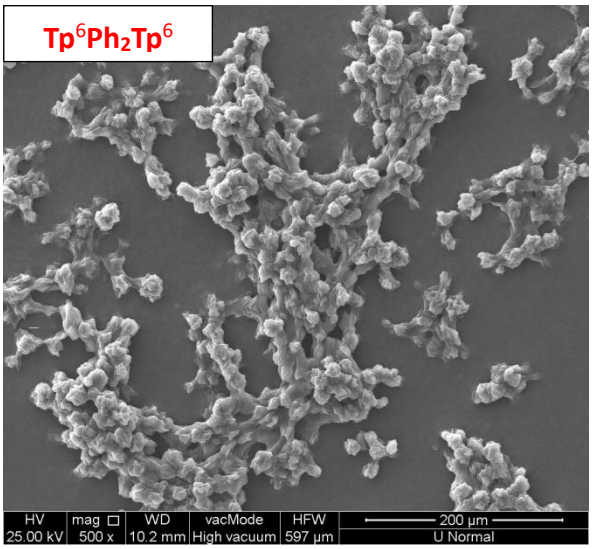
Tp6Ph2Tp6
HV 25.00 kV
mag 500 x
WD 10.2 mm
vacMode High vacuum
HFW 597 µm
200 µm
U Normal

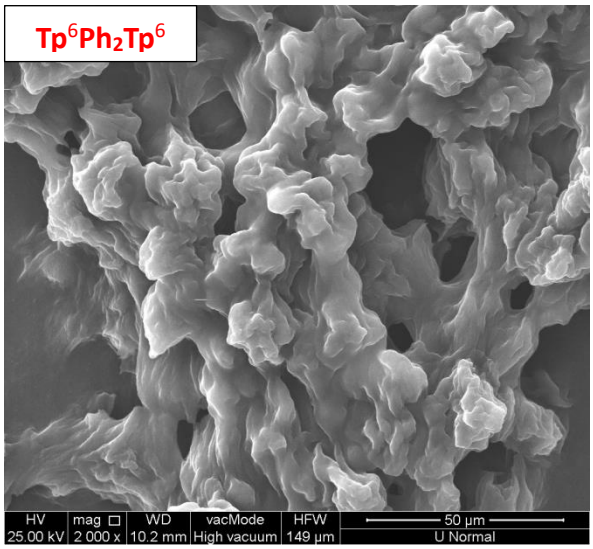
Tp6Ph2Tp6
HV 25.00 kV
mag 2 000 x
WD 10.2 mm
vacMode High vacuum
HFW 149 µm
50 µm
U Normal

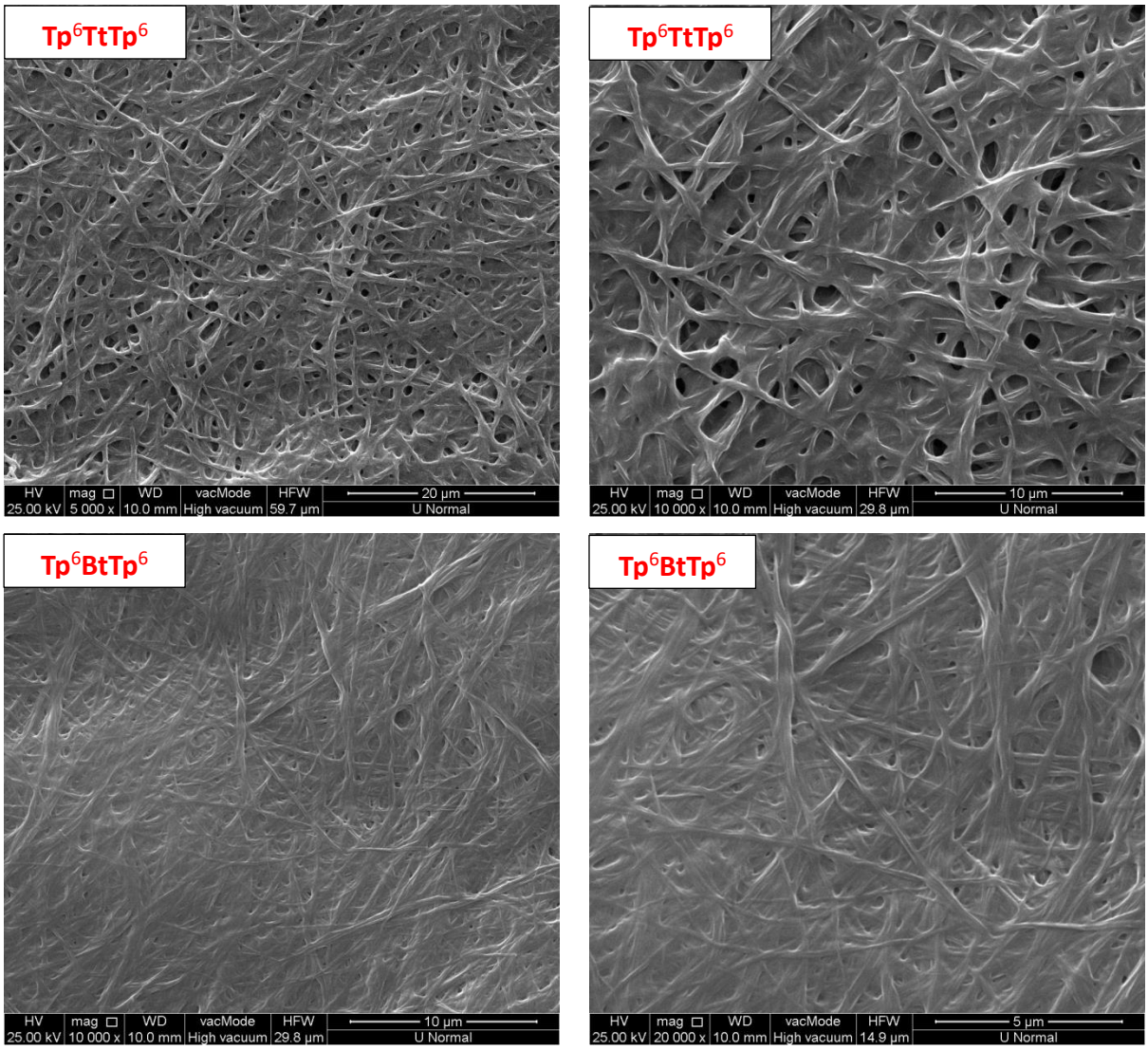

Figure S54. Xero-gel SEM images of representative target dimeric compounds in different solvents. **Tp^{6}Th$_2$Tp^6**, **Tp^{6}β-Th$_2$Tp^6**, **Tp^{6}Fu$_2$Tp^6**, **Tp^{6}PhTp^6**, **Tp^{6}Ph$_2$Tp^6**, **Tp^{6}TtTp^6**, **Tp^{6}BtTp^6** in ethyl acetate and ethanol; **Tp^{6}Tt$_2$Tp^6**, **Tp^{6}Dt^6** in toluene and light petroleum.

7. DFT

Compds	top-views	side-views
M0	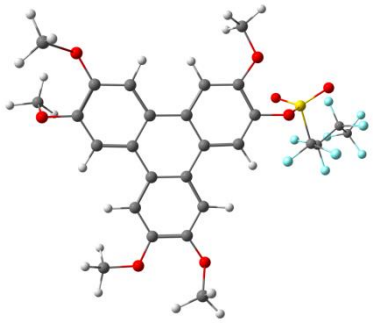	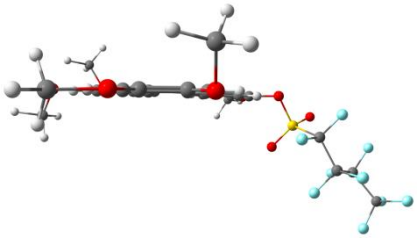
M1/5	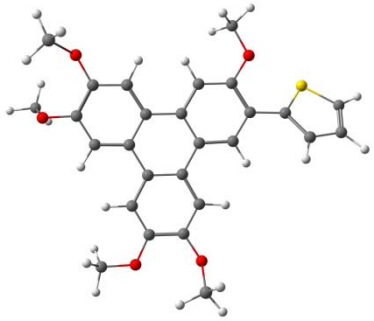	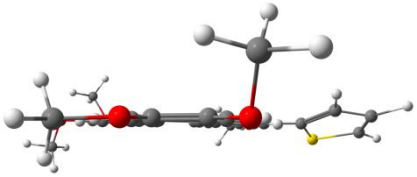
M2	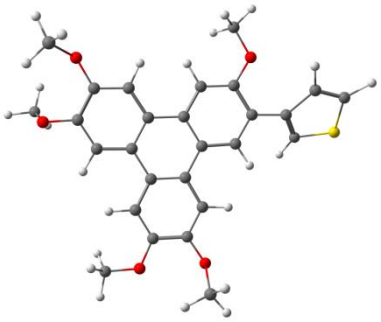	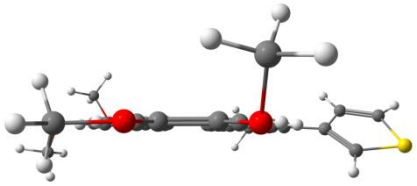
M3	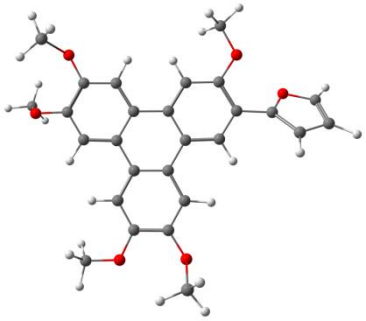	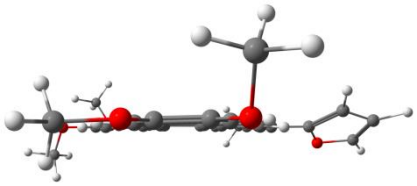
M4	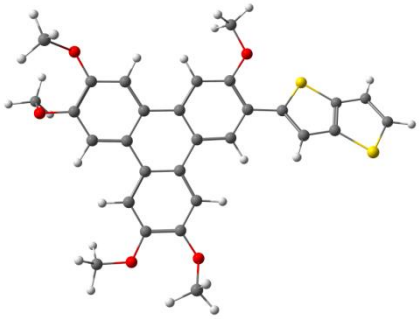	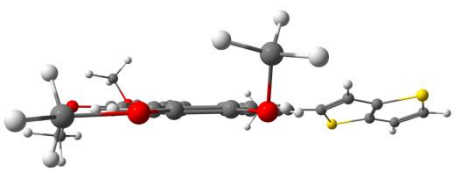

Figure S55. Calculated optimized molecular structures of the methoxy homologues of **M0-M5**.

Table S3. List of selected molecular orbital energies for the methoxy homologues of **M0-M5** and their HOMO-LUMO energy gaps (△E).

	HOMO-2 (eV)	HOMO-1 (eV)	HOMO (eV)	△E (eV)	LUMO (eV)	LUMO+1 (eV)	LUMO+2 (eV)
M0	-6.40	-5.77	-5.47	4.22	-1.25	-0.95	-0.72
M1/5	-5.95	-5.33	-5.15	3.98	-1.17	-0.75	-0.45
M2	-6.01	-5.40	-5.19	4.19	-1.00	-0.74	-0.43
M3	-5.90	-5.31	-5.10	4.06	-1.04	-0.73	-0.41
M4	-5.85	-5.33	-5.09	3.76	-1.33	-0.78	-0.50

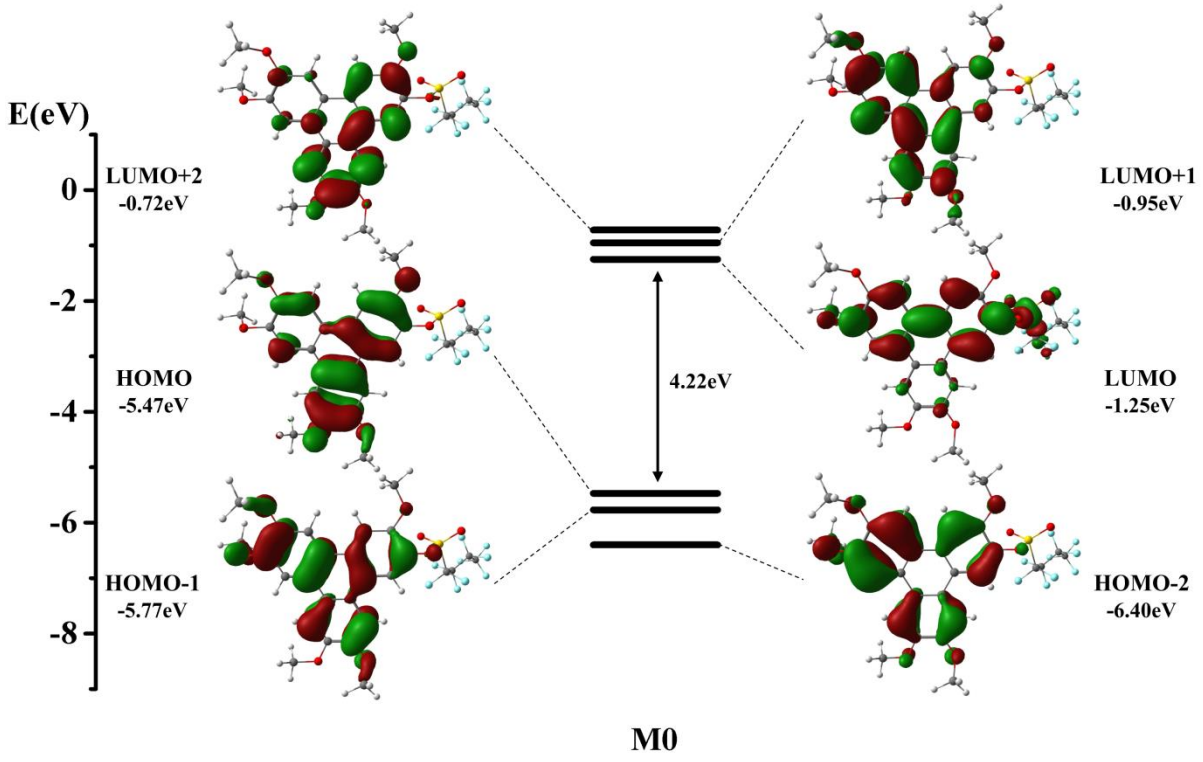

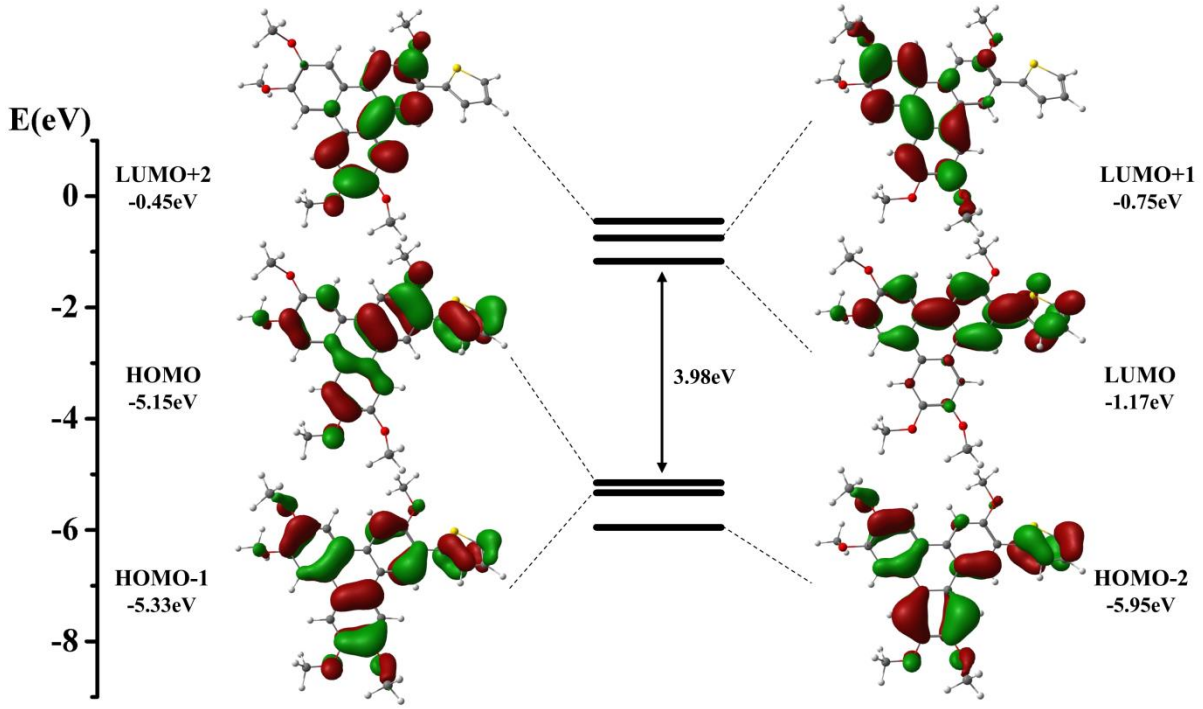
E(eV)
0
-2
-4
-6
-8
LUMO+2
-0.45eV
HOMO
-5.15eV
HOMO-1
-5.33eV
3.98eV
LUMO+1
-0.75eV
LUMO
-1.17eV
HOMO-2
-5.95eV

M1/5

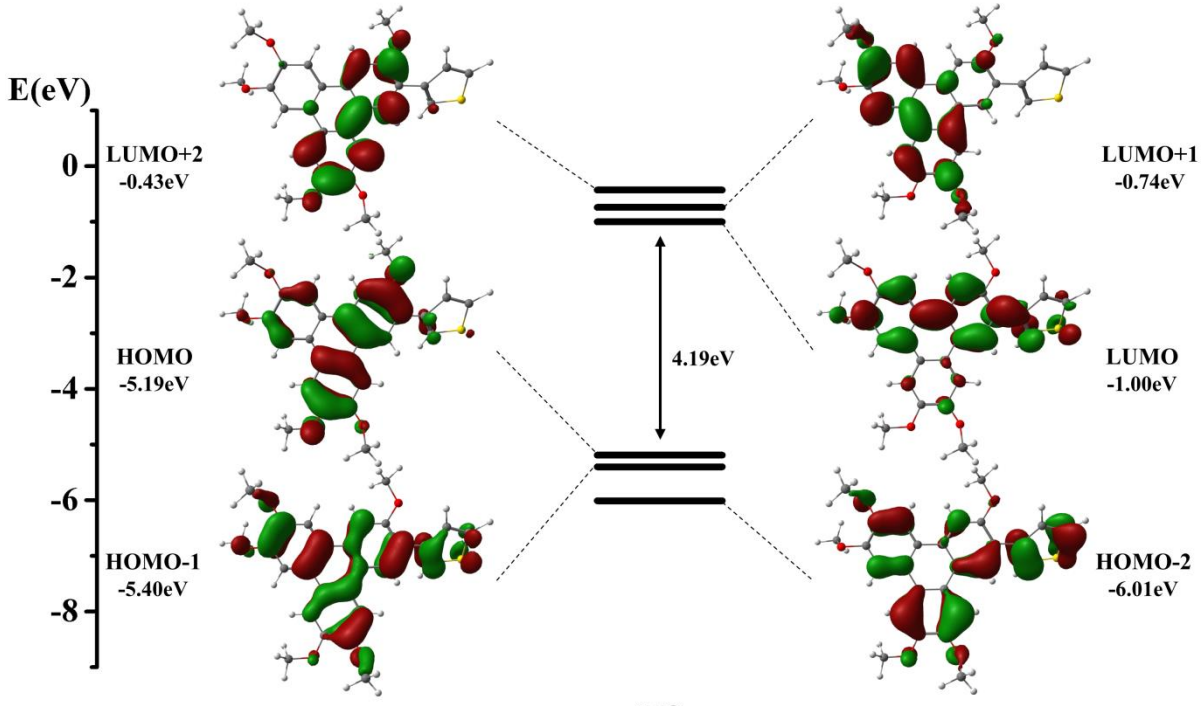
E(eV)
0
-2
-4
-6
-8
LUMO+2
-0.43eV
HOMO
-5.19eV
HOMO-1
-5.40eV
4.19eV
LUMO+1
-0.74eV
LUMO
-1.00eV
HOMO-2
-6.01eV

M2

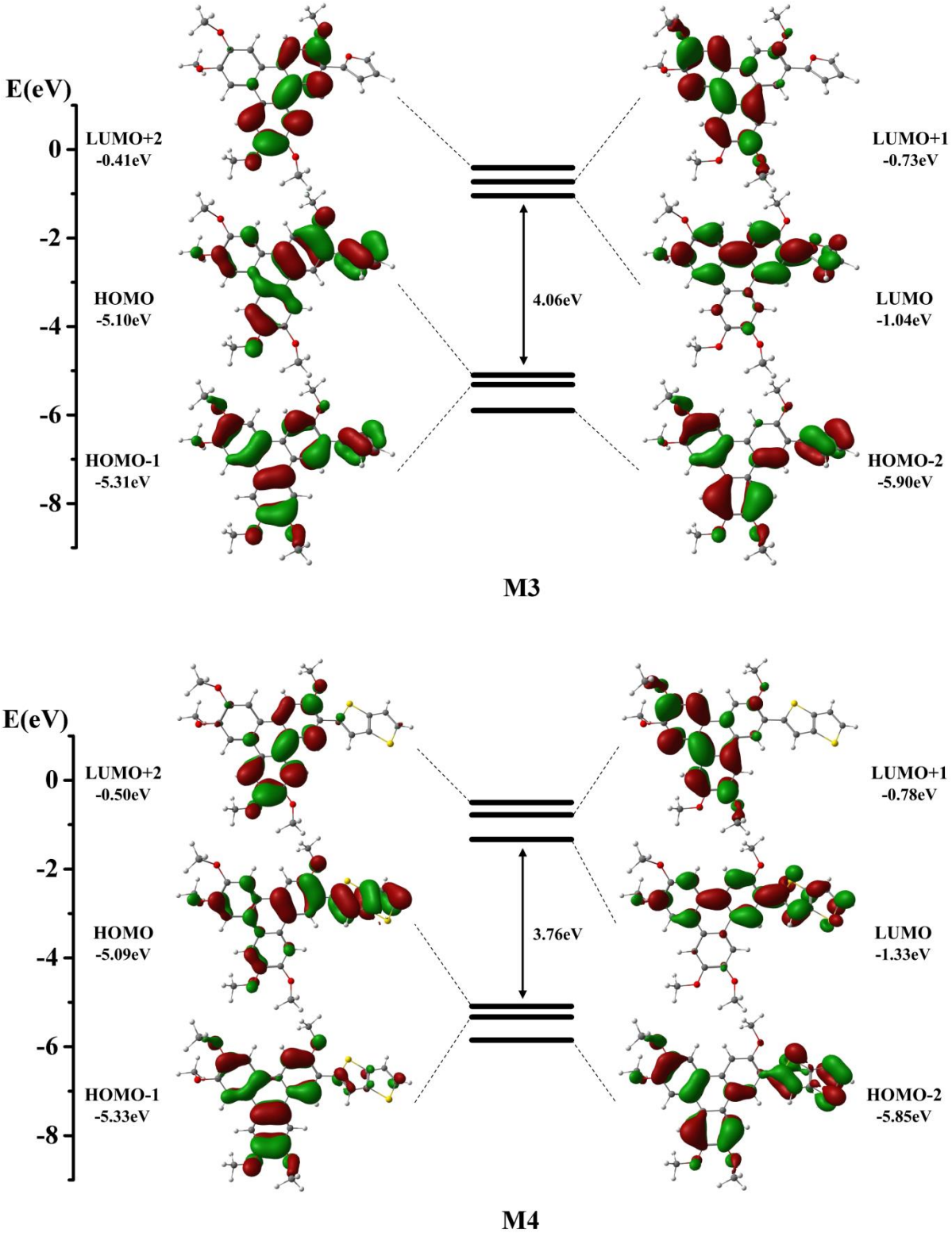

Figure S56. Partial molecular orbital diagram for the methoxy homologues of **M0-M5** with some selected isodensity frontier molecular orbital mainly involved in the electronic transitions. All the DFT energy values are given in electronvolts. The arrows are intended to highlight the HOMO-LUMO energy gaps.

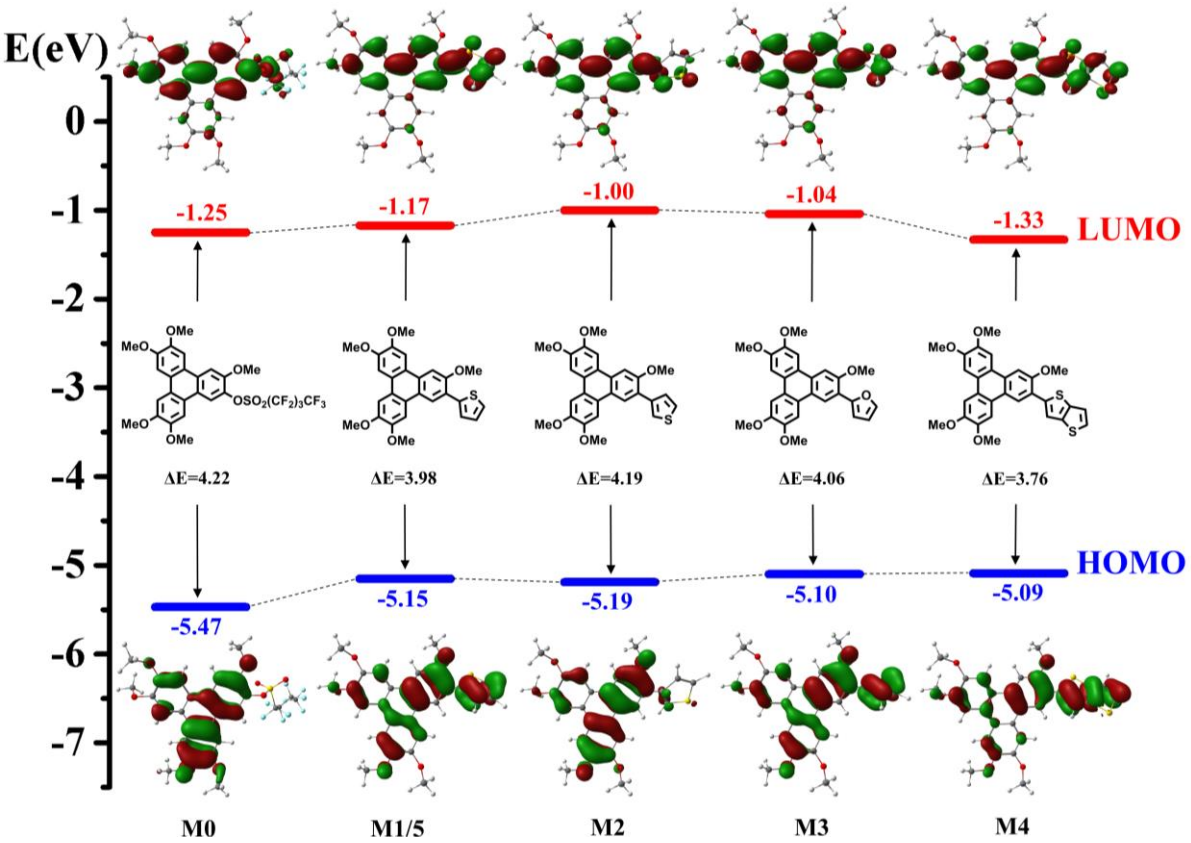

Figure S57. Comparison of HOMO-LUMO energy levels for the methoxy homologues of **M0-M5**.

Table S4. Selected calculated excitation energies (ΔE), oscillator strengths (f), main orbital components,and assignment for the methoxy homologues of **M0-M5** in THF solution.[a]

Compd.	λ_{exc}/nm	ΔE/eV	f	Transitions (Percentage Contribution)
M0	341.7	3.63	0.0401	H-0→L+0(+65%), H-1→L+1(+25%)
	319.2	3.88	0.0102	H-1→L+0(+50%)
	305.7	4.06	0.0159	H-0→L+2(+49%), H-1→L+0(+30%), H-1→L+1(+26%)
	294.3	4.21	0.2736	H-0→L+1(+33%), H-2→L+0(+28%), H-1→L+0(+27%)
	273.6	4.53	0.6569	H-1→L+2(+34%), H-1→L+0(+27%), H-0→L+1(+26%)
	271.7	4.56	0.4261	H-1→L+2(+43%), H-0→L+2(+24%), H-0→L+0(+21%)
	262.2	4.73	0.2838	H-2→L+0(+57%), H-1→L+2(+27%), H-1→L+1(+17%)
	255.7	4.85	0.2454	H-0→L+3(+56%), H-2→L+1(+30%), H-1→L+1(+20%)
	253.1	4.90	0.2327	H-2→L+1(+45%), H-3→L+0(+35%), H-1→L+1(+12%)
	244.8	5.06	0.0039	H-2→L+2(+46%), H-2→L+1(+22%), H-4→L+0(+18%)
	239.9	5.17	0.0448	H-3→L+0(+45%), H-2→L+2(+41%), H-0→L+3(+11%)
	237.9	5.21	0.0395	H-1→L+3(+62%), H-2→L+2(+18%)
	234.1	5.30	0.0502	H-4→L+0(+63%), H-3→L+1(+11%)
	230.9	5.37	0.0675	H-3→L+1(+61%), H-2→L+2(+17%), H-1→L+3(+13%)
	227.9	5.44	0.0526	H-5→L+0(+49%), H-4→L+1(+35%), H-4→L+0(+11%)
	226.4	5.48	0.0083	H-4→L+1(+41%), H-0→L+5(+12%)

	222.3	5.58	0.0244	H-3→L+2(+51%), H-0→L+4(+20%), H-5→L+1(+11%)
	220.9	5.61	0.0442	H-5→L+1(+40%), H-6→L+0(+27%), H-0→L+5(+25%)
	220.4	5.63	0.0511	H-5→L+1(+37%), H-7→L+0(+14%), H-3→L+1(+12%)
	219.0	5.66	0.0195	H-0→L+5(+40%), H-0→L+4(+15%)
	218.4	5.68	0.0011	H-0→L+4(+63%), H-0→L+6(+18%), H-6→L+0(+17%)
	216.2	5.74	0.0434	H-7→L+0(+38%), H-7→L+1(+19%), H-6→L+1(+19%)
	213.9	5.80	0.0426	H-2→L+3(+61%), H-6→L+1(+18%), H-1→L+5(+18%)
	212.6	5.83	0.0339	H-1→L+5(+35%), H-1→L+7(+12%)
	211.7	5.86	0.0097	H-4→L+2(+33%), H-6→L+1(+31%), H-1→L+6(+22%)
	208.6	5.95	0.0099	H-6→L+1(+40%), H-1→L+4(+18%), H-5→L+1(+13%)
	208.0	5.96	0.0023	H-0→L+7(+58%), H-0→L+6(+11%)
	207.4	5.98	0.0028	H-1→L+4(+60%), H-0→L+7(+25%), H-7→L+1(+10%)
	205.2	6.04	0.0071	H-1→L+6(+42%), H-6→L+2(+26%), H-7→L+2(+20%)
	203.8	6.08	0.0272	H-7→L+1(+34%), H-1→L+6(+21%), H-7→L+2(+20%)
M1/5	356.7	3.48	0.0986	H-0→L+0(+55%), H-0→L+1(+17%), H-1→L+1(+16%)
	338.2	3.67	0.3264	H-1→L+0(+51%), H-0→L+0(+37%), H-1→L+1(+11%)
	316.9	3.91	0.1035	H-0→L+1(+56%), H-1→L+0(+29%), H-0→L+2(+25%)
	304.5	4.07	0.1969	H-1→L+1(+49%), H-0→L+2(+33%), H-1→L+2(+22%)
	292.5	4.24	0.4972	H-2→L+0(+53%), H-1→L+1(+27%)
	289.9	4.28	0.2971	H-0→L+2(+46%), H-2→L+1(+26%), H-0→L+0(+10%)
	280.0	4.43	0.0503	H-1→L+2(+47%), H-2→L+0(+36%), H-0→L+3(+17%)
	268.3	4.62	0.0833	H-3→L+0(+52%), H-0→L+3(+38%), H-2→L+1(+15%)
	259.4	4.78	0.1730	H-0→L+3(+44%), H-5→L+0(+12%), H-0→L+2(+12%)
	256.4	4.83	0.0127	H-4→L+0(+68%)
	255.1	4.86	0.5475	H-2→L+1(+57%), H-1→L+2(+19%), H-1→L+1(+12%)
	253.4	4.89	0.0207	H-3→L+1(+36%), H-5→L+0(+36%), H-1→L+3(+30%)
	249.1	4.98	0.0685	H-2→L+2(+59%), H-5→L+0(+26%), H-5→L+1(+13%)
	244.0	5.08	0.0063	H-1→L+3(+42%), H-0→L+3(+19%), H-6→L+0(+19%)
	241.0	5.14	0.0290	H-5→L+0(+39%), H-6→L+0(+25%), H-7→L+0(+11%)
	235.8	5.26	0.0010	H-6→L+0(+53%), H-3→L+1(+24%)
	233.6	5.31	0.0494	H-3→L+2(+58%), H-6→L+0(+21%), H-0→L+4(+11%)
	231.7	5.35	0.0004	H-4→L+1(+67%)
	229.5	5.40	0.0362	H-5→L+1(+54%), H-3→L+2(+21%), H-7→L+1(+15%)
	227.3	5.46	0.0221	H-7→L+0(+60%), H-2→L+3(+22%), H-1→L+4(+11%)
	225.4	5.50	0.0232	H-6→L+1(+46%), H-1→L+4(+20%), H-0→L+5(+12%)
	223.4	5.55	0.0153	H-4→L+2(+47%), H-4→L+1(+13%), H-8→L+0(+10%)
	223.0	5.56	0.0181	H-4→L+2(+47%), H-0→L+5(+34%), H-4→L+1(+16%)
	221.9	5.59	0.0287	H-2→L+3(+54%)
	220.8	5.62	0.0402	H-0→L+6(+42%), H-1→L+6(+17%), H-2→L+3(+16%)
	218.7	5.67	0.0167	H-7→L+1(+44%), H-0→L+5(+20%)
	217.3	5.71	0.0591	H-5→L+2(+41%), H-7→L+1(+30%), H-8→L+0(+24%)
	216.6	5.72	0.0021	H-8→L+0(+45%), H-9→L+0(+27%), H-8→L+1(+23%)
	214.3	5.78	0.0131	H-1→L+5(+48%), H-9→L+0(+19%), H-5→L+2(+17%)
	214.0	5.79	0.0800	H-7→L+1(+32%), H-0→L+4(+21%), H-6→L+1(+21%)

M2	344.5	3.60	0.0503	H-0→L+0(+60%), H-1→L+1(+24%), H-0→L+1(+13%)
	325.3	3.81	0.0615	H-0→L+1(+49%)
	308.8	4.02	0.1127	H-1→L+0(+42%), H-0→L+2(+37%), H-0→L+1(+36%)
	297.8	4.16	0.2643	H-1→L+1(+44%), H-1→L+2(+29%), H-0→L+2(+24%)
	283.0	4.38	0.6194	H-0→L+2(+44%)
	278.9	4.45	0.5019	H-1→L+2(+39%), H-2→L+0(+29%), H-0→L+0(+25%)
	271.9	4.56	0.0194	H-2→L+0(+52%), H-0→L+3(+19%)
	266.0	4.66	0.0115	H-0→L+3(+49%), H-3→L+0(+41%), H-1→L+2(+16%)
	260.4	4.76	0.1872	H-0→L+3(+44%)
	255.5	4.85	0.4318	H-2→L+1(+50%), H-4→L+0(+34%), H-0→L+2(+22%)
	251.3	4.94	0.1121	H-4→L+0(+51%), H-1→L+3(+31%), H-3→L+1(+10%)
	248.4	4.99	0.0375	H-3→L+1(+36%), H-1→L+3(+28%), H-2→L+1(+22%)
	246.2	5.04	0.0699	H-2→L+2(+52%), H-1→L+3(+31%), H-5→L+0(+18%)
	243.5	5.09	0.0124	H-3→L+1(+38%), H-5→L+0(+26%), H-2→L+2(+26%)
	237.4	5.22	0.0203	H-5→L+0(+47%), H-4→L+1(+25%), H-3→L+2(+17%)
	236.4	5.24	0.0018	H-3→L+2(+41%), H-4→L+1(+40%), H-2→L+2(+21%)
	233.0	5.32	0.0231	H-3→L+2(+47%), H-4→L+2(+15%), H-3→L+1(+12%)
	231.7	5.35	0.0168	H-6→L+0(+46%), H-3→L+2(+18%), H-3→L+1(+15%)
	228.5	5.43	0.0481	H-5→L+1(+41%), H-6→L+0(+40%), H-0→L+4(+20%)
	226.1	5.48	0.0329	H-0→L+4(+46%), H-4→L+2(+17%), H-2→L+2(+10%)
	225.1	5.51	0.0356	H-4→L+2(+50%), H-7→L+1(+17%), H-5→L+1(+16%)
	224.4	5.52	0.0051	H-4→L+2(+38%), H-0→L+5(+32%), H-6→L+1(+31%)
	223.3	5.55	0.0036	H-7→L+0(+44%), H-3→L+3(+14%)
	221.1	5.61	0.0052	H-2→L+3(+45%), H-7→L+0(+38%), H-1→L+6(+14%)
	220.9	5.61	0.0247	H-1→L+4(+35%), H-7→L+0(+18%), H-5→L+1(+14%)
	217.7	5.70	0.0306	H-5→L+2(+36%), H-6→L+1(+23%), H-0→L+6(+21%)
	217.3	5.70	0.0051	H-1→L+4(+42%), H-0→L+6(+31%), H-1→L+6(+22%)
	216.8	5.72	0.0433	H-7→L+1(+49%), H-5→L+2(+35%), H-1→L+5(+17%)
	215.0	5.77	0.0072	H-8→L+0(+35%), H-8→L+1(+29%), H-9→L+0(+25%)
	212.1	5.84	0.1039	H-8→L+0(+43%), H-5→L+2(+27%), H-1→L+5(+17%)
M3	350.7	3.54	0.0841	H-0→L+0(+54%), H-0→L+1(+20%), H-1→L+1(+18%)
	332.9	3.72	0.2012	H-1→L+0(+44%), H-0→L+0(+36%), H-1→L+1(+14%)
	315.6	3.93	0.1316	H-0→L+1(+49%), H-1→L+0(+37%), H-0→L+2(+30%)
	302.7	4.10	0.2734	H-1→L+1(+49%), H-0→L+2(+32%), H-1→L+2(+24%)
	291.0	4.26	0.3387	H-0→L+2(+45%), H-2→L+1(+25%), H-2→L+0(+21%)
	290.0	4.28	0.3594	H-2→L+0(+47%), H-1→L+1(+34%)
	277.8	4.46	0.0515	H-1→L+2(+45%), H-2→L+0(+39%), H-0→L+1(+14%)
	262.5	4.72	0.4073	H-3→L+0(+50%), H-2→L+1(+31%), H-1→L+2(+15%)
	255.3	4.86	0.5326	H-2→L+1(+50%), H-1→L+2(+19%), H-0→L+3(+13%)
	251.9	4.92	0.0157	H-3→L+1(+47%), H-4→L+0(+11%)
	249.6	4.97	0.0776	H-4→L+0(+43%), H-2→L+2(+39%), H-3→L+1(+25%)
	245.2	5.06	0.0156	H-0→L+3(+48%), H-2→L+2(+29%), H-3→L+1(+18%)
	239.1	5.19	0.0374	H-4→L+0(+41%), H-0→L+3(+29%), H-5→L+0(+14%)
	235.4	5.27	0.0340	H-3→L+2(+64%), H-4→L+0(+13%)

	234.1	5.30	0.0101	H-1→L+3(+42%), H-0→L+3(+24%), H-0→L+4(+18%)
	232.8	5.33	0.0459	H-5→L+0(+56%), H-3→L+2(+12%), H-0→L+4(+11%)
	228.7	5.42	0.0173	H-4→L+1(+46%), H-1→L+3(+27%), H-5→L+0(+19%)
	225.4	5.50	0.0256	H-5→L+1(+46%), H-1→L+4(+23%)
	224.6	5.52	0.0108	H-6→L+0(+59%), H-4→L+1(+14%), H-0→L+4(+11%)
	221.6	5.60	0.0284	H-7→L+0(+41%), H-4→L+2(+32%), H-0→L+4(+23%)
	219.3	5.65	0.0227	H-7→L+0(+31%), H-6→L+1(+31%), H-6→L+0(+19%)
	218.1	5.68	0.0221	H-4→L+2(+37%), H-6→L+1(+36%)
	215.6	5.75	0.0349	H-8→L+0(+39%), H-8→L+1(+25%), H-5→L+1(+21%)
	214.6	5.78	0.0372	H-0→L+5(+36%), H-4→L+2(+29%), H-7→L+0(+20%)
	212.9	5.82	0.0184	H-1→L+4(+31%), H-2→L+3(+25%), H-0→L+4(+25%)
	211.6	5.86	0.1292	H-2→L+3(+49%), H-8→L+0(+28%), H-1→L+5(+21%)
	209.7	5.91	0.0032	H-1→L+4(+36%), H-8→L+0(+36%), H-1→L+5(+11%)
	207.3	5.98	0.0222	H-5→L+2(+50%), H-7→L+1(+15%), H-8→L+2(+12%)
	206.5	6.00	0.0157	H-1→L+5(+45%), H-8→L+1(+21%)
	205.3	6.04	0.0101	H-1→L+5(+34%), H-9→L+0(+33%), H-8→L+0(+15%)
M4	368.4	3.37	0.3877	H-0→L+0(+58%), H-0→L+1(+14%)
	354.5	3.50	0.4581	H-1→L+0(+56%), H-0→L+0(+37%)
	323.1	3.84	0.0565	H-0→L+1(+59%), H-1→L+0(+21%), H-0→L+2(+15%)
	309.0	4.01	0.1875	H-1→L+1(+49%), H-0→L+2(+43%), H-4→L+0(+15%)
	307.8	4.03	0.1412	H-2→L+0(+60%), H-1→L+1(+17%), H-0→L+1(+14%)
	297.9	4.16	0.1307	H-0→L+2(+39%), H-3→L+0(+23%), H-2→L+1(+20%)
	294.3	4.21	0.1295	H-3→L+0(+62%), H-1→L+2(+15%), H-2→L+0(+11%)
	290.2	4.27	0.1346	H-0→L+3(+46%), H-2→L+1(+16%), H-3→L+0(+12%)
	282.3	4.39	0.0086	H-4→L+0(+46%), H-2→L+1(+19%)
	271.1	4.57	0.1184	H-1→L+3(+61%), H-1→L+1(+12%)
	263.6	4.70	0.1284	H-4→L+0(+42%), H-0→L+3(+25%)
	259.7	4.77	0.4490	H-2→L+1(+48%), H-1→L+2(+30%), H-1→L+3(+25%)
	255.8	4.85	0.1139	H-3→L+1(+53%), H-4→L+1(+13%), H-4→L+0(+12%)
	254.5	4.87	0.2063	H-2→L+2(+50%), H-5→L+0(+32%), H-3→L+1(+23%)
	253.7	4.89	0.0104	H-5→L+0(+40%), H-4→L+1(+28%), H-0→L+3(+15%)
	248.7	4.99	0.0365	H-4→L+1(+42%), H-3→L+2(+23%), H-2→L+2(+11%)
	247.4	5.01	0.0011	H-0→L+5(+64%), H-1→L+5(+16%), H-0→L+4(+15%)
	244.8	5.07	0.0195	H-3→L+2(+63%), H-2→L+3(+16%), H-3→L+1(+13%)
	240.5	5.15	0.0053	H-6→L+0(+56%), H-4→L+1(+13%)
	239.3	5.18	0.0198	H-2→L+3(+43%), H-4→L+1(+29%), H-0→L+4(+13%)
	237.6	5.22	0.0230	H-0→L+4(+49%), H-4→L+2(+20%)
	236.6	5.24	0.1287	H-4→L+2(+51%), H-3→L+3(+30%), H-6→L+0(+21%)
	234.8	5.28	0.0399	H-3→L+3(+58%), H-5→L+1(+15%), H-0→L+4(+14%)
	233.1	5.32	0.0084	H-0→L+7(+51%), H-1→L+7(+11%)
	231.0	5.37	0.0439	H-5→L+1(+46%), H-8→L+0(+32%), H-4→L+2(+18%)
	230.3	5.38	0.0239	H-8→L+0(+38%), H-1→L+4(+16%), H-3→L+3(+11%)
	226.0	5.49	0.0133	H-6→L+1(+43%), H-1→L+6(+28%), H-1→L+4(+13%)
	225.2	5.51	0.0053	H-1→L+4(+39%), H-0→L+6(+25%), H-5→L+1(+21%)

	223.1	5.56	0.0430	H-6→L+1(+26%), H-8→L+0(+25%), H-0→L+6(+22%)
	222.3	5.58	0.0105	H-3→L+5(+54%), H-2→L+5(+28%), H-3→L+4(+13%)
[a]H = HOMO, L = LUMO, H-n = HOMO-n and L+n = LUMO+n.				

Compounds	top-views	side-views
$Tp^1Th_2Tp^1$	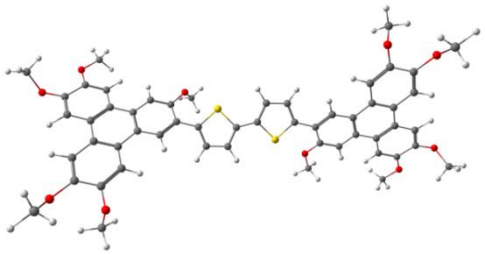	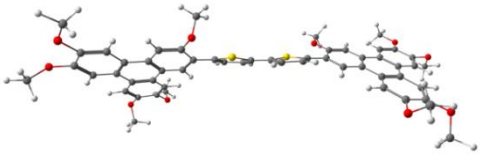
$Tp^1\beta$-Th_2Tp^1	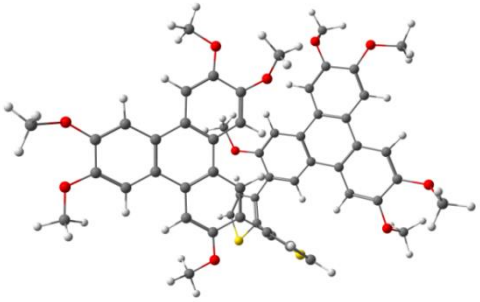	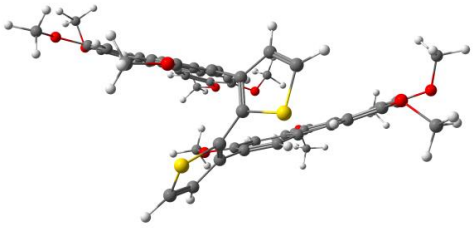
$Tp^1Fu_2Tp^1$	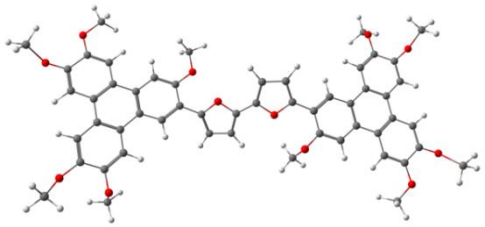	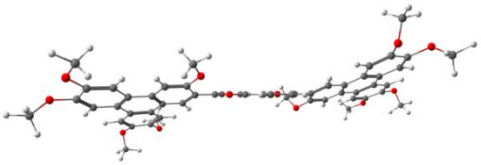
$Tp^1Tt_2Tp^1$	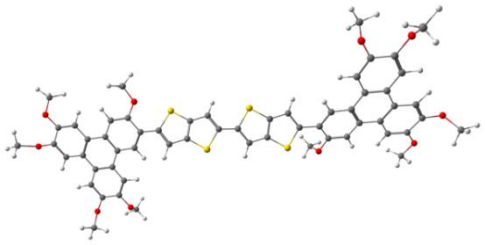	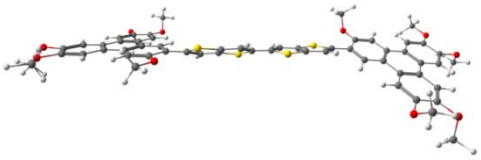
Tp^1T^1	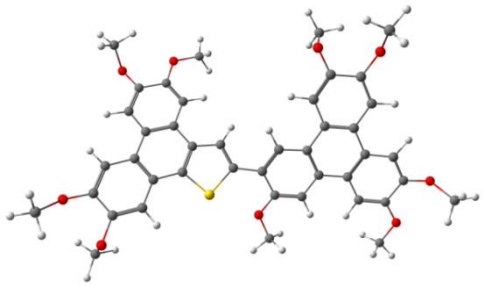	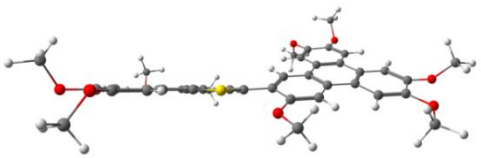

Tp^1Dt^1	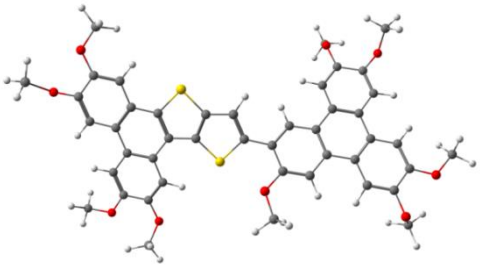	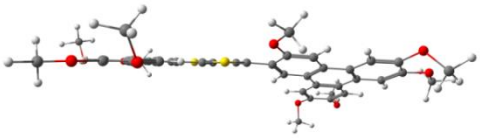
Tp^1PhTp^1	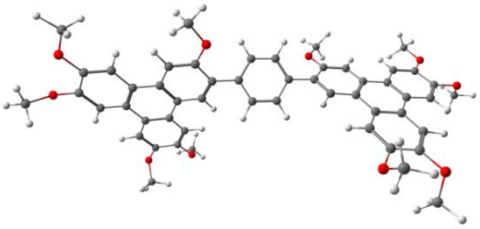	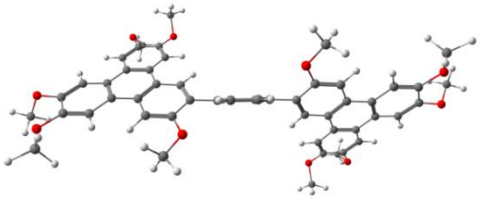
$Tp^1Ph_2Tp^1$	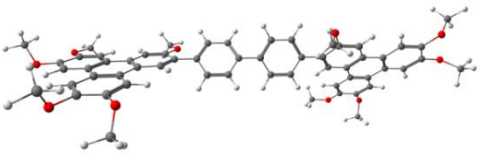	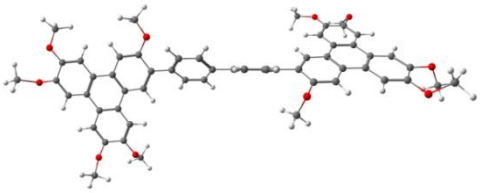
Tp^1TtTp^1	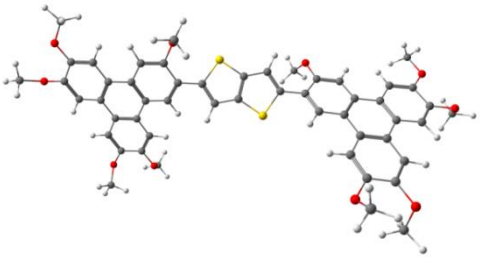	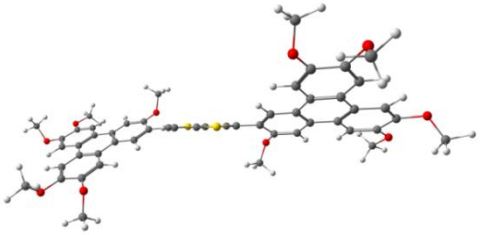
Tp^1BtTp^1	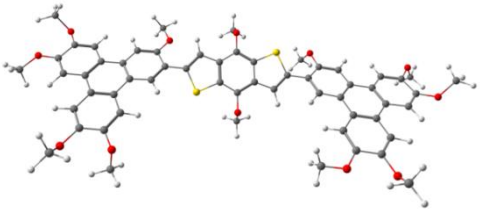	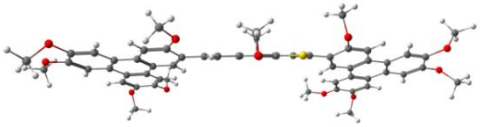

Figure S58. DFT calculated optimized molecular structures of the methoxy homologues of the dimeric compounds.

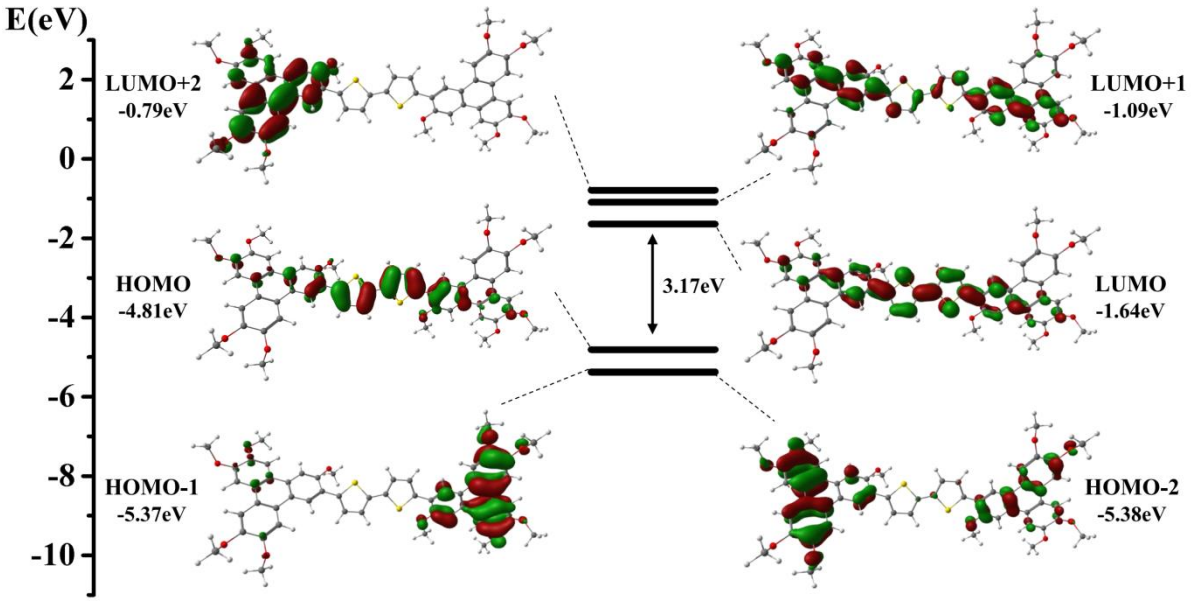

$Tp^1Th_2Tp^1$

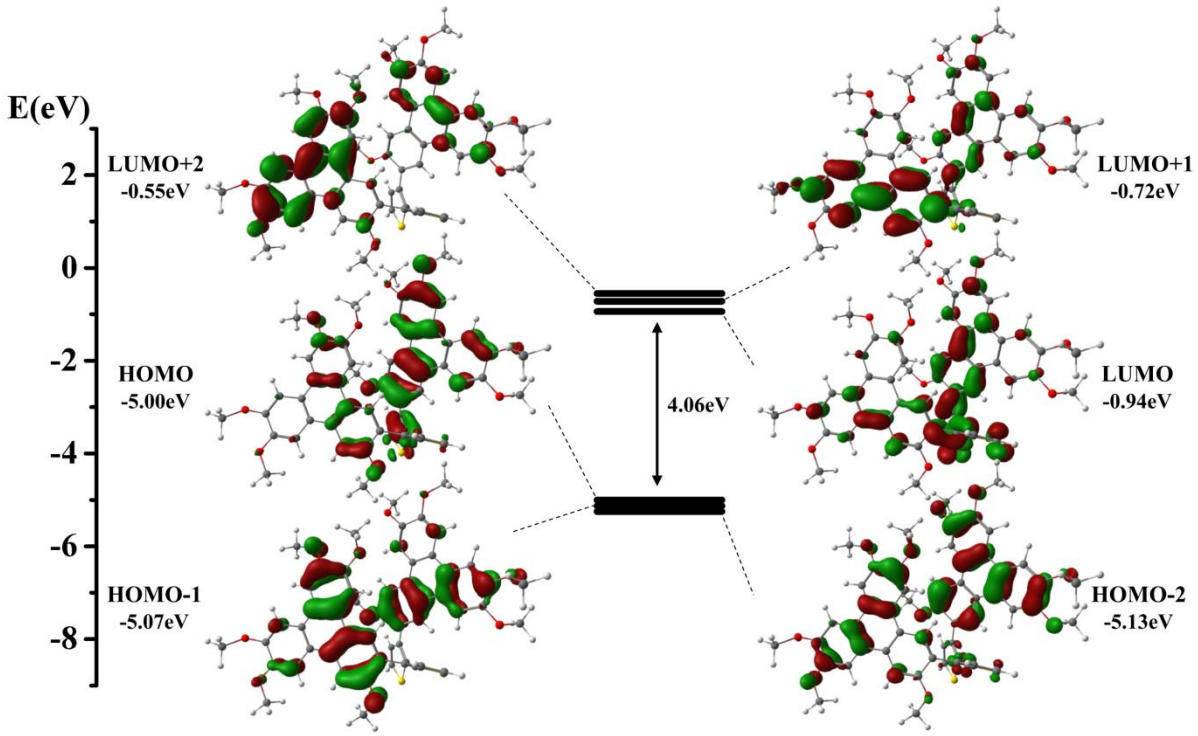

$Tp^1\beta\text{-}Th_2Tp^1$

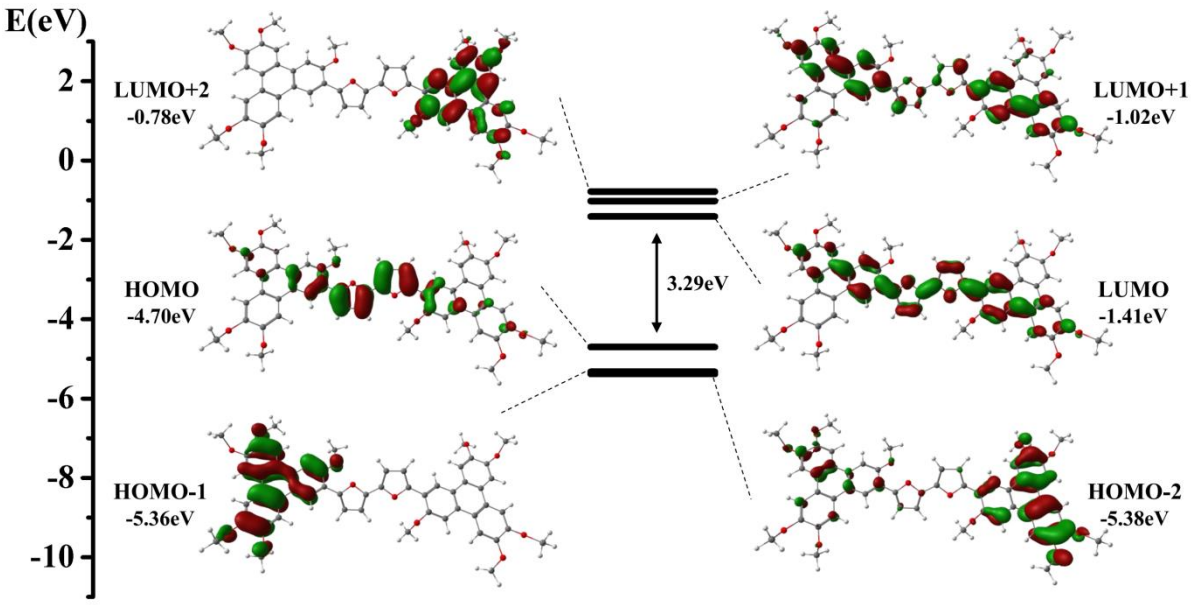

$Tp^1Fu_2Tp^1$

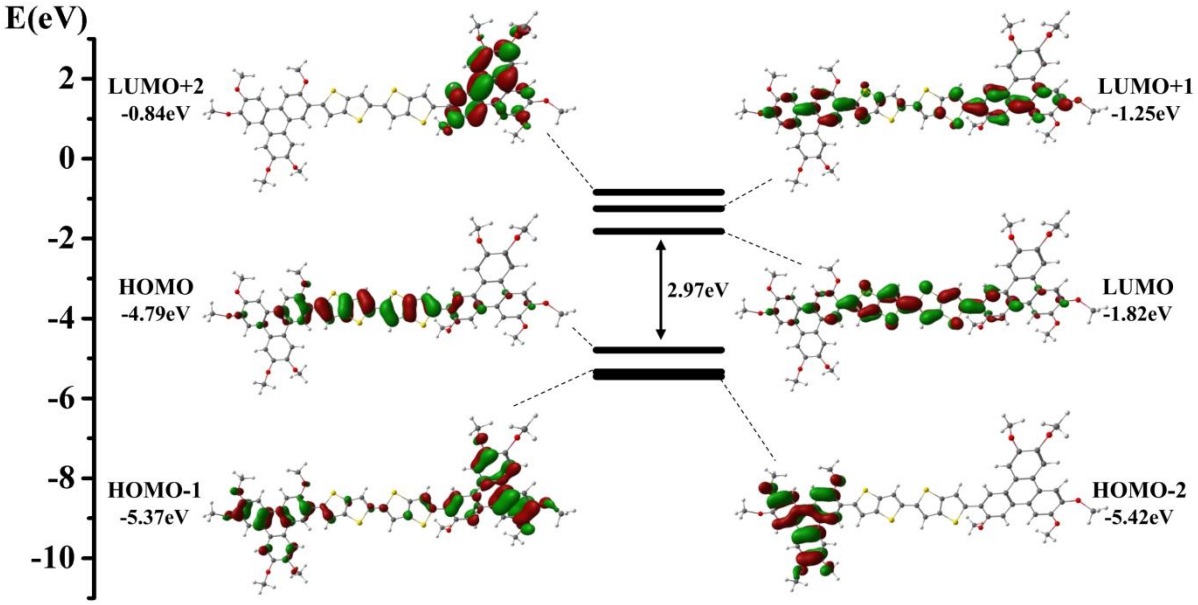

$Tp^1Tt_2Tp^1$

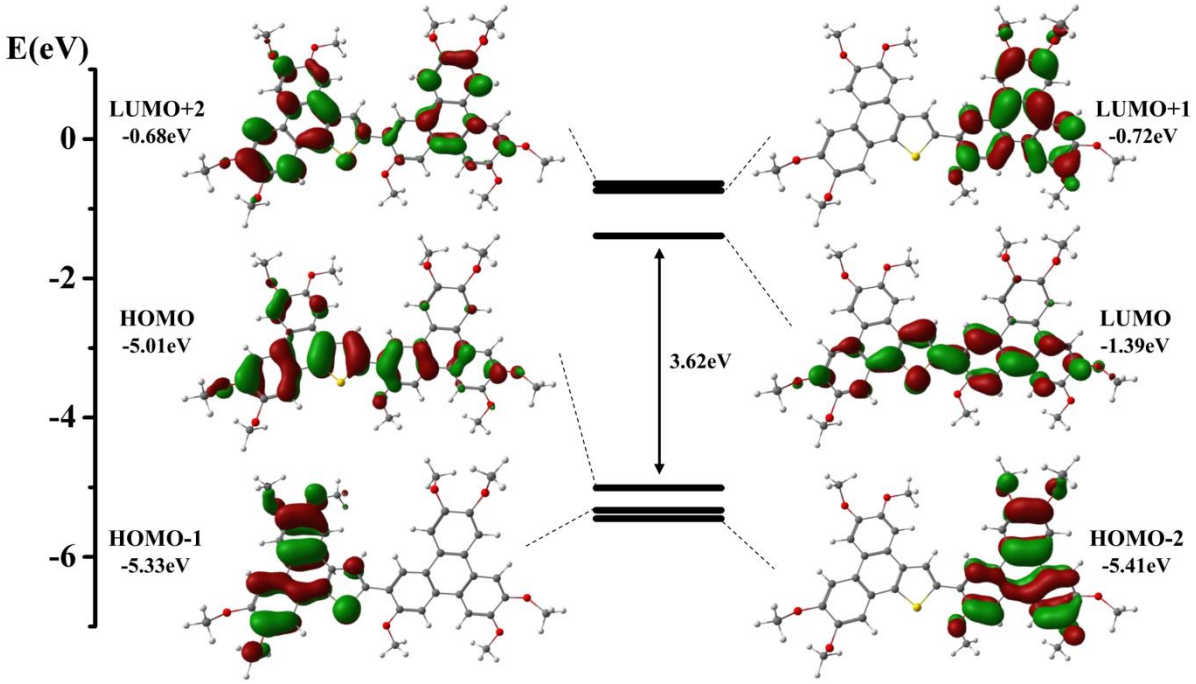

Tp^1T^1

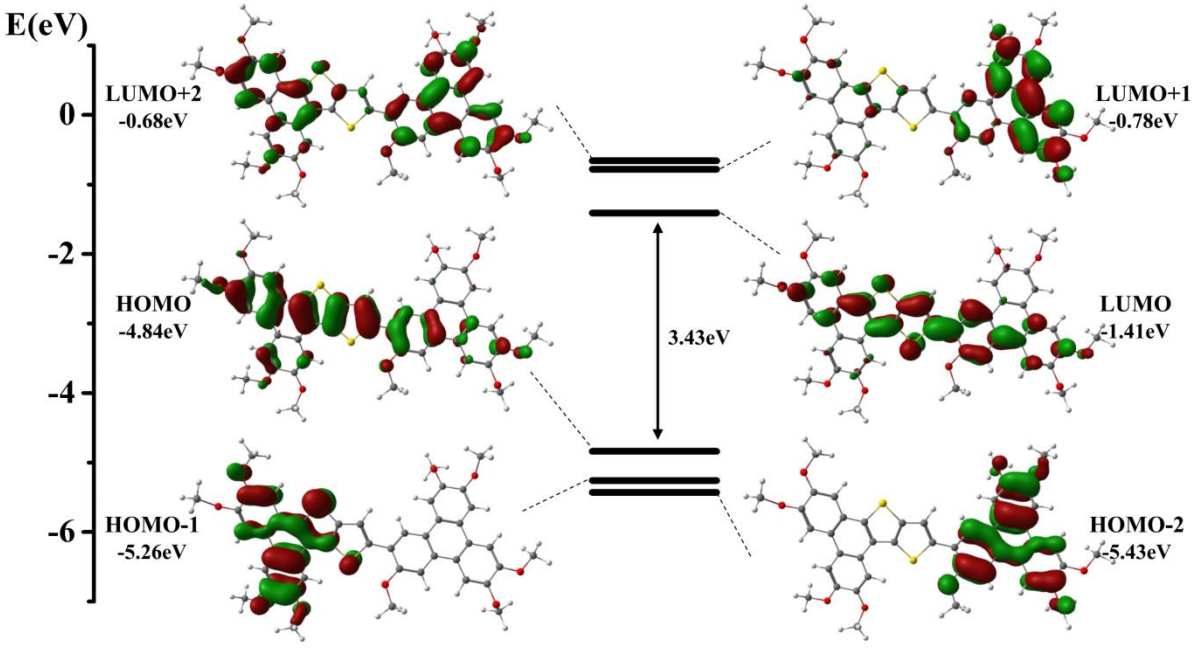

Tp^1Dt^1

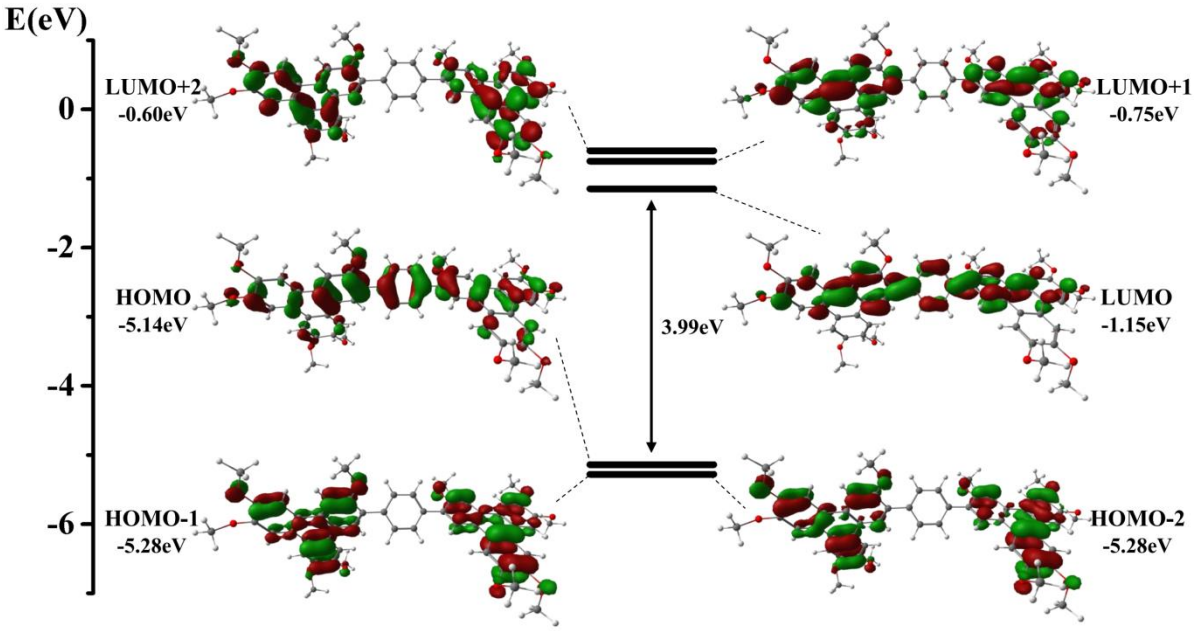

Tp^1PhTp^1

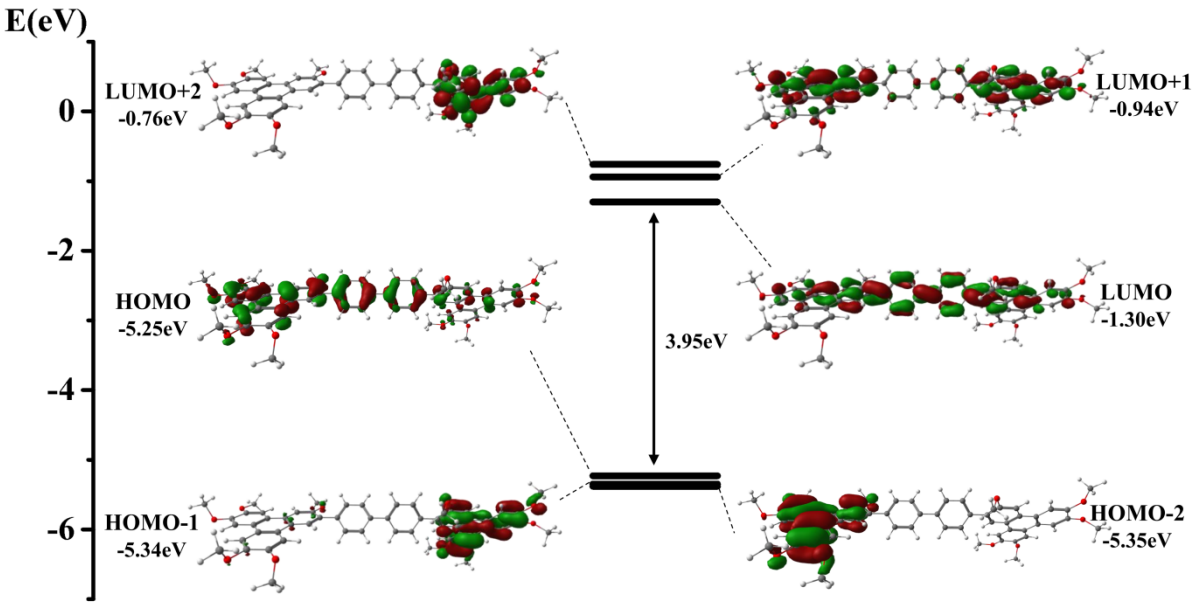

$Tp^1Ph_2Tp^1$

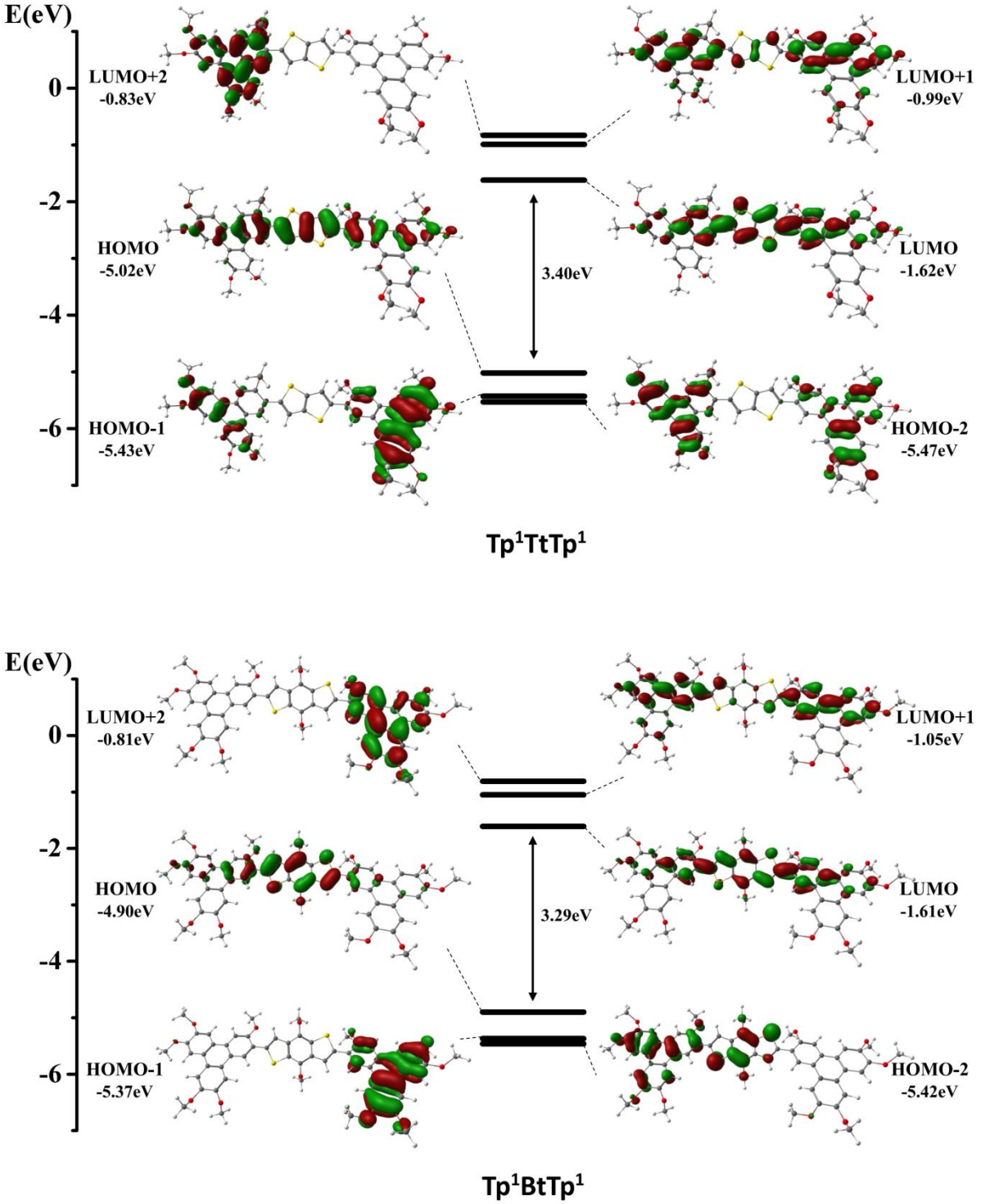

Figure S59. Partial molecular orbital diagram for the methoxy homologues of the dimers with some selected isodensity frontier molecular orbital mainly involved in the electronic transitions. All the DFT energy values are given in electronvolts. The arrows are intended to highlight the HOMO-LUMO energy gaps.

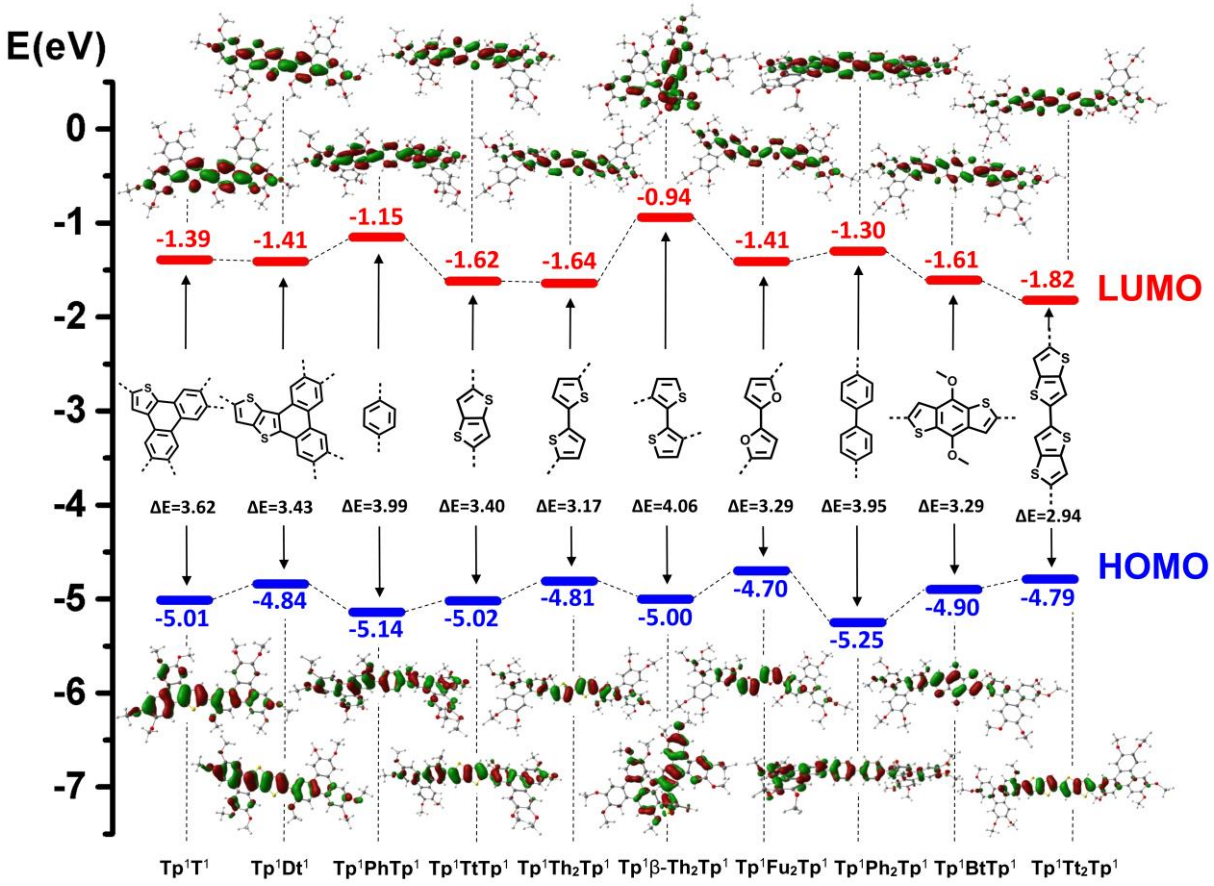

Figure S60. Comparison of HOMO-LUMO energy levels for the methoxy homologues of the dimeric compounds.

Table S5. List of selected molecular orbital energies for the methoxy homologues of the dimeric compounds and their HOMO-LUMO energy gaps (△E).

	HOMO-2 (eV)	HOMO-1 (eV)	HOMO (eV)	△E (eV)	LUMO (eV)	LUMO+1 (eV)	LUMO+2 (eV)
Tp¹Th₂Tp¹	-5.38	-5.37	-4.81	3.17	-1.64	-1.09	-0.79
Tp¹β-Th₂Tp¹	-5.13	-5.07	-5.00	4.06	-0.94	-0.72	-0.55
Tp¹Fu₂Tp¹	-5.38	-5.36	-4.70	3.29	-1.41	-1.02	-0.78
Tp¹Tt₂Tp¹	-5.42	-5.37	-4.79	2.97	-1.82	-1.25	-0.84
Tp¹T¹	-5.41	-5.33	-5.01	3.62	-1.39	-0.72	-0.68
Tp¹Dt¹	-5.43	-5.26	-4.84	3.43	-1.41	-0.78	-0.68
Tp¹PhTp¹	-5.28	-5.28	-5.14	3.99	-1.15	-0.75	-0.60
Tp¹Ph₂Tp¹	-5.35	-5.34	-5.25	3.95	-1.30	-0.94	-0.76
Tp¹TtTp¹	-5.47	-5.43	-5.02	3.40	-1.62	-0.99	-0.83
Tp¹BtTp¹	-5.42	-5.37	-4.90	3.29	-1.61	-1.05	-0.81

Table S6. Selected calculated excitation energies (ΔE), oscillator strengths (f), main orbital components, and assignment for the methoxy homologues of the dimers in THF solution.[a]

Compounds	λ_{exc}/nm	ΔE/eV	f	Transitions (Percentage Contribution)
Tp¹Th₂Tp¹	442.9	2.80	2.0778	H-0→L+0(+70%)
	374.4	3.31	0.0138	H-1→L+0(+57%), H-0→L+3(+19%), H-1→L+1(+15%)
	370.5	3.35	0.0029	H-2→L+0(+48%), H-1→L+0(+21%)
	365.2	3.40	0.0073	H-0→L+1(+46%), H-2→L+0(+17%)
	355.2	3.49	0.0062	H-3→L+0(+40%), H-2→L+0(+32%), H-0→L+1(+31%)

	340.9	3.64	0.0237	H-0→L+2(+51%), H-2→L+0(+13%)
	334.1	3.71	0.0121	H-0→L+3(+51%), H-1→L+1(+19%), H-3→L+0(+13%)
	330.8	3.75	0.0158	H-4→L+0(+53%), H-0→L+2(+21%), H-0→L+3(+21%)
	323.3	3.83	0.0142	H-0→L+4(+49%), H-5→L+0(+12%), H-2→L+1(+11%)
	323.2	3.84	0.0360	H-0→L+5(+46%), H-0→L+4(+37%), H-1→L+3(+16%)
	315.1	3.94	0.0124	H-2→L+1(+47%), H-1→L+1(+30%), H-4→L+2(+10%)
	312.5	3.97	0.0412	H-1→L+1(+46%), H-3→L+3(+10%)
	310.6	3.99	0.0077	H-3→L+1(+37%), H-2→L+2(+36%), H-0→L+2(+18%)
	307.8	4.03	0.1809	H-0→L+6(+54%), H-2→L+1(+21%), H-3→L+1(+19%)
	302.3	4.10	0.0223	H-3→L+1(+38%), H-4→L+1(+18%), H-1→L+5(+12%)
	300.7	4.12	0.0028	H-5→L+0(+58%), H-0→L+5(+17%), H-3→L+2(+12%)
	299.1	4.14	0.0129	H-1→L+5(+41%), H-5→L+0(+17%), H-1→L+1(+14%)
	295.2	4.20	0.1360	H-6→L+0(+49%), H-0→L+4(+15%), H-2→L+3(+13%)
	293.0	4.23	0.0024	H-4→L+1(+36%), H-3→L+2(+21%), H-3→L+4(+13%)
	284.0	4.37	0.0161	H-4→L+1(+42%), H-5→L+0(+23%), H-3→L+4(+19%)
	281.7	4.40	0.0005	H-1→L+2(+65%)
	279.5	4.44	0.1474	H-3→L+2(+31%), H-6→L+0(+31%), H-4→L+1(+22%)
	278.4	4.45	0.2253	H-7→L+0(+39%), H-2→L+4(+21%), H-2→L+2(+21%)
	277.8	4.46	0.0359	H-7→L+0(+39%), H-2→L+5(+28%), H-6→L+0(+21%)
	276.4	4.49	0.1791	H-2→L+3(+44%), H-1→L+5(+19%), H-1→L+3(+15%)
	275.9	4.49	0.5920	H-3→L+4(+26%), H-7→L+0(+21%), H-6→L+0(+21%)
	274.7	4.51	0.0131	H-2→L+5(+29%), H-3→L+5(+22%), H-3→L+4(+19%)
	272.2	4.56	0.0035	H-8→L+0(+43%), H-2→L+3(+24%), H-3→L+4(+18%)
	271.2	4.57	0.0170	H-1→L+4(+34%), H-2→L+3(+32%), H-1→L+6(+20%)
	268.6	4.62	0.0742	H-9→L+0(+47%), H-5→L+0(+21%), H-0→L+7(+12%)
$Tp^1\beta$-Th_2Tp^1	350.8	3.53	0.1647	H-0→L+0(+67%)
	347.7	3.57	0.0245	H-1→L+0(+56%), H-2→L+0(+24%), H-0→L+3(+16%)
	340.3	3.64	0.0117	H-2→L+0(+53%), H-1→L+1(+20%), H-0→L+3(+16%)
	329.7	3.76	0.0045	H-0→L+1(+54%), H-2→L+1(+15%), H-2→L+0(+11%)
	327.5	3.79	0.0212	H-1→L+1(+40%), H-0→L+2(+22%), H-2→L+1(+12%)
	322.4	3.85	0.0398	H-0→L+1(+34%), H-1→L+1(+27%), H-3→L+0(+24%)
	316.0	3.92	0.0096	H-3→L+0(+48%), H-2→L+1(+40%), H-1→L+1(+22%)
	315.3	3.93	0.0136	H-1→L+2(+36%), H-0→L+3(+35%), H-2→L+1(+15%)
	310.2	4.00	0.0125	H-0→L+2(+43%), H-0→L+4(+20%), H-3→L+0(+16%)
	306.9	4.01	0.0232	H-0→L+4(+39%), H-1→L+3(+26%), H-0→L+5(+24%)
	304.4	4.07	0.0097	H-0→L+2(+38%), H-1→L+2(+36%), H-0→L+5(+15%)
	303.4	4.09	0.0040	H-1→L+4(+34%), H-0→L+4(+31%), H-3→L+1(+20%)
	302.6	4.10	0.0384	H-2→L+2(+32%), H-1→L+4(+19%), H-2→L+4(+19%)
	300.6	4.12	0.0073	H-4→L+0(+51%), H-1→L+3(+18%), H-1→L+2(+13%)
	299.3	4.14	0.0120	H-1→L+3(+31%), H-3→L+1(+28%), H-1→L+2(+23%)
	296.5	4.18	0.0982	H-3→L+1(+31%), H-2→L+3(+28%), H-0→L+3(+15%)
	294.0	4.22	0.0363	H-2→L+2(+47%), H-1→L+2(+10%)
	292.9	4.23	0.0538	H-2→L+3(+32%), H-2→L+4(+18%), H-2→L+2(+17%)
	291.6	4.25	0.0490	H-2→L+4(+28%), H-0→L+6(+18%), H-3→L+3(+16%)
	288.4	4.30	0.1400	H-1→L+5(+47%), H-2→L+4(+32%), H-1→L+6(+17%)
	287.4	4.31	0.0632	H-0→L+6(+50%), H-4→L+1(+25%), H-3→L+2(+23%)
	286.7	4.32	0.2200	H-0→L+6(+33%), H-2→L+5(+26%), H-1→L+3(+13%)
	285.8	4.34	0.1592	H-2→L+5(+41%), H-1→L+6(+36%), H-3→L+1(+16%)
	282.7	4.39	0.1867	H-4→L+1(+47%), H-2→L+5(+13%), H-0→L+3(+10%)
	280.5	4.42	0.0198	H-3→L+3(+50%), H-2→L+6(+19%), H-1→L+5(+19%)
	278.6	4.45	0.0189	H-5→L+0(+51%), H-0→L+7(+23%), H-3→L+3(+15%)
	276.5	4.48	0.0150	H-2→L+6(+54%), H-0→L+7(+16%), H-4→L+3(+11%)
	275.8	4.50	0.1091	H-3→L+4(+42%), H-5→L+0(+18%), H-3→L+3(+15%)
	275.1	4.51	0.2961	H-3→L+4(+34%), H-1→L+6(+25%), H-4→L+3(+18%)
	274.5	4.52	0.2571	H-3→L+5(+43%), H-3→L+4(+14%), H-3→L+6(+14%)
$Tp^1Fu_2Tp^1$	427.5	2.90	1.9861	H-0→L+0(+70%)

	368.8	3.36	0.0005	H-0→L+1(+67%), H-2→L+0(+13%), H-0→L+2(+13%)
	362.1	3.42	0.0036	H-0→L+2(+51%), H-2→L+0(+23%), H-3→L+0(+21%)
	361.3	3.43	0.0080	H-1→L+0(+48%), H-0→L+3(+34%)
	342.2	3.62	0.0138	H-2→L+0(+59%), H-0→L+4(+13%)
	335.9	3.69	0.0352	H-3→L+0(+37%), H-0→L+3(+30%), H-0→L+4(+27%)
	333.7	3.72	0.0206	H-0→L+3(+43%)
	330.5	3.75	0.0151	H-0→L+5(+62%)
	329.1	3.77	0.0268	H-0→L+4(+53%), H-0→L+2(+22%)
	319.1	3.89	0.0168	H-4→L+0(+50%), H-2→L+2(+27%), H-2→L+1(+19%)
	311.9	3.98	0.0166	H-1→L+1(+57%), H-0→L+3(+20%), H-1→L+0(+19%)
	308.6	4.02	0.0134	H-2→L+1(+52%), H-3→L+1(+13%), H-3→L+4(+13%)
	305.3	4.06	0.1086	H-0→L+6(+36%), H-4→L+0(+32%), H-3→L+1(+16%)
	300.7	4.12	0.4523	H-0→L+6(+45%), H-2→L+1(+18%)
	299.6	4.14	0.0155	H-1→L+5(+42%), H-1→L+1(+23%)
	298.5	4.15	0.0405	H-1→L+5(+28%), H-3→L+1(+27%), H-0→L+6(+17%)
	293.4	4.23	0.0015	H-5→L+0(+38%), H-2→L+4(+31%), H-3→L+2(+24%)
	290.3	4.27	0.0821	H-6→L+0(+38%), H-3→L+2(+23%), H-1→L+3(+20%)
	287.8	4.31	0.0122	H-4→L+1(+46%), H-3→L+4(+20%), H-3→L+0(+16%)
	282.7	4.39	0.0021	H-1→L+2(+70%)
	278.0	4.46	0.1616	H-3→L+2(+42%), H-4→L+4(+10%)
	276.3	4.49	0.0656	H-4→L+1(+38%), H-5→L+0(+37%), H-1→L+3(+13%)
	275.1	4.51	0.1243	H-2→L+3(+36%), H-2→L+5(+34%), H-1→L+3(+17%)
	274.1	4.52	0.1579	H-2→L+3(+47%), H-3→L+5(+21%), H-4→L+4(+11%)
	273.7	4.53	0.0014	H-3→L+4(+38%), H-3→L+2(+22%), H-2→L+6(+14%)
	270.2	4.59	0.0556	H-1→L+4(+46%), H-1→L+6(+14%)
	269.0	4.61	0.1861	H-1→L+4(+48%), H-3→L+3(+44%)
	268.2	4.62	0.5421	H-6→L+0(+49%), H-4→L+0(+10%)
	265.9	4.66	0.1418	H-4→L+2(+50%), H-6→L+2(+10%), H-3→L+2(+10%)
	263.8	4.70	0.1013	H-2→L+5(+42%), H-3→L+5(+40%), H-4→L+2(+27%)
$Tp^1Tt_2Tp^1$	470.4	2.64	2.6883	H-0→L+0(+70%)
	387.8	3.20	0.0045	H-0→L+1(+52%)
	383.7	3.23	0.0116	H-2→L+0(+65%), H-2→L+1(+17%), H-0→L+4(+14%)
	377.4	3.28	0.0059	H-1→L+0(+42%), H-0→L+1(+35%)
	369.7	3.35	0.0072	H-3→L+0(+50%), H-1→L+0(+30%), H-0→L+1(+30%)
	349.9	3.54	0.0133	H-4→L+0(+50%), H-0→L+2(+33%), H-0→L+3(+22%)
	343.2	3.61	0.0133	H-0→L+2(+51%), H-3→L+0(+18%)
	339.9	3.65	0.0092	H-0→L+4(+50%), H-2→L+1(+30%), H-1→L+4(+13%)
	332.7	3.73	0.0370	H-0→L+3(+58%), H-0→L+4(+13%), H-2→L+4(+12%)
	327.0	3.79	0.0006	H-5→L+0(+43%), H-0→L+6(+27%), H-1→L+6(+12%)
	326.2	3.80	0.1036	H-1→L+1(+58%)
	324.4	3.82	0.0015	H-5→L+0(+47%), H-6→L+0(+33%), H-0→L+5(+23%)
	322.6	3.84	0.0416	H-0→L+6(+40%), H-0→L+5(+33%), H-1→L+1(+30%)
	319.9	3.88	0.0308	H-2→L+1(+51%)
	317.7	3.90	0.0236	H-3→L+1(+44%), H-4→L+2(+13%)
	314.7	3.94	0.0498	H-7→L+0(+53%), H-0→L+5(+15%), H-5→L+0(+13%)
	312.9	3.96	0.0043	H-7→L+0(+43%), H-6→L+0(+37%), H-3→L+1(+18%)
	308.3	4.02	0.0158	H-1→L+2(+32%), H-4→L+1(+27%), H-3→L+1(+22%)
	302.3	4.10	0.0469	H-8→L+0(+35%), H-2→L+4(+24%), H-2→L+3(+15%)
	301.3	4.11	0.0022	H-8→L+0(+44%), H-2→L+6(+28%), H-1→L+4(+16%)
	299.2	4.14	0.0143	H-4→L+1(+36%), H-4→L+2(+17%), H-2→L+5(+13%)
	294.8	4.21	0.0057	H-9→L+0(+41%), H-4→L+1(+30%), H-3→L+2(+21%)
	292.1	4.24	0.0010	H-0→L+7(+34%), H-9→L+0(+30%)
	287.2	4.32	0.4720	H-2→L+4(+34%), H-1→L+1(+17%), H-3→L+3(+16%)
	285.3	4.35	0.0170	H-1→L+3(+31%), H-0→L+7(+30%), H-0→L+8(+23%)
	285.0	4.35	0.0275	H-2→L+3(+45%), H-2→L+6(+35%), H-2→L+1(+17%)
	284.4	4.36	0.1028	H-1→L+5(+37%), H-3→L+1(+16%), H-9→L+0(+14%)

	283.2	4.38	0.1355	H-5→L+1(+51%), H-1→L+2(+17%), H-0→L+7(+13%)
	281.4	4.41	0.1054	H-5→L+1(+29%), H-9→L+0(+25%), H-1→L+6(+16%)
	279.7	4.43	0.0097	H-0→L+8(+55%), H-2→L+2(+14%)
Tp^1T^1	383.6	3.23	1.0294	H-0→L+0(+70%)
	358.6	3.46	0.0082	H-1→L+0(+62%), H-0→L+3(+14%)
	357.7	3.47	0.0232	H-2→L+0(+59%), H-0→L+1(+25%), H-1→L+0(+19%)
	327.7	3.78	0.0027	H-3→L+0(+62%), H-0→L+3(+15%), H-2→L+1(+14%)
	321.9	3.85	0.0219	H-0→L+2(+46%), H-1→L+0(+26%), H-0→L+1(+22%)
	319.1	3.89	0.0160	H-0→L+3(+36%), H-0→L+1(+30%), H-0→L+2(+20%)
	316.0	3.92	0.0469	H-0→L+1(+41%), H-3→L+0(+20%), H-2→L+1(+18%)
	313.7	3.95	0.0257	H-0→L+4(+47%), H-0→L+3(+35%), H-0→L+1(+15%)
	298.4	4.16	0.1409	H-2→L+3(+36%), H-2→L+2(+29%), H-2→L+4(+13%)
	294.1	4.22	0.6569	H-2→L+1(+36%), H-4→L+0(+27%), H-2→L+3(+19%)
	292.3	4.24	0.0020	H-4→L+0(+54%), H-2→L+2(+11%)
	290.2	4.27	0.0072	H-1→L+1(+65%)
	288.8	4.29	0.0211	H-1→L+2(+43%), H-4→L+0(+21%), H-0→L+3(+18%)
	287.0	4.32	0.1379	H-5→L+0(+41%), H-1→L+4(+30%), H-0→L+2(+20%)
	283.6	4.37	0.0159	H-2→L+2(+44%), H-2→L+1(+25%), H-1→L+2(+10%)
	280.0	4.43	0.0529	H-1→L+3(+46%), H-1→L+4(+37%), H-1→L+1(+20%)
	277.7	4.47	0.1595	H-1→L+3(+36%), H-5→L+0(+32%), H-1→L+5(+12%)
	272.4	4.55	0.0145	H-2→L+4(+58%), H-2→L+2(+21%), H-3→L+1(+13%)
	269.6	4.60	0.0902	H-3→L+2(+42%), H-3→L+3(+41%), H-3→L+4(+12%)
	267.2	4.64	0.3332	H-3→L+2(+42%), H-3→L+1(+24%), H-2→L+2(+12%)
	265.4	4.67	0.2697	H-3→L+1(+35%), H-3→L+3(+34%), H-2→L+3(+23%)
	261.7	4.74	0.0824	H-3→L+4(+41%), H-2→L+1(+14%), H-1→L+5(+10%)
	258.4	4.80	0.1950	H-3→L+4(+36%), H-0→L+5(+32%), H-6→L+0(+27%)
	256.1	4.84	0.0965	H-6→L+0(+41%), H-4→L+1(+21%), H-5→L+2(+12%)
	254.1	4.88	0.3780	H-7→L+0(+34%), H-5→L+1(+19%), H-4→L+4(+18%)
	251.4	4.93	0.0255	H-7→L+0(+45%), H-6→L+0(+30%), H-1→L+5(+18%)
	250.5	4.95	0.0427	H-4→L+1(+34%), H-4→L+2(+17%), H-3→L+4(+12%)
	249.7	4.97	0.0388	H-4→L+1(+40%), H-8→L+0(+36%), H-7→L+0(+19%)
	248.1	5.00	0.1295	H-4→L+2(+51%), H-1→L+5(+20%), H-9→L+0(+19%)
	246.8	5.02	0.0683	H-8→L+0(+38%), H-4→L+3(+12%)
Tp^1Dt^1	404.3	3.07	1.4008	H-0→L+0(+70%)
	366.6	3.38	0.0265	H-1→L+0(+63%), H-0→L+2(+13%)
	358.8	3.46	0.0126	H-2→L+0(+57%)
	339.0	3.66	0.0211	H-3→L+0(+50%), H-0→L+1(+36%), H-2→L+0(+12%)
	334.8	3.70	0.0673	H-0→L+1(+43%), H-1→L+0(+18%), H-2→L+0(+14%)
	329.8	3.76	0.0164	H-0→L+3(+41%), H-3→L+0(+31%), H-1→L+0(+21%)
	325.4	3.81	0.0213	H-0→L+2(+43%), H-2→L+0(+21%), H-0→L+3(+14%)
	324.2	3.82	0.0325	H-0→L+4(+47%), H-0→L+3(+36%), H-2→L+0(+25%)
	306.1	4.05	0.1799	H-4→L+0(+61%), H-1→L+2(+14%), H-3→L+1(+11%)
	303.2	4.09	0.0387	H-2→L+1(+40%), H-3→L+1(+25%), H-3→L+2(+21%)
	300.9	4.12	0.1990	H-1→L+2(+32%), H-5→L+0(+13%), H-3→L+1(+12%)
	296.3	4.18	0.1031	H-1→L+1(+35%), H-1→L+4(+32%), H-3→L+1(+18%)
	294.8	4.21	0.0085	H-5→L+0(+46%), H-2→L+2(+20%), H-2→L+1(+16%)
	291.1	4.26	0.0327	H-1→L+2(+46%), H-1→L+1(+44%), H-1→L+3(+18%)
	286.5	4.33	0.1090	H-5→L+0(+32%), H-1→L+3(+11%), H-3→L+4(+10%)
	284.2	4.36	0.0232	H-1→L+3(+35%), H-1→L+4(+34%), H-2→L+2(+13%)
	282.4	4.39	0.0176	H-2→L+4(+33%), H-1→L+3(+28%), H-2→L+3(+26%)
	280.7	4.42	0.0295	H-6→L+0(+55%), H-3→L+4(+16%)
	277.5	4.47	0.1752	H-3→L+2(+46%), H-1→L+4(+15%), H-3→L+3(+14%)
	274.8	4.51	0.0534	H-3→L+3(+47%), H-3→L+4(+37%), H-0→L+5(+17%)
	273.5	4.53	0.4020	H-3→L+1(+37%), H-2→L+2(+36%), H-3→L+2(+28%)
	270.5	4.58	0.0475	H-2→L+3(+47%), H-3→L+2(+17%)
	267.5	4.63	0.1555	H-0→L+5(+45%), H-6→L+0(+16%), H-1→L+4(+15%)

	267.0	4.64	0.2656	H-3→L+4(+44%), H-2→L+3(+19%), H-0→L+6(+13%)
	264.8	4.68	0.0014	H-0→L+7(+68%)
	261.7	4.74	0.0340	H-6→L+0(+52%), H-3→L+4(+19%), H-4→L+2(+14%)
	258.6	4.79	0.0988	H-4→L+1(+49%), H-7→L+0(+25%), H-4→L+4(+19%)
	257.4	4.82	0.0669	H-1→L+5(+29%), H-8→L+0(+26%), H-4→L+3(+24%)
	255.4	4.85	0.0710	H-4→L+2(+48%), H-4→L+1(+33%), H-4→L+3(+20%)
	254.4	4.87	0.0442	H-8→L+0(+55%)
Tp^1PhTp^1	351.6	3.53	1.0767	H-0→L+0(+67%)
	344.1	3.60	0.0123	H-1→L+0(+59%), H-2→L+1(+22%)
	342.9	3.62	0.1577	H-2→L+0(+58%), H-0→L+2(+23%), H-1→L+1(+22%)
	324.2	3.82	0.0019	H-3→L+0(+60%), H-1→L+2(+20%)
	312.3	3.97	0.0018	H-0→L+1(+50%), H-3→L+0(+22%), H-1→L+0(+21%)
	309.8	4.00	0.0149	H-1→L+1(+36%), H-0→L+2(+32%), H-3→L+3(+20%)
	308.1	4.02	0.0065	H-0→L+3(+30%), H-1→L+0(+27%), H-1→L+4(+20%)
	301.8	4.11	0.3299	H-0→L+4(+36%), H-2→L+2(+33%), H-3→L+1(+25%)
	299.2	4.14	0.1753	H-0→L+4(+38%), H-3→L+5(+20%), H-1→L+3(+18%)
	297.6	4.17	0.0011	H-0→L+5(+55%), H-3→L+4(+23%), H-5→L+0(+23%)
	293.9	4.22	0.0472	H-1→L+1(+40%), H-2→L+4(+34%), H-4→L+2(+11%)
	293.6	4.22	0.0010	H-2→L+1(+42%), H-1→L+4(+33%), H-5→L+2(+10%)
	286.4	4.33	0.1466	H-0→L+3(+55%), H-2→L+1(+26%), H-2→L+5(+13%)
	286.3	4.33	0.1580	H-0→L+2(+54%), H-2→L+4(+13%), H-4→L+2(+12%)
	282.5	4.39	0.0005	H-1→L+2(+36%), H-0→L+5(+29%), H-0→L+1(+26%)
	282.0	4.40	0.6260	H-4→L+0(+52%), H-0→L+4(+23%)
	280.1	4.43	0.3870	H-3→L+1(+40%), H-1→L+3(+30%), H-0→L+4(+30%)
	278.0	4.46	0.0169	H-2→L+3(+51%), H-1→L+2(+47%)
	278.0	4.46	0.0227	H-2→L+2(+51%), H-1→L+3(+46%)
	271.2	4.57	0.1694	H-1→L+5(+44%), H-3→L+5(+26%), H-2→L+4(+22%)
	270.9	4.58	0.0002	H-3→L+4(+36%), H-1→L+4(+36%), H-2→L+5(+35%)
	270.2	4.59	0.3564	H-3→L+2(+48%), H-2→L+5(+30%), H-2→L+1(+22%)
	269.7	4.60	0.3023	H-3→L+3(+45%), H-2→L+4(+30%), H-3→L+5(+27%)
	268.6	4.62	0.0411	H-7→L+0(+43%), H-0→L+7(+37%), H-5→L+0(+20%)
	268.1	4.62	0.0488	H-3→L+5(+47%)
	267.7	4.63	0.1254	H-1→L+4(+31%), H-7→L+0(+27%), H-2→L+5(+20%)
	266.0	4.66	0.0000	H-5→L+0(+54%), H-0→L+1(+13%), H-1→L+2(+13%)
	260.5	4.76	0.1698	H-6→L+0(+56%), H-0→L+6(+26%), H-3→L+5(+21%)
	259.2	4.78	0.0273	H-4→L+1(+64%)
	252.3	4.91	0.2537	H-4→L+3(+50%), H-8→L+0(+22%), H-1→L+4(+15%)
$Tp^1Ph_2Tp^1$	353.6	3.51	1.4897	H-0→L+0(+67%), H-3→L+1(+12%), H-2→L+0(+10%)
	347.3	3.57	0.0205	H-1→L+0(+56%), H-3→L+2(+18%), H-2→L+0(+17%)
	346.2	3.58	0.2023	H-2→L+0(+55%), H-2→L+1(+20%), H-0→L+3(+19%)
	328.6	3.77	0.0270	H-3→L+0(+58%), H-0→L+1(+20%), H-1→L+0(+10%)
	314.6	3.94	0.0090	H-0→L+1(+39%), H-2→L+1(+27%), H-0→L+3(+21%)
	312.9	3.96	0.0671	H-1→L+1(+33%), H-1→L+0(+29%), H-0→L+2(+27%)
	311.4	3.98	0.0225	H-0→L+1(+44%), H-2→L+0(+22%)
	307.4	4.03	0.4355	H-1→L+2(+38%), H-3→L+1(+29%), H-1→L+1(+23%)
	300.3	4.13	0.0060	H-0→L+4(+42%), H-3→L+5(+21%), H-5→L+1(+16%)
	299.1	4.15	0.0037	H-0→L+5(+35%), H-1→L+1(+26%), H-5→L+0(+21%)
	297.5	4.17	0.0132	H-2→L+4(+36%), H-2→L+5(+26%), H-1→L+5(+16%)
	296.6	4.18	0.0284	H-1→L+5(+24%), H-3→L+1(+18%), H-4→L+0(+18%)
	290.7	4.26	0.4718	H-4→L+0(+39%), H-0→L+2(+33%), H-1→L+2(+12%)
	287.9	4.31	0.3079	H-0→L+2(+44%), H-3→L+1(+31%), H-3→L+2(+16%)
	284.9	4.35	0.0324	H-2→L+3(+39%), H-0→L+5(+25%), H-0→L+1(+24%)
	282.4	4.39	0.2694	H-0→L+3(+51%)
	281.3	4.41	0.2199	H-2→L+2(+30%), H-0→L+4(+27%), H-3→L+1(+23%)
	280.9	4.41	0.0610	H-2→L+2(+60%), H-1→L+2(+23%)
	277.5	4.47	0.2379	H-3→L+2(+41%), H-1→L+5(+21%), H-1→L+1(+18%)

	275.6	4.50	0.0358	H-5→L+0(+51%), H-1→L+3(+13%)
	275.1	4.51	0.0432	H-1→L+3(+57%), H-0→L+6(+21%)
	274.8	4.51	0.0156	H-1→L+3(+35%), H-6→L+0(+32%), H-0→L+4(+28%)
	271.1	4.57	0.0003	H-0→L+7(+50%), H-0→L+8(+14%), H-7→L+0(+13%)
	269.8	4.59	0.1712	H-3→L+3(+52%)
	268.6	4.62	0.0374	H-1→L+4(+50%), H-1→L+5(+30%)
	268.0	4.63	0.0267	H-3→L+4(+38%), H-2→L+4(+14%), H-1→L+4(+11%)
	266.8	4.65	0.0390	H-4→L+1(+36%), H-2→L+4(+33%), H-5→L+0(+17%)
	266.6	4.65	0.0026	H-0→L+8(+41%), H-10→L+0(+26%), H-7→L+0(+26%)
	265.7	4.67	0.0318	H-4→L+1(+38%), H-2→L+5(+21%), H-3→L+4(+16%)
	264.7	4.68	0.0136	H-3→L+5(+41%), H-3→L+4(+37%), H-2→L+5(+14%)
Tp^{1}TtTp^1	410.7	3.02	1.9236	H-0→L+0(+70%)
	366.2	3.39	0.0153	H-1→L+0(+62%), H-0→L+3(+18%), H-3→L+0(+14%)
	363.9	3.41	0.0176	H-2→L+0(+61%), H-0→L+2(+20%), H-1→L+0(+11%)
	346.1	3.58	0.0049	H-3→L+0(+56%), H-0→L+2(+21%), H-0→L+3(+14%)
	337.9	3.67	0.0204	H-0→L+1(+65%), H-1→L+3(+11%), H-0→L+2(+11%)
	331.7	3.74	0.0861	H-0→L+3(+43%), H-2→L+0(+27%), H-1→L+2(+10%)
	326.5	3.80	0.0194	H-0→L+2(+44%), H-0→L+3(+29%), H-2→L+1(+14%)
	318.7	3.89	0.0514	H-4→L+0(+55%), H-0→L+3(+23%), H-2→L+0(+10%)
	314.5	3.94	0.1085	H-0→L+4(+42%), H-0→L+5(+31%), H-2→L+3(+17%)
	313.9	3.95	0.0125	H-0→L+5(+42%), H-6→L+0(+18%), H-2→L+2(+16%)
	307.6	4.03	0.0301	H-5→L+0(+66%)
	303.9	4.08	0.0235	H-1→L+1(+52%), H-4→L+0(+20%), H-3→L+2(+16%)
	303.2	4.09	0.0346	H-2→L+2(+29%), H-1→L+2(+26%), H-0→L+4(+22%)
	302.2	4.10	0.0276	H-1→L+3(+33%), H-0→L+5(+27%), H-0→L+4(+23%)
	297.7	4.16	0.0103	H-2→L+1(+50%), H-2→L+2(+19%), H-6→L+0(+16%)
	293.5	4.22	0.0004	H-6→L+0(+53%), H-1→L+4(+16%), H-1→L+5(+13%)
	292.1	4.24	0.0104	H-3→L+1(+37%), H-1→L+5(+29%), H-7→L+0(+15%)
	289.5	4.28	0.0059	H-7→L+0(+51%)
	286.1	4.33	0.3945	H-3→L+1(+42%), H-3→L+2(+16%), H-3→L+3(+13%)
	283.6	4.37	0.0039	H-6→L+0(+30%), H-4→L+1(+27%), H-2→L+5(+18%)
	281.2	4.41	0.0335	H-1→L+2(+56%)
	279.4	4.44	0.0543	H-2→L+3(+53%), H-1→L+3(+38%), H-2→L+5(+11%)
	274.7	4.51	0.0809	H-4→L+1(+32%), H-3→L+2(+29%), H-1→L+4(+15%)
	273.3	4.54	0.1047	H-3→L+2(+32%), H-3→L+3(+31%), H-3→L+5(+29%),
	271.8	4.56	0.2146	H-1→L+4(+26%), H-4→L+1(+26%), H-7→L+0(+18%)
	271.3	4.57	0.1932	H-1→L+5(+36%), H-4→L+1(+35%), H-3→L+3(+27%)
	269.2	4.61	0.1370	H-3→L+4(+30%), H-5→L+1(+29%), H-3→L+2(+19%)
	267.9	4.63	0.2762	H-0→L+6(+29%), H-2→L+4(+28%), H-7→L+0(+27%)
	266.5	4.65	0.0846	H-5→L+1(+55%), H-1→L+4(+17%), H-2→L+5(+13%)
	266.1	4.66	0.0594	H-2→L+5(+36%), H-1→L+4(+34%), H-4→L+3(+30%)
Tp^{1}BtTp^1	423.2	2.93	1.6740	H-0→L+0(+70%)
	371.2	3.34	0.0233	H-1→L+0(+64%), H-1→L+1(+16%)
	368.4	3.37	0.3360	H-2→L+0(+66%)
	364.2	3.40	0.0527	H-3→L+0(+61%), H-2→L+3(+11%)
	356.5	3.48	0.0583	H-0→L+1(+63%)
	348.3	3.56	0.0338	H-4→L+0(+56%), H-0→L+1(+24%), H-0→L+2(+18%)
	334.7	3.70	0.0448	H-0→L+2(+60%), H-1→L+0(+17%)
	331.6	3.74	0.0222	H-0→L+3(+59%), H-3→L+0(+27%), H-3→L+1(+15%)
	324.8	3.82	0.0055	H-0→L+4(+62%), H-5→L+0(+19%), H-3→L+0(+10%)
	317.2	3.91	0.2016	H-5→L+0(+49%), H-0→L+2(+12%), H-2→L+2(+10%)
	316.5	3.92	0.0024	H-1→L+1(+46%)
	314.1	3.95	0.0008	H-2→L+1(+63%), H-3→L+3(+17%), H-0→L+3(+13%)
	311.7	3.98	0.0222	H-0→L+5(+48%), H-1→L+1(+32%), H-0→L+2(+17%)
	310.1	4.00	0.0163	H-3→L+1(+45%), H-3→L+0(+11%), H-2→L+1(+11%)
	305.6	4.06	0.0097	H-5→L+0(+35%), H-1→L+2(+28%), H-4→L+1(+27%)

	300.6	4.12	0.0020	H-1→L+5(+32%), H-3→L+3(+28%), H-4→L+1(+22%)
	300.1	4.13	0.0031	H-6→L+0(+40%), H-1→L+5(+27%), H-4→L+1(+19%)
	297.1	4.17	0.0534	H-3→L+4(+35%), H-3→L+1(+33%), H-4→L+1(+24%)
	296.3	4.18	0.0309	H-7→L+0(+45%), H-2→L+4(+20%), H-0→L+4(+14%)
	294.5	4.21	0.5067	H-0→L+6(+47%), H-4→L+1(+31%), H-2→L+1(+12%)
	289.8	4.28	0.0666	H-6→L+0(+37%), H-3→L+3(+26%), H-4→L+2(+19%)
	287.0	4.32	0.0212	H-2→L+2(+61%), H-4→L+1(+11%)
	284.9	4.35	0.0251	H-2→L+4(+52%), H-3→L+3(+22%), H-3→L+4(+17%)
	283.4	4.37	0.2069	H-2→L+3(+49%), H-3→L+1(+20%), H-7→L+0(+17%)
	280.9	4.41	0.0181	H-1→L+3(+59%), H-4→L+2(+18%), H-1→L+5(+16%)
	279.8	4.43	0.1156	H-1→L+3(+30%), H-7→L+0(+23%), H-4→L+5(+23%)
	278.4	4.45	0.3152	H-3→L+2(+32%), H-1→L+3(+16%), H-2→L+5(+15%)
	277.4	4.47	0.1068	H-3→L+2(+57%), H-4→L+2(+28%), H-1→L+5(+15%)
	277.2	4.47	0.5535	H-0→L+7(+41%), H-4→L+5(+24%), H-5→L+1(+15%)
	274.8	4.51	0.0860	H-8→L+0(+30%), H-2→L+6(+21%), H-0→L+7(+20%)
[a]H = HOMO, L = LUMO, H-n = HOMO-n and L+n = LUMO+n.				

8. POM

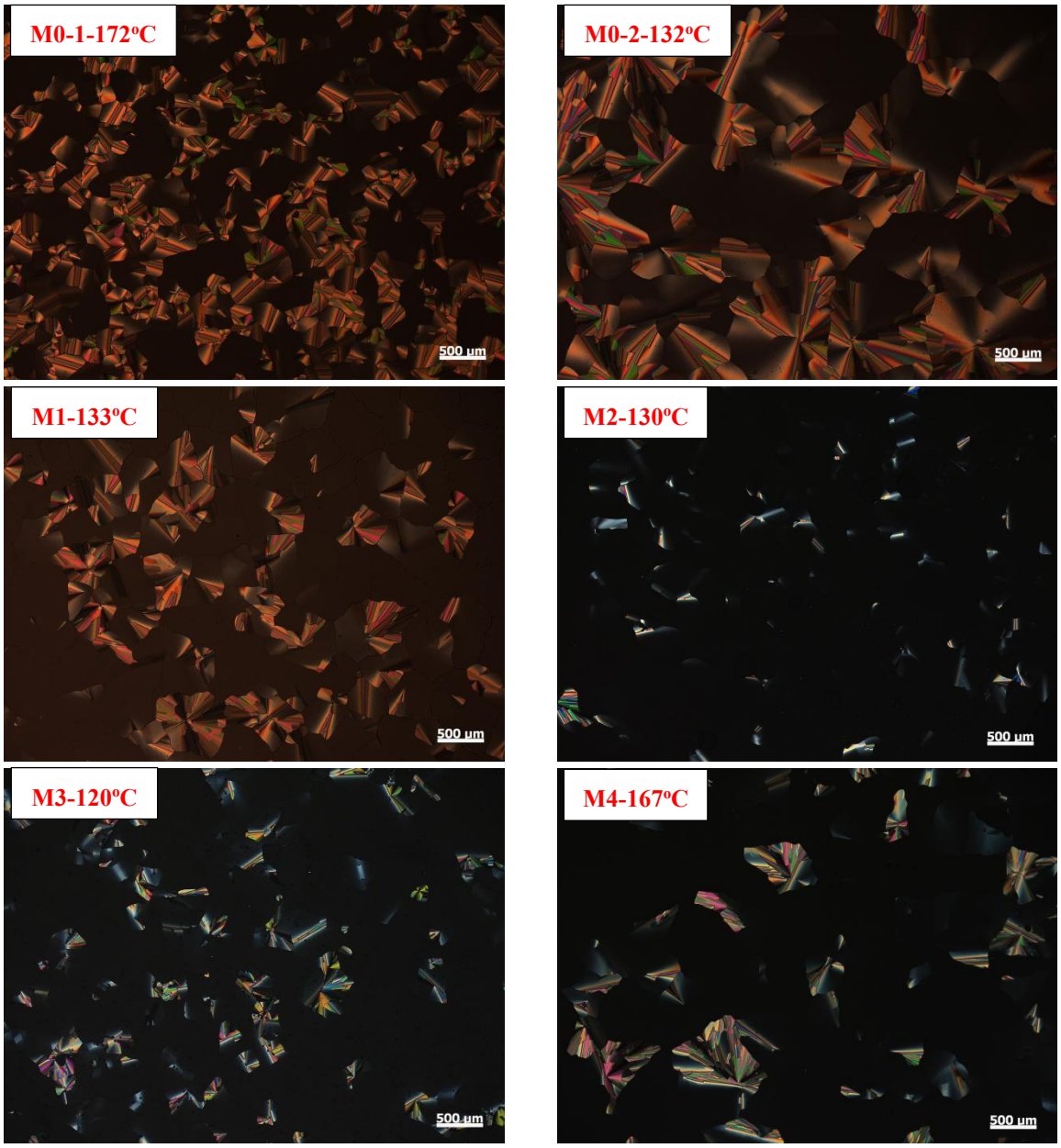

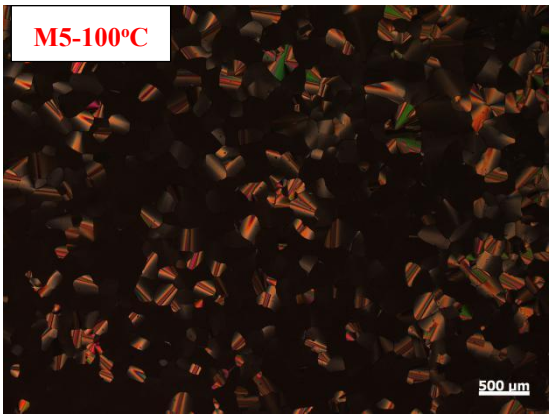
M5-100°C
500 µm

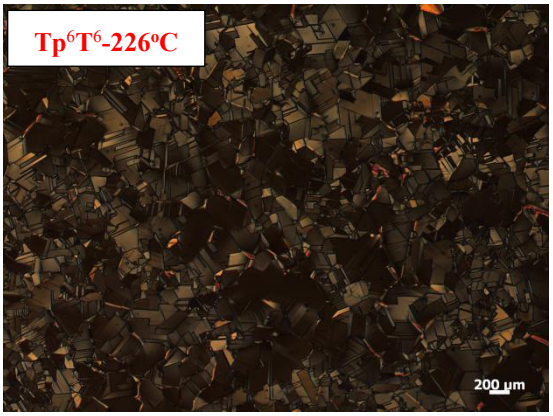
Tp⁶T⁶-226°C
200 µm

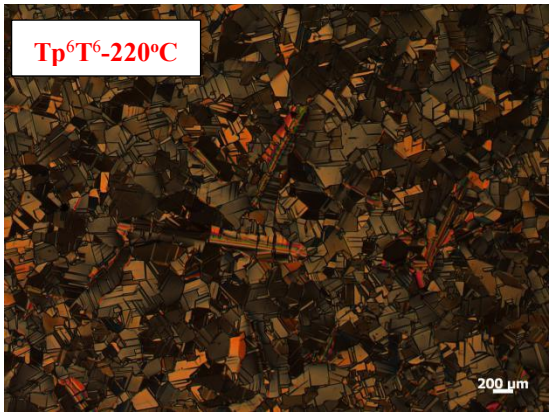
Tp⁶T⁶-220°C
200 µm

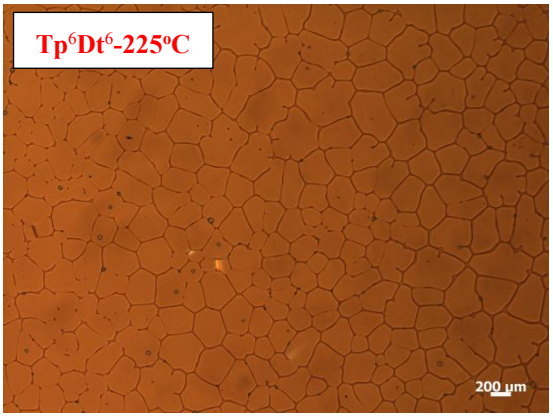
Tp⁶Dt⁶-225°C
200 µm

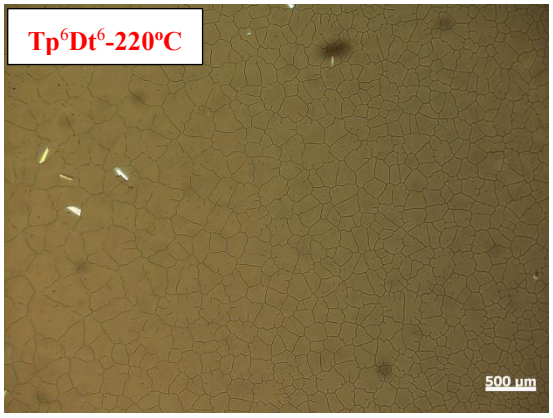
Tp⁶Dt⁶-220°C
500 µm

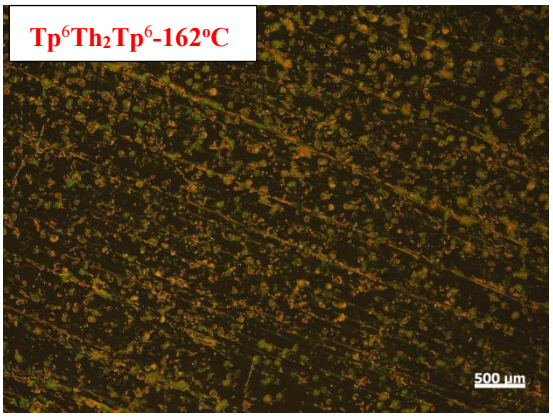
Tp⁶Th₂Tp⁶-162°C
500 µm

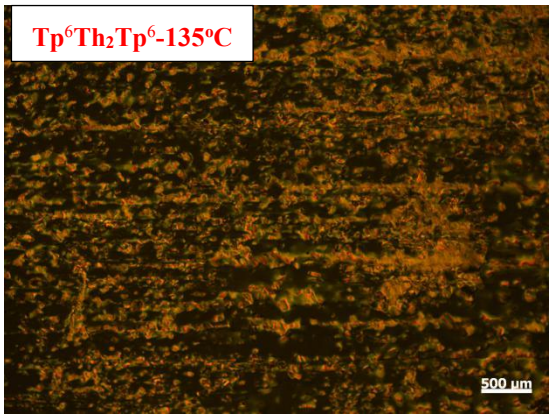
Tp⁶Th₂Tp⁶-135°C
500 µm

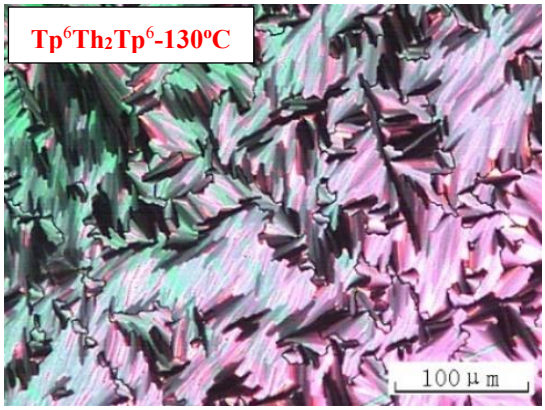
Tp⁶Th₂Tp⁶-130°C
100 μ m

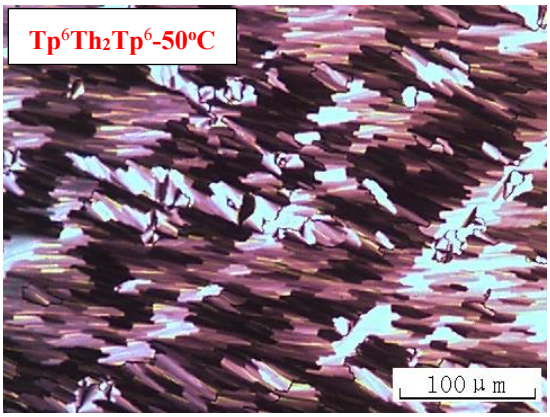
Tp⁶Th₂Tp⁶-50°C
100 μ m

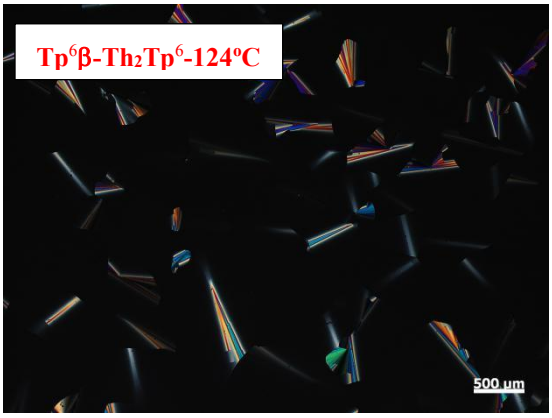
Tp⁶β-Th₂Tp⁶-124°C
500 μm

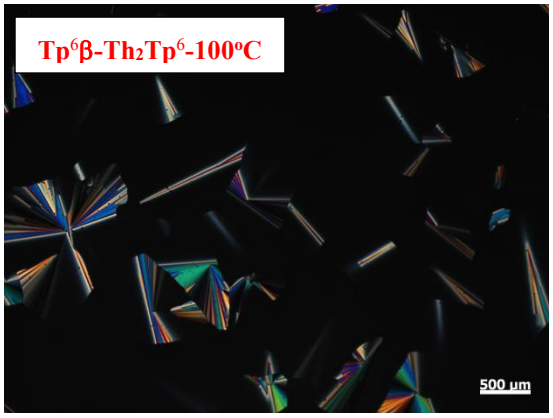
Tp⁶β-Th₂Tp⁶-100°C
500 μm

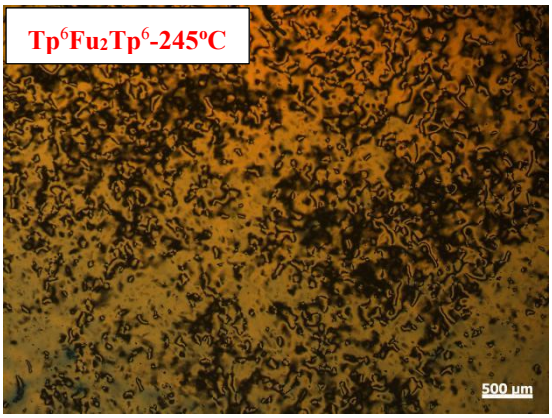
Tp⁶Fu₂Tp⁶-245°C
500 μm

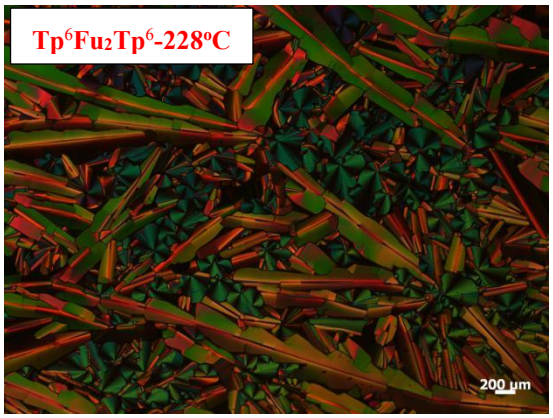
Tp⁶Fu₂Tp⁶-228°C
200 μm

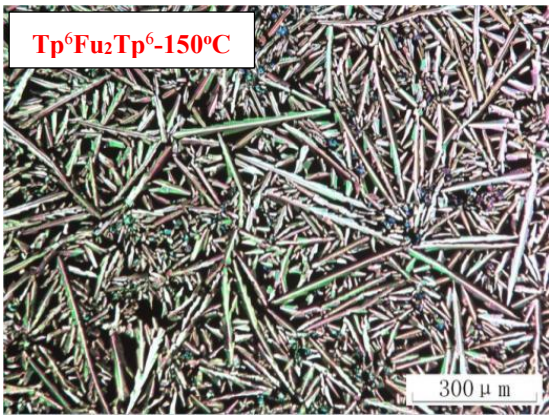
Tp⁶Fu₂Tp⁶-150°C
300 μ m


Tp⁶Tt₂Tp⁶-305°C
200 μm

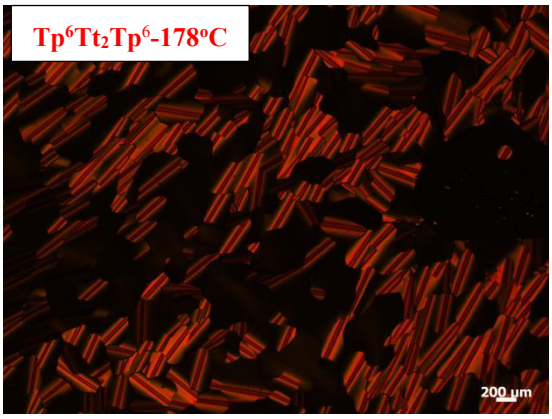
Tp⁶Tt₂Tp⁶-178ºC
200 μm

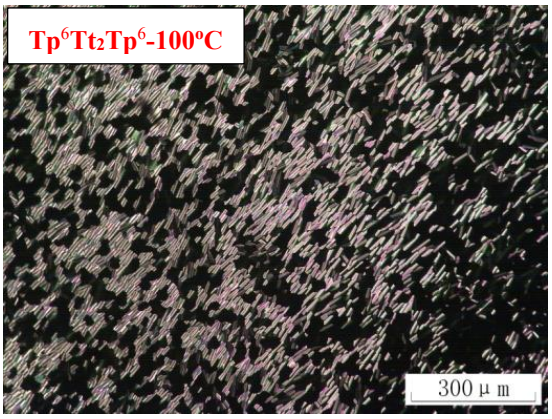
Tp⁶Tt₂Tp⁶-100ºC
300 μ m

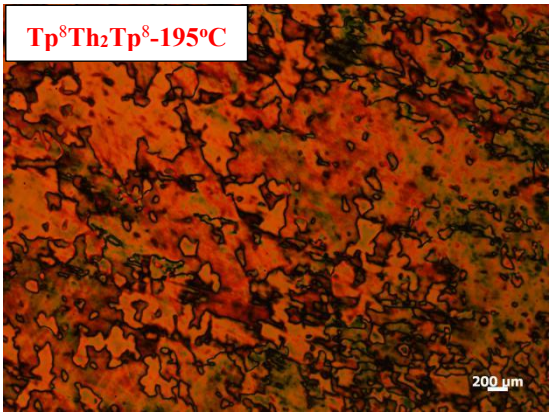
Tp⁸Th₂Tp⁸-195ºC
200 μm


Tp⁸Th₂Tp⁸-123ºC
200 μm

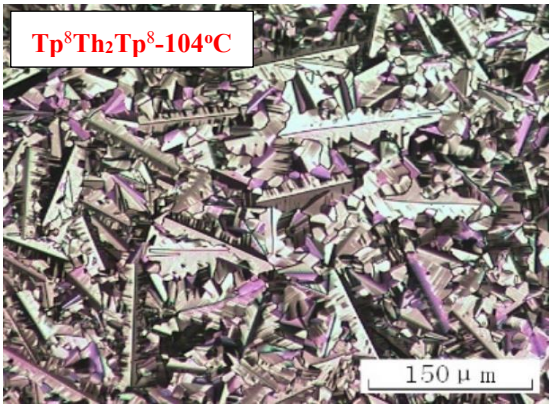
Tp⁸Th₂Tp⁸-104ºC
150 μ m

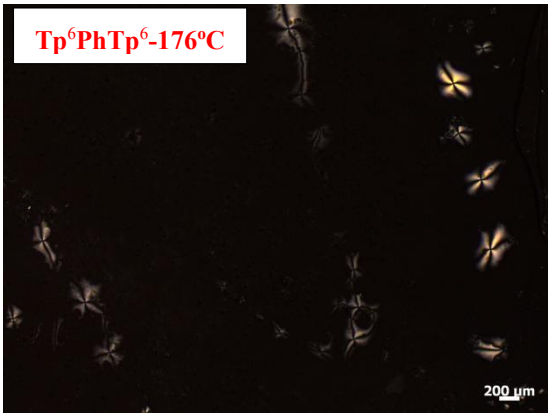
Tp⁶PhTp⁶-176ºC
200 μm

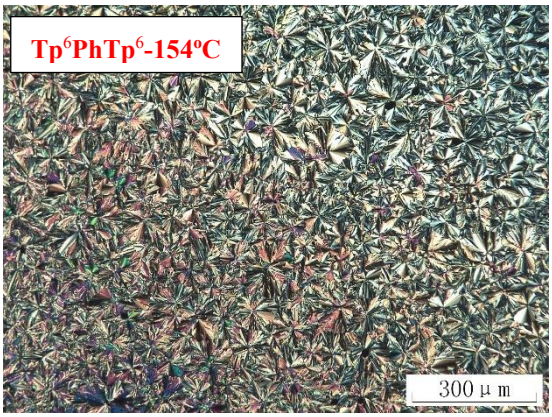
Tp⁶PhTp⁶-154ºC
300 μ m

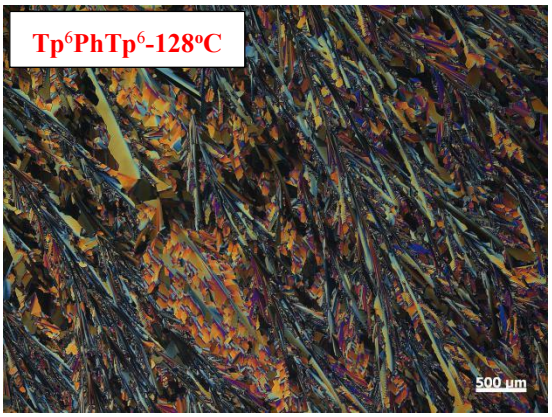
Tp⁶PhTp⁶-128ºC
500 μm

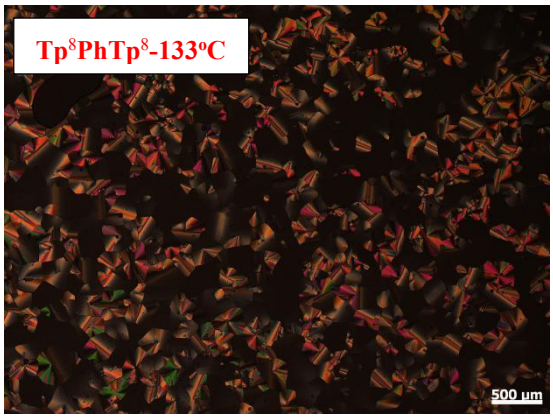
Tp8PhTp8-133ºC
500 µm

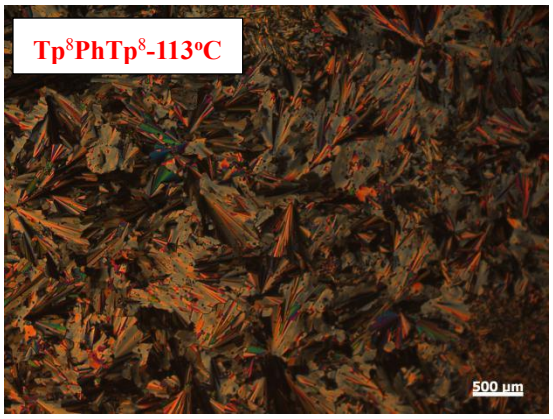
Tp8PhTp8-113ºC
500 µm

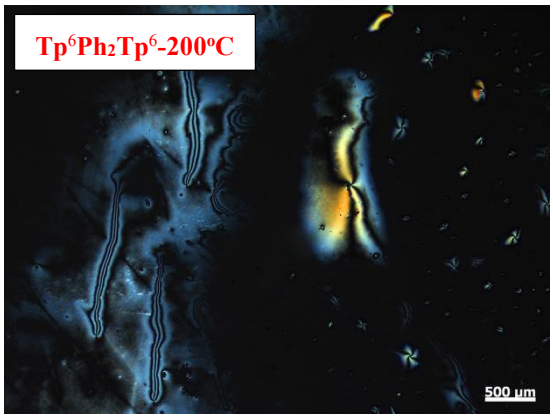
Tp6Ph2Tp6-200ºC
500 µm

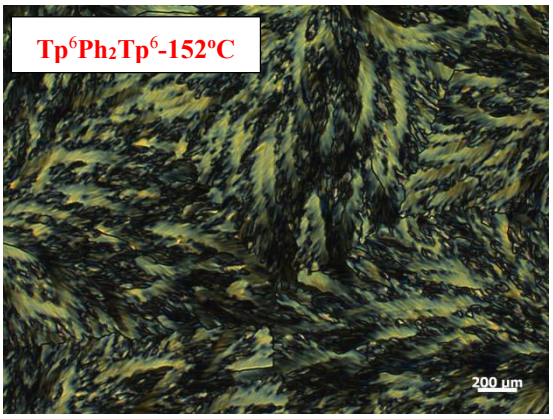
Tp6Ph2Tp6-152ºC
200 µm

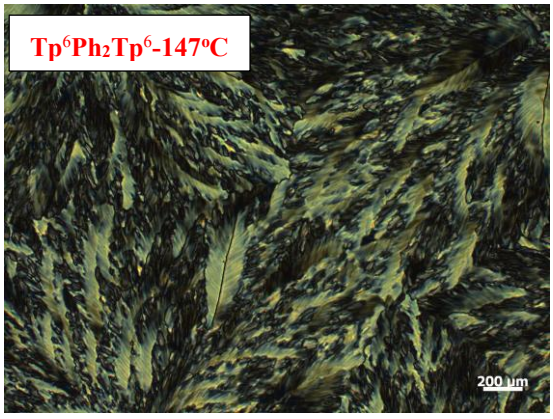
Tp6Ph2Tp6-147ºC
200 µm

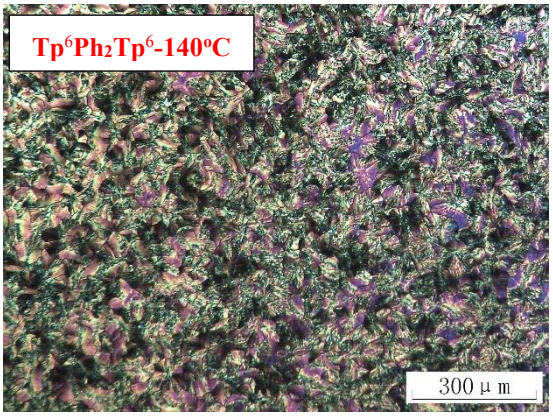
Tp6Ph2Tp6-140ºC
300 µ m

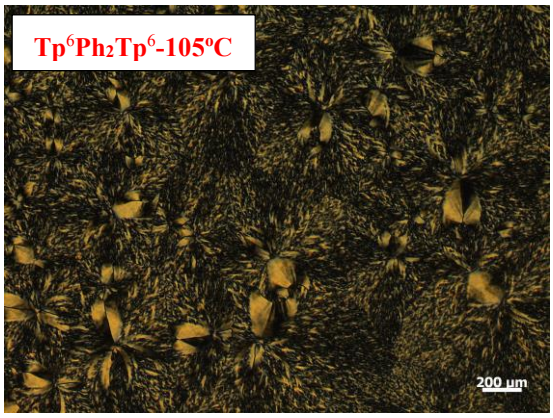
Tp6Ph2Tp6-105ºC
200 µm

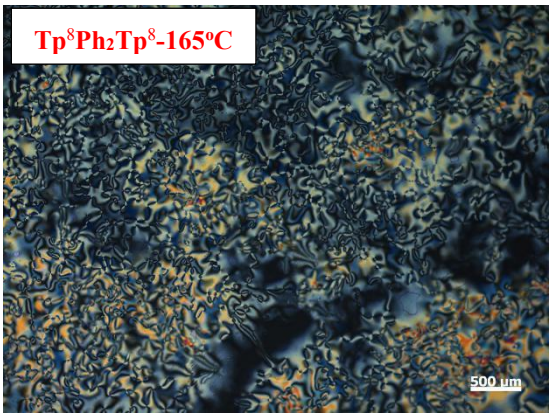
Tp8Ph2Tp8-165ºC
500 µm

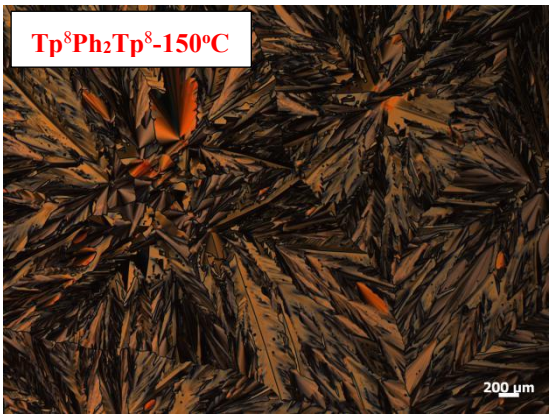
Tp8Ph2Tp8-150°C
200 μm

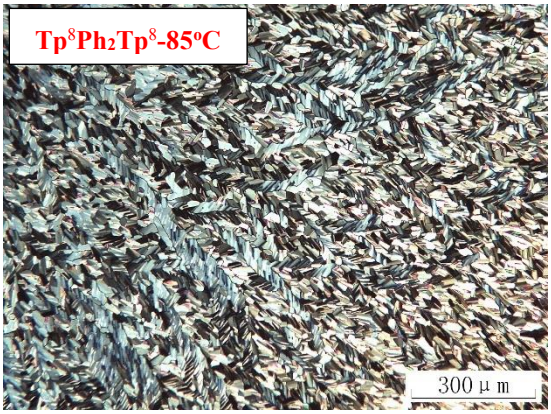
Tp8Ph2Tp8-85°C
300 μm

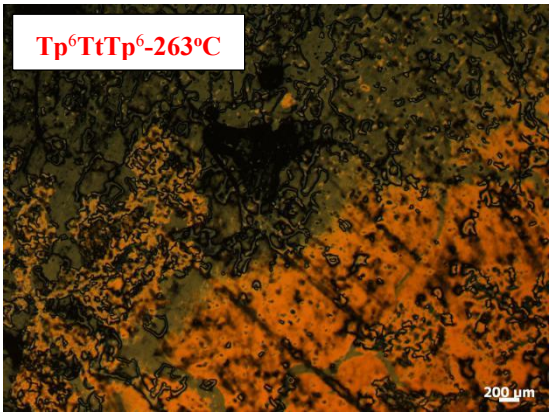
Tp6TtTp6-263°C
200 μm

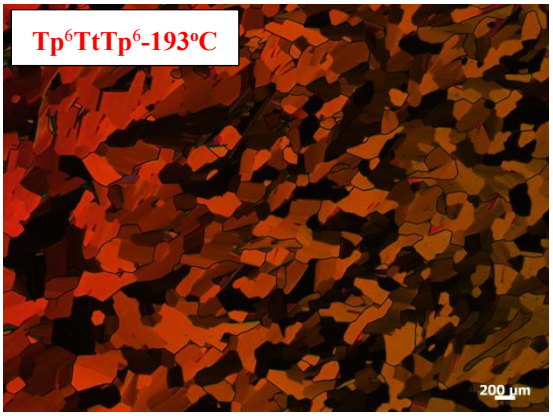
Tp6TtTp6-193°C
200 μm

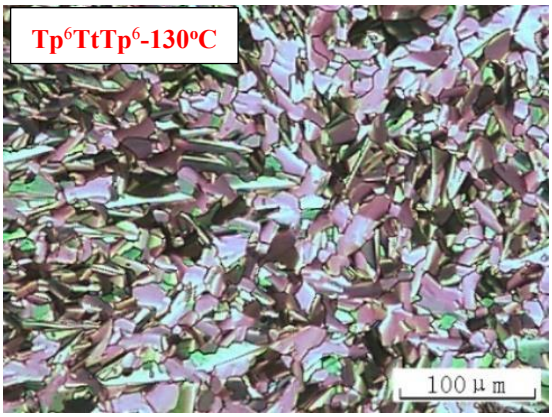
Tp6TtTp6-130°C
100 μm

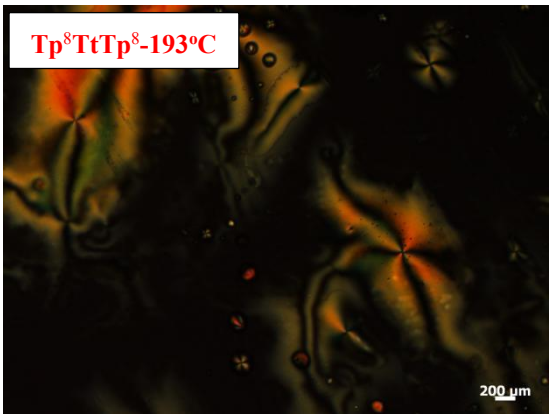
Tp8TtTp8-193°C
200 μm

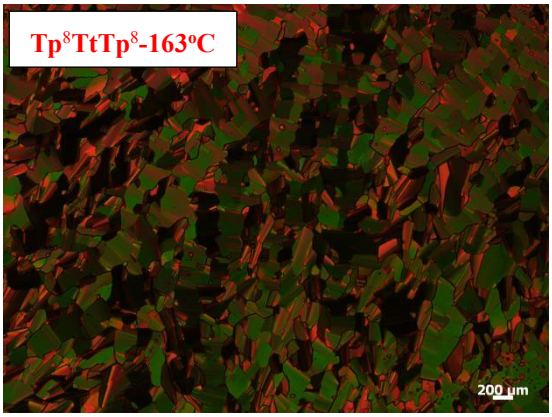
Tp8TtTp8-163°C
200 μm

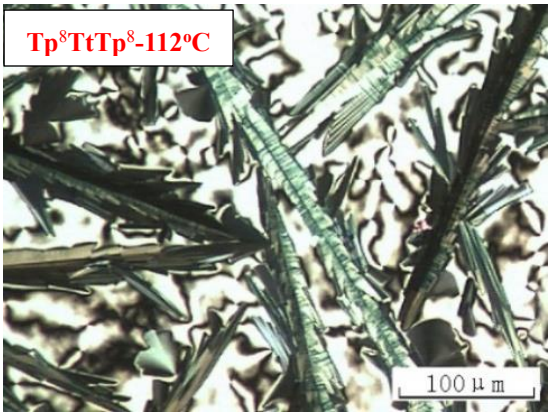
Tp8TtTp8-112°C
100 μm

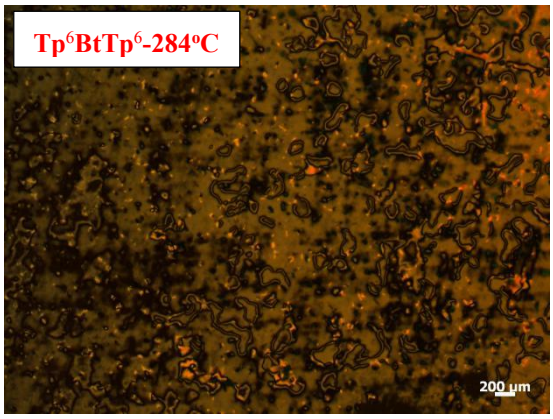
Tp⁶BtTp⁶-284ºC
200 µm


Tp⁶BtTp⁶-179ºC
200 µm

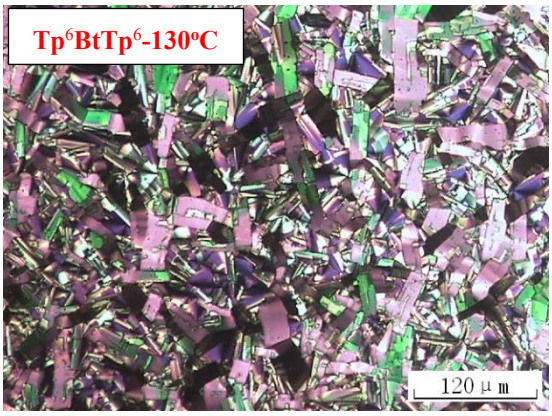
Tp⁶BtTp⁶-130ºC
120 µ m

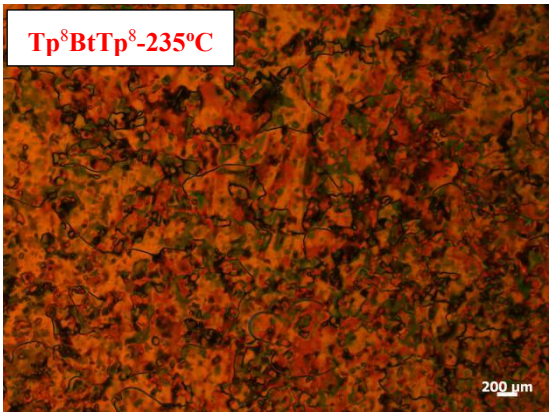
Tp⁸BtTp⁸-235ºC
200 µm

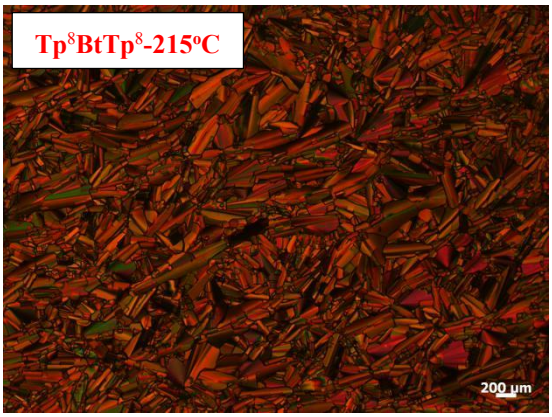
Tp⁸BtTp⁸-215ºC
200 µm

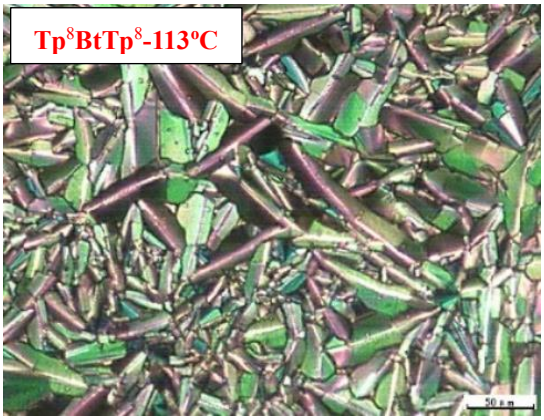
Tp⁸BtTp⁸-113ºC

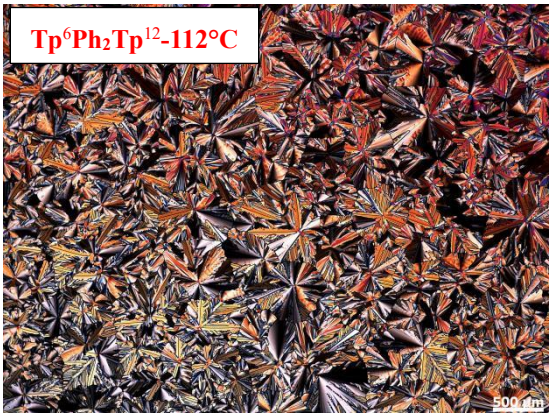
Tp⁶Ph₂Tp¹²-112°C

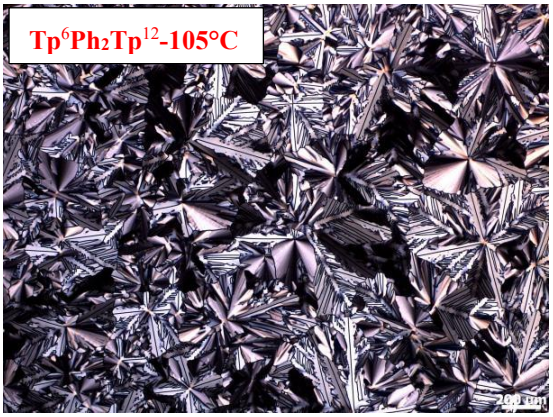
Tp⁶Ph₂Tp¹²-105°C

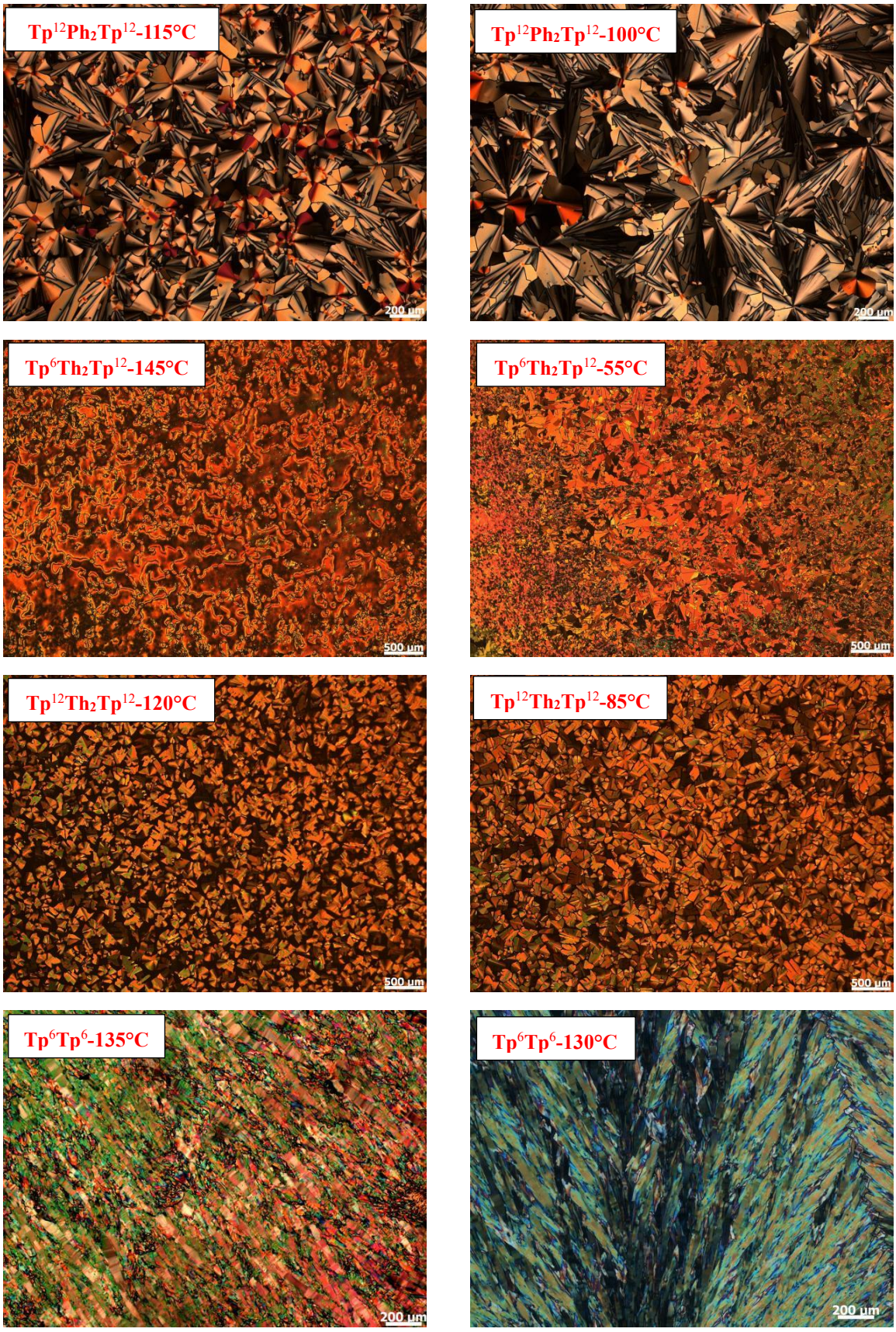

Figure S61. POM images of the mesophases of the triphenylene-based precursors, monomers, unsymmetrical dimers and π-bridged dimers, at various temperatures. Note that some temperature shifts may occur due to small variations in the calibration of the measuring devices (DSC and POM). All these microscopic observations were made on slow cooling from the isotropic liquid.

9. TGA

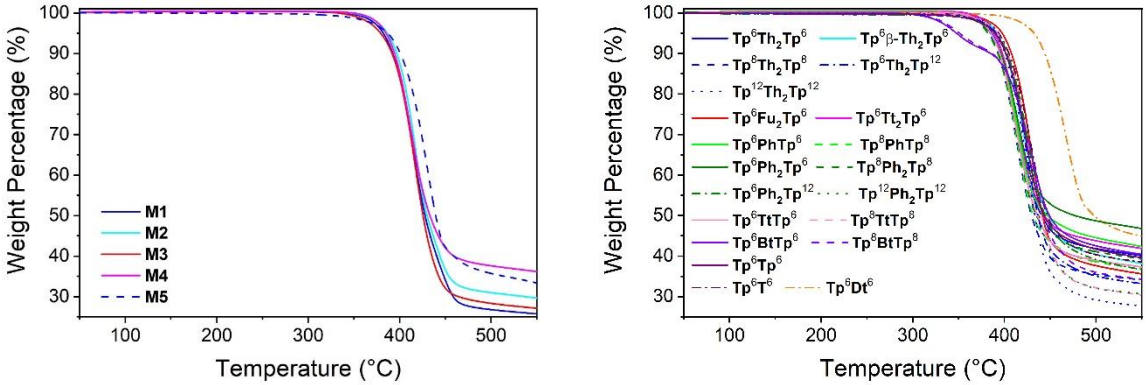

Figure S62. From top to bottom, TGA curves of monomeric (**M1-M5**) and dimeric compounds.

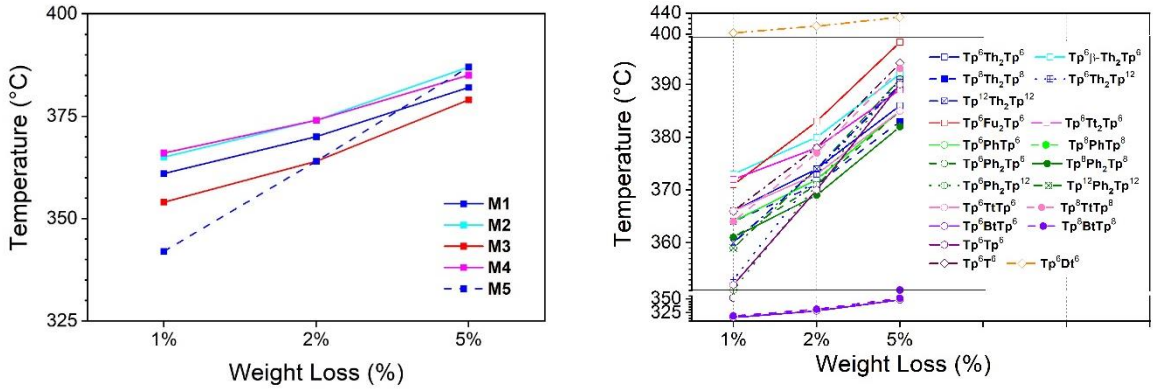

Figure S63. From top to bottom, weight loss % variation with temperature of monomeric (**M1-M5**) and dimeric compounds.

Table S7. Decomposition temperatures (TGA) of **M1-M5** monomers and dimeric DLCs.

Compound	$T_{dec.}$/°C (1% loss)	$T_{dec.}$/°C (2% loss)	$T_{dec.}$/°C (5% loss)
M1	361	370	382
M2	365	374	387
M3	354	364	379
M4	366	374	385
M5	342	364	387
$Tp^6Th_2Tp^6$	366	374	386
$Tp^6\beta$-Th_2Tp^6	373	380	392
$Tp^6Fu_2Tp^6$	371	383	398
$Tp^6Tt_2Tp^6$	372	378	389
$Tp^8Th_2Tp^8$	364	371	383
Tp^6T^6	366	378	394
Tp^6Dt^6	402	415	432
Tp^6PhTp^6	364	372	385
Tp^8PhTp^8	361	369	382
$Tp^6Ph_2Tp^6$	361	371	385
$Tp^8Ph_2Tp^8$	361	369	382
Tp^6TtTp^6	366	373	385
Tp^8TtTp^8	364	377	393
Tp^6BtTp^6	316	328	348
Tp^8BtTp^8	319	331	351
$Tp^6Ph_2Tp^{12}$	351	371	391
$T^{12}Ph_2Tp^{12}$	359	374	391
$Tp^6Th_2Tp^{12}$	353	373	391
$T^{12}Th_2Tp^{12}$	360	374	390
Tp^6Tp^6	352	370	390

$T_{dec.}$: Temperature at 1, 2 and 5% weight-loss.

10. DSC (heating/cooling rate 10 °C/min)

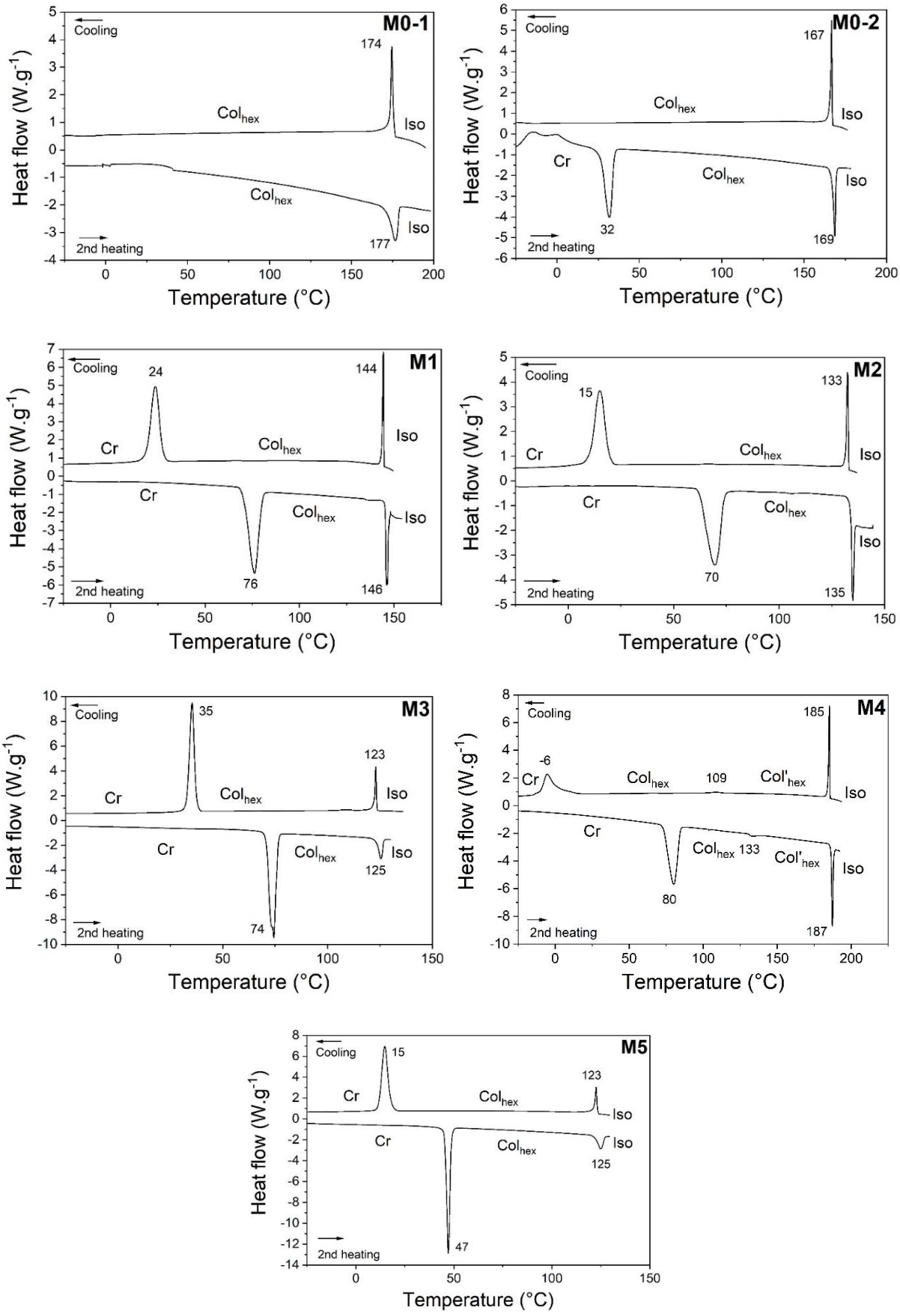

Figure S64. DSC curves of intermediates **M0** and monomers **M1**-**M5**.

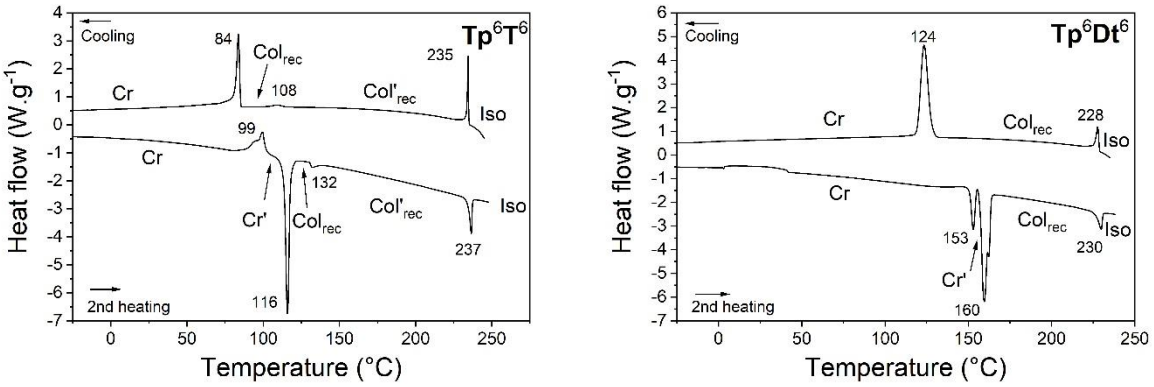

Figure S65. DSC curves of the unsymmetrical dimeric compounds **Tp^{6}T^6** and **Tp^{6}Dt^6**.

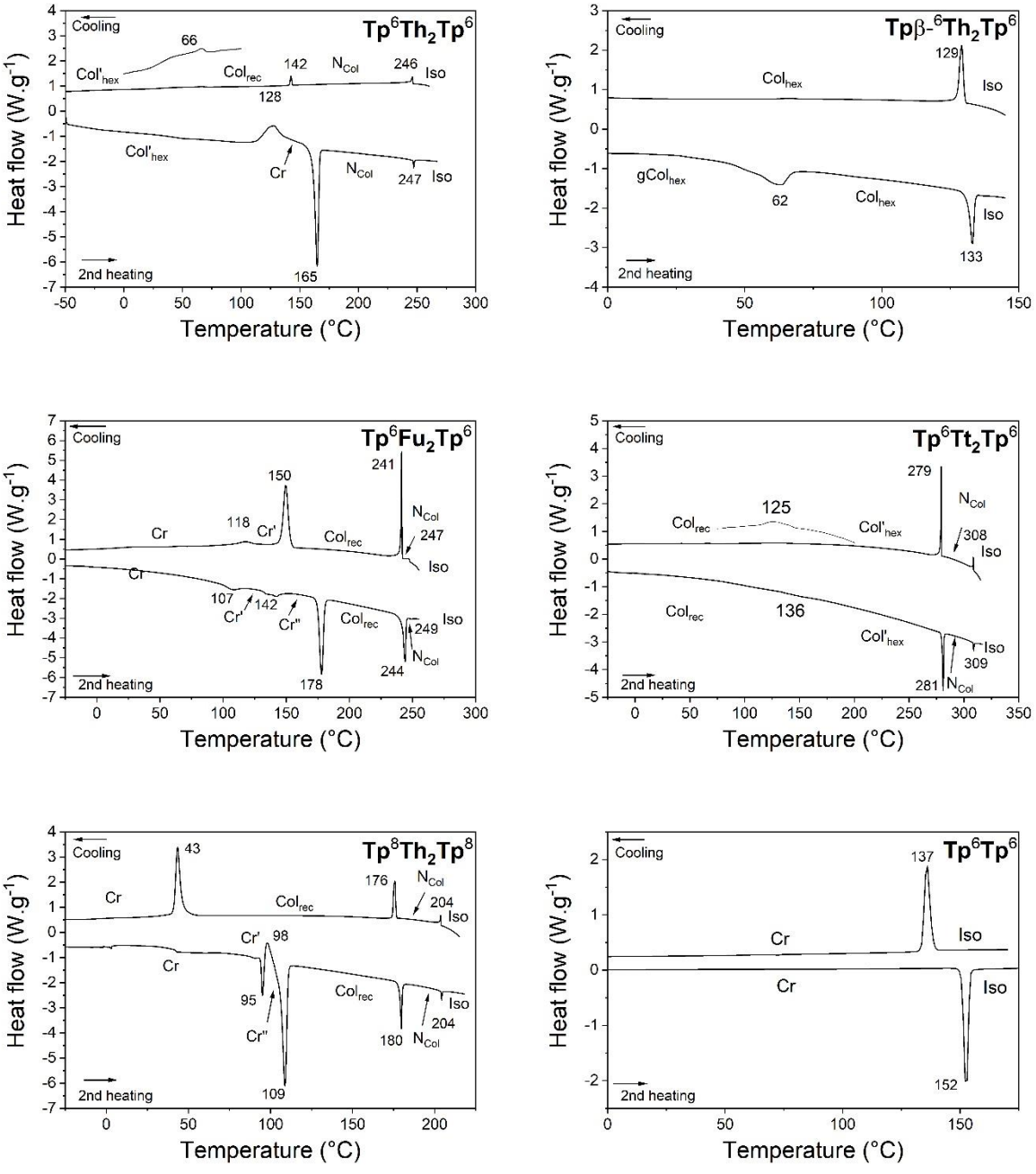

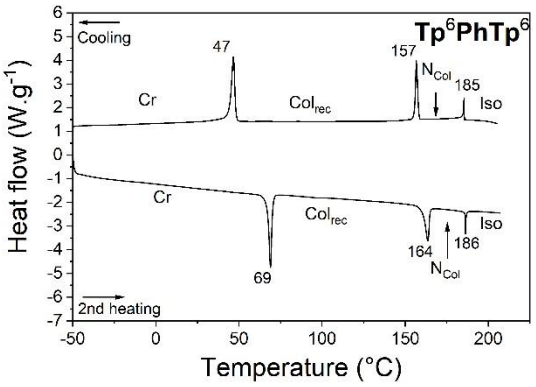
Tp6PhTp6
Cooling
Cr
47
Colrec
157
NCol
185
Iso
Cr
Colrec
Iso
164
186
NCol
69
2nd heating
Heat flow (W.g-1)
Temperature (°C)

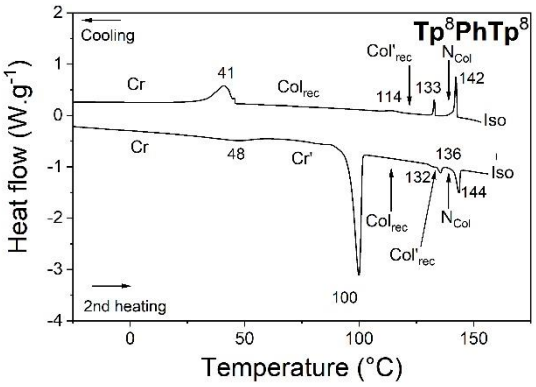
Tp8PhTp8
Cooling
Cr
41
Colrec
Col'rec
NCol
114
133
142
Iso
Cr
48
Cr'
136
132
144
Iso
Colrec
NCol
Col'rec
100
2nd heating
Heat flow (W.g-1)
Temperature (°C)

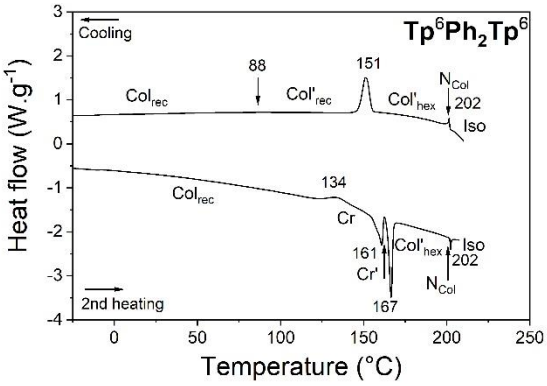
Tp6Ph2Tp6
Cooling
Colrec
88
Col'rec
151
Col'hex
NCol
202
Iso
Colrec
134
Cr
161
Cr'
Col'hex
Iso
202
NCol
167
2nd heating
Heat flow (W.g-1)
Temperature (°C)

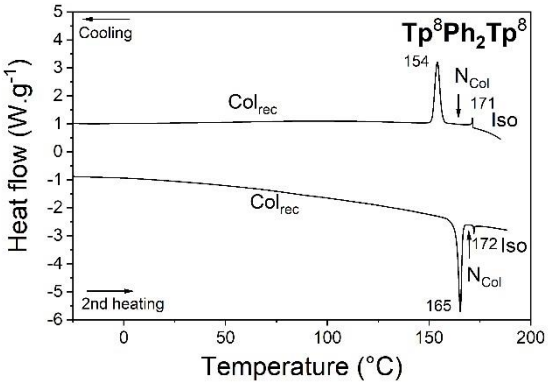
Tp8Ph2Tp8
Cooling
154
NCol
Colrec
171
Iso
Colrec
172
Iso
NCol
165
2nd heating
Heat flow (W.g-1)
Temperature (°C)

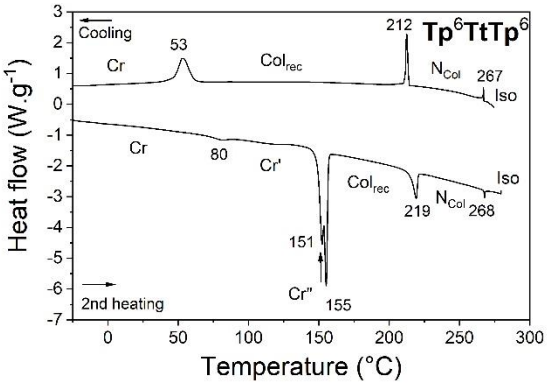
Tp6TtTp6
Cooling
212
53
Cr
Colrec
NCol
267
Iso
Cr
80
Cr'
Colrec
Iso
219
NCol
268
151
Cr''
155
2nd heating
Heat flow (W.g-1)
Temperature (°C)

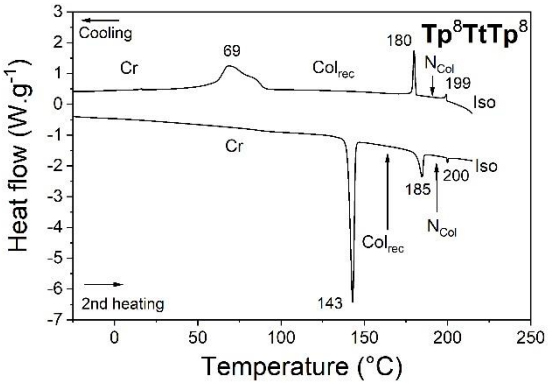
Tp8TtTp8
Cooling
69
Cr
Colrec
180
NCol
199
Iso
Cr
Iso
185
200
NCol
Colrec
143
2nd heating
Heat flow (W.g-1)
Temperature (°C)

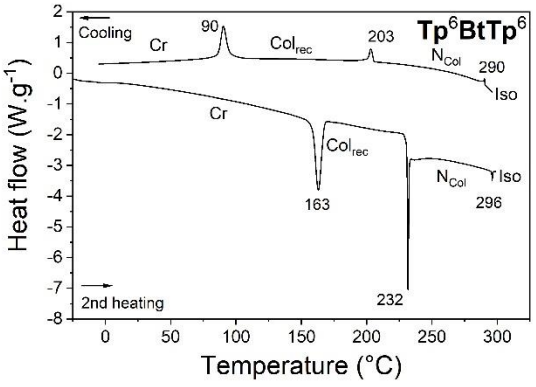
Tp6BtTp6
Cooling
Cr
90
Colrec
203
NCol
290
Iso
Cr
Colrec
NCol
Iso
163
296
232
2nd heating
Heat flow (W.g-1)
Temperature (°C)

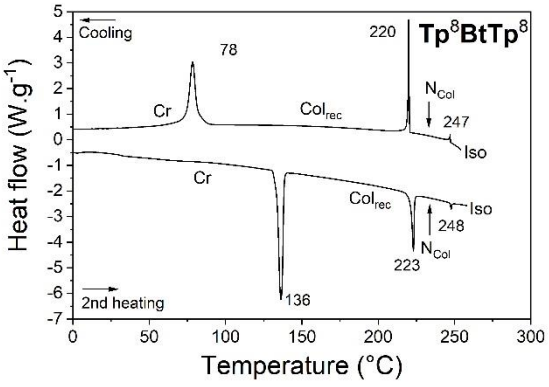
Tp8BtTp8
Cooling
78
220
Cr
Colrec
NCol
247
Iso
Cr
Colrec
Iso
248
NCol
223
136
2nd heating
Heat flow (W.g-1)
Temperature (°C)

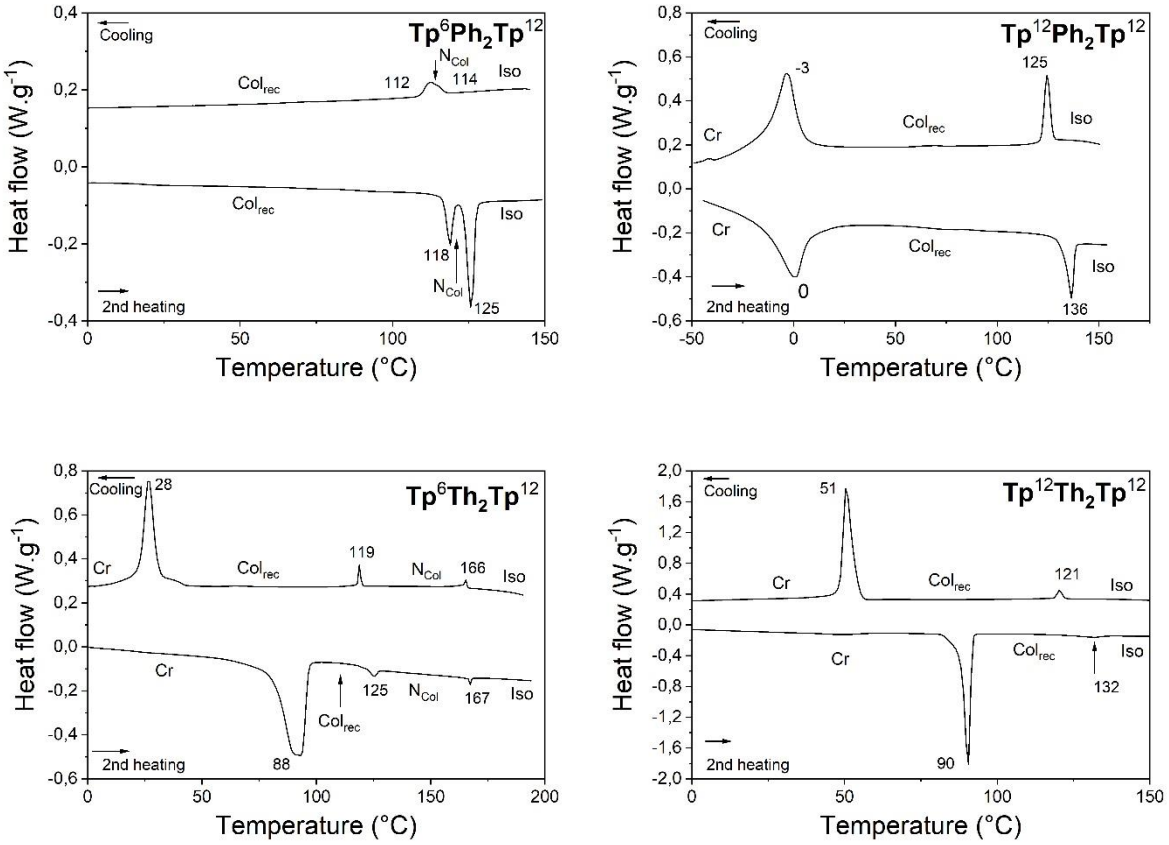

Figure S66. DSC curves of dimeric DLC compounds.

Table S8. Phase transition temperatures and associated enthalpy changes of monomeric precursors (**M0-M5**) and dimeric σ- and π-bridged triphenylenes (heating and cooling rates of 10°C/min).

Cpds	Second heating {First heating} / °C (ΔH, kJ·mol^{-1}); (ΔCp, kJ·mol^{-1} K^{-1})*	First cooling / °C (ΔH, kJ·mol^{-1})
M0-1	**Col$_{hex}$** 177 (11.6) **I**	**I** 174 (-12.0) **Col$_{hex}$**
M0-2	**Cr** 32 (38.1) **Col$_{hex}$** 169 (13.2) **I**	**I** 167 (-13.6) **Col$_{hex}$**
M1	**Cr** 76 (37.8) **Col$_{hex}$** 146 (8.9) **I**	**I** 144 (-8.1) **Col$_{hex}$** 24 (-31.8) **Cr**
M2	**Cr** 70 (35.1) **Col$_{hex}$** 135 (7.1) **I**	**I** 133 (-6.9) **Col$_{hex}$** 15 (-28.2) **Cr**
M3	**Cr** 74 (43.8) **Col$_{hex}$** 125 (5.1) **I**	**I** 123 (-5.0) **Col$_{hex}$** 35 (-36.6) **Cr**
M4	**Cr** 80 (40.5) **Col$_{hex}$** 133 (-) **Col$_{hex}$'** 187 (10.4) **I**	**I** 185 (-10.0) **Col'$_{hex}$** 109 (-) **Col$_{hex}$** -6 (-21.3) **Cr**
M5	**Cr** 47 (42.6) **Col$_{hex}$** 125 (6.4) **I**	**I** 123 (-6.5) **Col$_{hex}$** 15 (-38.5) **Cr**
Tp^{6}T^6	**Cr** 99 (-14.9) **Cr'** 116 (47.2) **Col$_{rec}$** 132 (1.6) **Col'$_{rec}$** 237 (7.3) **I**	**I** 235 (-6.8) **Col'$_{rec}$** 108 (-1.4) **Col$_{rec}$** 84 (-20.9) **Cr**
Tp^{6}Dt^6	**Cr** 153 (11.1) **Cr'** 160 (50.1) **Col$_{rec}$** 230 (5.5) **I**	**I** 228 (-5.8) **Col$_{rec}$** 124 (-51.5) **Cr**
Tp^{6}Th$_2$Tp^6	**Col'$_{hex}$** 128 (-26.7) **Cr** 165 (49.6) **N$_{Col}$** 247 (0.9) **I**	**I** 246 (-1.4) **N$_{Col}$** 142 (-1.5) **Col$_{rec}$** 66 (-0.5) **Col'$_{hex}$**
Tp^{6}β-Th$_2$Tp^6	**gCol$_{hex}$** 62 (0.03)* **Col$_{hex}$** 133 (7.2) **I**	**I** 129 (-7.5) **Col$_{hex}$**
Tp^{6}Fu$_2$Tp^6	**Cr** 107 (4.8) **Cr'** 142 (6.3) **Cr''** 178 (43.2) **Col$_{rec}$** 244 (17.0)† **N$_{Col}$** 249 (-) **I**	**I** 247 (-1.0) **N$_{Col}$** 241 (-16.6) **Col$_{rec}$** 150 (-44.9) **Cr'** 118 (-4.8) **Cr**
Tp^{6}Tt$_2$Tp^6	**Col$_{rec}$** 136 (-) **Col'$_{hex}$** 281 (9.1) **N$_{Col}$** 309 (0.7) **I**	**I** 308 (-0.8) **N$_{Col}$** 279 (-8.4) **Col'$_{hex}$** 125 (-) **Col$_{rec}$**
Tp^{6}PhTp^6	**Cr** 69 (13.5) **Col$_{rec}$** 164 (7.7) **N$_{Col}$** 186 (1.1) **I**	**I** 185 (-1.7) **N$_{Col}$** 157 (-7.0) **Col$_{rec}$** 47 (-15.3) **Cr**
Tp^{6}Ph$_2$Tp^6	**Col$_{rec}$** 134 (-6.3) **Cr** 161 (6.2) **Cr'** 167 (10.6) **Col'$_{hex}$** 200 (-) **N$_{Col}$** 202 (0.9)† **I**	**I** 202 (-0.8) **N$_{Col}$** 200 (-) **Col'$_{hex}$** 151 (-10.3) **Col'$_{rec}$** 88 (-) **Col$_{rec}$**
Tp^{6}TtTp^6	**Cr** 80 (-) **Cr'** 151 (-) **Cr''** 155 (57.3) **Col$_{rec}$** 219 (8.8) **N$_{Col}$** 268 (0.4) **I**	**I** 267 (-0.7) **N$_{Col}$** 212 (-8.2) **Col$_{rec}$** 53 (-21.5) **Cr**
Tp^{6}BtTp^6	**Cr** 163 (44.2) **Col$_{rec}$** 232 (17.4) **N$_{Col}$** 296 (0.7) **I**	**I** 290 (-1.2) **N$_{Col}$** 203 (-4.9) **Col$_{rec}$** 90 (-23.2) **Cr**
Tp^{8}Th$_2$Tp^8	**Cr** 95 (12.1) **Cr'** 98 (9.0) **Cr''** 109 (77.9) **Col$_{rec}$** 180 (9.4) **N$_{Col}$** 204 (0.9) **I**	**I** 204 (-1.0) **N$_{Col}$** 176 (-8.9) **Col$_{rec}$** 43 (-37.4) **Cr**
Tp^{8}PhTp^8	**Cr** 48 (-) **Cr'** 100 (81.8) **Col$_{rec}$** 132 (-)**Col'$_{rec}$** 136 (2.3) **N$_{Col}$** 144 (7.2)	**I** 144 (-8.6) **N$_{Col}$** 133 (-2.2) **Col'$_{rec}$** 114 (-) **Col$_{rec}$** 41

	I	(-25.5) **Cr**
Tp^{8}P90h$_2$Tp^{8}	**Col$_{rec}$** 165 (19.2) **N$_{Col}$** 172 (0.4) **I**	**I** 171 -(0.5) **N$_{Col}$** 154 (-18.2) **Col$_{rec}$**
Tp^{8}TtTp^{8}	**Cr** 143 (64.7) **Col$_{rec}$** 185 (8.6) **N$_{Col}$** 200 (0.5) **I**	**I** 199 (-0.8) **N$_{Col}$** 180 (-8.6) **Col$_{rec}$** 69 (-60.9) **Cr**
Tp^{8}BtTp^{8}	**Cr** 136 (66.3) **Col$_{rec}$** 223 (15.9) **N$_{Col}$** 248 (0.6) **I**	**I** 247 (-0.8) **N$_{Col}$** 220 (-16.2) **Col$_{rec}$** 78 (-58.1) **Cr**
Tp^{6}Ph$_2$Tp^{12}	**Col$_{rec}$** 118 (2.6) **N$_{Col}$** 125 (8.4) **I**	**I** 114 (-) **N$_{Col}$** 113 (-7.4)† **Col$_{rec}$**
Tp^{12}Ph$_2$Tp^{12}	**Cr** 0 (71.7) **Col$_{rec}$** 136 (15.7) **I**	**I** 125 (-15.0) **Col$_{rec}$** -3 (-76.9) **Cr**
Tp^{6}Th$_2$Tp^{12}	**Cr** 88 (48.2) **Col$_{rec}$** 125 (1.8) **N$_{Col}$** 167 (0.4) **I**	**I** 166 (-0.9) **N$_{Col}$** 119 (-1.4) **Col$_{rec}$** 28 (-37.1) **Cr**
Tp^{12}Th$_2$Tp^{12}	**Cr** 90 (71.7) **Col$_{rec}$** 132 (2.8) **I**	**I** 121 (-3.2) **Col$_{rec}$** 51 (-77.7) **Cr**
Tp^{6}Tp^{6}	**Cr** 152 (45.1) **I**	**I** 137 (-39.4) **Cr**

Cr, **Cr'**, **Cr"**: crystalline phases; **Col$_{hex}$**, **Col'$_{hex}$** hexagonal columnar phases; **Col$_{rec}$** and **Col'$_{rec}$**: (multi)columnar rectangular mesophases (see main text and Table 3 for details); **N$_{Col}$**: nematic columnar phase; **I**: isotropic liquid. †Cumulated enthalpy.

11. SWAXS patterns and indexation tables

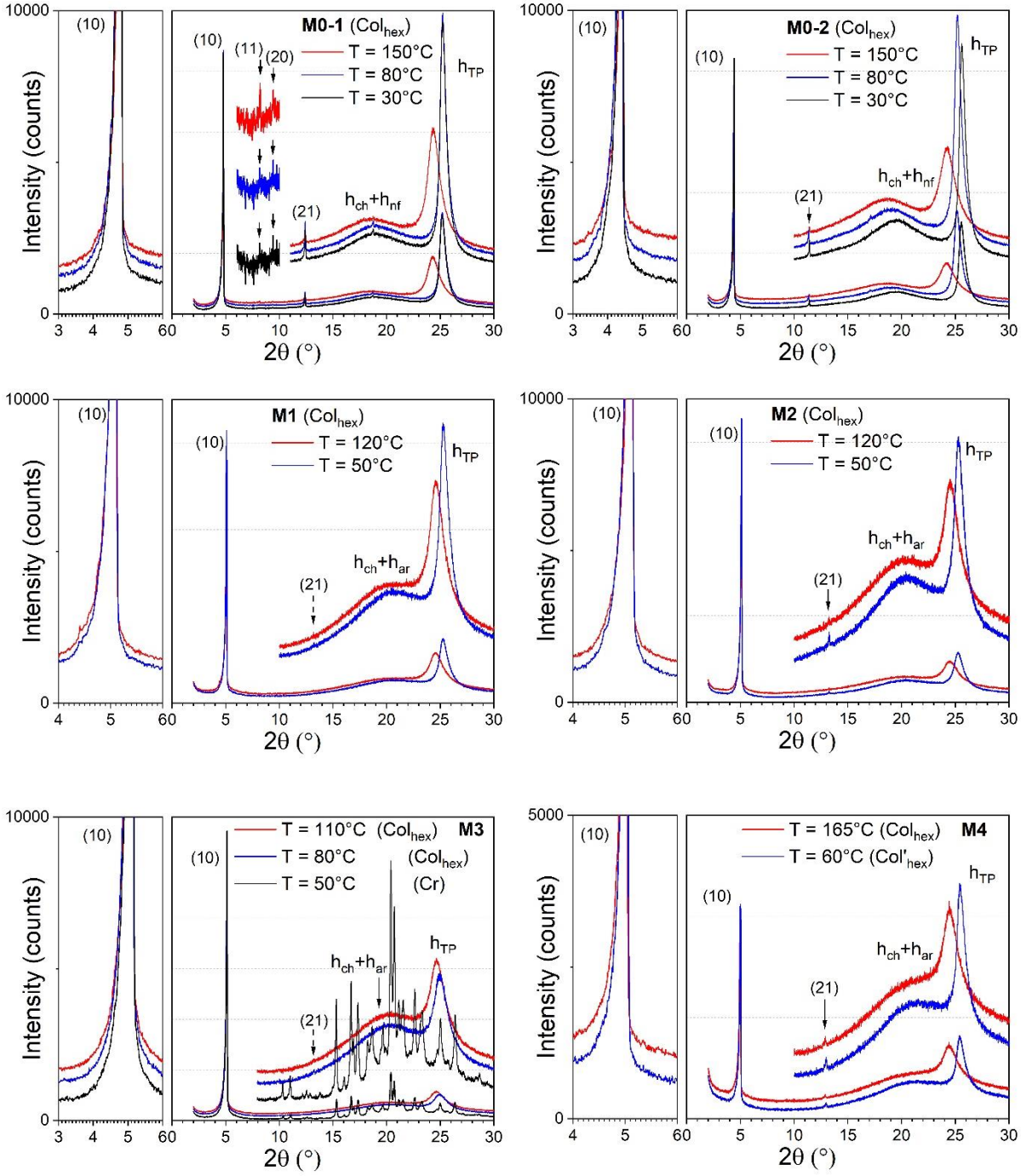

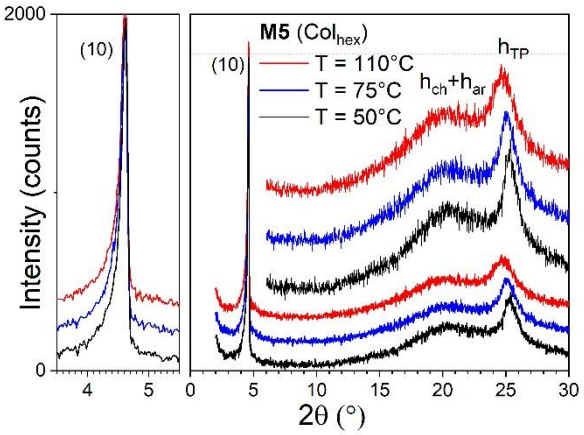

Figure S67. SWAXS patterns of monomeric precursors, **M0**-**M5**

Table S9. Table of indexation of mesophases of monomeric species **M0-M5**.

$2\theta_{exp}$	$d_{exp.}$	I [%]	*hk*	Line shape (ξ)	$d_{calc.}$	Δ
M0-1 (T = 150°C): **Col$_{hex}$**-*p6mm*; **a**$_{hex}$ = 21.75Å						
4.68(6)	18.84	VS	10	sh	18.84	0.00
8.15(0)	10.83	W	11	sh	10.87	0.04
9.37(2)	9.43	W	20	sh	9.42	0.01
12.39(1)	7.14	M	21	sh	7.12	0.02
18.69	4.74	VS	h$_{ch}$	br	-	-
24.34	3.65	VS	h$_{TP}$	sh (46)	-	-
M0-1 (T = 80°C): **Col$_{hex}$**-*p6mm*; **a**$_{hex}$ = 21.71Å						
4.69(6)	18.80	VS	10	sh	18.80	0.00
8.14(2)	10.85	W	11	sh	10.85	0.00
9.42(0)	9.38	W	20	sh	9.40	0.02
12.42(1)	7.12	M	21	sh	7.11	0.01
18.71	4.74	VS	h$_{ch}$	br	-	-
25.24	3.53	VS	h$_{TP}$	sh (99)	-	-
M0-1 (T = 30°C): **Col$_{hex}$**-*p6mm*; **a**$_{hex}$ = 21.68Å						
4.70(1)	18.78	VS	10	sh	18.78	0.00
8.14(9)	10.84	W	11	sh	10.84	0.00
9.40(0)	9.40	W	20	sh	9.39	0.01
12.47(4)	7.09	M	21	sh	7.10	0.01
18.82	4.71	VS	h$_{ch}$	br	-	-
25.24	3.53	VS	h$_{TP}$	sh (99)	-	-
M0-2 (T = 150°C): **Col$_{hex}$**-*p6mm*; **a**$_{hex}$ = 23.55Å						
4.32(5)	20.41	VS	10	sh	20.40	0.00
11.46(7)	7.71	M	21	sh	7.71	0.00
18.84	4.70	VS	h$_{ch}$	br	-	-
24.19	3.67	VS	h$_{TP}$	sh (35)	-	-
M0-2 (T = 80°C): **Col$_{hex}$**-*p6mm*; **a**$_{hex}$ = 23.68Å						
4.30(5)	20.51	VS	10	sh	20.51	0.00
11.40(7)	7.75	M	21	sh	7.75	0.00
18.76	4.72	VS	h$_{ch}$	br	-	-
25.20	3.53	VS	h$_{TP}$	sh (88)	-	-
M0-2 (T = 30°C): **Col$_{hex}$**-*p6mm*; **a**$_{hex}$ = 23.60Å						
4.32(1)	20.43	VS	10	sh	20.44	0.00
11.44(3)	7.73	M	21	sh	7.72	0.01
19.75	4.49	VS	h$_{ch}$	br	-	-
25.63	3.47	VS	h$_{TP}$	sh (101)	-	-
M1 (T = 120°C): **Col$_{hex}$**-*p6mm*; **a**$_{hex}$ = 20.46Å						
4.98(3)	17.72	VS	10	sh	17.72	0.00
13.20(3)	6.70	VW	21	sh	6.70	0.00
19.76	4.49	VS	h$_{ch}$+h$_{ar}$	br	-	-
24.57	3.62	VS	h$_{TP}$	sh (36)	-	-
M1 (T = 50°C): **Col$_{hex}$**-*p6mm*; **a**$_{hex}$ = 20.44Å						
4.98(3)	17.71	VS	10	sh	17.70	0.00
13.21(1)	6.69	VW	21	sh	6.69	0.00
20.48	4.33	VS	h$_{ch}$+h$_{ar}$	br	-	-
25.31	3.52	VS	h$_{TP}$	sh (64)	-	-
M2 (T = 120°C): **Col$_{hex}$**-*p6mm*; **a**$_{hex}$ = 20.40Å						

4.99(7)	17.67	VS	10	sh	17.67	0.00
13.24(8)	6.68	M	21	sh	6.68	0.00
19.96	4.44	VS	$h_{ch}+h_{ar}$	br	-	-
24.46	3.64	VS	h_{TP}	sh (30)	-	-
M2 (T = 50°C): **Col$_{hex}$**-*p6mm*; **a**$_{hex}$ = 20.38Å						
5.00(2)	17.65	VS	10	sh	17.65	0.00
13.26(0)	6.67	M	21	sh	6.67	0.00
20.31	4.39	VS	$h_{ch}+h_{ar}$	br	-	-
25.29	3.52	VS	h_{TP}	sh (58)	-	-
M3 (T = 110°C): **Col$_{hex}$**-*p6mm*; **a**$_{hex}$ = 20.44Å						
5.98(8)	17.70	VS	10	sh	17.70	0.00
13.21(3)	6.69	VW	21	sh	6.69	0.00
20.45	4.33	VS	$h_{ch}+h_{ar}$	br	-	-
24.59	3.62	VS	h_{TP}	sh (27)	-	-
M3 (T = 80°C): **Col$_{hex}$**-*p6mm*; **a**$_{hex}$ = 20.35Å						
5.01(1)	17.62	VS	10	sh	17.62	0.00
13.27(4)	6.66	VW	21	sh	6.66	0.00
19.74	4.49	VS	$h_{ch}+h_{ar}$	br	-	-
24.89	3.57	VS	h_{TP}	sh (31)	-	-
M4 (T = 165°C): **Col$_{hex}$**-*p6mm*; **a**$_{hex}$ = 20.96Å						
4.86(5)	18.15	VS	10	sh	18.15	0.00
12.90(1)	6.86	M	21	sh	6.86	0.00
19.85	4.47	VS	$h_{ch}+h_{ar}$	br	-	-
24.41	3.64	VS	h_{TP}	sh (30)	-	-
M4 (T = 60°C): **Col'$_{hex}$**-*p6mm*; **a**$_{hex}$ = 20.86Å						
4.88(6)	18.07	VS	10	sh	18.07	0.00
12.94(1)	6.83	M	21	sh	6.93	0.00
20.60	4.31	VS	$h_{ch}+h_{ar}$	br	-	-
25.47	3.49	VS	h_{TP}	sh (69)	-	-
M5 (T = 110°C): **Col$_{hex}$**-*p6mm*; **a**$_{hex}$ = 22.18Å						
4.59(5)	19.21	VS	10	sh	-	-
20.00	4.44	VS	$h_{ch}+h_{ar}$	br	-	-
24.66	3.60	VS	h_{TP}	sh (25)	-	-
M5 (T = 75°C): **Col$_{hex}$**-*p6mm*; **a**$_{hex}$ = 22.20Å						
4.59(2)	19.23	VS	10	sh	-	-
20.25	4.38	VS	$h_{ch}+h_{ar}$	br	-	-
25.09	3.55	VS	h_{TP}	sh (45)	-	-
M5 (T = 50°C): **Col$_{hex}$**-*p6mm*; **a**$_{hex}$ = 22.22Å						
4.58(8)	19.24	VS	10	sh	-	-
20.25	4.38	VS	$h_{ch}+h_{ar}$	br	-	-
25.31	3.51	VS	h_{TP}	sh (46)	-	-

$2\theta_{exp}$ (°), $d_{exp.}$ (Å), $d_{calc.}$ (Å): experimental and calculated angles and d-spacings from peak position of maximum; $|\Delta| = |d_{exp.}-d_{calc.}|$; I: intensity of reflection, signal intensity code: VS = very strong, S = strong, M = medium, W = weak, VW = very weak; (*hk*) are the Miller indices of reflections from the columnar lattice; Line shape of reflections: sh stands for sharp and br for broad, ξ(Å): correlation length from peak width using the Debye-Scherrer equation with shape factor K = 0.9 (no indication: long-range periodicity from sharp reflection); h_{ch} (Å): liquid-like lateral distances between molten chains; h_{ar} (Å): liquid-like distance between grafted aromatic parts; h_{TP} (Å): average piling distance along triphenylene columns; **a**$_{hex}$: hexagonal lattice parameter.

Table S10. Structural and geometrical parameters of the monomers mesophases at various temperatures.

Cpds	T[a]	Phase[b]	V_{mol}[c]	ρ[c]	a_{hex}[d]	A[d]	h_{mol}[e]	h_{TP} (ξ)[f]	ψ[g]	D_{TP}[h]	S_{ch}[i]	q[j]
M0-1	150	Col$_{hex}$-*p6mm*	1609	1.061	21.75	409.68	3.92	3.65 (46)	21	11.58	23.76	0.94
	80	Col$_{hex}$-*p6mm*	1490	1.129	21.71	408.18	3.65	3.53 (99)	15	11.80	22.54	0.94
	30	Col$_{hex}$-*p6mm*	1436	1.188	21.68	407.05	3.53	3.53 (99)	0	11.80	21.82	0.94
M0-2	150	Col$_{hex}$-*p6mm*	1903	1.019	23.55	480.30	3.96	3.67 (35)	22	11.52	23.92	0.95
	80	Col$_{hex}$-*p6mm*	1771	1.081	23.68	485.62	3.65	3.53 (88)	16	11.80	22.55	0.94
	30	Col$_{hex}$-*p6mm*	1684	1.136	23.60	482.34	3.49	3.47 (101)	6	11.87	21.69	0.94
M1	120	Col$_{hex}$-*p6mm*	1442	0.934	20.46	362.53	3.98	3.62 (36)	24	11.26	23.46	1.03
	50	Col$_{hex}$-*p6mm*	1394	0.966	20.44	361.82	3.85	3.52 (64)	24	11.28	22.75	1.05
M2	120	Col$_{hex}$-*p6mm*	1442	0.934	20.40	360.40	4.00	3.64 (30)	24	11.23	23.51	1.03
	50	Col$_{hex}$-*p6mm*	1394	0.966	20.38	359.70	3.88	3.52 (58)	25	11.25	22.84	1.05
M3	110	Col$_{hex}$-*p6mm*	1420	0.930	20.44	361.82	3.92	3.62 (27)	22	11.31	23.22	1.02
	80	Col$_{hex}$-*p6mm*	1383	0.954	20.35	358.64	3.86	3.57 (31)	22	11.35	22.91	1.03
M4	165	Col'$_{hex}$-*p6mm*	1558	0.925	20.96	380.46	4.09	3.64 (30)	27	11.19	24.00	1.02
	60	Col$_{hex}$-*p6mm*	1413	1.019	20.86	376.84	3.75	3.49 (69)	21	11.60	22.76	1.04
M5	110	Col$_{hex}$-*p6mm*	1728	0.914	22.18	426.11	4.06	3.60 (25)	27	11.13	23.65	1.04

	75	Col_{hex}-*p6mm*	1667	0.947	22.20	427.00	3.90	3.55 (45)	25	11.26	23.03	1.04
	50	Col_{hex}-*p6mm*	1635	0.966	22.22	427.44	3.82	3.51 (46)	23	11.33	22.69	1.04

[a]Temperature of experiment (°C); [b]Mesophase type and symmetry; [c]Molecular volume (Å^3) and density (g.cm^{-3}) calculated by additivity of partial elementary volumes; [d]Hexagonal lattice parameter a_{hex} (Å) and cross-section areas A (Å^2) of the Col_{hex}: $A = a_{hex}^2 \sin\gamma$, where $\gamma = 120°$ (number of TP columns per lattice, Z =1); [e]Columnar slice thickness: $h_{mol} = V_{mol}/(A/Z)$ in Å; [f]Face-to-face π-π stacking distance, h_{TP}, (Å) from scattering maximum from SWAXS pattern, and ζ, correlation length (Å) determined by the Debye-Scherrer formula; [g]Out-of-plane tilt angle ψ (°) of TP-based mesogen cores inside columns: $\psi = \arccos(h_{TP}/h_{mol})$. [h]Diameter of triphenylene core, $D_{TP} = (\chi_{TP} 4A/\pi)^{1/2}$, where χ_{TP} is the volume fraction of triphenylene core (V_{TP}/V_{mol}); [i]$\langle s_{ch} \rangle$ is the average cross-section chain area: $\langle s_{ch} \rangle = \pi D_{TP} \times h_{mol}/6$; [j]Chain packing ratio: $\langle q \rangle = \langle s_{ch} \rangle / \sigma_{ch}$, σ_{ch} being the available cross-sectional area for a molten chain. For **M0-1** and **M0-2**, $\langle q \rangle = (\pi D_{TP} \times h_{mol})/(5\sigma_{ch}+1\sigma_{cf})$, where σ_{cf} being the available cross-sectional area for a molten fluorinated chain.[1]

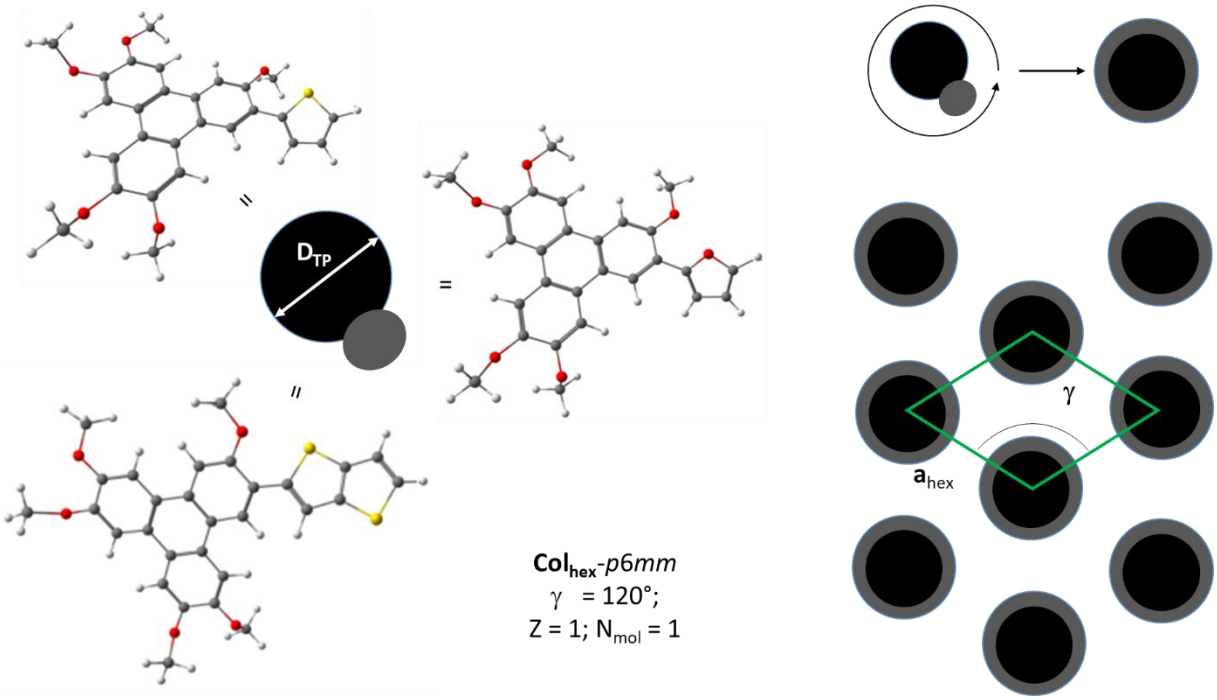

Figure S68. Schematic representations of the molecular self-assemblies and supramolecular organizations in the hexagonal mesophase of **M1**, **M3** and **M4**; a_{hex}, γ: lattice parameter and angle, Z: number of columns per lattice and N_{mol}: number of mesogens per lattice (the chains are not represented for clarity). D_{TP} defined above.

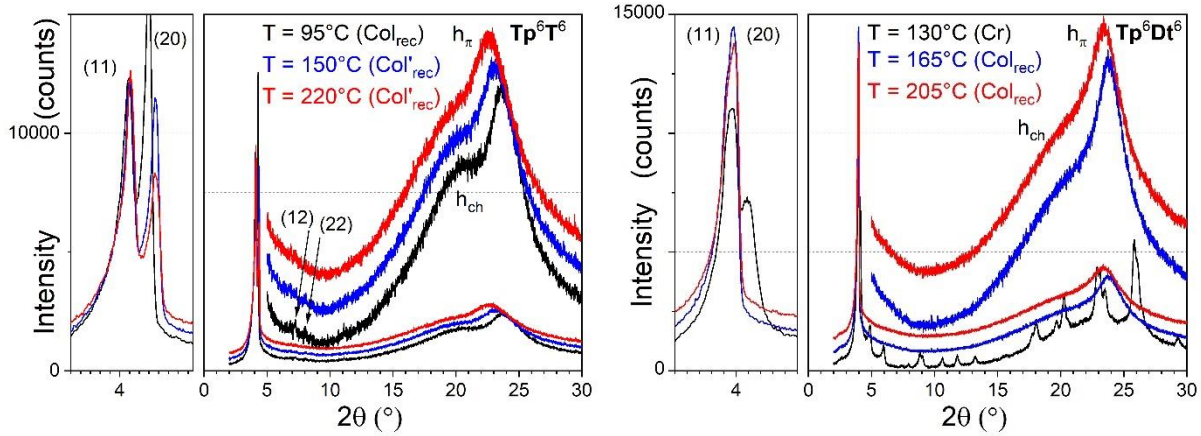

Figure S69. SWAXS patterns of the unsymmetrical dimers, **Tp^{6}T^6** - **Tp^{6}Dt^6**

[1] B. Alameddine, O. F. Aebischer, B. Heinrich, D. Guillon, B. Donnio, T. A. Jenny, *Supramol. Chem*. **2014**, *26*, 125-137.

Table S11. Table of indexation of mesophases of the unsymmetrical dimers **Tp^{6}T^6** - **Tp^{6}Dt^6**.

$2\theta_{exp}$	d_{exp}	I [%]	Line shape (ξ)	*hk*	d_{calc}	Δ
Tp^{6}T^6 (T = 220°C): **Col'$_{rec}$-*c2mm***; $\mathbf{a}_{rec}$ = 40.66Å; $\mathbf{b}_{rec}$ = 25.64Å / $\mathbf{a}_{rec}$ = 43.38Å; $\mathbf{b}_{rec}$ = 23.01Å						
4.06(9)	21.69	VS	sh	11/20	-	-
4.34(2)	20.33	VS	sh	20/11	-	-
17.84	4.97	VS	br	h_{ch}	-	-
22.69	3.92	VS	sh (10)	h_{TP}	-	-
Tp^{6}T^6 (T = 150°C): **Col'$_{rec}$-*c2mm***; $\mathbf{a}_{rec}$ = 40.72Å; $\mathbf{b}_{rec}$ = 25.73Å / $\mathbf{a}_{rec}$ = 43.50Å; $\mathbf{b}_{rec}$ = 23.04Å						
4.05(9)	21.75	VS	sh	11/20	-	-
4.33(7)	20.36	VS	sh	20/11	-	-
18.49	4.79	VS	br	h_{ch}	-	-
23.17	3.84	VS	sh (11)	h_{TP}	-	-
Tp^{6}T^6 (T = 95°C): **Col$_{rec}$-*p2gg***; $\mathbf{a}_{rec}$ = 41.10Å; $\mathbf{b}_{rec}$ = 25.62Å						
4.06(1)	21.74	VS	sh	11	-	-
4.29(5)	20.55	VS	sh	20	-	-
7.21(3)	12.24	VW	sh	12	12.23	0.01
8.13(3)	10.86	VW	sh	22	10.87	0.01
19.44	4.56	VS	br	h_{ch}	-	-
23.89	3.72	VS	sh (15)	h_{TP}	-	-
Tp^{6}Dt^6 (T = 205°C): **Col$_{rec}$-*c2mm***; $\mathbf{a}_{rec}$ = 44.32Å; $\mathbf{b}_{rec}$ = 25.79Å / $\mathbf{a}_{rec}$ = 44.58Å; $\mathbf{b}_{rec}$ = 25.54Å						
3.96(0)	22.29	VS	sh	11/20	-	-
3.99(0)	22.16	VS	sh	20/11	-	-
18.48	4.79	S	br	h_{ch}	-	-
23.36	3.80	S	sh (12)	h_{TP}	-	-
Tp^{6}Dt^6 (T = 165°C): **Col$_{rec}$-*c2mm***; $\mathbf{a}_{rec}$ = 44.30Å; $\mathbf{b}_{rec}$ = 25.98Å / $\mathbf{a}_{rec}$ = 44.82Å; $\mathbf{b}_{rec}$ = 25.48Å						
3.93(9)	22.41	VS	sh	11/20	-	-
3.98(5)	22.15	VS	sh	20/11	-	-
19.18	4.62	VS	br	h_{ch}	-	-
23.77	3.74	VS	sh (14)	h_{TP}	-	-

As **Table S9** above. Rectangular lattice parameters: $\mathbf{a}_{rec}$ and $\mathbf{b}_{rec}$.

Table S12. Structural and geometrical parameters of the mesophases of **Tp^{6}T^6** and **Tp^{6}Dt^6** at various temperatures.

Cpds	T[a]	Phase[b]	V_{mol}[c]	ρ[c]	$\mathbf{a}_{rec}$[d]	$\mathbf{b}_{rec}$[d]	$\mathbf{a}_{rec}$/ $\mathbf{b}_{rec}$	A[d]	γ, Z[d]	h_{mol}[e]	h_{TP} (ξ)[f]	ψ[g]
Tp^{6}T^6	220	Col'$_{rec}$-*c2mm*	2667	0.848	40.66	25.64	1.58	1042.52	90, 2	5.11	3.92 (10)	40
		-	-	-	43.38	23.01	1.88	998.17	-, -	5.34	-	43
	150	Col'$_{rec}$-*c2mm*	2489	0.909	40.72	25.73	1.58	1047.72	90, 2	4.75	3.84 (11)	36
		-	-	-	43.50	23.04	1.89	1002.24	-, -	4.97	-	41
	95	Col$_{rec}$-*p2gg*	2367	0.955	41.10	25.62	1.60	1052.99	90, 2	4.49	3.72 (15)	34
Tp^{6}Dt^6	205	Col$_{rec}$-*c2mm*	2646	0.899	44.32	25.79	1.72	1143.01	90, 2	4.63	3.80 (12)	35
		-	-	-	44.58	25.54	1.74	1138.57	-, -	4.65	-	35
	165	Col$_{rec}$-*c2mm*	2548	0.906	44.30	25.98	1.70	1150.9	90, 2	4.43	3.74 (14)	32
		-	-	-	44.82	25.48	1.76	1142.01	-, -	4.46	-	33

[a,b,c,e,f,g] As in **Tables S10** [d]Lattice parameters $\mathbf{a}_{rec}$, $\mathbf{b}_{rec}$ and γ (Å,°), number of TP columns per lattice (Z) and cross-section areas A (Å^2) of the Col$_{rec}$: A = a×bsinγ. The two possible rectangular lattices, when applicable, are considered.

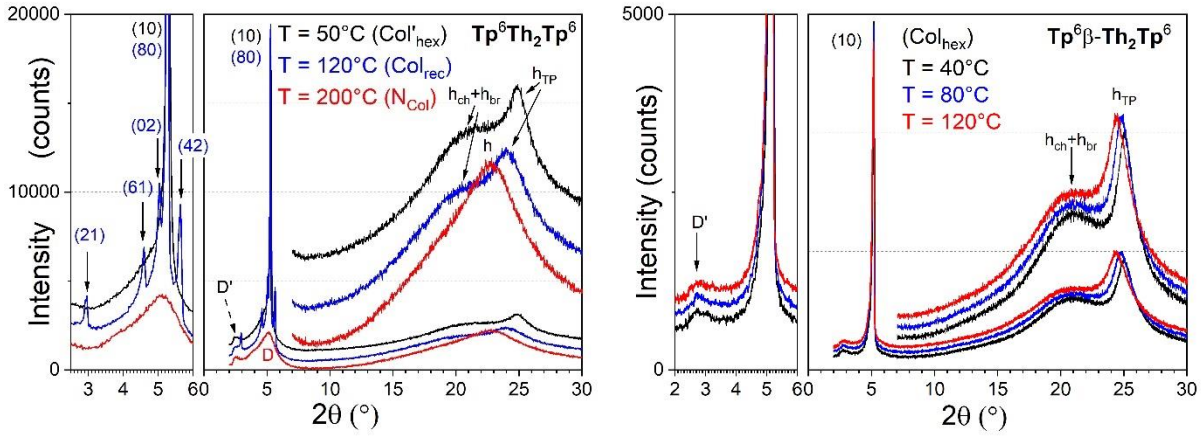

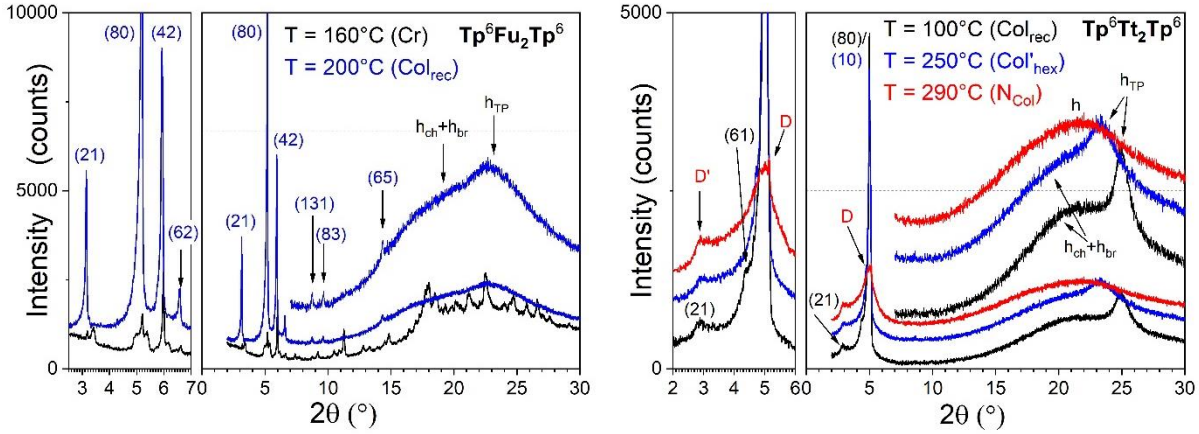
Tp⁶Fu₂Tp⁶
T = 160°C (Cr)
T = 200°C (Col_rec)
Tp⁶Tt₂Tp⁶
T = 100°C (Col_rec)
T = 250°C (Col'_hex)
T = 290°C (N_Col)
Intensity (counts)
2θ (°)

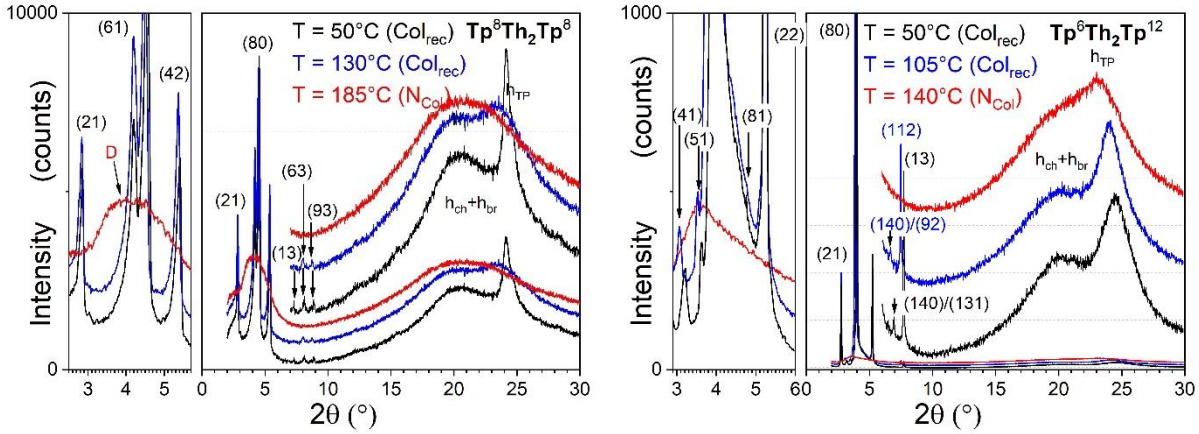
Tp⁸Th₂Tp⁸
T = 50°C (Col_rec)
T = 130°C (Col_rec)
T = 185°C (N_Col)
Tp⁶Th₂Tp¹²
T = 50°C (Col_rec)
T = 105°C (Col_rec)
T = 140°C (N_Col)
Intensity (counts)
2θ (°)

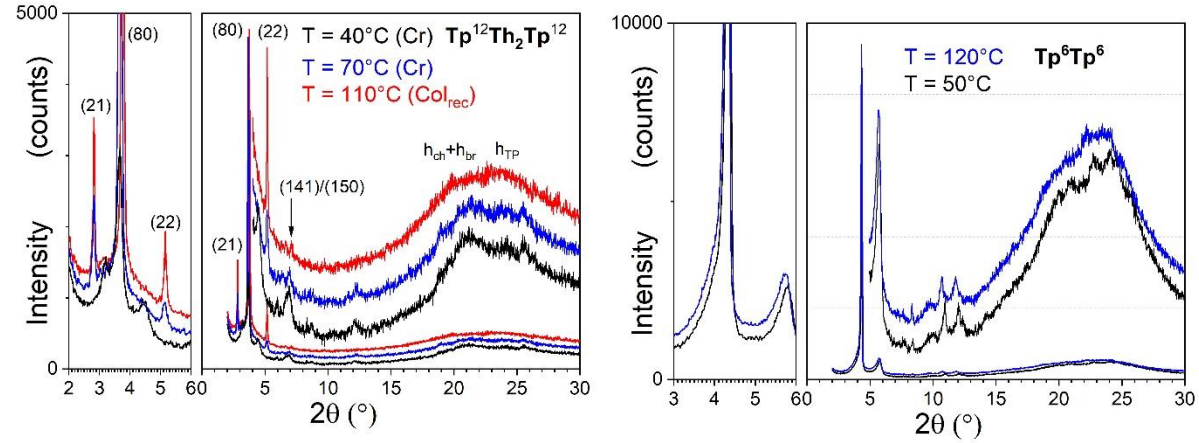
Tp¹²Th₂Tp¹²
T = 40°C (Cr)
T = 70°C (Cr)
T = 110°C (Col_rec)
Tp⁶Tp⁶
T = 120°C
T = 50°C
Intensity (counts)
2θ (°)

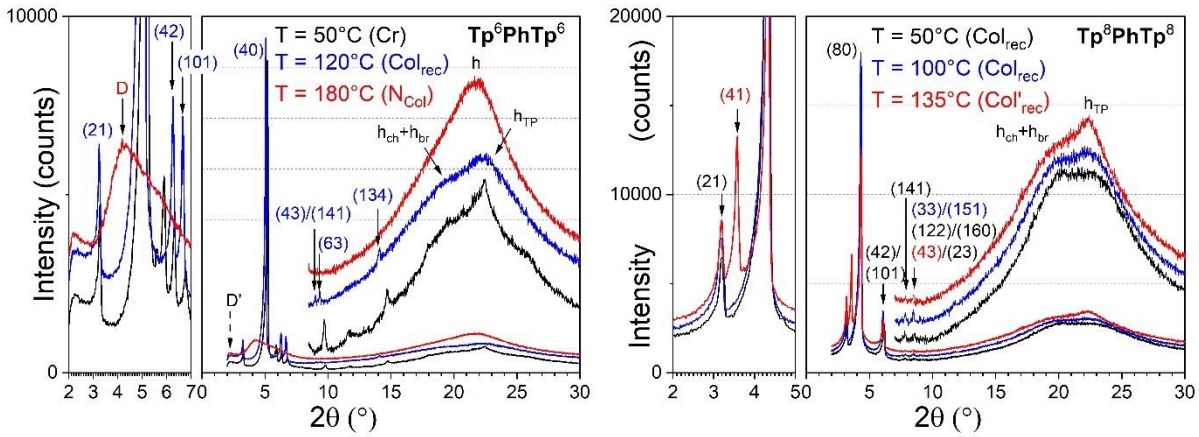
Tp⁶PhTp⁶
T = 50°C (Cr)
T = 120°C (Col_rec)
T = 180°C (N_Col)
Tp⁸PhTp⁸
T = 50°C (Col_rec)
T = 100°C (Col_rec)
T = 135°C (Col'_rec)
Intensity (counts)
2θ (°)

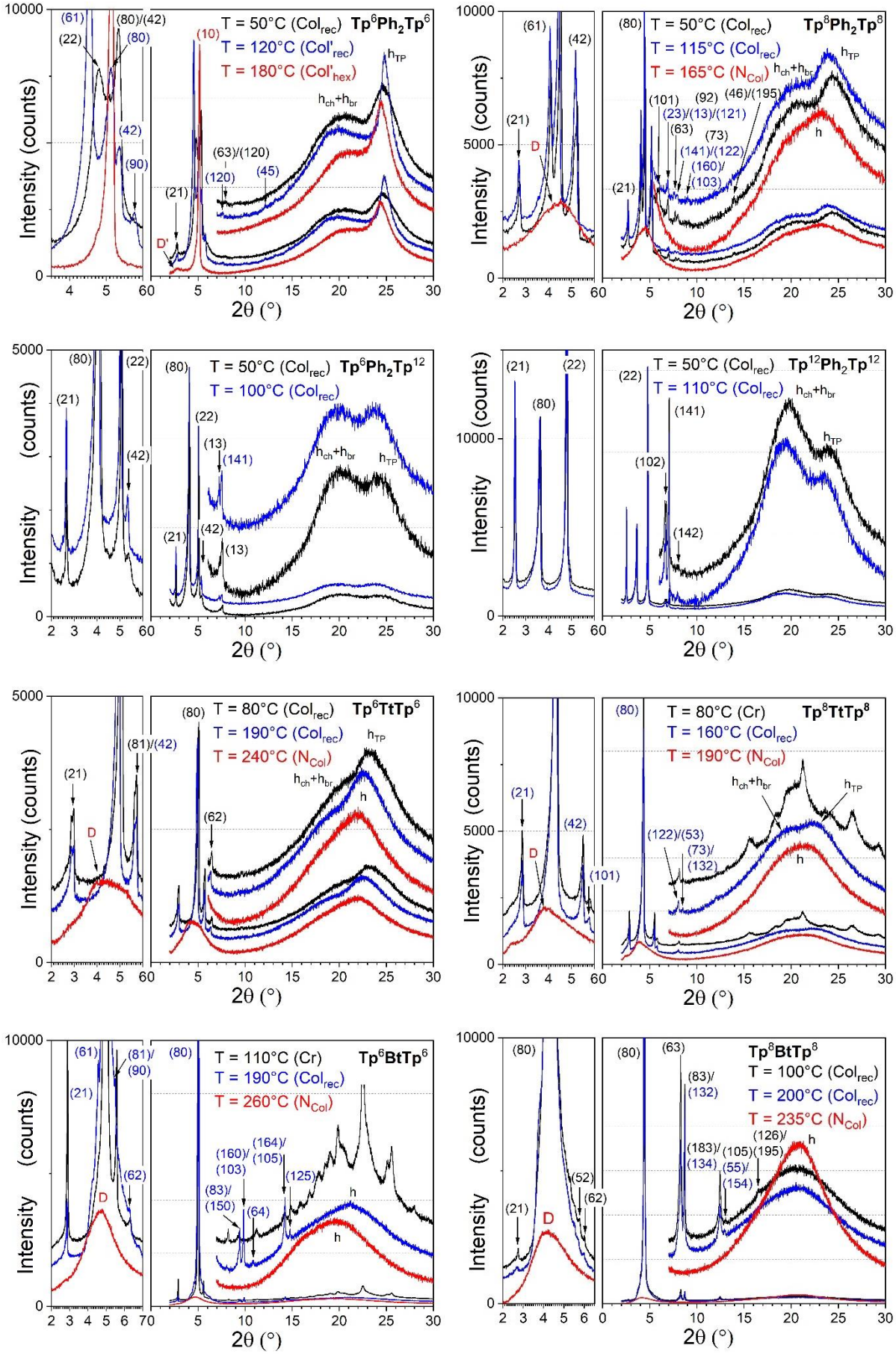

Figure S70. SWAXS patterns of the mesophases of the dimeric compounds (recorded on cooling), with indexations (considering the small lattice).

Table S13. Table of indexation of mesophases of the π-bridged dimeric compounds.

$2\theta_{exp}$	$d_{exp.}$	I	Line shape (ξ)	Single lattice		Double lattice		Δ
				hk	$d_{calc.}$	*hk*	$d_{calc.}$	
Tp^{6}Th$_2$Tp^6 (T = 200°C): **N$_{Col}$**; D = 17.96Å								
(2.45)	(36.03)	VW	br	D'~2D		-		-
4.92	17.94	S	br (33)	D		-		-
22.43	3.96	VS	br (6)	$h=h_{ch}+h_{br}+h_{TP}$		-		-
Tp^{6}Th$_2$Tp^6 (T = 120°C): **Col$_{rec}$**; **a**$_{rec}$ = 67.00Å; **b**$_{rec}$ = 35.01Å; γ = 90° ➡**a**$_{rec}$ = 134.00Å; **b**$_{rec}$ = 35.01Å; γ = 90°								
2.84(5)	31.03	M	sh	11	31.03	21	31.03	0.00
4.66(1)	18.94	M	sh	31	18.83	61	18.83	0.11
5.03(9)	17.52	S	sh	02	17.51	02	17.51	0.01
5.27(1)	16.75	VS	sh	40	16.75	80	16.75	0.00
5.68(2)	15.54	S	sh	22	15.51	42	15.51	0.03
18.98	4.68	VS	br	$h_{ch}+h_{br}$	-	$h_{ch}+h_{br}$	-	-
23.89	3.72	VS	sh (9)	h_{TP}	-	h_{TP}	-	-
Tp^{6}Th$_2$Tp^6 (T = 50°C): **Col'$_{hex}$**; **a**$_{hex}$ = 19.64Å; γ = 120°								
2.63	33.57	VW	br	sp		-		-
5.19(1)	17.01	VS	sh	10		17.01		-
20.40	4.35	VS	br	$h_{ch}+h_{br}$		-		-
24.84	3.58	VS	sh (15)	h_{TP}		-		-
Tp^{6}β-Th$_2$Tp^6 (T = 120°C): **Col$_{hex}$**; **a**$_{hex}$ = 19.87Å; γ = 120°								
2.96	29.81	W	br	D'		-		-
5.13(0)	17.21	VS	sh	10		17.21		-
20.24	4.38	VS	br	$h_{ch}+h_{br}$		-		-
24.52	3.63	VS	sh (23)	h_{TP}		-		-
Tp^{6}β-Th$_2$Tp^6 (T = 80°C): **Col$_{hex}$**; **a**$_{hex}$ = 19.81Å; γ = 120°								
2.97	29.70	W	br	D'		-		-
5.14(7)	17.15	VS	sh	10		17.15		0.00
20.65	4.30	VS	br	$h_{ch}+h_{br}$		-		-
24.99	3.58	VS	sh (31)	h_{TP}		-		-
Tp^{6}β-Th$_2$Tp^6 (T = 40°C): **Col$_{hex}$**; **a**$_{hex}$ = 19.73Å; γ = 120°								
2.98	29.58	W	br	D'		-		-
5.16(8)	17.08	VS	sh	10		17.08		0.00
20.84	4.26	VS	br	$h_{ch}+h_{br}$		-		-
25.11	3.54	VS	sh (33)	h_{TP}		-		-
Tp^{6}Fu$_2$Tp^6 (T = 200°C): **Col$_{rec}$**; **a**$_{rec}$ = 69.56Å; **b**$_{rec}$ = 32.08Å; γ = 90° ➡**a**$_{rec}$ = 139.12Å; **b**$_{rec}$ = 32.08Å; γ = 90°								
3.03(0)	29.13	S	sh	11	29.13	21	29.13	0.00
5.08(8)	17.39	VS	sh	40	17.39	80	17.39	0.00
6.06(5)	14.56	S	sh	22	14.56	42	14.56	0.00
6.62(9)	13.32	M	sh	32	13.19	62	13.19	0.13
8.74(2)	10.11	M	sh	23	10.22	131	10.15	0.11/0.04
9.64(9)	9.16	M	sh	43	9.11	83	9.11	0.05
14.28(9)	6.19	M	sh	35/111	6.18/6.20	65	6.18	0.01
18.87	4.70	VS	br	$h_{ch}+h_{br}$	-	$h_{ch}+h_{br}$	-	-
22.70	3.91	VS	br	h_{TP}	-	h_{TP}	-	-
Tp^{6}Tt$_2$Tp^6 (T = 290°C): **N$_{Col}$**; D = 18.15Å								
2.81	31.44	W	br	D'		-		-
4.86	18.15	S	br (46)	D		-		-
21.84	4.06	VS	br	$h=h_{ch}+h_{br}+h_{TP}$		-		-
Tp^{6}Tt$_2$Tp^6 (T = 250°C): **Col'$_{hex}$**; **a**$_{hex}$ = 20.95Å								
2.87	30.76	W	br	D'		-		0.00
4.86(4)	18.15	VS	sh	10		18.15		0.00
20.22	4.39	VS	br	$h_{ch}+h_{br}$		-		-
23.05	3.85	VS	sh (13)	h_{TP}		-		-
Tp^{6}Tt$_2$Tp^6 (T = 100°C): **Col$_{rec}$**; **a**$_{rec}$ = 70.64Å; **b**$_{rec}$ = 33.98Å; γ = 90° ➡**a**$_{rec}$ = 141.28Å; **b**$_{rec}$ = 33.98Å; γ = 90°								

2.88	30.62	W	br	11	30.62	21	30.62	0.00
4.54	19.45	W	sh	31	19.35	61	19.35	0.10
5.00(0)	17.66	VS	sh	40	17.66	80	17.66	0.00
20.85	4.26	VS	br	$h_{ch}+h_{br}$	-	$h_{ch}+h_{br}$	-	-
25.02	3.55	VS	sh (35)	h_{TP}	-	h_{TP}	-	-
$Tp^8Th_2Tp^8$ (T = 185°C): **N_{Col}**; D = 21.38Å								
4.13	21.38	VS	br (24)	D		-		-
21.54	4.12	VS	br	$h=h_{ch}+h_{br}+h_{TP}$		-		-
$Tp^8Th_2Tp^8$ (T = 130°C): **Col_{rec}**; a_{rec} = 78.84Å; b_{rec} = 36.15Å; γ = 90° ➡ a_{rec} = 157.68Å; b_{rec} = 36.15Å; γ = 90°								
2.68(6)	32.86	S	sh	11	32.86	21	32.86	0.00
4.16(0)	21.22	S	sh	31	21.26	61	21.26	0.04
4.47(9)	19.71	VS	sh	40	19.71	80	19.71	0.00
5.37(3)	16.43	S	sh	22	16.43	42	16.43	0.00
8.04(0)	10.99	W	sh	33	10.95	63	10.95	0.04
8.722(0)	9.98	W	sh	80	9.86	93	9.93	0.12/0.05
19.88	4.46	VS	br	$h_{ch}+h_{br}$	-	$h_{ch}+h_{br}$	-	-
23.44	3.79	M	br	h_{TP}	-	h_{TP}	-	-
$Tp^8Th_2Tp^8$ (T = 50°C): **Col_{rec}**; a_{rec} = 77.80Å; b_{rec} = 35.93Å; γ = 90° ➡ a_{rec} = 155.60Å; b_{rec} = 35.93Å; γ = 90°								
2.85(5)	32.62	S	sh	11	32.62	21	32.62	0.00
4.20(0)	21.02	S	sh	31	21.03	61	21.03	0.01
4.54(0)	19.45	VS	sh	40	19.45	80	19.45	0.00
5.41(3)	16.31	S	sh	22	16.31	42	16.31	0.00
7.41(5)	11.91	W	sh	13/03	11.84/11.98	13/130	11.94/11.97	0.07/0.03
8.14(2)	10.85	W	sh	33	10.87	63	10.87	0.02
8.97(6)	9.84	W	sh	80	9.72	93	9.84	0.12/0.00
20.06	4.42	VS	br	$h_{ch}+h_{br}$	-	$h_{ch}+h_{br}$	-	-
24.20	3.67	VS	sh (67)	h_{TP}	-	h_{TP}	-	-
Tp^6PhTp^6 (T = 180 °C): **N_{Col}**; D = 21.12Å								
2.20	40.15	VW	br	D'		-		-
4.18	21.12	S	br	D		-		-
21.58	4.11	VS	br	$h=h_{ch}+h_{br}+h_{TP}$		-		-
Tp^6PhTp^6 (T = 120°C): **Col_{rec}**; a_{rec} = 72.28Å; b_{rec} = 30.47Å; γ = 90° ➡ a_{rec} = 144.56Å; b_{rec} = 30.47Å; γ = 90°								
2.94(0)	28.08	S	sh	11	28.08	21	28.08	0.00
4.88(7)	18.07	VS	sh	40	18.07	80	18.07	0.00
6.27(7)	14.07	S	sh	22	14.04	42	14.04	0.03
6.75(2)	13.08	S	sh	51	13.06	101	13.06	0.02
9.06(3)	9.75	W	sh	71	9.78	43/141	9.78	0.03
9.45(3)	9.35	W	sh	33	9.36	63	9.36	0.01
14.12(3)	6.26	W	sh	93	6.30	183/134	6.30/6.28	0.04/0.02
19.41	4.57	VS	br	$h_{ch}+h_{br}$	-	$h_{ch}+h_{br}$	-	-
22.55	3.94	VS	br	h_{TP}	-	h_{TP}	-	-
Tp^8PhTp^8 (T = 135°C): **Col'_{rec}**; a_{rec} = 81.72Å; b_{rec} = 32.15Å; γ = 90° ➡ a_{rec} = 163.44Å; b_{rec} = 32.15Å; γ = 90°								
2.95(0)	29.92	S	sh	11	29.92	21	29.92	0.00
3.50(6)	25.18	S	sh	21	25.27	41	25.27	0.09
4.32(0)	20.43	VS	sh	40	20.43	80	20.43	0.00
6.06(3)	14.57	S	sh	51	14.57	101	14.57	0.00
8.00(0)	11.04	W	sh	71	10.97	141	10.97	0.07
8.48(8)	10.39	W	sh	62/23	10.39/10.37	122/43	10.39/10.37	0.02/0.00
19.11	4.64	VS	br	$h_{ch}+h_{br}$	-	$h_{ch}+h_{br}$	-	-
22.40	3.96	VS	br	h_{TP}	-	h_{TP}	-	-
Tp^8PhTp^8 (T = 100°C): **Col_{rec}**; a_{rec} = 82.08Å; b_{rec} = 31.59Å; γ = 90° ➡ a_{rec} = 164.16Å; b_{rec} = 31.59Å; γ = 90°								

2.99(4)	29.48	S	sh	11	29.48	21	29.48	0.00
4.30(1)	20.52	VS	sh	40	20.52	80	20.52	0.00
6.06(2)	14.57	S	sh	51	14.57	101	14.57	0.00
7.95(1)	11.11	W	sh	71	10.99	141	10.99	0.12
8.56(7)	10.31	W	sh	62	10.34	33/122/151	10.34	0.03
19.62	4.52	VS	br	$h_{ch}+h_{br}$	-	$h_{ch}+h_{br}$	-	-
22.46	3.95	VS	br	h_{TP}	-	h_{TP}	-	-
Tp^8PhTp^8 (T = 50°C): **Col_{rec}**; $\mathbf{a}_{rec}$ = 81.96Å; $\mathbf{b}_{rec}$ = 30.97Å; γ = 90° ➡ $\mathbf{a}_{rec}$ = 163.92Å; $\mathbf{b}_{rec}$ = 30.97Å; γ = 90°								
3.04(7)	28.97	S	sh	11	28.97	21	28.97	0.00
4.30(9)	20.49	VS	sh	40	20.49	80	20.49	0.00
6.09(7)	14.48	S	sh	22/51	14.48/14.49	42/101	14.48/14.49	0.00/0.01
7.97(2)	11.08	W	sh	71	10.95	141	10.95	0.13
8.61(5)	10.25	W	sh	13/80/62	10.24	23/160/122	10.24	0.01
19.33	4.58	VS	br	$h_{ch}+h_{br}$	-	$h_{ch}+h_{br}$	-	-
22.87	3.88	VS	br	h_{TP}	-	h_{TP}	-	-
$Tp^6Ph_2Tp^6$ (T = 180°C): **Col'_{hex}**; $\mathbf{a}_{hex}$ = 19.92Å								
2.81	31.36	W	br	D		-		-
5.12(0)	17.25	VS	sh	10		17.25		0.00
20.18	3.40	VS	br	$h_{ch}+h_{br}$		-		-
24.32	3.66	VS	sh (21)	h_{TP}		-		-
$Tp^6Ph_2Tp^6$ (T = 120°C): **Col'_{rec}**; $\mathbf{a}_{rec}$ = 68.84Å; $\mathbf{b}_{rec}$ = 37.51Å; γ = 90° ➡ $\mathbf{a}_{rec}$ = 137.68Å; $\mathbf{b}_{rec}$ = 37.51Å; γ = 90°								
2.67(9)	32.94	M	sh	11	32.94	21	32.94	0.00
4.51(4)	19.56	VS	sh	31	19.57	61	19.57	0.01
5.11(8)	17.21	VS	sh	40	17.21	80	17.21	0.00
5.36(0)	16.46	S	sh	22	16.47	42	16.47	0.01
5.75(1)	15.35	M	sh	41	15.64	90	15.30	0.29/0.05
7.67(2)	11.51	W	sh	60	11.47	120	11.47	0.04
12.10(2)	7.31	W	sh	25	7.33	45	7.33	0.02
20.21	4.39	VS	br	$h_{ch}+h_{br}$	-	$h_{ch}+h_{br}$	-	-
24.79	3.59	VS	sh (42)	h_{TP}	-	h_{TP}	-	-
$Tp^6Ph_2Tp^6$ (T = 50°C): **Col_{rec}**; $\mathbf{a}_{rec}$ = 66.16Å; $\mathbf{b}_{rec}$ = 38.19Å; γ = 90° ➡ $\mathbf{a}_{rec}$ = 132.32Å; $\mathbf{b}_{rec}$ = 38.19Å; γ = 90°								
2.66(8)	33.08	M	sh	11	33.08	21	33.08	0.00
4.81(0)	18.36	VS	sh	12	18.35	22	18.35	0.01
5.34(0)	16.54	VS	sh	40	16.54	80/42	16.54	0.00
7.99(0)	11.04	W	sh	33	11.02	63/120	11.02	0.02
19.90	4.46	VS	br	$h_{ch}+h_{br}$	-	$h_{ch}+h_{br}$	-	-
24.94	3.57	VS	sh (32)	h_{TP}	-	h_{TP}	-	-
$Tp^8Ph_2Tp^8$ (T = 165°C): **N_{Col}**; D = 20.20Å								
4.37	20.20	VS	br (23)	D		-		-
22.92	3.88	VS	br	$h=h_{ch}+h_{br}+h_{TP}$		-		-
$Tp^8Ph_2Tp^8$ (T = 115°C): **Col_{rec}**; $\mathbf{a}_{rec}$ = 79.52Å; $\mathbf{b}_{rec}$ = 38.02Å; γ = 90° ➡ $\mathbf{a}_{rec}$ = 159.04Å; $\mathbf{b}_{rec}$ = 38.02Å; γ = 90°								
2.57(3)	34.30	S	sh	11	34.30	21	34.30	0.00
4.06(1)	21.74	S	sh	31	21.74	61	21.74	0.00
4.44(1)	19.88	VS	sh	40	19.88	80	19.88	0.00
5.18(0)	17.05	S	sh	22	17.15	42	17.15	0.10
7.02(2)	12.58	M	sh	13/61	12.51	13/23/121	12.51/12.63	0.07/0.05
7.71(0)	11.46	W	sh	33	11.43	63	11.43	0.03
8.06(7)	10.95	W	sh	71/62	10.88/10.87	141/122	10.88/10.87	0.07/0.08
8.89(0)	9.93	W	sh	80/53	9.94/9.91	160/103	9.94/9.91	0.01/0.02
20.08	4.42	VS	br	$h_{ch}+h_{br}$	-	$h_{ch}+h_{br}$	-	-
24.04	3.70	VS	br (13)	h_{TP}	-	h_{TP}	-	-
$Tp^8Ph_2Tp^8$ (T = 50°C): **Col_{rec}**; $\mathbf{a}_{rec}$ = 78.12Å; $\mathbf{b}_{rec}$ = 37.57Å; γ = 90° ➡ $\mathbf{a}_{rec}$ = 156.24Å; $\mathbf{b}_{rec}$ = 37.57Å; γ = 90°								
2.60(7)	33.86	S	sh	11	33.86	21	33.86	0.00
4.12(3)	21.40	S	sh	31	21.40	61	21.40	0.00
4.52(0)	19.53	VS	sh	40	19.53	80	19.53	0.00
5.20(2)	16.97	S	sh	22	16.93	42	16.93	0.04
6.11(7)	14.44	W	sh	51	14.43	101	14.43	0.01

6.92(8)	12.75	M	sh	x	x	92	12.75	0.01
7.83(0)	11.28	W	sh	33	11.29	63	11.29	0.01
8.06(5)	10.95	W	sh	x	x	73	10.92	0.03
14.31(9)	6.18	W	sh	26	6.18	46/195	6.18	0.00
19.37	4.58	VS	br	$h_{ch}+h_{br}$	-	$h_{ch}+h_{br}$	-	-
24.56	3.62	VS	br (6)	h_{TP}	-	h_{TP}	-	-
$Tp^{6}TtTp^{6}$ (T = 240°C): **N_{Col}**; D = 19.46Å								
4.54	19.46	VS	br (23)	D		-		-
21.75	4.08	VS	br	$h=h_{ch}+h_{br}+h_{TP}$		-		-
$Tp^{6}TtTp^{6}$ (T = 190°C): **Col_{rec}**; **a_{rec}** = 72.96Å; **b_{rec}** = 33.85Å; γ = 90° ➡ **a_{rec}** = 145.92Å; **b_{rec}** = 33.85Å; γ = 90°								
2.86(5)	30.71	S	sh	11	30.71	21	30.71	0.00
4.84(0)	18.24	VS	sh	40	18.24	80	18.24	0.00
5.75(1)	15.35	S	sh	22	15.35	42	15.35	0.00
6.36(5)	13.87	M	sh	32	13.89	62	13.89	0.02
19.36	4.58	VS	br	$h_{ch}+h_{br}$	-	$h_{ch}+h_{br}$	-	-
22.64	3.92	VS	br (8)	h_{TP}	-	h_{TP}	-	-
$Tp^{6}TtTp^{6}$ (T = 80°C): **Col_{rec}**; **a_{rec}** = 71.52Å; **b_{rec}** = 32.67Å; γ = 90° ➡ **a_{rec}** = 143.04Å; **b_{rec}** = 32.67Å; γ = 90°								
2.97(0)	29.72	S	sh	11	29.72	21	29.72	0.00
4.93(8)	17.88	VS	sh	40	17.88	80	17.88	0.00
5.64(7)	15.64	VS	sh	41	15.68	81	15.68	0.04
6.55(2)	13.48	S	sh	32	13.47	62	13.47	0.01
19.36	4.58	VS	br	$h_{ch}+h_{br}$	-	$h_{ch}+h_{br}$	-	-
23.25	3.81	VS	br	h_{TP}	-	h_{TP}	-	-
$Tp^{8}TtTp^{8}$ (T = 190°C): **N_{Col}**; D = 21.59Å								
4.09	21.59	VS	br (31)	D		-		-
21.29	4.17	VS	br	$h=h_{ch}+h_{br}+h_{TP}$		-		-
$Tp^{8}TtTp^{8}$ (T = 160°C): **Col_{rec}**; **a_{rec}** = 85.24Å; **b_{rec}** = 34.80Å; γ = 90° ➡ **a_{rec}** = 170.48Å; **b_{rec}** = 34.80Å; γ = 90°								
2.73(9)	32.22	S	sh	11	32.22	21	32.22	0.00
4.14(3)	21.31	VS	sh	40	21.31	80	21.31	0.00
5.48(1)	16.11	S	sh	22	16.11	42	16.11	0.00
5.77(3)	15.30	M	sh	51	15.31	101	15.31	0.01
8.04(0)	10.99	M	sh	62	11.00	122/53	$11.00/10.9_{8}$	0.01
8.38(8)	10.53	W	sh	80	10.65	73/132	10.47	0.12/0.06
18.14	4.88	VS	br	$h_{ch}+h_{br}$	-	$h_{ch}+h_{br}$	-	-
23.20	3.83	VS	br	h_{TP}	-	h_{TP}	-	-
$Tp^{6}BtTp^{6}$ (T = 260°C): **N_{Col}**; D = 18.69Å								
4.72	18.69	VS	br (35)	D		-		-
19.60	4.52	VS	br	$h=h_{ch}+h_{br}+h_{TP}$		-		-
$Tp^{6}BtTp^{6}$ (T = 190°C): **Col_{rec}**; **a_{rec}** = 71.52Å; **b_{rec}** = 34.40Å; γ = 90° ➡ **a_{rec}** = 143.04Å; **b_{rec}** = 34.40Å; γ = 90°								
2.84(7)	31.00	M	sh	11	31.00	21	31.00	0.00
4.53(0)	19.49	S	sh	31	19.59	61	19.59	0.10
4.93(8)	17.88	VS	sh	40	17.88	80	17.88	0.00
5.56(0)	15.88	M	sh	41	15.86	81/90	$15.86/15.8_{9}$	0.02/0.01
6.35(7)	13.89	M	sh	32	13.95	62	13.95	0.06
9.28(6)	9.51	W	sh	43	9.65	83/150	9.65/9.54	0.14/0.03
9.90(0)	8.96	M	sh	53/80	8.95/8.94	103/160	8.95/8.94	0.01/0.02
10.94(0)	8.08	W	sh	34	8.09	64	8.09	0.01
14.27(2)	6.20	M	sh	84/55	6.20	164/105	6.20	0.00
14.84(9)	5.96	W	sh	120/65	5.96	125	5.96	0.00
21.01	4.21	VS	br	$h=h_{ch}+h_{br}+h_{TP}$	-	h	-	-
$Tp^{8}BtTp^{8}$ (T = 235°C): **N_{Col}**; D = 20.24Å								
4.36	20.24	VS	br (35)	D		-		-
20.88	4.25	VS	br	$h=h_{ch}+h_{br}+h_{TP}$		-		-
$Tp^{8}BtTp^{8}$ (T = 200°C): **Col_{rec}**; **a_{rec}** = 81.92Å; **b_{rec}** = 34.78Å; γ = 90° ➡ **a_{rec}** = 163.84Å; **b_{rec}** = 34.78Å; γ = 90°								

2.74(9)	32.10	VW	sh	11	32.01	21	32.01	0.09
4.31(1)	20.48	VS	sh	40	20.48	80	20.48	0.00
6.00(8)	14.70	W	sh	32	14.67	62	14.67	0.03
8.29(0)	10.66	M	sh	33	10.67	63	10.67	0.01
8.69(9)	10.16	M	sh	43/80	10.09/10.24	83/132	10.09/10.2$_0$	0.07/0.04
12.37(7)	7.14	M	sh	93	7.16	183/134	7.16	0.02
12.96(6)	6.82	W	sh	25/112	6.86/6.85	55/154	6.80	0.04-0.02
20.65	4.30	VS	br	h=h_{ch}+h_{br}+h_{TP}	-	h	-	-
Tp^{8}BtTp^8 (T = 100°C): **Col$_{rec}$**; **a**$_{rec}$ = 81.44Å; **b**$_{rec}$ = 34.81Å; γ = 90° ➡**a**$_{rec}$ = 162.88Å; **b**$_{rec}$ = 34.81Å; γ = 90°								
2.75(2)	32.08	VVW	sh	11	32.01	21	32.01	0.07
4.33(6)	20.36	VS	sh	40	20.36	80	20.36	0.00
5.74(1)	15.38	W	sh	x	x	52	15.35	0.03
6.01(5)	14.68	W	sh	32	14.65	62	14.65	0.03
8.29(0)	10.66	S	sh	33	10.67	63	10.67	0.01
8.73(0)	10.12	S	sh	43	10.08	83	10.08	0.04
12.45(0)	7.10	M	sh	93	7.13	183	7.13	0.03
13.07(2)	6.41	W	sh	55	6.40	105	6.40	0.01
16.48(6)	5.37	VW	sh	66/124/151	5.33/5.35/5.36	195/126	5.40/5.33	0.03/0.04
20.74	4.28	VS	br	h=h_{ch}+h_{br}+h_{TP}	-	h	-	-
Tp^{6}Ph$_2$Tp^{12} (T = 100°C): **Col$_{rec}$**; **a**$_{rec}$ = 86.64Å; **b**$_{rec}$ = 35.96Å; γ = 90° ➡**a**$_{rec}$ = 173.28Å; **b**$_{rec}$ = 35.96Å; γ = 90°								
2.65(8)	33.21	S	sh	11	33.21	21	33.21	0.00
4.07(5)	21.66	VS	sh	40	21.66	80	21.66	0.00
5.02(9)	17.56	VS	sh	12	17.60	22	17.60	0.04
5.32(0)	16.60	M	sh	22	16.61	42	16.61	0.01
7.39(1)	11.95	W	sh	03	11.99	13	11.96	0.04/0.01
7.51(5)	11.70	W	sh	71	11.70	141	11.70	0.00
19.79	4.48	VS	br	h_{ch}+h_{br}	-	h_{ch}+h_{br}	-	-
23.83	3.72	VS	br	h_{TP}	-	h_{TP}	-	-
Tp^{6}Ph$_2$Tp^{12} (T = 50°C): **Col$_{rec}$**; **a**$_{rec}$ = 86.56Å; **b**$_{rec}$ = 35.11Å; γ = 90° ➡**a**$_{rec}$ = 173.12Å; **b**$_{rec}$ = 35.11Å; γ = 90°								
2.71(3)	32.54	S	sh	11	32.54	21	32.54	0.00
4.07(9)	21.64	VS	sh	40	21.64	80	21.64	0.00
5.11(7)	17.25	VS	sh	12	17.20	22	17.20	0.05
5.41(6)	16.30	M	sh	22	16.27	42	16.27	0.02
7.55(8)	11.69	W	sh	03	11.70	13	11.68	0.01
19.83	4.47	W	br	h_{ch}+h_{br}	-	h_{ch}+h_{br}	-	-
24.56	3.62	VS	br	h_{TP}	-	h_{TP}	-	-
Tp^{12}Ph$_2$Tp^{12} (T = 110°C): **Col$_{rec}$**; **a**$_{rec}$ = 97.20Å; **b**$_{rec}$ = 37.33Å; γ = 90° ➡**a**$_{rec}$ = 194.40Å; **b**$_{rec}$ = 37.33Å; γ = 90°								
2.53(3)	34.85	S	sh	11	34.85	21	34.85	0.00
3.63(2)	24.30	S	sh	40	24.30	80	24.30	0.00
4.79(7)	18.40	VS	sh	12	18.33	22	18.33	0.07
6.58(7)	13.41	W	sh	52	13.46	102	13.46	0.05
6.74(9)	13.08	W	br	71	13.01	141	13.01	0.07
7.89(6)	11.19	W	sh	72	11.14	142	11.14	0.05
19.51	4.55	VS	br	h_{ch}+h_{br}	-	h_{ch}+h_{br}	-	-
23.65	3.76	VS	br	h_{TP}	-	h_{TP}	-	-
Tp^{12}Ph$_2$Tp^{12} (T = 50°C): **Col$_{rec}$**; **a**$_{rec}$ = 96.80Å; **b**$_{rec}$ = 37.26Å; γ = 90° ➡**a**$_{rec}$ = 193.60Å; **b**$_{rec}$ = 37.26Å; γ = 90°								
2.53(9)	34.77	S	sh	11	34.77	21	34.77	0.00
3.64(8)	24.20	S	sh	40	24.20	80	24.20	0.00
4.83(0)	18.28	VS	sh	12	18.29	22	18.29	0.01
6.60(5)	13.37	W	sh	52	13.42	102	13.42	0.05
6.78(9)	13.01	W	br	71	12.96	141	12.96	0.05
19.82	4.47	VS	br	h_{ch}+h_{br}	-	h_{ch}+h_{br}	-	-
24.32	3.66	VS	br	h_{TP}	-	h_{TP}	-	-
Tp^{6}Th$_2$Tp^{12} (T = 50°C): **Col$_{rec}$**; **a**$_{rec}$ = 88.80Å; **b**$_{rec}$ = 34.39Å; γ = 90° ➡**a**$_{rec}$ = 177.60Å; **b**$_{rec}$ = 34.39Å; γ = 90°								
2.75(2)	32.07	S	sh	11	32.07	21	32.07	0.00
3.24(0)	27.24	W	sh	21	27.19	41	27.19	0.05
3.62(0)	24.39	W	sh	x	x	51	24.71	0.32

3.97(6)	22.20	VS	sh	40	22.20	80	22.20	0.00
4.74(3)	18.61	W	br	41	18.65	81	18.65	0.04
5.23(8)	16.86	S	sh	12	16.88	22	16.88	0.02
6.99(1)	12.63	W	sh	70	12.68	140/131	12.69	0.05/0.06
7.71(2)	11.45	M	sh	03	11.46	13	11.44	0.01/0.01
20.08	4.42	VS	br	$h_{ch}+h_{br}$	-	$h_{ch}+h_{br}$	-	-
24.57	3.62	VS	br	h_{TP}	-	h_{TP}	-	-
$Tp^{6}Th_2Tp^{12}$ (T = 105°C): **Col_{rec}**; **a_{rec}** = 91.40Å; **b_{rec}** = 34.25Å; γ = 90° ➡ **a_{rec}** = 182.80Å; **b_{rec}** = 34.25Å; γ = 90°								
2.75(2)	32.07	S	sh	11	32.07	21	32.07	0.00
3.15(9)	27.94	W	sh	21	27.41	41	27.41	0.53
3.53(2)	24.99	W	sh	x	x	51	25.00	0.01
3.86(3)	22.85	VS	sh	40	22.85	80	22.85	0.00
5.23(8)	16.86	W	br	12	16.83	22	16.83	0.03
6.72(5)	13.13	S	sh	70	13.06	140/92	13.09	0.07/0.04
7.41(3)	11.92	W	sh	71	12.20	112	11.92	0.00
20.01	4.43	VS	br	$h_{ch}+h_{br}$	-	$h_{ch}+h_{br}$	-	-
24.15	3.68	VS	br	h_{TP}	-	h_{TP}	-	-
$Tp^{12}Th_2Tp^{12}$ (T = 110°C): **Col_{rec}**; **a_{rec}** = 93.64Å; **b_{rec}** = 34.42Å; γ = 90° ➡ **a_{rec}** = 187.28Å; **b_{rec}** = 34.42Å; γ = 90°								
2.73(2)	32.31	M	sh	11	32.31	21	32.31	0.00
3.77(1)	23.41	VS	sh	40	23.41	80	23.41	0.00
5.20(3)	16.97	M	sh	12	16.93	22	16.93	0.04
7.06(8)	12.49	W	sh	71	12.47	141/150	12.47/12.48	0.02/0.01
20.17	4.40	VS	br	$h_{ch}+h_{br}$	-	$h_{ch}+h_{br}$	-	-
23.97	3.71	VS	br	h_{TP}		h_{TP}		-

As above for **Table S9**.

12. STM

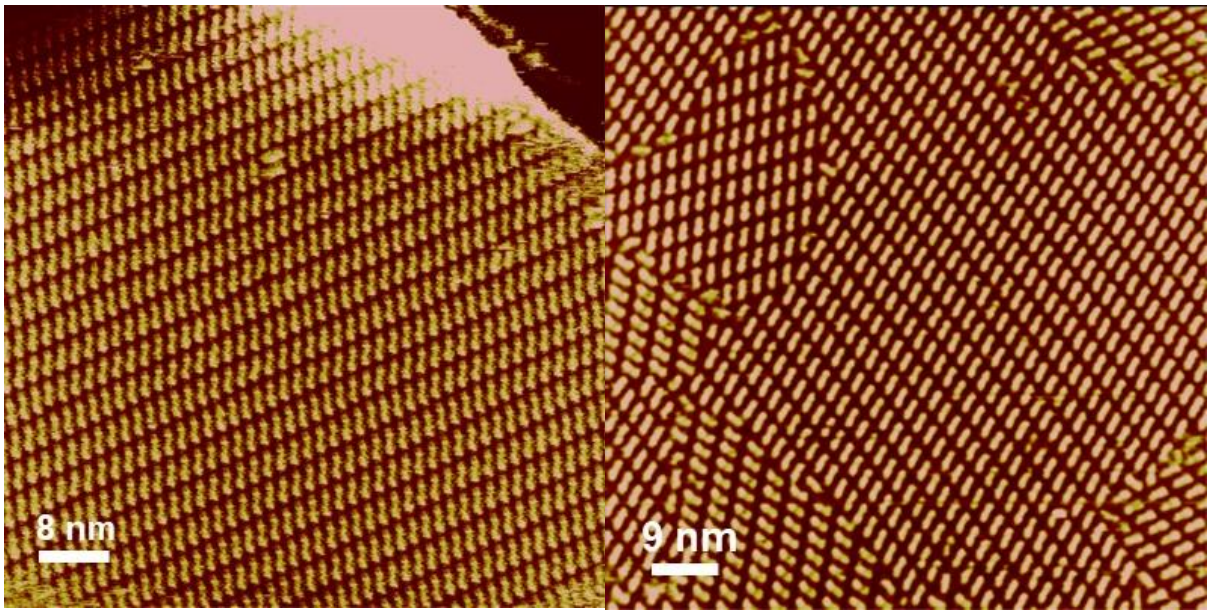

Figure S71. Large-scale STM images of the self-assembly of **$Tp^{6}Tt_2Tp^{6}$** (left) and **$Tp^{8}Th_2Tp^{8}$** (right)on the interface of 1-phenyloctane/HOPG. Conditions: I_{set} = 247.2 pA, V_{bis} = 847.2 mV and I_{set} = 271.6 pA, V_{bis} = 770.0 mV

13. Models' variations

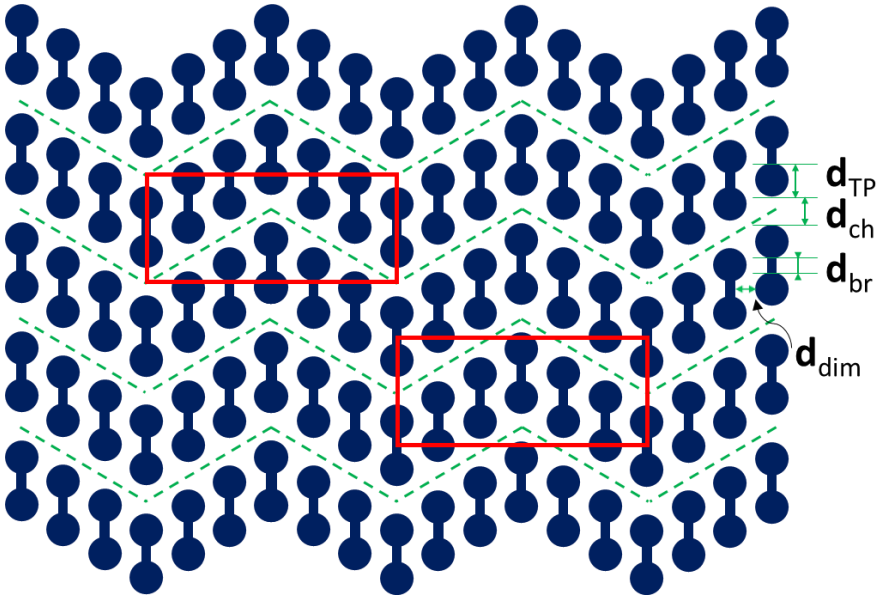

Figure S72. Parameters controlling the chevron columnar phase of symmetry *pm*: $\mathbf{d}_{TP}$ = diameter of cylinder (see Table 3); $\mathbf{d}_{br}$, length of bridge; $\mathbf{d}_{ch}$, chain separation; $\mathbf{d}_{dim}$, distance between bridge and TP unit; $\mathbf{b}_{rec} = 2\mathbf{d}_{TP}+\mathbf{d}_{br}+\mathbf{d}_{ch}$. Single multicolumnar lattice shown in red.

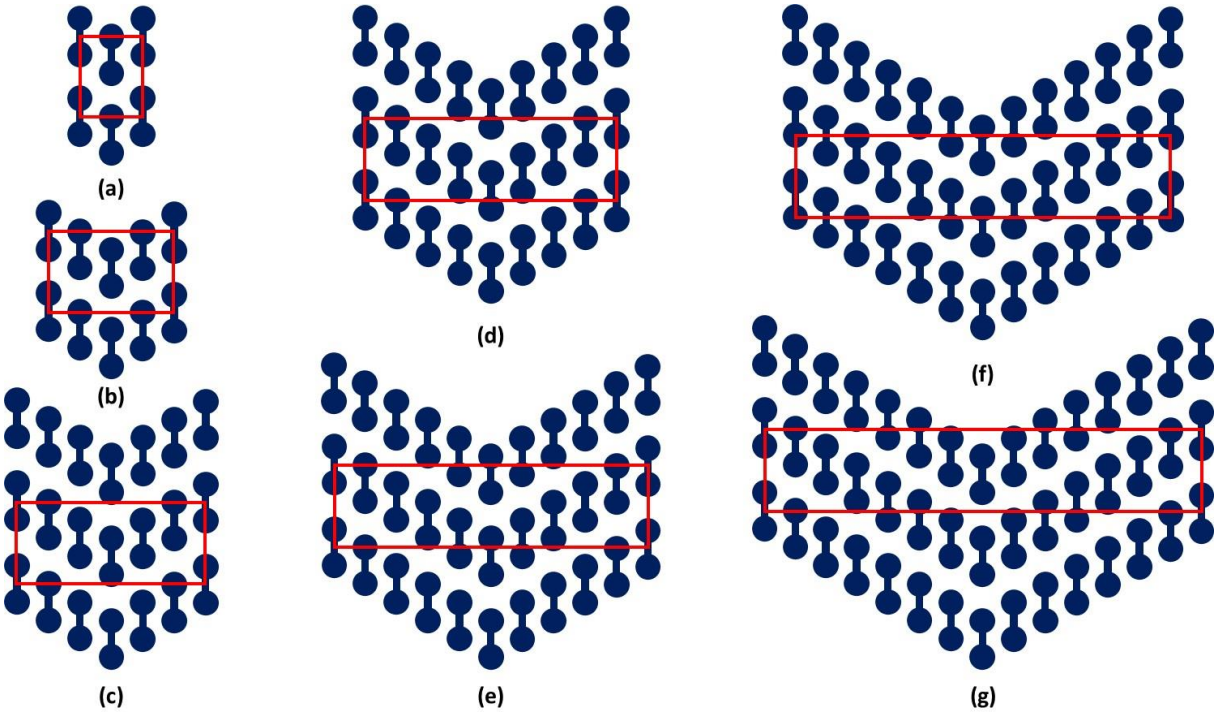

Figure S73. Idealized representations of the potentially extended family of *pm* chevron columnar phases containing increasing numbers of columns (and dimers) per rectangular superlattice: (**a**), Z = 4, n_{mol} = 2; (**b**), Z = 8, n_{mol} = 4; (**c**), Z = 12, n_{mol} = 6; (**d**), Z = 16, n_{mol} = 8; (**e**), Z = 20, n_{mol} = 10; (**f**), Z = 24, n_{mol} = 12; (**g**), Z = 28, n_{mol} = 14.

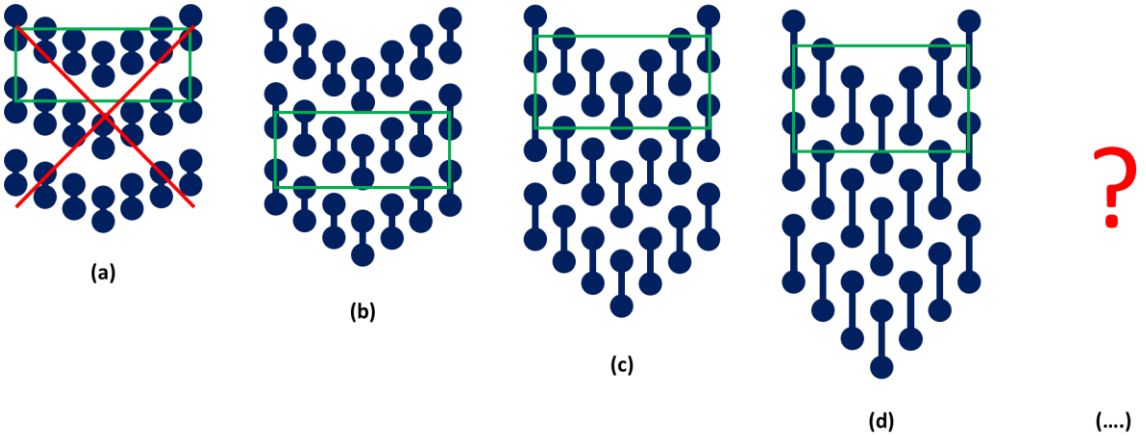

Figure S74. Effect of bridge length: induction of stalking faults and symmetry changes. (**a**), $\mathbf{d}_{br}$ = 0 (not mesomorphous); (**b**), $\mathbf{d}_{br}$ = $\mathbf{d}_{TP}$ (Col_{rec}-*pm*); (**c**), $\mathbf{d}_{br}$ = 2$\mathbf{d}_{TP}$ (Col_{rec}-*pm*); (**d**), $\mathbf{d}_{br}$ = 3$\mathbf{d}_{TP}$ (Col_{rec}-*pm*); ……. (?).